AN INVESTIGATION TOWARDS A CONJUGATE VACCINE AGAINST *STREPTOCOCCUS PNEUMONIAE* SEROTYPE 19A

By

Astrid Joan Trimmel

Thesis Presented for the Degree of

DOCTOR OF PHILOSOPHY

In the Department of Chemistry

UNIVERSITY OF CAPE TOWN

March 2017

Supervisors: Associate Professor Neil Ravenscroft
Dr. Seanette Wilson

WITH ALL MY LOVE

TO

MY FAMILY

Declaration

I declare that “An investigation towards a conjugate vaccine against *Streptococcus pneumoniae* serotype 19A“ is my own work and that all sources that I have used or quoted have been indicated and acknowledged by means of complete references.

Astrid Joan Trimmel

Parts of this thesis have been presented at conferences

Poster presentation (2011) - African Network for Drugs and Diagnostics (ANDI) in Kenya, Africa, abstract p 142.

Poster entitled: Production of *Streptococcus pneumoniae* capsular polysaccharide using disposable bag technology.

Oral presentation (2011) - South Africa Society of Microbiology (SASM) in Cape Town, South Africa, abstract p 140.

Talk entitled: Production of *Streptococcus pneumoniae* serotype 19A capsular polysaccharide using disposable bag technology.

Poster presentation (2012) - Pneumococci & Pneumococcal Diseases (ISPPD) in Iguassu Falls, Brazil**,** abstract p 107.

Poster entitled: *Streptococcus pneumoniae* serotype 19A capsular polysaccharide production using disposable bag and single step chromatographic purification.

Abstract

Streptococcus pneumoniae is a human pathogen that causes invasive pneumococcal diseases (IPD) such as pneumonia, otitis media and sepsis particularly in children, the elderly, and patients with HIV, and other immunosuppressive conditions. Conjugate vaccines comprised of the bacterial surface polysaccharide conjugated to a carrier protein are very effective in protecting young children against disease by inducing immunological memory and reducing carriage of the bacteria. A pneumococcal conjugate vaccine against seven serotypes (PCV7) was licensed in 2000, which resulted in a dramatic reduction of IPD. However; there was a gradual increase in the number of cases due to non–vaccine serotypes (serotype replacement).

Serotype 19A, not included in PCV7 as the structurally similar serotype 19F was assumed to cross-protect against 19A disease, emerged as the most prevalent serotype in several studies with significant presence in Sub-Saharan Africa and South-East Asia and is associated with multidrug resistance. As a result a 13-valent conjugate vaccine that includes serotype 19A was developed and licensed which provided broader coverage.

The aim of the work presented in this thesis was to develop processes for the manufacture of 19A capsular polysaccharide (CPS) for the production of a conjugate vaccine based on work performed on the model Pn1. The cultivation process included clonal selection for the growth and isolation of a serotype 19A clone producing high levels of CPS and cultivation using disposable bag technology as an alternative to the traditional fermentor. The culture was inactivated at low temperatures using cold phenol to prevent CPS degradation and to improve the release of CPS from the bacteria. The culture was clarified using a scalable flow-through centrifugation process. The Pn19A polysaccharide was purified using a single step process utilizing differential filtration with ethanol. Analytical tests including identity, purity (from nucleic acid and protein) and size analysis were optimized and performed on Pn19A CPS lots. All purified batches of polysaccharide met World Health Organisation (WHO) specifications as defined in the Technical Report Series.

Structural studies were performed on closely related CPS namely; 19F and 19A CPS, both of which contain a labile phosphodiester linkage. The composition of the polysaccharides determined by colorimetric assays was confirmed by hydrolysis and monomeric analysis using gas chromatography/mass spectroscopy (GC/MS) of the methyl glycoside derivatives. Use of ^{1}H, ^{13}C and ^{31}P nuclear magnetic resonance (NMR) experiments confirmed the structure of the 19F and 19A CPS repeating units and permitted determination of the extent of the cell wall polysaccharide contamination.

CPS was size-reduced by microfluidization prior to conjugation experiments using cyanylating chemistry and a model carrier protein bovine serum albumin (BSA) and tetanus toxoid (TT). Pn19F and Pn19A conjugates prepared using TT were subjected to thermal stability studies and demonstrated similar stability based on the free saccharide generated.

This proof of concept study established small-scale processes that can be further optimized for the manufacture of a conjugate vaccine against Pn19A disease.

Acknowledgements

I would like to extend my thanks and appreciation to the following people for their contribution to the preparation of this degree.

To my supervisors, Associate Professor Neil Ravenscroft and Dr. Seanette Wilson for their patience, guidance and thorough proof-reading of my thesis. Thanks for your enthusiasm in all things vaccines and especially on the focus of Pn19A.

To Dr. Ebrahim Mohammed and Dr. Ike James for all your help and guidance in and out of the laboratory. Thanks for your friendship and words of encouragement.

To all the staff past and present in the R&D/PD department at The Biovac Institute those in the pneumococcal project, I feel privileged to have worked with this team; Dr. Nelius Swart, Dr. Melinda Scanlen, Shantal, Jill, Charlie, Margaret, Lizelle, Gloria, Londiwe, Fran, Rochelle, Daria, Peter, Brian, Michelle, Kashief, Sihle, Lesetja and Patrick.

To the chemistry department at UCT and the other students in this group, thanks for the chats and motivation.

Special thanks to Dr. Cesarina Edmonds-Smith for her encouragement, chats, motivation, and friendship. Thanks to Dr. Aneesa Omar and Mrs. Hendricks for proof-reading my thesis.

Thank you to The Biovac Institute and NRF for funding this study.

To my family who had to endure these last few years with me, thank you for standing by me and encouraging me to strive for the best. For all the motivation and scoldings, it has gotten me through the good and the tough times. I love you all.

To my husband and daughter, all I can say is thank you for being such a special part of my life, you make it whole and worth it. I will love you always.

I am entirely grateful to the One who watches over my soul. To him be all the glory, honour and praise.

Contents

Abbreviations

ACN	Acetonitrile
ADH	Adipic acid dihydrazide
BCA	Bicinchoninic acid
BSA	Bovine serum albumin
BSL	Biological safety level
CDAP	1-cyano-4-dimethylaminopyridinium tetrafluoroborate
CDC	Centers for Disease Control and Prevention
CDIBP	Chengdu Institute of Biological Products
CFU	Colony forming units
cGMP	Current Good Manufacturing Practices
CNBr	Cyanogen bromide
COSY	Correlation spectroscopy
CPS	Capsular polysaccharides
CRM_{197}	Cross-reactive material 197
CTAB	Cetyltrimethylammonium bromide
CWPS	Cell wall polysaccharide
Cys.HCl	Cysteine hydrochloric acid
^oC	Degrees Celsius
D_2O	Deuterium oxide
Da	Daltons
DAD	Diode array detector
DOC	Deoxycholic acid
DMAB	Dimethylaminobenzaldehyde
EDC	N-(3-dimethylaminopropyl)-N'-ethyl carbodiimide hydrochloride
ELISA	Enzyme-linked immunosorbent assay
EPI	Expanded Program of Immunization
EtOH	Ethanol
FTC	Flow-through centrifuge
GC	Gas chromatography
GERMS-SA	Group for Enteric, Meningeal and Respiratory disease Surveillance in South Africa
Glc	Glucose
Gly	Glycine
GSK	GlaxoSmithKline
h	Hour
H_2SO_4	Sulfuric acid
HCl	Hydrochloric acid
Hib	*Haemophilus influenzae* type b
HIV	Human immunodeficiency virus

HPAEC-PAD	High-performance anion-exchange chromatography with pulsed amperometric detection
HSQC	Heteronuclear single quantum correlation
IPD	Invasive pneumococcal diseases
IR	Infrared
L	Litre
LMSL	Laboratory master seed lot
LOD	Limit of detection
LWSL	Laboratory working seed lot
M	Molarity
ManNAc	N-acetyl mannosamine
MES	2-(*N*-morpholino)ethane sulfonic acid
mg	Milligrams
min	Minute
mL	Millilitres
mM	Millimolar
µL	Microliters
MS	Mass spectroscopy
MSLT	Multilocus sequence typing
MW	Molecular weight
MWCO	Molecular weight cut-off
NaCl	Sodium chloride
Na_2CO_3	Sodium carbonate
NaOH	Sodium hydroxide
nm	Nanometres
NMR	Nuclear magnetic resonance
OD	Optical density
PAGE	Polyacrylamide gel electrophoresis
PBS	Phosphate buffered saline
PCV	Pneumococcal conjugate vaccine
PEG	Polyethylene glycol
p.i	Post inoculation
Pn	Pneumococcal
Pn1	*Streptococcus pneumoniae* serotype 1
Pn19A	*Streptococcus pneumoniae* serotype 19A
PPV	Pneumococcal polysaccharide vaccine
PRP	Polyribosylribitol phosphate
PS	Pre-seed
Rha	Rhamnose
rH	Relative humidity

RID	Refractive index detector
RPM	Revolutions per minute
RT	Room temperature
RU	Repeating unit
SDS	Sodium dodecyl sulfate
SEC-HPLC	Size exclusion high-performance liquid chromatography
TEA	Triethylamine
TFA	Trifluoroacetic acid
TNBS	2, 4, 6-trinitrobenzenesulfonic acid
TOCSY	Total correlation spectroscopy
TT	Tetanus toxoid
Trp	Tryptophan
TRS	Technical report series
Tyr	Tyrosine
UV	Ultraviolet
U	Units
WHO	World Health Organization

CHAPTER 1. INTRODUCTION

The pneumococcus bacterium, *Streptococcus pneumoniae* (*S. pneumoniae*) is known for being the most frequent causative agent of acute bacterial pneumonia, meningitis, sinusitis and otitis media [1, 2]. *S. pneumoniae* causes infections some of which are invasive pneumococcal disease (IPD) that are responsible for substantial morbidity and mortality among the young and the elderly in both developed and developing countries [3]. An increased risk of IPD has been observed in immunocompromised persons where individuals infected with the Human Immunodeficiency Virus (HIV) have rates of IPD that are up to 100 fold higher than those of the general population [4, 5]. *S. pneumoniae* causes IPD and public health problems because of its increasing resistance to penicillin, the antibiotic of choice. The impact of IPD is of major concern to developing countries as it accounts for an estimated 1.2 million deaths of young children per year [5]. A study by O'Brien et al. [3] conducted in 2009 estimated that Africa has the highest incidence of cases of pneumococcal disease (38/100000) and Europe the lowest (6/100000). The Group for Enteric, Meningeal and Respiratory Disease Surveillance in South Africa (GERMS-SA) recorded that in South Africa in 2007 pneumococcal meningitis was the predominant cause of acute bacterial meningitis in children younger than 5 years, followed by meningitis due to *Neisseria meningitides* (meningococcus) and *Haemophilus influenzae* type b (Hib) [3, 6]. Case fatality ratios were reported to be higher for pneumococcal meningitis 28%, (44/156), while both meningococcus and Hib appeared to have a similar incidence of 9%, (6/65) and 10%, (3/30) respectively [7].

1.1 The pneumococcus

The pneumococcal bacterium was first isolated in the 1880s by two independent laboratories, one in Europe and one in the United States [8]. In the 1920s the morphology was identified as a diplococci structure but was reclassified in 1974 as *S. pneumoniae* due to its growth in chains in solid and liquid media [9]. *S. pneumoniae* is an alpha-haemolytic pathogen that is typically observed in pairs (diplococci) as well as in short chains [10]. It is a fastidious Gram-positive, catalase-negative coccus that generates hydrogen peroxide (H_2O_2) via a flavoenzyme system in the cells [10, 11]. The ability to colonize and survive in different environments is facilitated by the synthesis and regulation of capsular polysaccharides (CPS). The CPS of *S. pneumoniae* is recognized as the major virulence factor and used as an antigen for pneumococcal vaccine development [6, 12]. As shown in Figure 1.1, the CPS forms part of the outer layer of the surface structure of *S. pneumoniae* and is considered the first line of defense [13]. *S. pneumoniae* is capable of synthesizing more than 90 structurally unique CPS, which forms the basis of serotyping [14-16]. It is the distinct chemical composition of the capsule that determines the different pneumococcal serotypes. Pneumococcus is very versatile in that it can spontaneously switch its phases between two colony phenotypes i.e. transparent and opaque [17, 18]. The transparent variants of *S. pneumoniae,* which are more adapted for intranasal colonization, are known to have lower amounts of CPS whereas the opaque variants produce higher amounts of CPS [17]. The CPS are high molecular weight polymers of oligosaccharides repeating units. Of the more than 90 serotypes that have been identified, 23 are responsible for the majority of human infections. In most cases, the invasive infections appear to be caused by these serotypes of which *S. pneumoniae*

serotype 19A (Pn19A) is one of the most common serotypes in children and therefore an important serotype to include in vaccines [19].

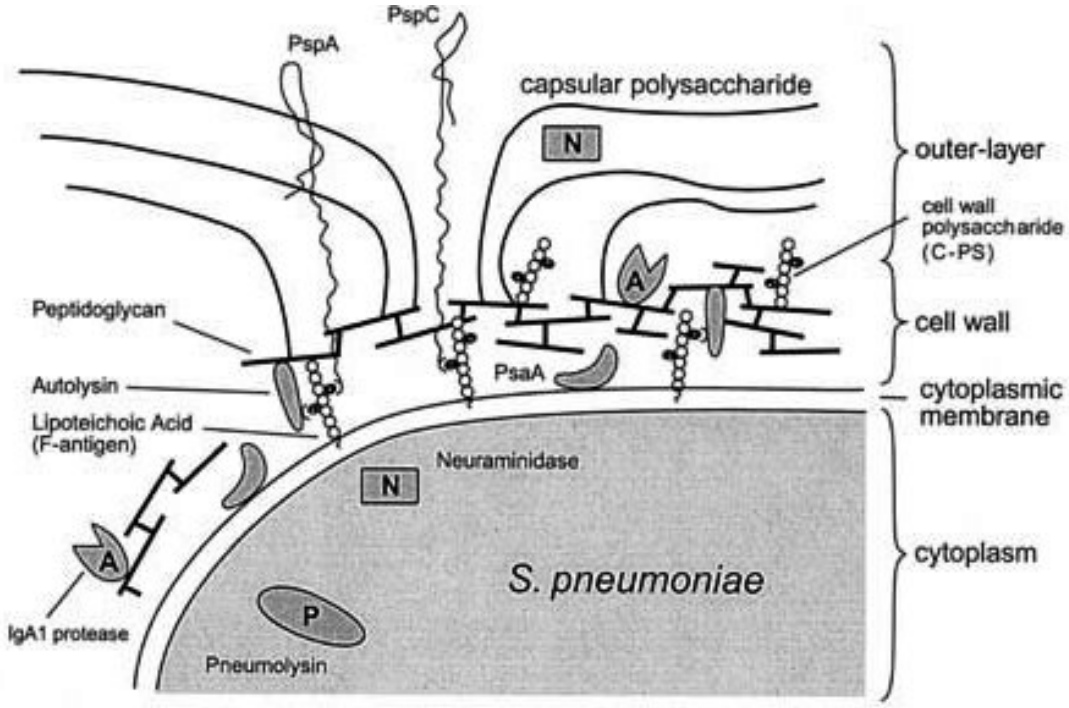

Figure 1.1: The surface structure of *S. pneumoniae* bacteria composed of three layers; cytoplasmic membrane, cell wall, and outer layer [13].

1.2 Pneumococcal disease burden

The pneumococcus commonly inhabits the respiratory tract of humans and colonizes the nasopharynx. With the acquisition of new strains, it can spread to surrounding tissue and cause acute otitis media (AOM) and sinusitis or invade the bloodstream as illustrated in Figure 1.2 [10, 20]. Pneumococcal disease can be divided into the non-invasive and invasive disease. The non-invasive pneumococcal disease can further be divided into sinusitis, AOM and community-acquired pneumonia whereas IPD is defined as an infection confirmed by the isolation of *S. pneumoniae* from a normally sterile site, such as blood or cerebrospinal fluid [21]. The IPD burden is predominantly characterized by pneumococcal meningitis, bacteraemic pneumococcal pneumonia, and pneumococcal bacteremia without a primary focus [22].

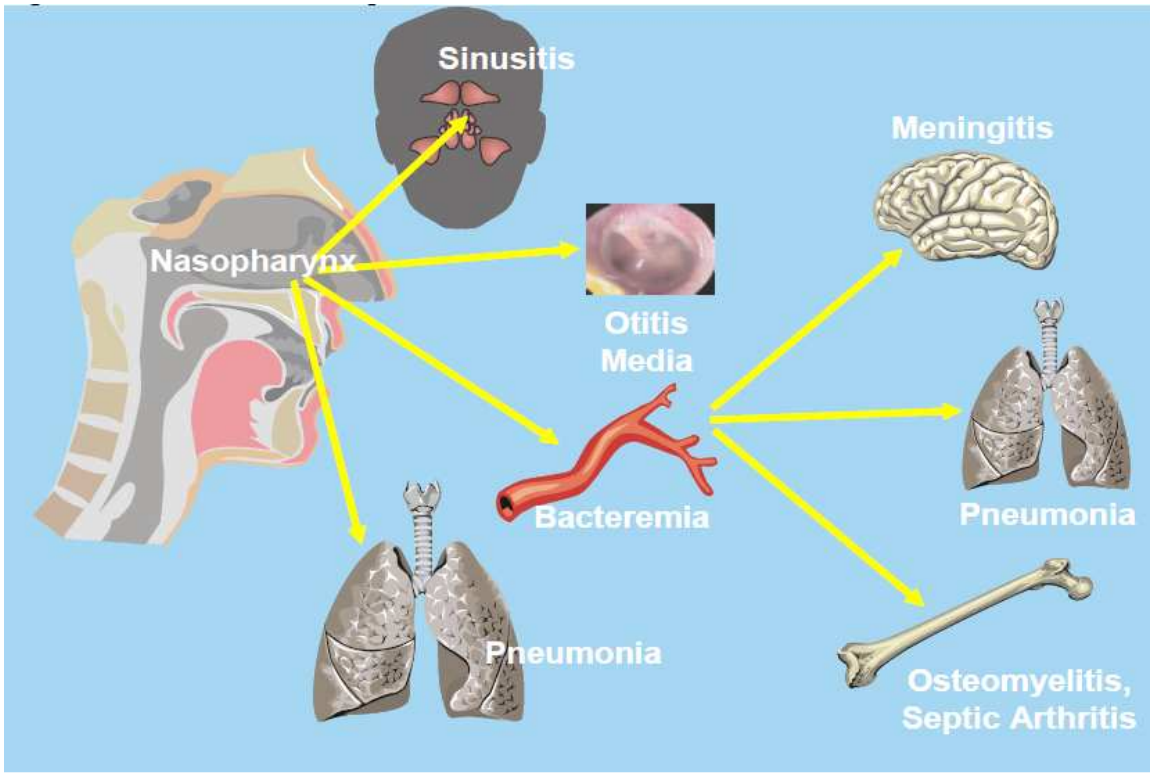

Figure 1.2: Common forms of IPD caused by infection at sites such as the nose and throat and subsequent invasion of the bloodstream [20].

The burden of disease is highest in young children (<2 years) and the elderly (>65 years of age) because their immune systems are either immature and unprepared or unable to respond effectively to pneumococcal infections [14]. There are clinical and economic burdens of this disease related to age. A study by Song et al. [23] showed there was a significant increase in case fatality rates of adults older than 50 years of age suffering from IPD. Globally, IPD has been estimated to account for approximately 1.4 million deaths annually in children younger than 5 years of age according to the WHO media fact sheet [24]. Figure 1.3 displays the total number of deaths caused by *S. pneumoniae* in children younger than 5 years of age in 2009, which was higher than the incidence caused by HIV.

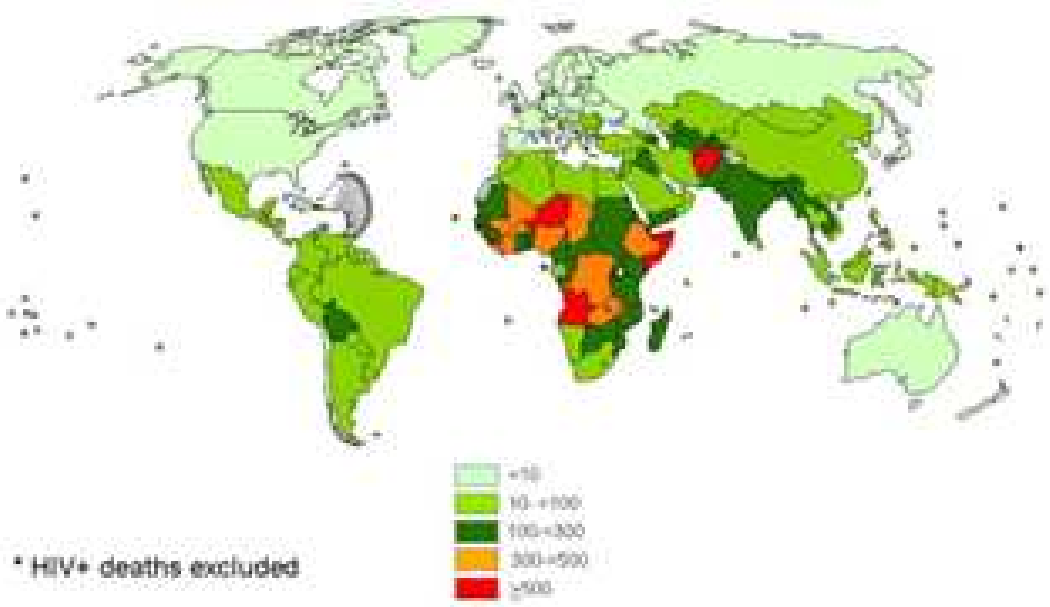

Figure 1.3: The total number of deaths (per 100000) in children younger than 2 years of age in 2009 caused by *S. pneumoniae* was higher than the incidence caused by HIV [3].

1.3 Pneumococcal capsule

The chemical structure and, to a lesser extent the thickness of the capsule determines the differential ability of the serotype to survive in the bloodstream which consequently results in invasive disease in the host [25]. The CPS determines the pathogenicity of the organism and allows for the classification of the pneumococci [25]. The classification of the more than 90 serotypes is based on composition and the carbohydrate structure of the capsule and its antigenic properties [25]. The difference between the serotypes is a result of the difference in the repeating unit structure of the CPS which results in varying potential to cause disease. Consequently, relatively few serotypes are associated with severe disease in children [20].

1.4 Pneumococcal serotypes

Approximately 23 serotypes account for over 70% of invasive disease in all age groups worldwide [21]. Based on the molecular typing of multiple housekeeping genes, pneumococcal strains can be characterized into clonal groups. The most common serogroups and serotypes worldwide are 6, 14, 19 and 23 but other serotypes including 1, 5 and 7 contribute greatly to IPD in young children in developing countries [26]. Occurrence varies throughout the world but some serotypes, such as 14, are consistently more abundant. Figure 1.4 shows that Pn19A is one of the main causes of IPD on three of the five continents and is one of the most common serotypes that causes invasive pneumococcal infection in Asia and, most importantly, in Africa [25, 27]. In addition, according to a literature survey performed by Hausdorff et al. [5] in 2000, serotypes 6A and 19A account for more invasive pneumococcal disease in the United States of America (USA) in children under 2 years of age than serotypes 1, 3, 5 and 7F combined.

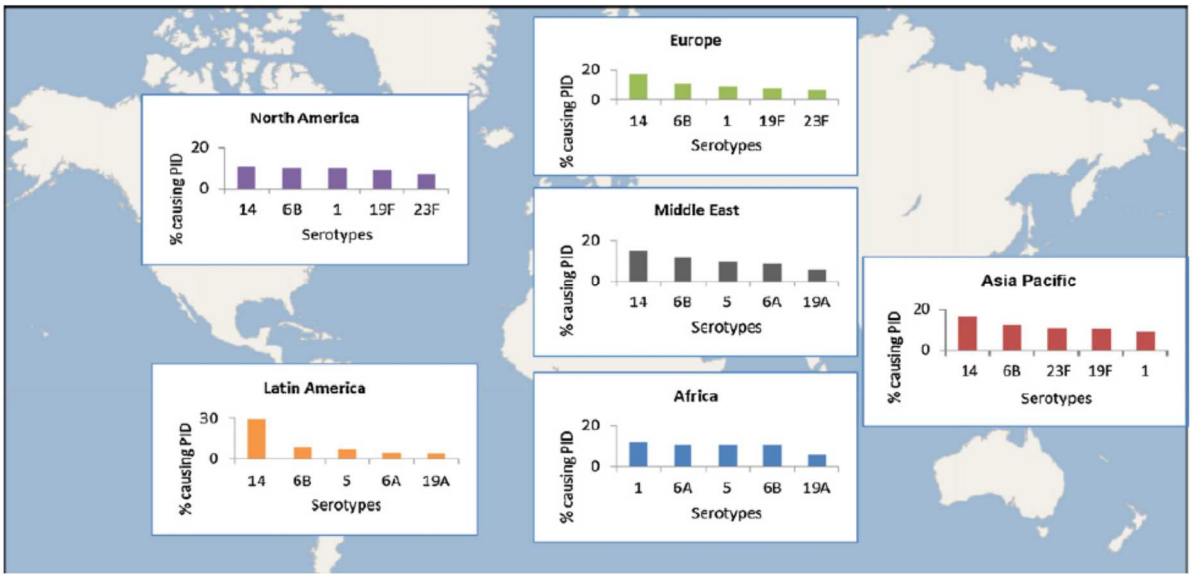

Figure 1.4: The five most common serotypes (1, 5, 6A, 6B and 19A) causing invasive pneumococcal infection by continent, as shown by Mehr et al. [12] in 2012 causes 70 – 80% IPD.

1.5 Pneumococcal polysaccharide vaccines

Polysaccharide vaccines prepared from the polysaccharide isolated from the surface of certain bacteria provide serotype and serogroup protection against pneumococcal and meningococcal disease [28]. The first pneumococcal polysaccharide vaccine (PPV) was released in 1946 but was soon removed from the market when anti-microbial therapies such as penicillin and sulfa drugs became readily available for the treatment of pneumococcal diseases [29]. The PPV was reintroduced in the 1970s in the form of a 14-valent vaccine which was licensed in 1977 (Table 1.1) [30].

Table 1.1 Pneumococcal polysaccharide vaccines [27].

Year of first licensure	Valency	Vaccine serotypes	Licensed formulations
1977	14-valent CPS	1, 2, 3, 4, 6A, 7F, 8, 9N, 12F, 14, 18C, 19F, 23F, 25F	Pneumovax (Merck & Co., Inc) Pnu-Immune (Lederle-Praxis Biologicals)
1980's	17-valent CPS	1, 2, 3, 4, 6A, 7F, 8, 9N, 11A, 12F, 14, 15F, 17F, 18C, 19F, 23F, 25	Moniarix (SmithKline Beecham) (used from 1986-88 in Belgium)
1983	23-valent CPS	1, 2, 3, 4, 5, 6B, 7F, 8, 9N, 9V, 10A, 11A, 12F, 14, 15B, 17F, 18C, 19A, 19F, 20, 22F, 23F, 33	Pneumovax 23 (Merck & Co., Inc) PNEUMO 23 (Sanofi Pasteur)

It was predicted that PPV would cross-protect against related serotypes in the individual serogroups but this vaccine only provided protection against 70 – 80% pneumococcal infections leaving pneumococcal experts recognizing the need for expanded protection against a wider range of serotypes [31, 32]. Cross-protection was observed for serotype 6B as it showed cross protection against the unstable serotype 6A and therefore 6A was replaced by 6B in the 23-valent PPV [32]. This, however, was not the case between serotypes 19F and 19A as there was no satisfactory cross-protection and therefore both serotypes 19F and 19A were required in the pneumococcal vaccine [33]. The 14-valent

PPV was replaced in 1983 by the 23-valent vaccine (PPV23) which included the serotypes 1, 2, 3, 4, 5, 6B, 7F, 8, 9N, 9V, 10A, 11A, 12F, 14, 15B, 17F, 18C, 19A, 19F, 20, 22F, 23F and 33 thus providing for coverage of more than 85% of adult pneumococcal infections [34, 35]. The pneumococcal serotypes 6B, 9V, and 19A were included in the PPV23 as they were the most frequent cause of invasive drug-resistant disease in the USA.

1.6 Conjugate vaccines

The immune response to PPV23 is highly age-dependent. In infants, immunogenicity is uniformly poor and boosters do not elicit anamnestic responses [36]. Pneumococcal CPS is a T-cell independent immunogen and is not capable of inducing an immune memory effect in children under 2 years of age. At the time of introduction, the PPV23 focussed on IPD in adults but was found to be ineffective in infants younger than 18 months and adults over the age of 60 years [37]. Polysaccharide vaccines are still available and affordable and are used to prevent diseases in older children and adults due to meningococcus and pneumococcus, as this age group continues to be at risk of diseases due to these pathogens [10].

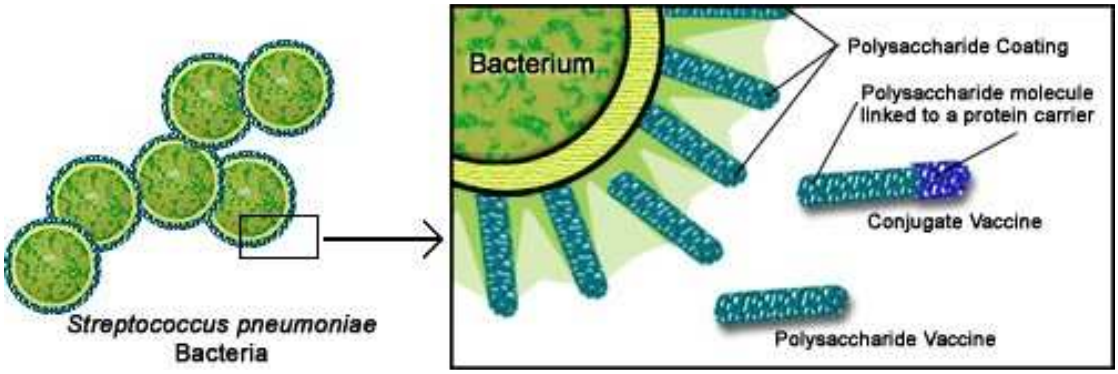

Figure 1.5: This diagram represents the two types of pneumococcal vaccines, the polysaccharide vaccine and the conjugate vaccine [38].

Although PPV23 covers a wide range of serotypes there are several disadvantages to its usage: (1) poorly immunogenic in infants younger than 2 years of age, (2) poorly effective against nonbacteremic or CAP and IPD in older adults (3) may not prevent nasopharyngeal colonization and mucosal infections and (4) antibody levels drop after primary vaccination [39]. To combat these disadvantages, the development of a conjugate vaccine was deemed necessary. While the impact of PPV23 led to the decrease of pneumococcal incidences in adults, it also led to an understanding of the need for a vaccine that would induce a protective immune response in children under the age of 2.

To improve upon the current pneumococcal polysaccharide vaccines, efforts have focused on the development of a second generation vaccine in which the CPS is covalently attached to an immunogenic carrier protein thus rendering the CPS immunogenic in young children (Figure 1.5) [35]. Covalent conjugation of CPS haptens to carrier proteins making them capable of inducing humoral immune responses with the characteristics of T-cell dependent antigens [40].

The first conjugate vaccine was licensed in 1987 against Hib. The success of Hib conjugate vaccines in eliminating Hib among immunized children was a demonstration that this approach was effective [41].

The carrier proteins successfully utilized for the Hib vaccines, namely tetanus toxoid (TT), diphtheria toxoid (DT), the outer membrane protein from Men B and the non-toxic mutant of diphtheria toxin, CRM_{197}, were the initial candidates for the pneumococcal conjugate vaccine [41].

1.7 Pneumococcal conjugate vaccines

The first PCV (PCV7) was licensed in 2000 by Pfizer in the USA (Table 1.2). The introduction of PCV led to an increase in the protective response of all individuals thereby significantly reducing the burden of disease [42]. Three additional PCVs have been developed in the last 15 years (Table 1.2).

Table 1.2: Pneumococcal conjugate vaccines [27].

Year of first licensure	Valency	Carrier protein	Vaccine serotypes	Licensed formulations
2000	PCV7	CRM_{197}	4, 6B, 9V, 14, 18C, 19F, 23F	Prevnar (Pfizer)
Clinical trial use only	PCV9	CRM_{197}	1, 4, 5, 6B, 9V, 14, 18C, 19F, 23F	Not licensed (Pfizer)
2009	PCV10	Protein D (*H. influenzae*), DT & TT	1, 4, 5, 6B, 7F, 9V, 14, 18C, 19F, 23F	Synflorix (GlaxoSmithKline)
2010	PCV13	CRM_{197}	1, 3, 4, 5, 6A, 6B, 7F, 9V, 14, 18C, 19A, 19F, 23F	Prevnar 13 (Pfizer)

The introduction of PCV7 led to an overall decrease in IPD due to vaccine serotypes. The vaccine consisted of seven different serotypes individually conjugated to the cross–reactive material 197 (CRM_{197}) carrier protein, a non-toxic form of diphtheria toxin (DT) that had already been successfully used in Hib as well as meningococcal group C (MenC) vaccines. The seven serotypes used in this vaccine were 4, 6B, 9V, 14, 18C, 19F and 23F which accounted for approximately 86% of bacteremia, 83% of meningitis and 65% of middle ear infections in children under 5 years of age in the USA [43]. A few years later there was an increase in disease caused by serotypes 1, 5 and 19A that were not included in PCV7. The increase in IPD due to serotypes 1 and 5 in the developing countries led to the testing of PCV9 that was never licensed [44]. It did, however, emphasize the need for a pneumococcal vaccine with broader serotype coverage [45]. Around the time PCV9 was tested in South Africa, GlaxoSmithKline (GSK) brought to market PCV10 which included serotypes 1, 5 and 7F [46]. PCV10 increased the serotype coverage against IPD; however, the more prevalent serotypes, namely 19A, was excluded from this vaccine. As 19A was seen to be the cause of IPD in PCV7 areas Pfizer introduced a 13-valent conjugate vaccine (PCV13) in 2010 and included the 13 most common serotypes to cause IPD in children and the elderly globally [47]. Figure 1.6 provides a summary of the development of pneumococcal conjugate vaccines and the increase in valency of serotypes as the increase in IPD due to non-vaccine types became more prevalent [47].

In 2009, South Africa was the first country in Africa to self-finance the introduction of a PCV7 in the Expanded Programme on Immunization (EPI) [6]. Studies conducted in developing countries such as South Africa and Gambia demonstrated that PCV9, PCV7 plus serotypes 1 and 5, had high efficacy in the prevention of most vaccine-serotype disease with 92% in Gambia and 83% among HIV-uninfected children in South Africa [6, 14]. Good efficacy of 65% was also obtained among HIV-infected children in South Africa, as a result of the increase in efficacy of PCV9, an unlicensed product in South Africa.

In May 2011, South Africa introduced PCV13, a conjugate vaccine made up of serotypes 1, 3, 4, 5, 6A, 6B, 7F, 9V, 14, 18C, 19A, 19F, and 23F replacing PCV7.

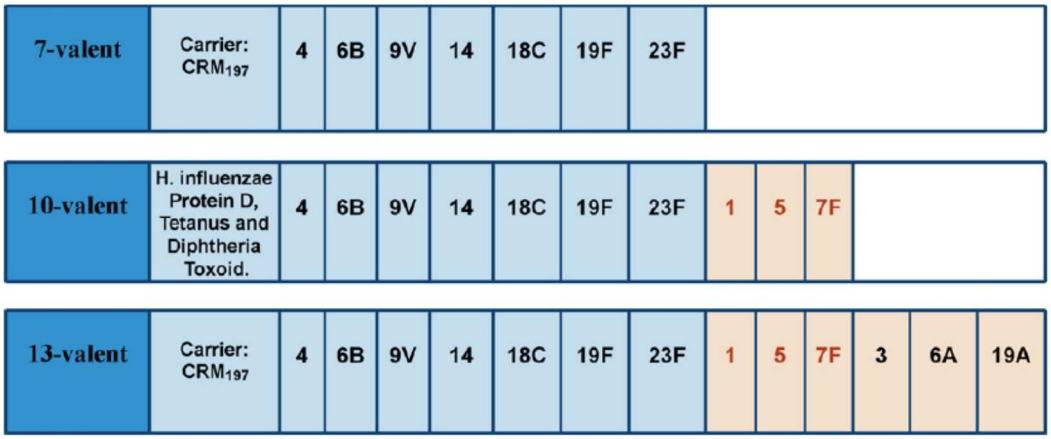

Figure 1.6: Pneumococcal serotypes included in the currently licensed 7-, 10- and 13-valent pneumococcal conjugate vaccines [47].

Data from WHO 2013 (Figure 1.7) shows the global distribution of IPD and the coverage afforded by different vaccine formulations currently available, based on the serotypes included in the vaccines [20].

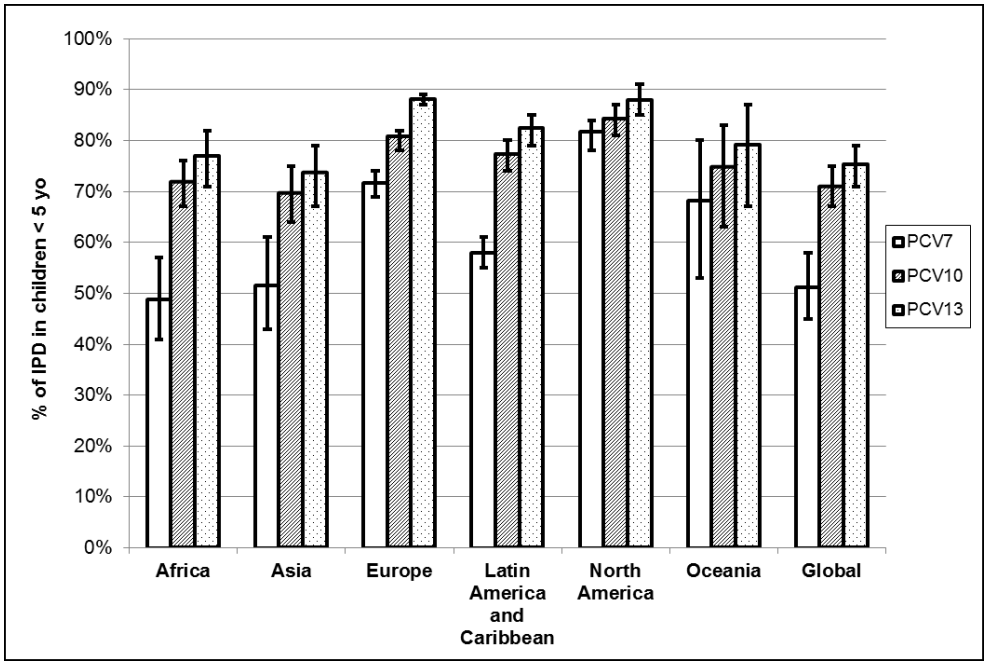

Figure 1.7: IPD represented by serotypes in vaccine formulations among children under 5 years of age [20].

1.8 Serogroup 19

Serogroup 19 pneumococci are among the most common pneumococcal disease causative agents throughout the world [48]. Serogroup 19 (Figure 1.8) consists of four serotypes 19F, 19A, 19B and 19C (equivalent to US types 19, 57, 58 and 59 respectively) [49].

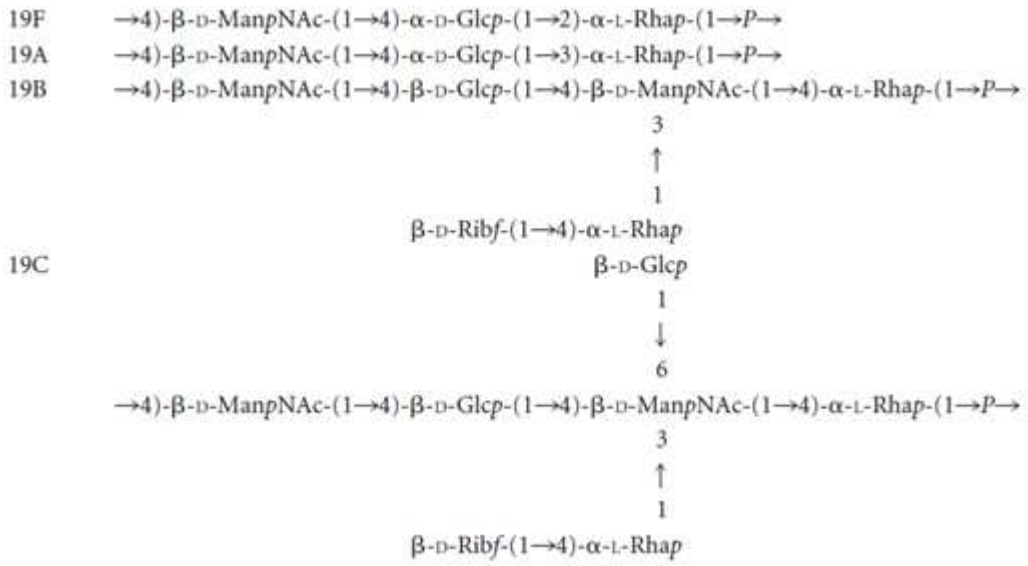

Figure 1.8: Structure of serogroup 19 [39].

Serotypes 19F and 19A account for about 99% of all disease caused by serogroup 19 pneumococci [50]. Studies reported by Beynon et al., (1992) postulated cross-serological protection within serogroups such as 19 (Figure 1.8) because: (1) the trisaccharide repeating unit (RU) of 19F and 19A are almost identical, (2) 19B and 19C share a common hexasaccharide RU and (3) serotypes 19F, 19A, 19B and 19C all contain a phosphodiester backbone in the RU of the CPS which could result in cross-protection in humans [51]. Serotype 19F was predominant among IPD isolates in the USA but similar cases of serotype 19F and 19A accounted for IPD in Denmark [52]. The serotype 19F and 19A monosaccharide components in the RU are identical and composed of L-rhamnose, D-glucose, 2-acetamido-2-deoxy-D-mannose and a phosphate moiety. The only difference between the two CPS is the linkage between the glucose and the rhamnose units: C1→C2 in the case of 19F and C1→C3 in the case of 19A. This difference in the linkage produces a rhamnose hydroxyl group adjacent to the phosphodiester bond in 19A and not 19F resulting in a less stable Pn19A due to facile cyclophosphate formation as observed for serotypes Pn6A but not Pn6B [53].

Serotype 19A is one of the most common serotypes found in children, especially in developing countries. The first 19A strain of *S. pneumoniae* with penicillin resistance was reported in the USA in 1986 [54]. In the pre-vaccine period, serotype 19A was the second leading serotype in children with pneumococcal meningitis in France and the fourth in bacteraemic children younger than 2 years old [55]. This led researchers to believe that infections caused by *S. pneumoniae* serotype 19A resulted in a 'superbug' strain [50]. Serotype 19A has received considerable attention as an important expanding serotype, and strain ST199 has been identified as a major lineage among serotype 19A strains but is also associated with capsule type 15B/C [56]. Among the multidrug-resistant strains, serotype 19A is predominant, especially in pneumococcal disease in Korean infants [57].

Serotype 19A is responsible for a significant proportion of IPD in Europe, with the highest rates reported in Spain (21%), France (16%) and Belgium (9.6%) in children younger than 5 years of age. It was thought that PCV7 containing serotype 19F would provide protection against 19A but instead, there

was an increase in IPD due to serotype 19A after the introduction of PCV7 in the Australia, the USA, and some European countries (Figure 1.9) [12].

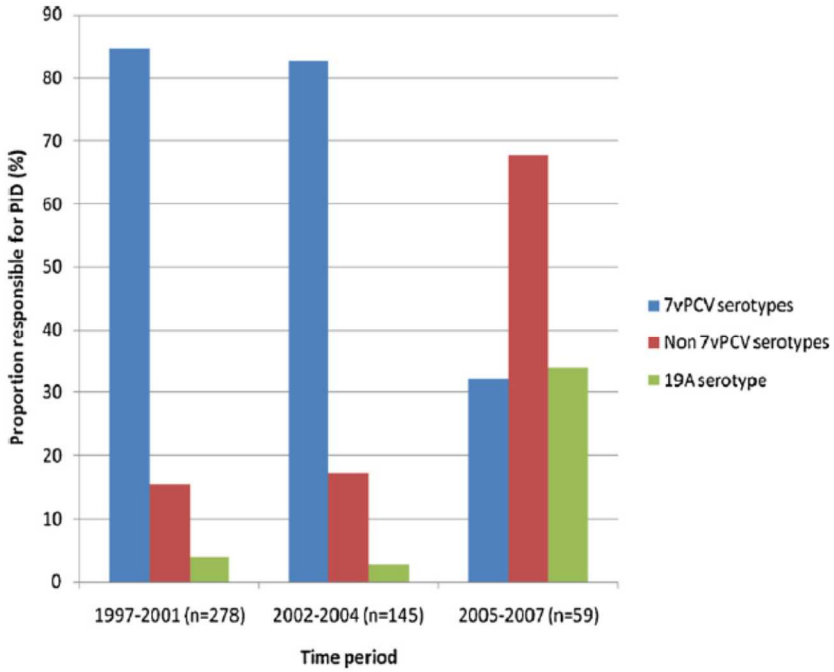

Figure 1.9: Increasing the proportion of IPD caused by non-PCV7 serotypes in Australia in children younger than 2 years of age [12].

Serotype 19A went from being the ninth leading cause of IPD in the USA, prior to the release of PCV7, to the most prominent serotype in 2011 [58]. Of concern, the prevalence of IPD due to penicillin-resistant and often multiple antibiotic resistant 19A isolates increased from 6.7% to 35% in the USA [59]. Figure 1.10 illustrates the increase in Pn19A in children younger than 5 years of age in Australia. Figure 1.11 indicates the rise of the non-PCV7 serotypes with the increase in serotype 19A.

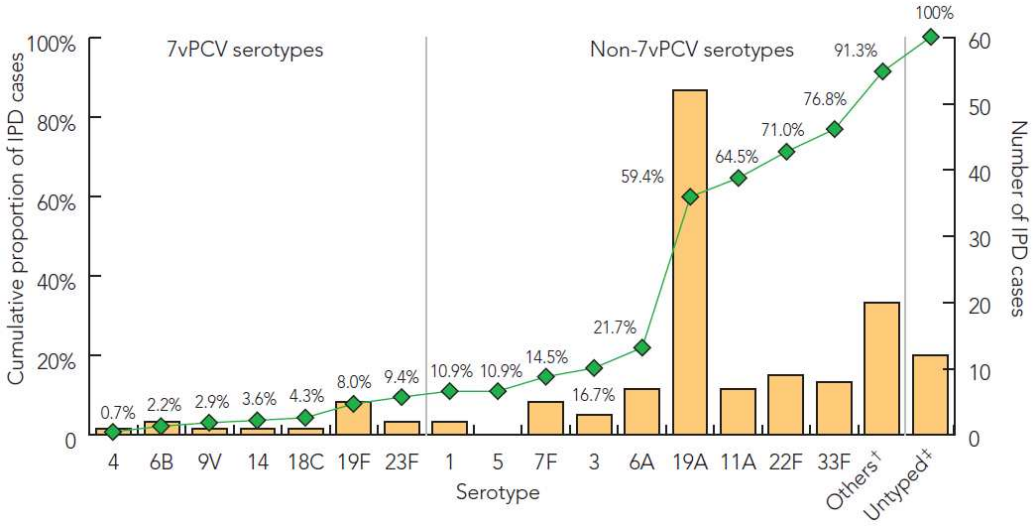

Figure 1.10: Proportion of IPD caused by PCV7 and non-PCV7 serotypes in Australian children younger than 5 years of age in 2007 [19].

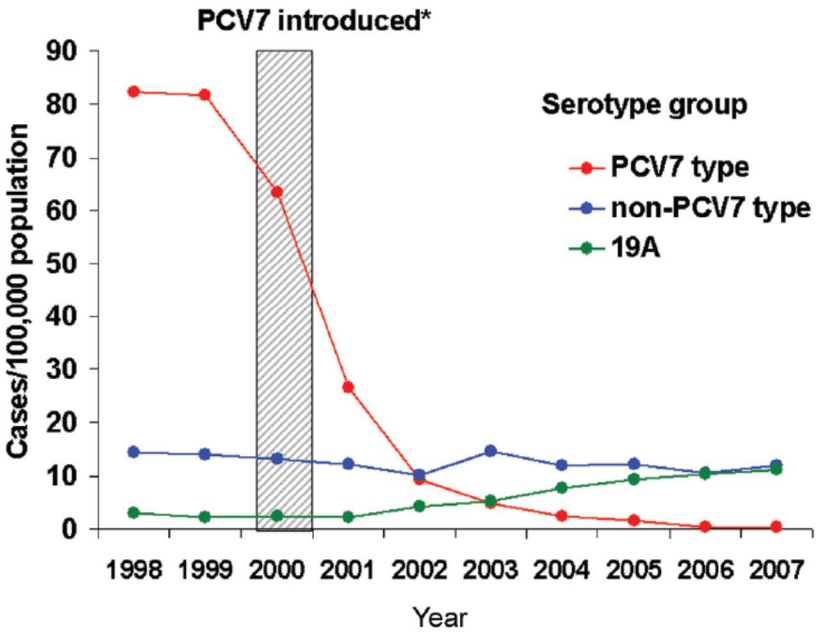

Figure 1.11: Rates of IPD among children aged younger than 5 years, 1998-2007 [45].

Looking at polysaccharide stability, when the hydrolytic stability for Pn6A and Pn6B was compared it was found that Pn6A was significantly less stable than Pn6B, which was attributed to the presence of the hydroxyl group adjacent to the phosphodiester linkage in serotype Pn6A. As Pn6A and Pn6B cross-protect, it was possible to replace Pn6A with the more stable Pn6B in the vaccine formulation [60]. Both Pn19F and Pn19A also contain a phosphodiester bond connecting the repeating units in these polymers. The phosphodiester bond is susceptible to hydrolysis under basic conditions resulting in an unstable linkage with the positioning of C1→C3 in Pn19A making this bond more susceptible to cleavage when compared to Pn19F [53]. As a result, Pn19A is considered less stable than Pn19F. However, cross-protection has not been shown between Pn19F and Pn19A so both would need to be included in the vaccine [61].

Hanage et al. [62] in 2007 described a phenomenon known as 'serotype replacement' which included a niche for an increase in IPD due to specific non-vaccine types. The primary contributor to this phenomenon was serotype 19A which colonized in the nasopharynx and caused AOM. A study reported in South Korea by Choi et al. [52] (2008), however, showed that there was an increase of 19A before the introduction of PCV7, a result of the expansion of a multidrug-resistant clone (ST320). According to Moore [63] (2008), the ineffectiveness of PCV7 against serotype 19A, antibiotic resistance, clonal expansion and emergence, and capsular switching contributed to the genetic diversity of 19A and to its emergence as the predominant invasive pneumococcal serotype in the USA.

1.9 Manufacturing of bulk conjugates

There are physical and chemical variables that need to be considered when preparing a PCV. These include (1) size of CPS, (2) chemistry for activation of CPS, (3) choice of carrier protein, (4) CPS-protein conjugation chemistry and (5) the ratio of CPS to protein [64]. The general processes in the manufacture of a conjugate vaccine involves multiple steps as shown in Figure 1.12.

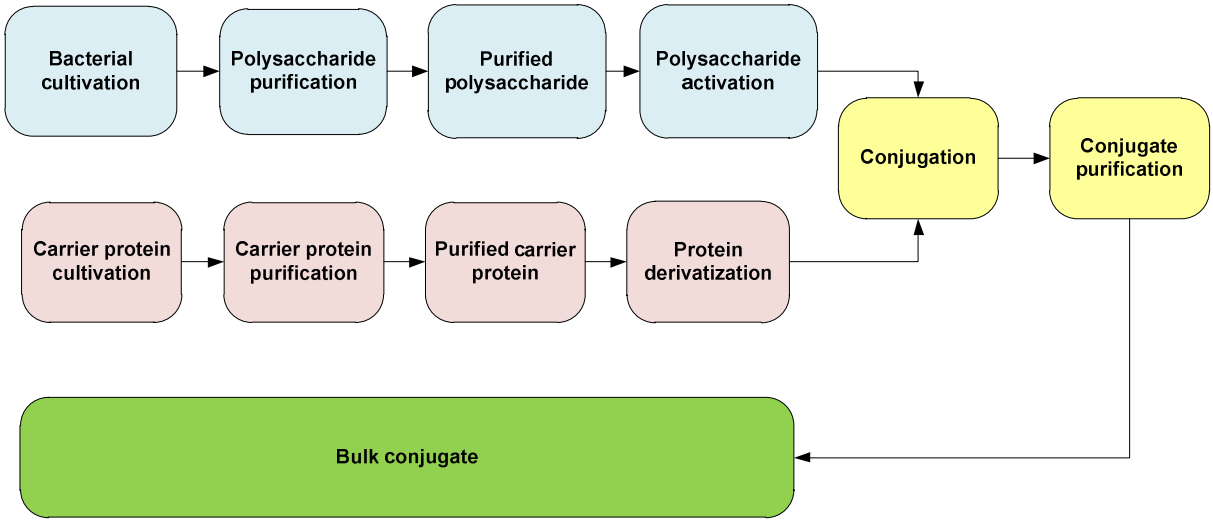

Figure 1.12: Representation of the manufacturing process of a bulk conjugate.

The development of a high polysaccharide producing strain within each serotype involves isolate and clonal selection, media selection, inoculum train development and preparation of seed lots for fermentations. These processes were based on work developed and optimized using serotype 1 (Pn1) and performed on serotype 19A as it was shown to perform similarly in terms of growth, nutritional requirements, polysaccharide production and other downstream processes discussed in this study.

The pneumococcal bacteria have been cultivated using traditional stainless steel stirred tank fermenters and bioreactors. A newer convenient approach using disposable bag technology first discussed and presented by Singh in 1999 was used during this study [65-67]. The polysaccharide purification process developed for polyribosylribitol phosphate (PRP) produced from the *Haemophilus influenzae* type b (Hib) was followed in this study. This method included the precipitation of the CPS using cetyl trimethylammonium bromide (CTAB), alcohol fractionation with the aid of a filter aid (celite) and finally diafiltration.

Conjugation of the CPS to the protein involved size reduction of the CPS, activation of the CPS, derivatization of the protein carrier, conjugation of the activated CPS to the protein carrier followed by purification of the conjugate to remove reagents and unconjugated components. Figure 1.13 shows four approaches that can be utilized to activate the polysaccharide in order to covalently link it to a carrier protein. The first three approaches utilize CPS produced from bacteria, either full-length or size-reduced, while the fourth approach makes use of polysaccharide produced synthetically. These approaches include: (i) random activation of CPS, (ii) bi-terminal activation with or without subsequent depolymerization, (iii) terminal activation with or without subsequent depolymerization and (iv) terminal activation of synthetically produced polysaccharide. Approach (i) using size-reduced CPS was utilized during this project [68]. During the activation of CPS, the integrity of the CPS must remain such that the antigen immunogenicity is retained [64]. The polysaccharide and conjugate must be well characterized both chemically and immunologically and the specifications must meet WHO Technical Series Report 927 (WHO TRS).

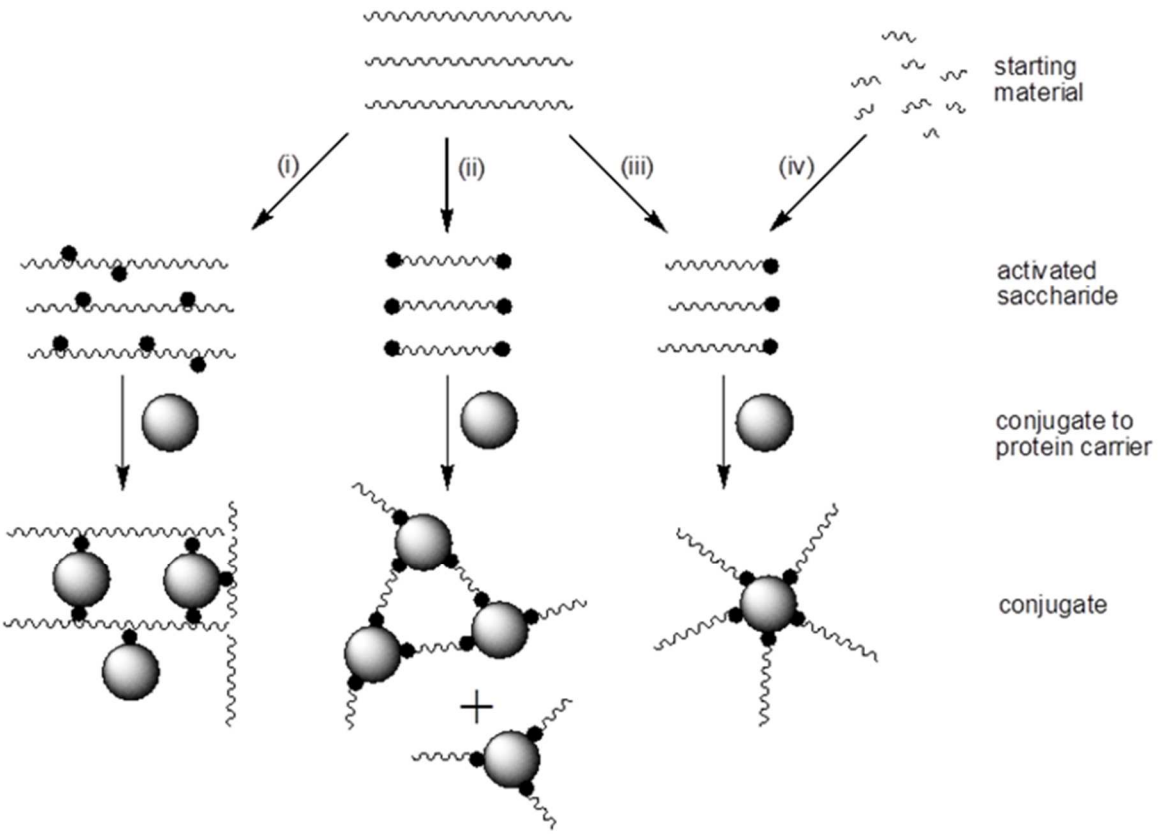

Figure 1.13: Production of conjugate vaccines. There are four approaches for the production of conjugate vaccines; (i) random activation of CPS, (ii) bi-terminal activation with or without depolymerisation, (iii) terminal activation with or without depolymerisation and (iv) terminal activation of synthetically produced polysaccharide [68].

1.10 Aims and objectives

The purpose of this study was to develop a process for the manufacture of Pn19A CPS as a proof of concept study, based on Pn1 process optimization studies due to the unavailability of Pn19A at the time the study was performed. Following this, the conjugation of Pn19F and Pn19A CPS to a carrier protein was investigated as well as the stability of these bulk conjugates in liquid form.

This study investigated the clonal selection, isolation, cultivation, purification, and characterization of the CPS from *S. pneumoniae* serotype 19A. The aim was to determine if *S. pneumoniae* serotype 19A CPS could be cultivated and harvested using disposable bag technology. The Pn19A CPS produced was conjugated to a carrier protein. Pn19F obtained from Chengdu Institute of Biological Products (CDIBP) based in China was also conjugated to a carrier protein. The structurally similar Pn19F and Pn19A CPS were compared during a characterization, conjugation and stability study. Cyanylation chemistry was the conjugation chemistry method of choice for the negatively charged Pn19F and Pn19A CPS.

In order to achieve this aim, the specific objectives of this study were:

i. To obtain an appropriate clone and screen for the isolation and production of *S. pneumoniae* serotype 19A CPS.
ii. Development of medium for the cultivation of *S. pneumoniae* serotype 19A using disposable bag technology.

iii. Purification of the polysaccharide using a modified method of differential filtration with ethanol.
iv. To establish characterization assays for the CPS based on WHO specifications including identity, purity, composition and size analysis.
v. To perform detailed structural characterization of purified 19A polysaccharide using a range of physiochemical methods and comparing it to 19F polysaccharide.
vi. To investigate the conjugation of Pn19A CPS to a suitable carrier protein using CDAP chemistry.
vii. To evaluate the thermal stability of Pn19F (control) and Pn19A (test) conjugates in an accelerated study.

CHAPTER 2. GENERAL METHODS

The outline shown in Figure 2.1 shows the processes and analytical methods utilized during the preparation of conjugates Pn19F and Pn19A. This chapter outlines the following processes and methods based on work performed on Pn1 as Pn19A was unavailable at the time that this study was conducted:

- Cultivation of bacteria, purification of CPS, size-reduction of CPS, protein derivatization, conjugation and conjugate purification.
- Microbiological and immunological techniques used to identify the bacteria and quantify the CPS produced from the bacteria during clonal selection.
- Microbiological, immunological and chemical assays during cultivation to quantify bacterial growth and CPS production.
- In-process chemical assay to monitor CPS elution during purification.
- Chemical and bio-analytical techniques used to analyze purified capsular polysaccharide (CPS).
- Chemical, immunological and bio-analytical assays to track the conjugation process and to analyze the purified conjugate bulk.

More detail on the fermentation, purification and conjugation methodologies are provided in Chapters 3, 4 and 6.

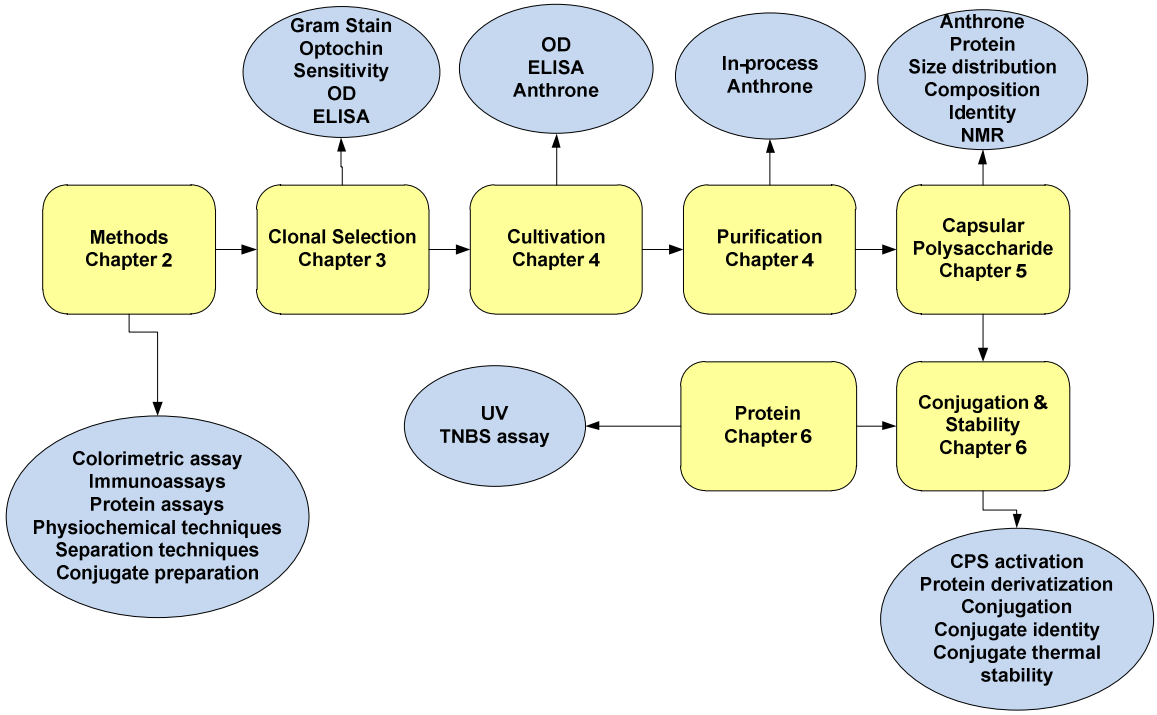

Figure 2.1: Procedure used in the analysis of a bulk conjugate vaccine.

2.1 Microbiological identification tests

Microbiological identity tests include colony morphology, Gram stain, hemolysis, quellung and optochin sensitivity [8]. The expected results for these assays are summarized in Table 2.1. The National Institute of Communicable Diseases (NICD) provided 13 clinical isolates of *S. pneumoniae* that were screened for identity and suitability for CPS production. The strains provided were isolated in 2009 from HIV

negative individuals who suffered from pneumococcal infections caused by serotype 19A. The NICD performed Multilocus sequence typing (MLST) to identify the pneumococcal serotype.

Table 2.1: Phenotypic identity tests for *Streptococcus pneumoniae* used during this investigation**.**

	Gram stain	Quellung	Optochin sensitivity	Hemolysis	Growth
Streptococcus pneumoniae	Positive	Halo	Sensitive	Alpha	36 – 37 ºC

2.1.1 Colony morphology

Phenotypic variation is an important mechanism that allows bacterial pathogens to adapt to different environmental niches. For *S. pneumoniae* the phenotypic variation can be observed through changes in the colony opacity. There are two variations: transparent and opaque. The opaque colonies of the bacteria are highly encapsulated compared to bacteria in the transparent colonies [69]. An opaque colony was selected using a sterile disposable inoculating loop and gently placed into liquid culture for further analysis. These opaque colonies were selected as part of the clonal and isolate selection process described in Chapter 3.

2.1.2 Gram stain

Gram staining is a technique that separates bacteria into two groups; Gram-positive and Gram-negative, based on their ability to retain crystal violet dye upon treatment with an organic solvent such as ethanol [70].

A loopful of culture broth was placed onto a labeled glass slide and the bacteria were heat-fixed. Once the slide was cool and dry, the slide was stained with crystal violet for 1 min and then rinsed with de-ionised water. Iodine solution was added for 1 min and the slide was subsequently rinsed with water. Ethanol (95%) was added for 10 seconds and immediately rinsed with water and finally, Safranin (counterstain, Merck) was added for 20 seconds. The slide was rinsed with water, blot-dried and viewed using oil-immersion under a microscope (Olympus cx31). Figure 2.2 shows a summary of the Gram stain procedure [71]. Gram-positive bacteria, such as *S. pneumoniae*, stain dark purple due to retention or uptake of crystal violet by the cell wall.

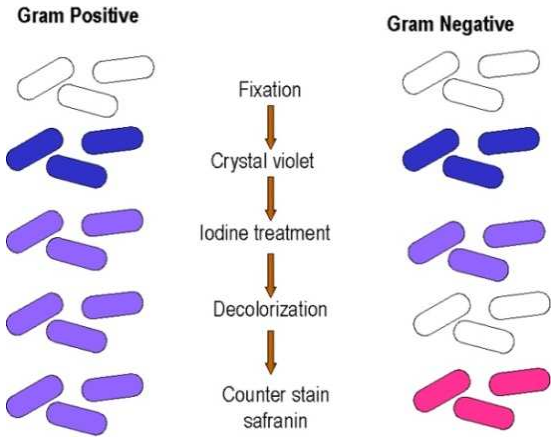

Figure 2.2: Colour changes that occur at each step in the Gram staining process [71].

2.1.3 Quellung reaction

The Quellung reaction or serotyping is a method used to differentiate between strains or serotypes of bacteria that differ in antigenic composition. Quellung is the increase in the swelling of the capsule of the bacteria in the presence of antibodies against capsular antigens. In the Quellung reaction, a cell suspension was prepared in 0.5 mL physiological saline from a blood agar plate (BAP) or broth to the equivalent of a 0.5 McFarland density standard. MacFarland density standards are a measure of the turbidity of bacterial suspension within a given range. The cell suspension (10 µL) was dispensed onto a microscopic slide and the same volume of typing serum for Pn19A CPS (Davies Diagnostics, lot no. K19c21 B1), containing 1% methylene blue was applied to the cell suspension. The slide was covered and placed in a petri dish to prevent dehydration and incubated at 20 – 25 ºC for 30 min. A negative control with non-specific rabbit serum (Davies Diagnostics) was included. After incubation, the slide was gently pressed to create a thin film and examined microscopically using the oil immersion lens (x100). The swelling of the capsule or halo surrounding the organisms and the clumping of the bacteria are indicative of a positive result.

2.1.4 Optochin sensitivity test

Optochin or ethylhydrocupreine is an antibiotic that is used in cell culture to interfere with adenosine triphosphate (ATP) and ATPase (enzyme) production in susceptible bacteria such as *S. pneumoniae,* and serves as a presumptive identification test for *S. pneumoniae* [70, 72]. An optochin disk (Davies Diagnostics, cat no. MAS-IDDS-D42) was placed on a BAP, incubated at 35 – 37 ºC for 18 – 24 h in 5% CO_2 and examined for a zone of inhibition around the disk. Inhibition of bacterial growth is one of the indicators of the presence of *S. pneumoniae.*

2.1.5 Alpha hemolytic activity

One of the characteristics of *S. pneumoniae* is alpha hemolysis which is the incomplete lysis of red blood cells which results in the formation of a greenish zone around a bacterial colony growing on blood agar [21]. The test involved inoculating BAP with the bacteria and incubating the plates at 37 ºC for 24 h.

2.2 Cultivation of Pn19A

In summary, clinical isolates were obtained from the National Institute of Communicable Diseases (NICD) and used to establish a laboratory master seed (LMS) and a laboratory working seed (LWS) for the production of *S. pneumoniae* serotype 19A (Pn19A) CPS. Cultivations were performed in a Wave bioreactor using disposable single-use bag technology, as presented in Figure 2.3 (explained in Chapters 3 and 4). The LWS (1 mL) was used to inoculate a 20 mL starting culture medium. After a further 3 passages, the Wave bioreactor was inoculated. On completion of cultivation, the culture was chemically inactivated and clarified before purification of the polysaccharide.

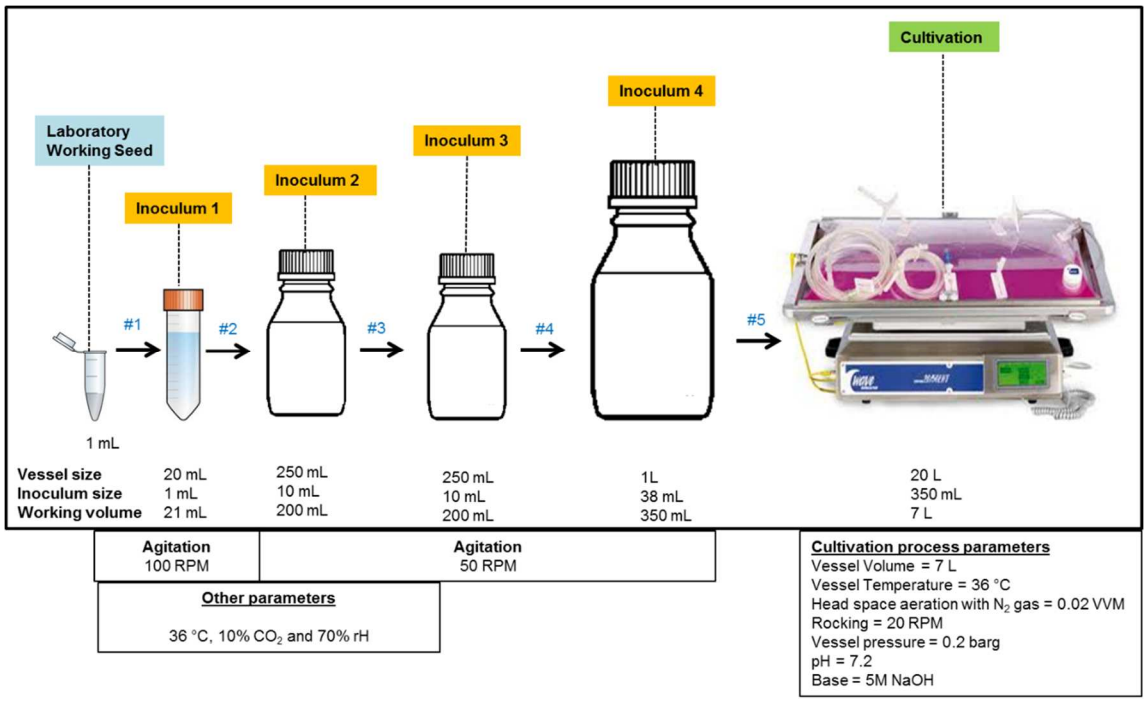

Figure 2.3: Process flow diagram outlining the stages during the fermentation of a single batch culture of Pn19A.

2.3 Cultivation media

2.3.1 Culture medium

Culture media for growth of *S. pneumoniae* is an important aspect of bacterial cultivation because it defines whether or not it will lead to optimal CPS production [65]. The culture media components of animal origin are preferred for *S. pneumoniae* growth but if used in a manufacturing process and not adequately removed may cause serious diseases such as prions, viruses, and mycoplasma. In addition to animal products, culture media should not contain any substances that have the possibility of inducing a pronounced allergic reaction in humans such as antibiotics. As such, non-animal media devoid of allergy-inducing components were investigated. All media components were either prepared in a biosafety cabinet (BSC) or autoclaved post-preparation to ensure sterility.

2.3.1.1 Liquid medium

S. pneumoniae is nutritionally fastidious and requires a defined medium for optimal growth [26]. Hoeprich's media, with modifications, was used for the cultivation of this facultative anaerobe. The Hoeprich's media used during this study was adapted from Gonçalves et al., (2002) and Hoeprich, (1957) [26, 73]. The modified Hoeprich's media consists of yeast extract, select soytone, glucose, magnesium sulfate ($MgSO_4$), Hoeprich's amino acids, Hoeprich's salts, Hoeprich's acids (thioglycolic acid and hydrochloric acid (HCl)) and catalase. The media components were prepared in purified water and the pH of the solution was adjusted to pH 7.2. The Hoeprich's media was stored at 2 – 8 ºC for up to 2 months.

2.3.1.2 Solid (agar) medium

Hoeprich's agar has the same media components as Hoeprich's liquid medium at the same concentrations with the addition of 20 g/L agar. The formulation of the components upon mixing was a

modification of the liquid form of the media. The agar was mixed with the Hoeprich's salts and purified water and placed in the autoclave for 30 min on a liquid cycle at 121 ºC. After autoclaving, the liquid agar was stored at 65 ºC to keep from solidifying. Glucose, yeast extract, select soytone, $MgSO_4$ and Hoeprich's acids (thioglycolic acid and HCl) were warmed to 65 ºC in a static incubator then added to the agar. The Hoeprich's amino acids were warmed to 37 ºC using the same method and also added to the agar. The solution was mixed gently in order to prevent bubble formation before being poured into 90 mm plastic sterile Petri dishes using approximately 15 mL per dish. The agar mixing and plate pouring were performed in the BSC to ensure sterility. When the plates were cool, the lids were fitted and the plates were placed in a plastic bag and stored at 2 – 8 ºC. Catalase was spread onto the Hoeprich's agar plates prior to use.

2.4 Purification of Pn19A CPS

After cultivation of *S. pneumoniae*, the Pn19A CPS isolated was purified to meet WHO specifications [65]. The process flow depicted in Figure 2.4 involves centrifugation of the fermentation broth, addition of celite and CTAB to the supernatant, packing of the celite slurry in a chromatography column, washing of the slurry to remove the fermentation media and selective elution of the polysaccharide using varying concentration of alcohol. The soluble polysaccharide was precipitated, collected through centrifugation diafiltered and lyophilized.

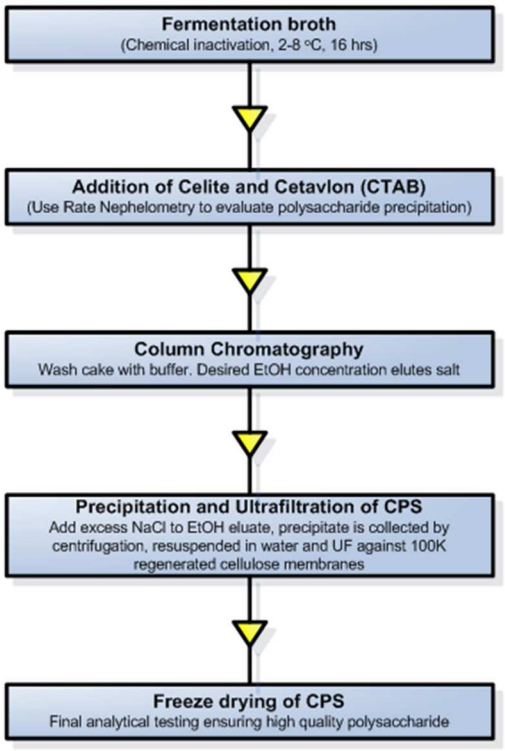

Figure 2.4: Overview of the process flow of purification of the polysaccharide.

2.5 Colorimetric assays

Colorimetric assays are employed to determine the concentration of an analyte by the generation of a chromophore in a solution that allows for absorption in the ultraviolet/visible (UV/Vis) region of the spectrum. For polysaccharides, these assays have been established by heating aqueous solutions of polysaccharides with strong acids converting them to furfurals or derivatives of furfurals. A color is then

produced by the addition of an organic developer such as phenol, cysteine.HCl or *p*–dimethylamino benzaldehyde (DMAB). According to WHO TRS 927, recommendations are provided on compositional assays in order to ascertain identity and purity [74].

Table 2.2: Testing conducted on the components found in the CPS and CPS-protein conjugates.

Components	CPS	Conjugate
CPS	x	x
Protein	x	x
Nucleic Acid	x	-
Phosphorus	x	x
Nitrogen	x	-

In order to determine the concentration of the various components listed in Table 2.2, the following assays were employed: methyl pentose [75], hexosamine [76] and anthrone [77] for determination of saccharide content and Bradford, BCA and/or micro-BCA for determination of protein content [78]. Other compositional assays for quantification of phosphorus, nucleic acid and hydrazides were also performed. All absorbance measurements were performed on a Shimadzu UV-Vis 1700 Spectrophotometer with UV Probe 2.2.1 software.

2.5.1 Methyl pentose assay

This is a spectrophotometric method used for the detection and quantification of methyl pentoses and specifically the identity of rhamnose. The estimation of the rhamnose monosaccharide is used to measure the concentration of pentoses in polysaccharides containing pentoses other than ribose [79]. The mechanism as shown in Figure 2.5 involves the conversion of polysaccharides into a furfural intermediate upon reaction with concentrated acid and a subsequent color formation upon reaction with cysteine hydrochloride.

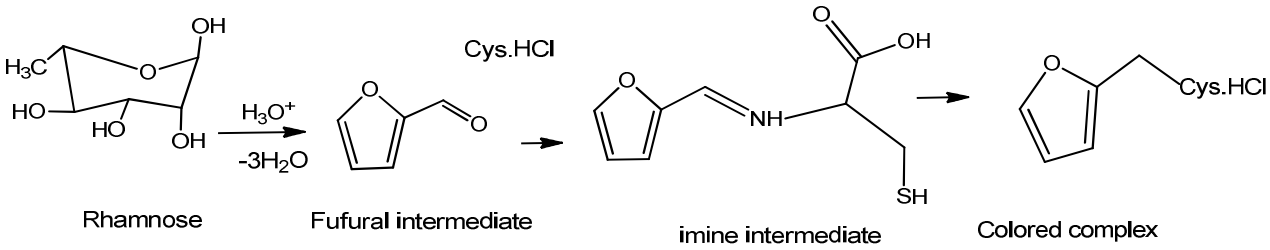

Figure 2.5: The mechanism of methyl pentose assay shows the formation of a furfural intermediate with the CPS in the presence of an acid and a color change from colorless to pale yellow complexation upon reaction with cysteine.hydrochloride [75].

The polysaccharide (Pn19A or Pn19F CPS), standards (rhamnose) and the gold standard (Pn19F or Pn6B CPS) (10 – 50 µg/mL) were hydrolyzed by the addition of 0.9 mL H_2SO_4 for 10 min at 100 ºC. The tubes were left to cool and 20 µL of cysteine hydrochloride (Cys.HCl) was added and the reaction left to develop in the dark for 90 minutes at 20 - 25 ºC. The absorbance was read at these 396 nm (maximum absorption for methyl pentose) and 430 nm (maximum absorption for hexoses) and the difference calculated which corrects for polysaccharides that have a negligible contribution such as pentoses, hexoses, hexuronic acids and 2-deoxyribose [75, 77].

2.5.2 Hexosamine assay

Determination of the hexosamine content present in the repeating units of polysaccharides, such as mannosamine in the case of Pn19A, was achieved using the hexosamine assay [76, 80]. This assay was not used to quantify the CPS but merely to indicate the presence of an *N*-acetylated component as per the TRS [74]. The mechanism, shown in Figure 2.6, required a two-step process to obtain a colored complex. Firstly hydrolysis and neutralization of the polysaccharides cleaved the glycosidic linkages and released the hexosamines which were then condensed with alkaline acetylacetone and DMAB.

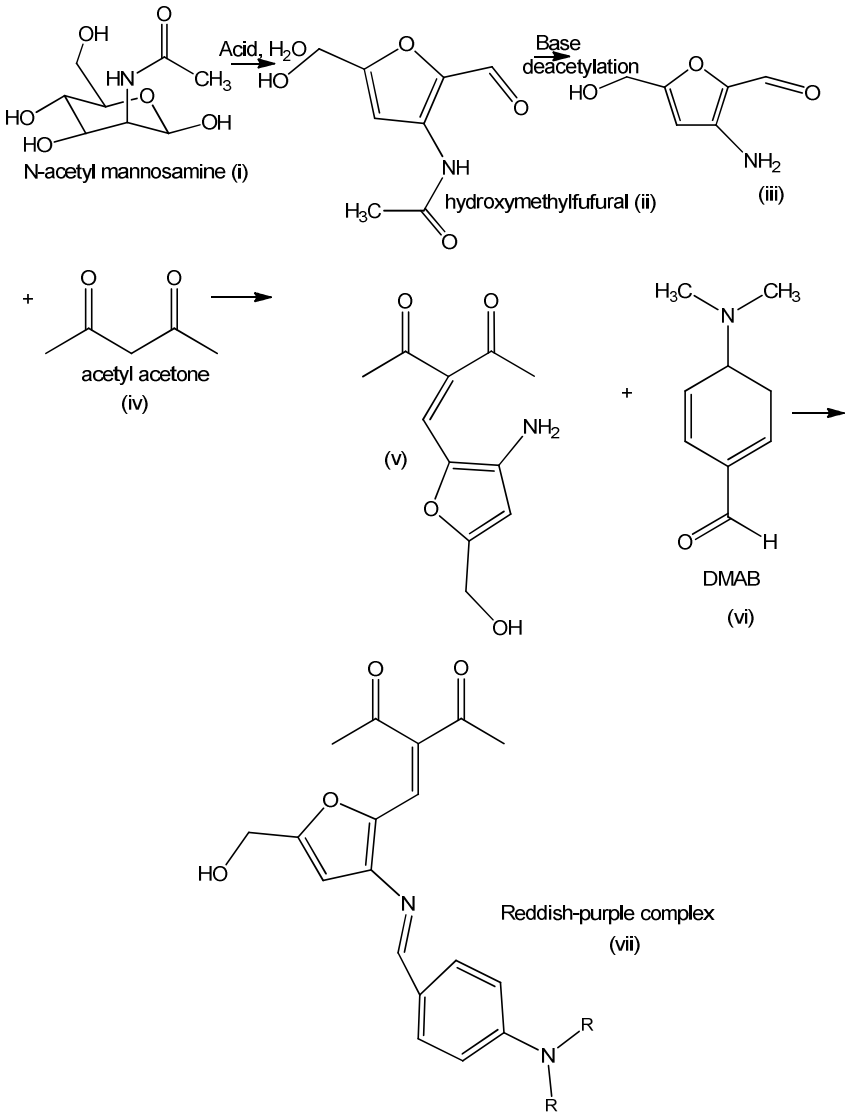

Figure 2.6: The mechanism for the hexosamine assay shows the formation a hydroxyl furfural intermediate upon hydrolysis with CPS and then a color complex upon reaction with DMAB to form a reddish-purple product [80]. R refers to methyl groups present on DMAB.

The samples (Pn19A CPS), standard (glucosamine hydrochloride) and gold standards (Pn19F, 100 - 500 µg/mL) were placed in hydrolysis tubes, 0.5 mL of 10 M HCl was added and the tubes incubated at 100 ºC for 10 min (standards) and 2 h (polysaccharides). All samples were cooled and 0.25 mL thymolphthalein added. NaOH (5 M) was added dropwise until the sample turned blue in color. HCl (1 M) was subsequently added dropwise until the solution went colorless. The neutralized samples were

diluted to 5 mL with water followed by the addition of 0.5 mL cold acetylacetone. The samples were concentrated by incubating the hydrolysis tubes at 100 ºC for 45 min and left to cool. 1.25 mL of 96% ethanol and 0.5 mL cold DMAB solution was added slowly and the volume was adjusted with 96% ethanol to give a final volume of 5 mL. The tubes were capped and incubated in the dark at room temperature (20 - 25 ℃) for 90 min. Absorbance was read at a wavelength of 530 nm.

2.5.3 Phosphorus assay

Samples were mineralized by heating with a sulfuric/perchloric acid mixture and the resultant inorganic phosphate was complexed with ammonium molybdate. Reduction of this phosphomolybdate complex by ascorbic acid resulted in a characteristic blue-coloured solution, detected using a spectrophotometer at a wavelength of 825 nm as described by Chen [81]. The samples (30 µg/mL phosphorus ~ 0.68 mg/mL Pn19A CPS), standards (7.5 – 60 µg/mL phosphorus – sodium hydrogen phosphate (Na_2HPO_4) used as reference standard) and gold standard (22 µg/mL phosphorus ~ 0.5 mg/mL Pn19F CPS) were mineralized by the addition of 100 µL sulfuric/perchloric acid (ratio 1:1) and incubated at 250 ºC for 1 h. This was followed by the addition of 3.9 mL water and 4 mL of a5 M sulfuric acid/ 2.5% ammonium molybdate/ 10% ascorbic acid mixture. Tubes were vortexed and incubated at 37 ºC for 2 h. The samples were cooled to room temperature and absorbance read at a wavelength of 825 nm.

2.5.4 Anthrone assay

The anthrone assay is used to measure the concentration of polysaccharides that contain neutral hexoses such as glucose, and methyl pentoses such as rhamnose [77, 82, 83]. No specifications for this assay are indicated in the TRS but the assay is rather used for the in-process tracking of polysaccharide content [84]. The mechanism, as shown in Figure 2.7, involves the conversion of polysaccharides into furfuraldehyde upon addition of sulfuric acid. Anthrone reacts by condensing with the carbohydrate furfural derivative to give a color complex. The intensity of the color produced by glucose is proportional to the amount of glucose present in the solution. In contrast, pentoses such as rhamnose are less sensitive thus resulting in a less intense color.

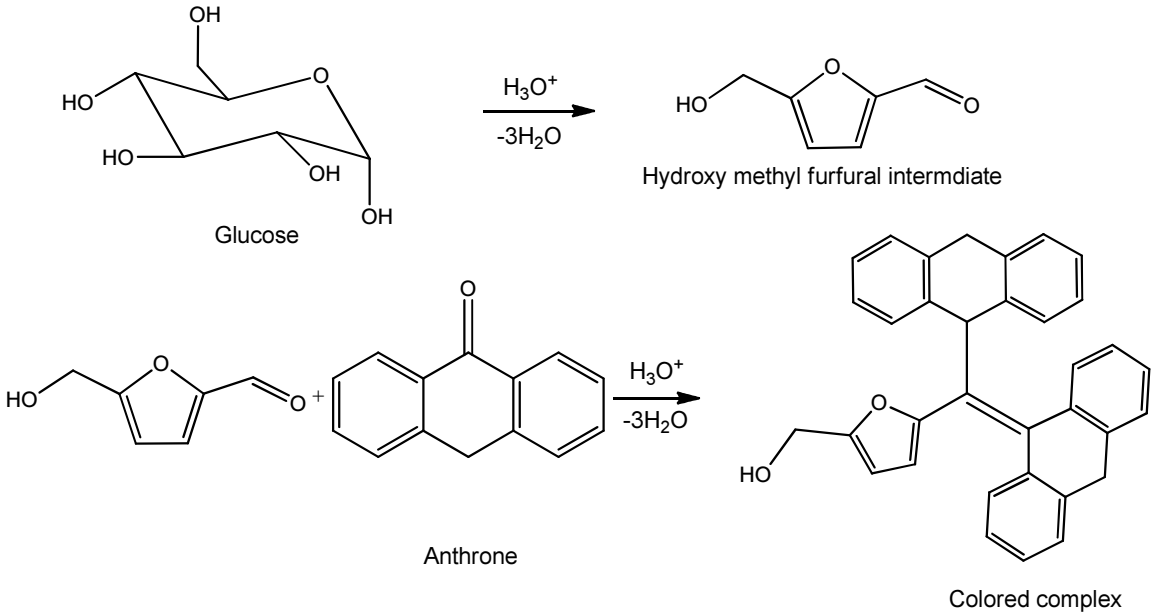

Figure 2.7: The mechanism of the anthrone assay shows the formation of a hydroxyl methyl furfural intermediate with CPS in the presence of anthrone-sulfuric acid solution. The colored complex product changes from yellow to green upon reaction.

The polysaccharides (Pn19A CPS), standards (glucose) and gold standards (Pn19F or Pn6B) (5 - 40 µg/mL) were placed in hydrolysis tubes and 1 mL of 2 mg/mL anthrone-sulfuric acid solution was added. The tubes were capped and placed at 100 ºC for 16 min. Standards and samples were cooled and the absorbance was read at a wavelength of 625 nm. A color change from yellow to green indicated the presence of neutral hexoses [77]. The color intensity for rhamnose was very low and hence the preferred assay for the determination of rhamnose was the methyl pentose assay.

2.6 Protein assays

Protein assays were performed in order to determine (1) the trace amounts of protein contamination present in the purified polysaccharides, (2) the protein concentration of the derivatized carrier protein and (3) the protein concentration of the carrier protein in the conjugated protein. Spectrophotometric assays include UV absorbance methods and dye-binding assays which use colorimetric and fluorescent-based detection. Examples include the bicinchoninic acid (BCA) and Bradford assays provided by Thermo Scientific Pierce protein kit [78].

2.6.1 UV spectrophotometric protein assay

Proteins display a characteristic ultraviolet (UV) absorption band near 280 nm predominantly due to the presence of the aromatic amino acids tyrosine (Tyr) and tryptophan (Trp) [85]. The UV method was employed to determine tetanus toxoid (TT) concentration before and after derivatization. A sample of TT was diluted 1: 50 before being transferred to a quartz cuvette and the absorbance read at 279 nm, with a path length of 1 cm. In order to calculate the concentration of protein present the Beer-Lambert law was applied:

$$A=\varepsilon cl$$

where ε is 185210 M/cm (molar extinction coefficient of TT), c the concentration of the analyte and l the path length in cm [86].

2.6.2 BCA assay

The BCA assay was first described by Smith et al., in 1985. It is based on and exploits the presence of peptide bonds within the protein to reduce Cu^{2+} to Cu^{+} under alkaline conditions [87]. The Cu^{+} is then detected with BCA reagent. The complex formed results in the development of an intense purple color with an absorbance maximum at 562 nm [87]. The 0.1 mL of standard (concentration range of 20 - 2000 µg/mL of Bovine serum albumin (BSA)) or sample was mixed with 2 mL of working reagent (BCA assay kit – Thermo Scientific) and incubated at 37 ºC for 30 min. Absorbance was read at a wavelength of 562 nm.

2.6.3 Micro-BCA assay

The assay principle is as per the BCA assay except the concentration range of the micro-BCA assay is between 0.5 - 20 µg/mL thus allowing for the measurement of low concentrations of the protein [78]. The 1 mL of standard (concentrations of 0.5 – 20 µg/mL) or sample was mixed with 1 mL of working reagent and incubated at 60 ºC for 1h. Absorbance was read at 562 nm.

2.6.4 Bradford (Coomassie) assay

The Bradford colorimetric method is based on an absorbance shift following the binding of Coomassie Brilliant Blue G-250 to a protein in an acidic medium. The development of color from brown to blue in Coomassie dye-based (Bradford) protein assays due to protonation of the dye has been associated with the presence of certain basic amino acids (primarily arginine, lysine, and histidine) in the protein [88]. Van der Waals forces and hydrophobic interactions also participate in the binding of the dye to the protein [88]. A 30 µL standard (concentration range of 100 - 1500 µg/mL of BSA) or sample was mixed with 1.5 mL of the Coomassie reagent and incubated at room temperature for 30 min. Absorbance was read at a wavelength of 595 nm.

2.7 Other characterization assays

2.7.1 Nucleic acid assay

The purpose of this test was to determine the nucleic acid content of purified CPS. The European Pharmacopoeia method for nucleic acids in polysaccharide vaccines was used as the reference method [89]. Nucleic acid concentration was determined by measuring the absorbance of the polysaccharide solution at 260 nm (A260). Samples were diluted in water to obtain a polysaccharide concentration of approximately 2 mg/mL and placed in quartz cuvettes. The absorbance was read at a wavelength of 260 nm (A260). Nucleic acid concentration was calculated in mg/mL using the following formula:

$$\text{Nucleic acid (mg/mL)} = ([\text{A260} \times \text{dilution factor}] / 20).$$

2.8 Immunoassays

2.8.1 Enzyme-linked immunosorbent assay (ELISA)

The ELISA is a very sensitive technique for detection and measurement of antigens or antibodies in solution. The assay combines the specificity of antibodies with the sensitivity of simple enzyme assays, by coupling antibodies or antigens into an easily assayable enzyme. The competition ELISA, used in this study, is based on the principle that the combination of an unknown amount of analyte introduced from the sample and the reference analyte compete for binding to a limited number of antibody binding sites (Figure 2.8). An inverse correlation between ELISA response and concentration of the analyte can be observed. This type of ELISA is applicable for quantifying antigens in complex matrixes [90, 91].

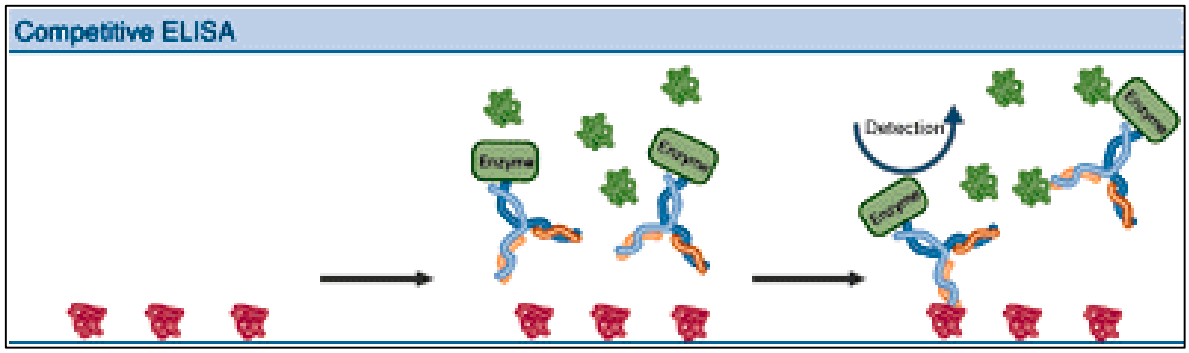

Figure 2.8: Schematic representation of the competition ELISA [92].

Table 2.3: Reagents used in competition ELISA experiments.

Primary antibody and CPS	
	Dilution
Pn19A CPS reference standard (ATCC)	1:100
Pn19A antiserum (SSI)	1: 32000
Secondary antibody	
Goat anti-rabbit HRP conjugate	1:4000 (45 min at RT)

Table 2.3 shows the reagents used in the competition ELISA experiments. A known concentration of Pn19A was used as the reference analyte or standard. The 96-well plates were coated with Pn19A CPS immobilized antigen working reagent (1.5 µg/mL in PBS), covered with plate film and incubated statically for 16 h at 2 – 8 ºC. The plates were washed with the wash solution (PBS 0.03% Tween mix) to remove excess antigen. The wells were covered with blocking solution (3% (w/v) BSA in PBS) and the plates covered with plate film and incubated for 1.5 h at 20 - 25 ºC with shaking at 190 RPM on an orbital shaker. Thereafter, plates were washed with the wash solution. Plates were set up as in Figure 2.9 with Ab/Ag diluent in all wells except in row A, columns 1 and 2 which were used as reference standard columns.

	Reference standard		samples 1 - 9								
	1	2	3	4	5	6	7	8	9	10	11
A	0.5	0.5	S1	S2	S3	S4	S5	S6	S7	S8	S9
B	0.25	0.25	S1	S2	S3	S4	S5	S6	S7	S8	S9
C	0.125	0.125	S1	S2	S3	S4	S5	S6	S7	S8	S9
D	0.063	0.063	S1	S2	S3	S4	S5	S6	S7	S8	S9
E	0.031	0.031	S1	S2	S3	S4	S5	S6	S7	S8	S9
F	0.016	0.016	S1	S2	S3	S4	S5	S6	S7	S8	S9
G	0.008	0.008	S1	S2	S3	S4	S5	S6	S7	S8	S9
H	0	0	S1	S2	S3	S4	S5	S6	S7	S8	S9

Figure 2.9: Pn19A competition ELISA 96-well ELISA plate layout.

The Pn19A CPS reference standard (ATCC) was added to each well in row A columns 1 and 2, in order to ensure the standard was present in duplicate. A two-fold serial dilution was carried out from rows B to H. The sample, diluted in Ab/Ag diluent was added to row A, columns 3 – 11 and a two-fold dilution was performed from row B – H. For antibody detection, Pn19A antiserum working reagent was added to each well and the plate incubated at 20 – 25 ºC with shaking at 190 RPM for 1.5 h. Plates were washed and goat anti-rabbit horseradish peroxidase (HRP) conjugate working reagent was added to every well and incubated at 20 - 25 ºC for 45 min with shaking at 190 RPM. Plates were washed and 3,3',5,5'-tetramethylbenzidine (TMB) substrate was added to each well and left to incubate in the dark for 20 min, tapping occasionally. The reaction was stopped by the addition of stop solution (0.5 M H_2SO_4) and the absorbance read at 450 nm within 30 min of stopping the reaction.

2.8.2 Rate nephelometry

Rate nephelometry is a technique used for the detection and quantification of antigens in solution. The distinguishing feature of nephelometry is the selectivity in complex matrices and assay speed compared to ELISA. Nephelometry measures the intensity of scattered light as it passes through the antigen-antibody complex formed by the precipitating reaction and is based on the measurement of aggregation rates of specific antibody (Ab)-antigen (Ag) interactions as shown in Figure 2.10 [93]. The aggregation rate is a function of the antigen concentration at a constant Ab titer. Rate nephelometry was used for measuring CPS concentrations in the fermentation broth and to monitor the efficiency of CTAB precipitation of the polysaccharide from the broth prior to purification. Table 2.4 summarizes the reagents used in the nephelometry assay. A Nephelometer with BMG lab tech software was employed.

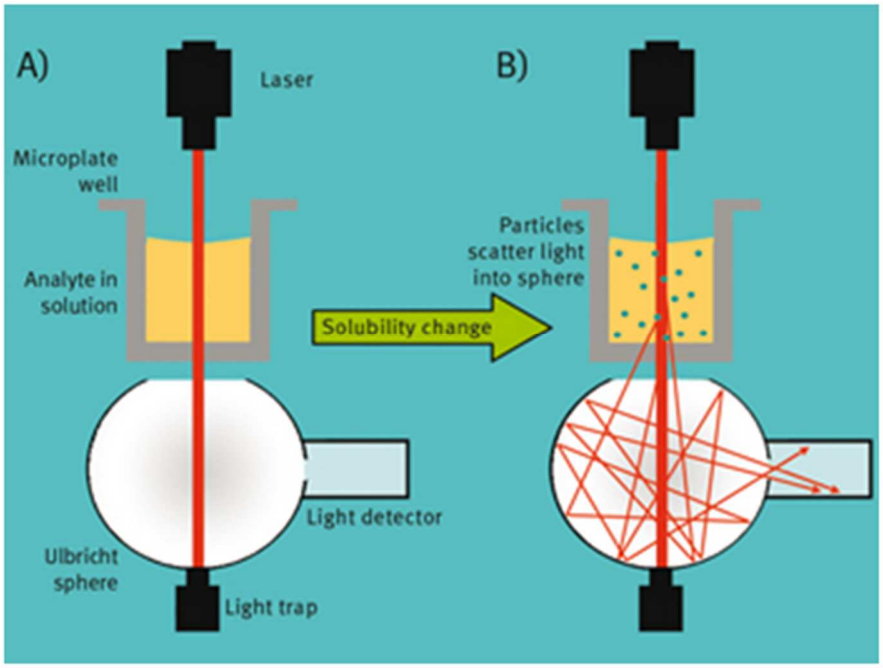

Figure 2.10: Nephelometric assay principle [94]. A laser-generated light beam is passed through a sample. The particles in solution will scatter light depending on particle size and/or shape.

Table 2.4: Reagents used in rate nephelometry

Reagent	Dilution
Pn19A CPS reference standard (ATCC)	1:200
Pn19A antiserum (SSI)	1: 4

Two 96-well plates were used for this assay, one for antigen preparation (Pn19A CPS reference standard and sample) and the other for the reaction and measurement. A serial two-fold dilution of the sample was prepared in Plate 1 using PBS as the diluent. Pn19A CPS reference standard (10 μg/mL) was also added to Plate 1. Four percent (4%) PEG solution, as well as the antisera, was added to Plate 2 and the solution was mixed by shaking at 120 RPM for 10 min at 20 – 25 ºC on the orbital shaker. Thereafter the Pn19A reference CPS and samples were transferred from Plate 1 to the PEG/antiserum mixture in Plate 2. The plate was immediately placed in the Nephelometer and the samples were analyzed. The nephelometry rate for each of the dilution points was calculated and used to calculate the concentration using the mathematical linear function obtained from the standard curve.

2.9 Physicochemical techniques

Physicochemical interactions involve the determination of the nature of the system by studying its physical properties and composition. This can be performed using various chromatographic and spectroscopic techniques such as size exclusion high-performance liquid chromatography (SEC-HPLC), gas chromatography (GC) and nuclear magnetic resonance (NMR).

2.9.1 Nuclear magnetic resonance (NMR) analysis

NMR is a spectroscopic analytical technique used to determine the molecular structure of a sample by detecting the reorientation of nuclear spin in an applied magnetic field [95]. It involves monitoring the absorption of energy associated with the transition of nuclei between two magnetic energy levels. NMR

provides information on the structural composition, linkage, sequence, substitutions and anomeric configurations of polysaccharides and can quantitatively define the composition of the purified polysaccharide [96]. The analytical non-destructive nature of this technique allows it to precede other techniques.

Approximately 5 - 20 mg of dried polysaccharide was dissolved in 0.5 mL 99.9% deuterated water (D_2O), lyophilized and re-suspended in 0.7 mL D_2O for NMR data acquisition. 1D-proton, 1D-carbon, 1D-phosphorus, 2D-COSY (^1H-^1H Correlation Spectroscopy), TOCSY (Total ^1H-^1H Correlation Spectroscopy), HSQC (Heteronuclear Single Quantum Coherence) and HMBC (Heteronuclear Multiple Bond Correlation) experiments were conducted. NMR analysis of Pn19F and Pn19A CPS and conjugates were performed using a Bruker Avance III 400 NMR with Ultra Shield 400 Plus magnet and a Bruker Advance III 600 MHz NMR spectrometer equipped with a BBO Prodigy cryoprobe. The probe temperature was set at 303 K and all experiments were recorded and processed using standard Bruker software (Topspin 2.1). Spectra were recorded using the standard Bruker pulse programs with the following setting: ^1H-^{13}C HSQC J = 145 Hz, ^1H-^{13}C HMBC J = 6 Hz, ^1H-^{31}P at J = 10 Hz and the ^1H-^1H (TOCSY) experiments used a mixing time of 120 ms.

2.9.2 Fourier transfer infrared (FTIR) spectroscopy

FTIR is the study of absorption of infrared (IR) radiation which causes vibrational transitions in the molecule and can be used to determine the presence of functional groups in a structure. An IR spectrum represents a fingerprint of a sample with absorption peaks which correspond to the frequencies of vibrations between the bonds of the atoms making up the material [97]. FTIR is a reliable and sensitive technique that identifies qualitatively different kinds of material, where the size of the peaks in a spectrum is a direct indication of the amount of material present [97]. As such IR radiation is passed through a sample to (1) identify the unknown material, (2) determine the quality or consistency of a sample and (3) quantify components of a mixture [97]. The FTIR spectrophotometer has an energy source, an interferometer and a detector that measures the signal which is displayed as a spectrum (Figure 2.11) [97]. This technique was used to analyze the polymer composition of the disposable cell culture bags and the bag itself used during the fermentation process. The disposable cell bags are multi-layered laminated clear plastic composed of ethylene vinyl acetate (EVA) and polyethylene.

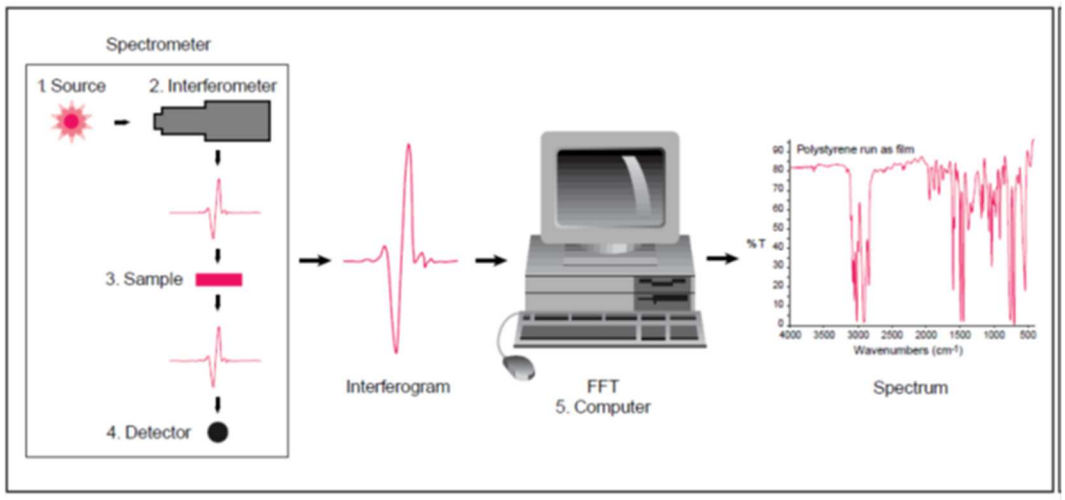

Figure 2.11: Schematic of sample analysis process from source to spectrum [97]. Each peak/band in the spectrum indicates the specific functional groups present in a region of the spectrum.

2.9.3 SDS-PAGE

Polyacrylamide gel electrophoresis (PAGE) is a versatile, gentle, high-resolution method for fractionation and physiochemical characterization of molecules on the basis of size, conformation and net charge [98]. SDS-PAGE uses sodium dodecyl sulfate (SDS), a detergent that denatures proteins and dissociates them from one another while conferring a negative charge, thereby allowing for their separation based on size. Electrophoresis relies on differences in the migration of charged molecules in a solution when an electrical field is applied across it. Hence, when an electric field is applied across the polyacrylamide gel the charged proteins or polysaccharides migrate through the gel to the anode based on the protein size. Coomassie dye R250 (protein) and Schiff's reagent (polysaccharide) are used for band visualization. The Schiff's reaction involves the reaction of the Schiff reagent with aldehydes generated by periodate oxidation to form Schiff bases which stain pink.

All samples were diluted in native sample buffer to give concentrations of 100 µg/mL. The 40 µL sample and 15 µL standard (Biorad) were loaded into wells on the gel. Gels were subjected to a constant current of 90 V for 2 h or until the dye reached the bottom of the gel. Products of conjugation reactions were assessed using 3 - 8% acetate SDS-PAGE under reducing conditions (with Tris-(2-carboxyethyl) phosphine, TCEP - XT reducing agent from Bio-Rad).

2.9.4 SEC-HPLC

High-performance liquid chromatography (HPLC) is a commonly used analytical tool for the analysis of compounds separated with the use of a chromatographic column as it offers a combination of speed, reproducibility, and sensitivity. Size exclusion chromatography (SEC) is a technique that provides molecular weight distribution information by separating molecules according to size as they pass through a SEC packed column. A typical SEC separation is shown in Figure 2.12. Depending on the detector, either proteins can be analyzed (diode array detector (DAD) or polysaccharides (refractive index detector (RID)) [99].

All SEC-HPLC chromatograms were generated on an Agilent 1200 HPLC system, equipped with micro vacuum degasser, quaternary gradient pump with degasser, autosampler, thermostatted column compartment, DAD and RID detectors (set at 35 ºC), fraction collector and Chemstation software. The columns consisted of a guard column (Shodex OH Pak SB-G) and Shodex OH Pak SB -805 HQ and SB -804 HQ columns mounted in series. These columns are packed with polyhydroxy methacrylate gels designed for use with high-resolution, high-speed aqueous size exclusion chromatography to separate water-soluble polymers and proteins. The Shodex OH Pak SB -805 HQ will separate polysaccharides in the molecular weight range of 100,000 - 1,000,000 Da while the SB -804 HQ has a molecular weight range of 5,000 - 400,000 Da, both ranges based on Pullulan standards.

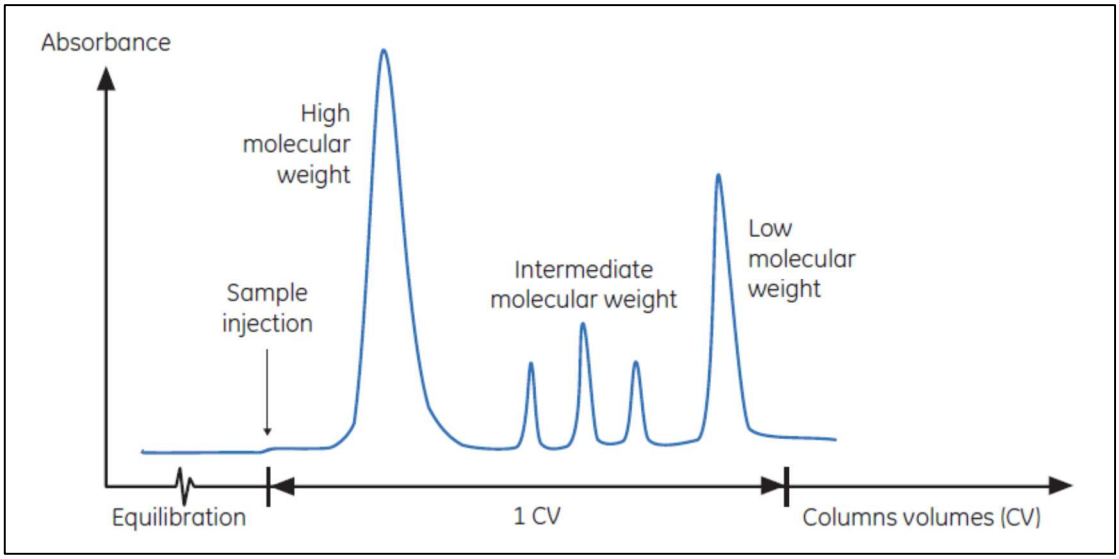

Figure 2.12: Typical high-resolution SEC separation [100].

SEC does not yield an absolute molecular weight. However, calibration of the column using standards of known molecular weight allows for the conversion of the retention time to a molecular weight for a given column set. The principle of SEC is that the smaller molecules will travel through the column entrapping themselves in the pores of the column whereas the larger molecules will simply pass by the pores because these molecules are too large to enter the pores. Larger molecules, therefore, flow through the column more quickly than smaller molecules, thus the smaller the molecule, the longer the retention time. For polysaccharides, Pullulan standards are used to determine the unknown molecular size and are supplied with known molecular weights. An example of the retention times determined after running the standards through the column can be seen in Figure 2.13.

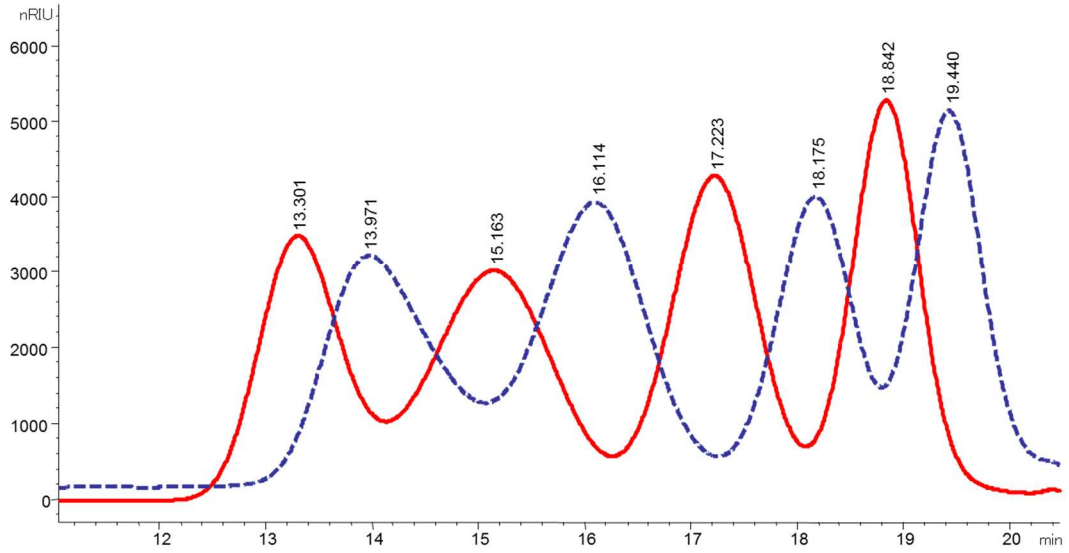

Figure 2.13: The Pullulan standards as presented in Table 2.5.

Pullulan standards were eluted through the Shodex columns using an eluent of 10 mM PBS buffer at pH 7.0. A summary of the Pullulan standards and their related molecular weights and elution times are provided in Table 2.5. The void and total volumes were determined using DNA molecular markers and ethylene glycol respectively. For the Shodex columns mentioned above, the retention times were 10 min for void volume and 20 min for total volume. Purified CPS and conjugates (CPS concentration of 2.5 mg/mL) samples were filtered through 0.22 µm nylon filters before injection. A 50 µL injection volume with a flow rate of 1 mL/min for both purified CPS and conjugates was employed using an eluent of 10 mM PBS buffer at pH 7.0.

Table 2.5: Molecular weight and elution times of Pullulan standards on pneumococcal CPS using Shodex columns.

Standard	MW (kDa)	Log (MW)	Shodex Columns Elution Time (min)
P-800	788	2.897	13.301
P-400	404	2.606	13.971
P-200	212	2.326	15.163
P-100	112	2.049	16.114
P-50	47.3	1.675	17.223
P-20	22.8	1.358	18.175
P-10	11.8	1.072	18.421
P-11	5.9	0.771	19.440

2.9.5 Composition analysis by HPAEC-PAD and GC

Compositional analysis offers greater specificity and sensitivity than colorimetric assays. In order to determine the composition, the CPS is hydrolyzed to release monomers [101]. Three different means of hydrolysis are described in the literature: (1) TFA hydrolysis (2) methanolysis followed by TFA hydrolysis and (3) HF hydrolysis followed by TFA hydrolysis [102]. Talaga et al., [102] showed that even though TFA hydrolysis is only partially satisfactory for the composition analysis of polysaccharides

containing phosphate (Pn6B and Pn19A), amino sugars (Pn14) and uronic acids (Pn1), it is still the most widely used as most monosaccharides can be recovered without extensive degradation. TFA alone is not effective due to the failure of the acid hydrolysis to completely cleave phosphate and glycosidic linkages. Methanolysis may be preferable to classical acid hydrolysis for certain sugars such as uronic acid as it results in a more stable product compared to TFA alone or harsher hydrolysis conditions which could lead to more monosaccharide degradation [102, 103].

2.9.5.1 High-performance anion-exchange chromatography with pulsed amperometric detection

HPAEC-PAD was used to determine the presence and quantity of monosaccharides present in the repeating unit of Pn19F and Pn19A CPS. HPAEC-PAD is a sensitive technique used for monomeric analysis and provides a high-resolution separation of carbohydrate components that require no sample derivatization and samples can be separated at high pH. HPAEC-PAD takes advantage of the weakly acidic nature of carbohydrates and provides separation using a high pH eluent and base stable polymer anion exchange stationary phase [104].

Purified polysaccharide, (400 µL of a 100 µg/mL sample), was mixed with 100 µL of 10 N TFA in a glass tube with a screw-cap. The samples were heated at 121 ºC for 2 h, and the hydrolyzates were cooled to room temperature then evaporated to dryness using a speed vac concentrator (Thermo Speedvac Savant SPD131DDA Concentrator, 1.3 mbar, 3 hours). Monosaccharide standards were subjected to the same hydrolysis conditions. Standards and sample hydrolyzates were reconstituted in 1 mL water and then filtered through a 0.22 µm nylon filter. The hydrolyzed samples were transferred to vials for analysis by HPAEC-PAD.

The analysis was performed using a Dionex BioLC chromatography system equipped with a CarboPac PA1 analytical column (code: 035391) and CarboPac PA1 guard (code: 043096) column. An injection volume of 25 µL was used for all samples. Carbohydrates were eluted with 18 mM sodium hydroxide (NaOH) over 18 min at a flow rate of 1 mL/min, followed by a regeneration step with a gradient. The gradients were achieved with three solvents: solvent A was water, solvent B was a 100 mM NaOH solution and solvent C was a 100 mM NaOH containing 1 M sodium acetate solution. These solutions in combination were used simultaneously to elute the carbohydrates. The gradients are summarized in Table 2.6.

Table 2.6: Solvent gradients used to eluent CPS.

Time (min)	Sodium hydroxide (mM)	Sodium Acetate (mM)
0 – 15	18	0
15 – 18	18 – 100	0 – 300
18 – 35	100	300
35 – 55	100 – 18	300 – 0

2.9.5.2 Gas chromatography (GC)

GC is an analytical technique used as a quantitative tool and it provides improved sensitivity with detectors such as mass selective detectors (MSD) over liquid chromatography techniques for polysaccharide analysis. A schematic representation of the general layout of the gas chromatographic instrument is shown in Figure 2.14. In order to analyze the polysaccharides, they are depolymerized with methanolic HCl to form methyl glycosides before further derivatization if required. Methyl glycosides are relatively stable products compared with monosaccharides released under aqueous conditions and can be subjected to harsher hydrolysis conditions with less degradation. Trimethylsilylation derivatization is a quantitative and rapid method for a range of carbohydrates including aldoses, ketoses, amino sugars and alditols [103]. The GC method followed in this study was described by Kim et al., and applied to pneumococcal CPS [103].

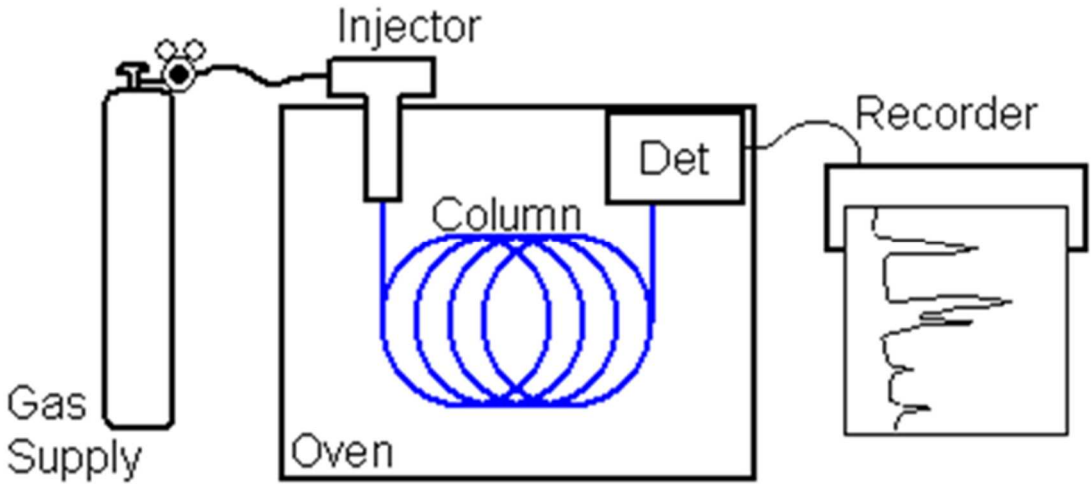

Figure 2.14: Schematic representation of an instrument used in gas chromatography [37].

Samples were transferred to screw cap tubes and dried at 40 ºC under a steady stream of nitrogen (N_2). To each tube, approximately 0.5 mL of methanolic 3 N HCl (Supelco, Sigma-Aldrich) was added, tubes were sealed with screw caps and incubated in a pre-heated block set at 121 ºC for 2 h. After incubation, the tubes were removed from the heating block and allowed to cool to room temperature (20 – 25 ºC), transferred to Reacti-therm vials (Thermo Scientific) and centrifuged for 1 min at 3500 RPM. Samples were dried under N_2 at 40 ℃ and washed 3 times with methanol to remov e residual HCl.

Post methanolysis; the samples were re-*N*-acetylated with the sequential addition of 10 drops of methanol, 1 drop of pyridine and 1 drop of acetic anhydride. The samples were sealed using screw caps and allowed to incubate at room temperature for 30 min. The caps were removed and the samples were once again dried under N_2 at 40 ºC. The samples were washed three times with 0.5 mL methanol. Approximately 0.2 mL of the Trisil reagent (Sweeley reagent, Thermo Scientific) was added to each tube. Tubes were recapped and incubated at 80 ºC for 20 min. After incubation, the samples were cooled to room temperature, mixed and dried under N_2 at 40 ºC. Hexane (1 mL) was added to each tube and the contents mixed prior to transferring to auto-sampler tubes via filtration through 0.22 µm filters. The GC system used for the separation of the hydrolyzed CPS was an Agilent 6820 gas

chromatograph with a flame ionization detector, fitted with a DB-5 column (30 m x 0.32 mm, 0.25 µm ID) and nitrogen was used as the carrier gas at a flow rate of 1 mL/min.

2.9.6 Size reduction of CPS

Size reduction was employed to reduce the size and viscosity of CPS prior to activation and conjugation. The reduction in viscosity allows easier manipulation of the CPS solution and allows for a more efficient conjugation. In addition to this separation of unreacted CPS from the final conjugated product is facilitated, provided there is sufficient differentiation between the full-length and size-reduced CPS. Mechanical methods including sonication and micro-fluidization were investigated.

Although mechanical methodologies require specialized instrumentation, the advantages of the mechanical over chemical methods include:

- Suitable fragmentation.
- Reproducible and scalable.
- Minimal post-fragmentation workup required.
- Relatively quick to perform.
- No additional chemicals or reagents required.

2.9.6.1 Sonication

Sonication generates emulsions by cavitation, a process whereby high-frequency vibrations give rise to many bubbles which form and implode at a very high rate [105]. Ultrasonic disruption is performed by ultrasonic vibrators that produce a high-frequency sound with a wave density of approximately 20 kHz/s. A transducer converts the waves into mechanical oscillations via a titanium probe immersed in the concentrated sample. Sonication is used to reduce the size of polysaccharides by disruption of the glycosidic bonds in the polysaccharide using the high-frequency sound waves with the energy of up to 10 KJ at 1-hour intervals. Provided the glycosidic linkages are not part of a branched chain in the repeating unit, size reduction results. For the sonication experimental work, the polysaccharide was first solubilized in water at concentrations of 10 mg/mL. The polysaccharide solutions were then placed in a 50 mL beaker and cooled in an ice bath. The sample was then exposed to a pre-set energy power output for a pre-determined time. The sonication cycle consisted of a 59 s pulse with 15 s break intervals. The total energy input was read from the sonicator display. Samples were passed through 0.45 µm filters to remove any trace metal shed by the sonicator probe before analysis on SEC-HPLC. Sonication was performed on a VibraCell model VCX 750 ultrasonic processor at the University of Stellenbosch.

2.9.6.2 Microfluidization

Microfluidization is a technique that involves the use of high shear fluid processors to reduce particle size and produces uniform size reduced particles. It is the preferred method for size reduction of polysaccharides as it does not require detergents or solvents. The microfluidizer that was utilized was Model M-110P from Microfluidics (Figure 2.15). It processes a minimum sample volume of 25 mL, has

a fixed geometry diamond interaction chamber and a ceramic (zirconia) plunger. The microfluidizer has an operating pressure range of 0-30 000 psi and the return coil has to be cooled to between 2 - 6 ºC to avoid the sample becoming heated.

The interaction chamber contains fixed geometry microchannels and a pump. The pump amplifies hydraulic pressure to the selected level which, in turn, imparts this pressure to the sample. The pressure is controllable between 2,500 and 30,000 psi where the pump delivers the desired pressure, at a constant rate, to the sample. As the pump travels through its pressure stroke, it drives the sample through the interaction chamber. The sample travels at a very high velocity through the microchannels which are designed to create high shearing and impact forces that disrupt (breaks) the glycosidic bonds in the polysaccharide, provided the glycosidic linkages are not part of a branched chain in the repeating unit, resulting in size reduction. As the pump completes its pressure stroke it reverses direction and draws the next volume of sample. At the end of the intake stroke it again reverses direction and drives the sample into the interaction chamber and the process is repeated. This allows for the processing of large volumes of sample in a reproducible manner.

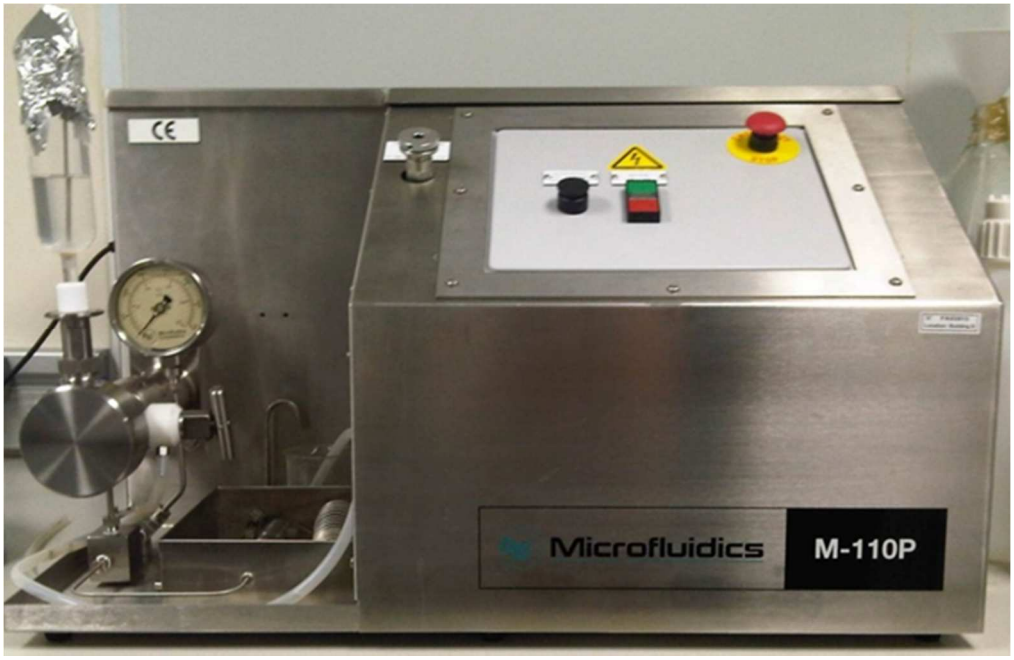

Figure 2.15: Microfluidizer M-110P used during this study.

The sample can then be recirculated through the chamber if the desired size is not achieved from the first pass. For micro-fluidization, polysaccharide samples of Pn19F and Pn19A were dissolved in water to obtain concentrations of 10 mg/mL. The samples were then passed through the Microfluidics M-110P microfluidizer processor at a variable pressure for a predetermined number of passes to obtain size reduced CPS.

2.9.7 Protein derivatization

Conjugation chemistry involves the linking (conjugation) of a protein to a CPS. Due to the high molecular weight of the commonly used proteins, steric hindrance impedes the coupling of the protein to the CPS. To overcome this, spacer molecule or linkers are included, the choice of which depends on the

chemistry used and length of the CPS needed to achieve conjugation. One such linker is adipic acid dihydrazide (ADH), a highly reactive homo-bifunctional linker used to derivatize carboxyl, carbonyl and hydroxyl groups present on proteins. The mechanism for the reaction, depicted in Figure 2.16, involves 1-Ethyl-3-(3-dimethylaminopropyl)carbodiimide (EDC) which is a water-soluble carbodiimide crosslinker that primes the carboxyl group for spontaneous reaction with the ADH [106, 107]. 2-(*N*-morpholino) ethane sulfonic acid **(**MES**)** is a suitable carbodiimide reaction buffer as it has a buffering capacity of pH 5.5 – 6.7, an ideal pH for this reaction.

The protein was dissolved in 0.1 M MES buffer at pH 6.0. Solid ADH was added to the protein at room temperature at a ratio of 3.5 mg ADH / mg protein and the reaction mixture was stirred until the complete dissolution of ADH. EDC, due to its hydroscopic nature, was first dissolved in water to make up a 20 mM solution and then added to the protein mixture at room temperature at a ratio of 0.15 mg EDC / mg protein. Both BSA and TT were derivatized for 4 hours at room temperature. The reaction mixture was then quenched by raising the pH to pH 10 with 1 M NaOH. After quenching, the reaction mixture was diafiltered against a 30 mM NaCl / 3 mM Na_2CO_3 buffer at pH 10.5 using regenerated cellulose (3 x 50K 50 cm^2) filters. Diafiltration continued until the permeate was clear of hydrazides (excess ADH). To test the permeate for ADH, 2 drops of permeate was added to 100 µL 0.1% TNBS and 100 µL 0.1 M sodium borate (pH 9.0) solution and incubated for 5 min at room temperature. An orange color was indicative of the presence of ADH.

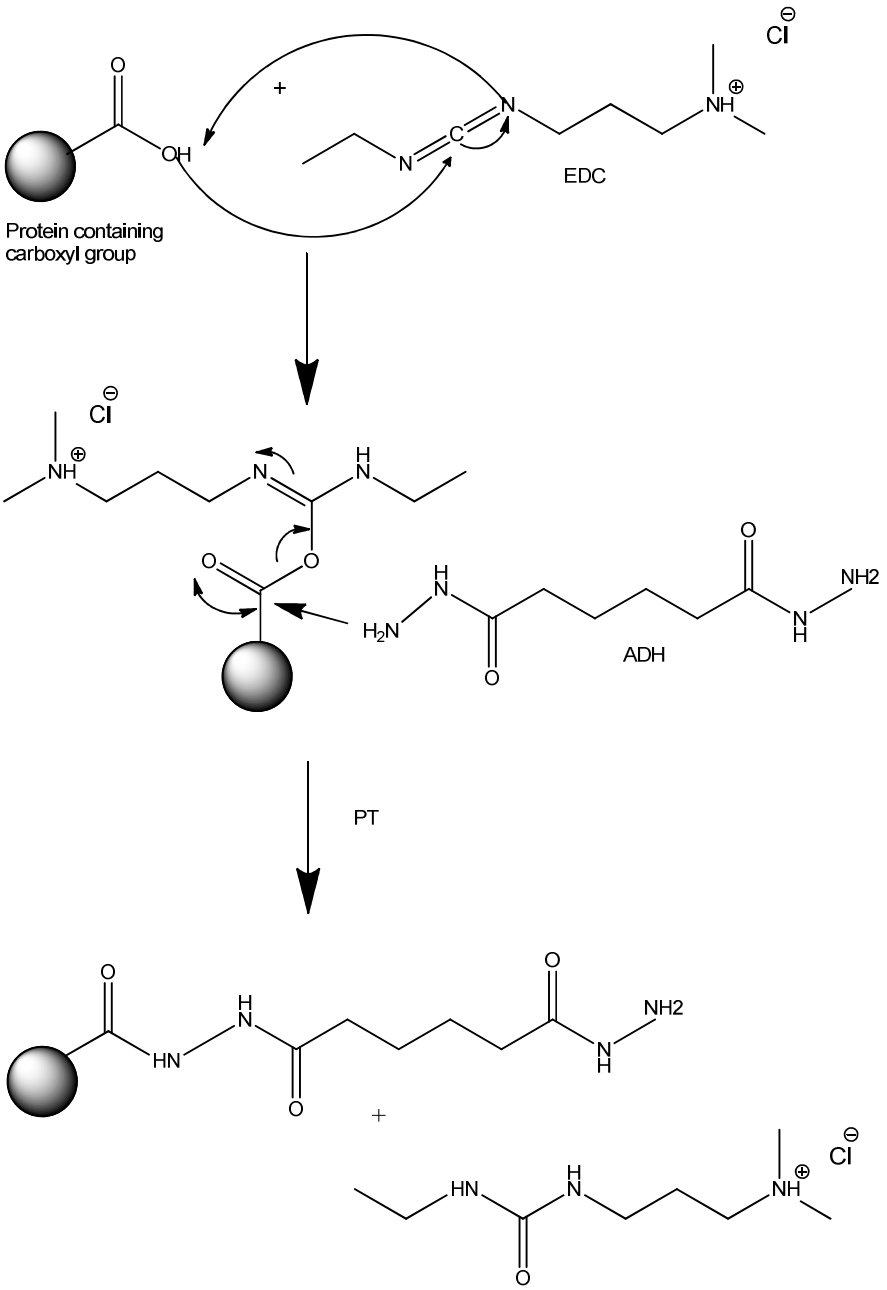

Figure 2.16: Schematic representing the mechanism of protein derivatization [108].

2.9.7.1 2,4,6-Trinitrobenzenesulfonic acid (TNBS) assay

The TNBS assay is used to quantify the free hydrazide groups in solutions following protein derivatization. This assay can also be used to determine free (unreacted) hydrazides present after conjugation of CPS to derivatized TT and BSA. The TNBS assay was adapted from Okuyama et al. [109] 1960, whereby the samples were incubated with TNBS at a high pH, resulting in chromogen formation at a maximum absorbance at 550 nm. ADH was employed as a standard thus enabling the molar concentration of hydrazides in the activated TT to be determined. This was converted into moles hydrazide per mole TT or, considering TT contains a total of 160 carboxyls (from the aspartic acid, glutamic acid, and C-terminus), as percentage activation (mole fraction of carboxyls converted to acid hydrazides). The results were expressed as moles of ADH with free hydrazide group per repeating unit of derivatized TT [109]. Samples and standards (0 – 625 mM) were placed in glass tubes, 1 mL of 0.1

M borate buffer (pH 9) and 0.5 mL of 0.1% TNBS solution was added to the tubes and incubated at 20 – 25 ºC for 2 h. The absorbance of samples and standards were measured at 550 and 750 nm, auto-zeroing the spectrophotometer with air at both wavelengths prior to reading. The difference in the absorbance readings accounts for the interference due to light scattering [110]. This reaction distinguishes between hydrazine and hydrazides by the specific absorbance maxima of each complex. The TNBS–hydrazine complex absorbance maxima are at 570 nm whereas hydrazides absorb most strongly at 550 nm. Amino acids do not interfere with this assay as the absorbance maxima for these complexes are approximately 420 nm [109].

2.9.8 Conjugation using CDAP activation and ammonium sulfate precipitation

The CDAP conjugation method investigated was originally established by Lees and Shafer [37, 111]. Figure 2.17 depicts the general mechanism of CDAP activation used to conjugate protein to polysaccharide. The mechanism will be discussed in more detail in Chapter 6. Only the pneumococcal polysaccharide that is covalently bound (conjugated) to the carrier protein is immunologically important for clinical protection. As such, following conjugation, the conjugates are purified to remove unconjugated CPS and reagents. This is achieved using saturated levels of ammonium sulfate which, when added to the conjugate solution, results in precipitation of all protein components, including the unreacted protein and conjugate, thus leaving the unreacted CPS in solution [112]. Separation of the unreacted CPS can then be achieved through centrifugation.

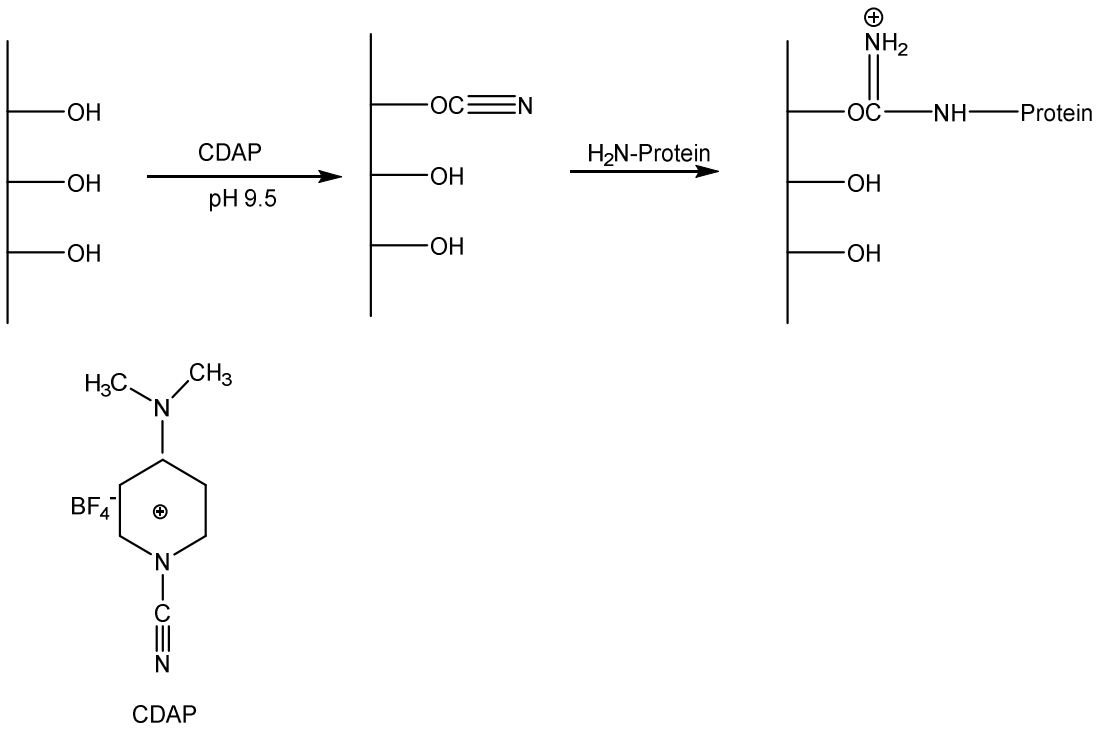

Figure 2.17: Schematic of CDAP mechanism used during conjugation of CPS to protein [111].

The general procedure for activation of CPS and conjugation of CPS to protein using CDAP is as follows: the polysaccharide was dissolved in a 0.2 M NaCl solution and cooled on ice. A 100 mg/mL solution of CDAP in acetonitrile was added to the CPS with vigorous stirring at a ratio of 0.75 mg CDAP per mg CPS. The mixture was left to react for 30 s followed by the addition of 0.2 M trimethylamine

(TEA) which was added at twice the volume of the CDAP solution. The pH increased from 5.5 to 9.0 – 9.5 on the addition of TEA. The CDAP activated polysaccharide was then added to the derivatized protein and the pH was maintained above 9.0 with the addition of 0.2 M TEA. The reaction was left to proceed for 20 hours, after which a molar equivalence of glycine to CDAP was added to quench the reaction.

A saturated ammonium sulfate solution was prepared by dissolving 550 g ammonium sulfate [$(NH_4)_2SO_4$] in 1 L water and cooling it at 2 - 8 ºC. Two volumes of saturated ammonium sulfate were added to one volume of the conjugate sample, mixed and left overnight at 2 - 8 ºC. The solution was centrifuged to pellet out the conjugate and the supernatant was removed. The procedure was repeated and the final pellet was re-dissolved in 10 mM phosphate buffered saline (PBS) (pH 7.2).

2.9.9 Free saccharide assay

The term free saccharide refers to the quantity of polysaccharide that is present but not covalently linked to the protein carrier. The aim was to determine the quantity of free or unconjugated polysaccharide remaining in the final polysaccharide-protein bulk conjugate as this is indicative of the both the success of purification and the stability of the conjugates during the stability studies.

A precipitation method adapted from Guo et al. [113] (1998), to separate unconjugated/ free polysaccharide from carrier protein bound material under acidic conditions using deoxycholate/HCl was applied to Pn19F and Pn19A CPS-protein conjugates. Deoxycholic acid (sodium deoxycholate or DOC) is a water-soluble, bile-acid ionic compound that binds to both the free and conjugated protein resulting in precipitation of the protein components after acidification. This is followed by centrifugation to remove free and conjugated protein from solution leaving the free polysaccharide in the supernatant which can then be quantified.

The pH of DOC solution was adjusted to between pH 6.3 - 6.8 with 1 M HCl. The sample (1 mL diluted with 0.15 M NaCl to give a polysaccharide concentration of 75 - 100 µg/mL), and a blank were placed into Eppendorf tubes to which 100 µL of 1% DOC solution was added and the tubes incubated at 2 – 8 ºC for 30 min. Samples were centrifuged at 13 400 RPM for 30 min and the supernatant transferred to hydrolysis tubes. The CPS concentration was determined using the anthrone assay.

CHAPTER 3. MICROBIOLOGICAL CHARACTERIZATION AND CULTIVATION OF PNEUMOCOCCI

This chapter describes the growth medium, clonal selection, inoculum train and bacterial inactivation strategies performed during this study. Some of the processes were initially established as a proof of principal for the Pn1 serotype before being applied to Pn19A.

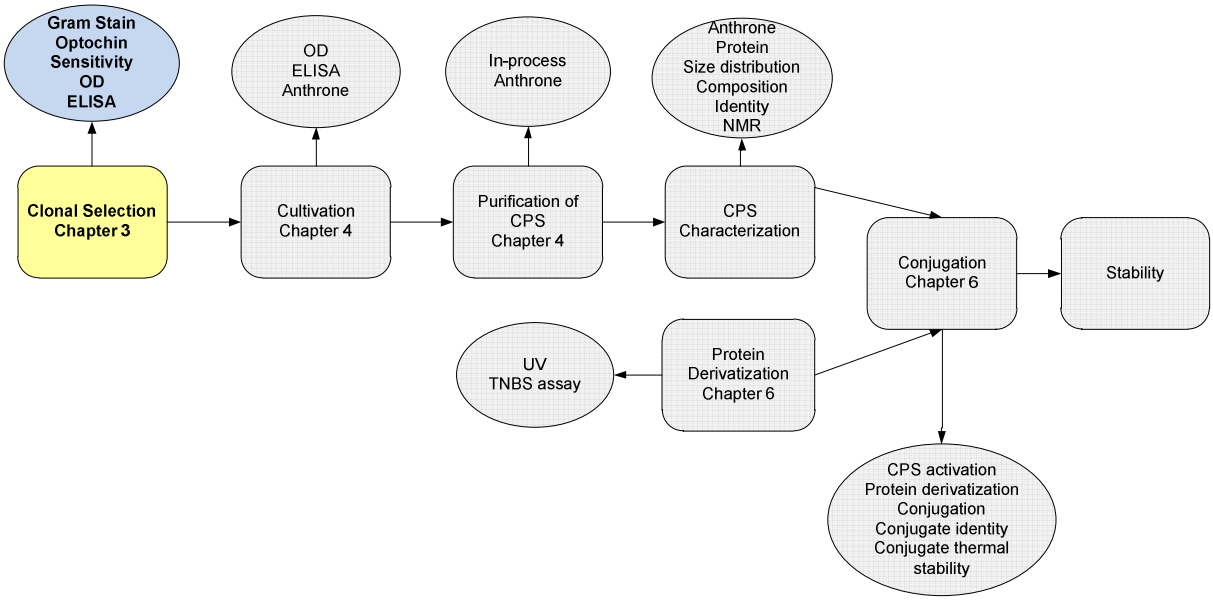

Figure 3.1: The process development steps for Pn19A conjugate vaccine production, highlighting the microbiological identification of pneumococci.

3.1 Introduction

The following steps towards the production of CPS were investigated in this study and discussed below:

- Medium and growth conditions.
- Clinical isolate screening.
- Seed development.
- Establishment of an inoculum train and small scale fermentation process using shaker cultures for Pn19A CPS production.
- Development of an inactivation method for both the killing of bacteria and the release of polysaccharide prior to CPS purification.
- Determination of a clarification technique to remove cell debris before purification of CPS.

Confirmatory ID tests were required throughout these steps, including Gram stain, colony morphology, hemolysis and optochin susceptibility, surrounding capsule identification by Quellung and bile solubility [114, 115].

3.2 Microbiological identity

The techniques used to phenotypically identify *S. pneumoniae* were the Gram stain, Quellung reaction, alpha hemolysis and optochin susceptibility [116].

Gram-positive bacteria have a thick and relatively impermeable cell wall composed of peptidoglycan and secondary polymers that retain a crystal violet stain (purple) and resist decolorization [117]. The purple stain presented in Figure 3.2 (A) shows the presence of Gram-positive diplococci characteristic of *S. pneumoniae*.

A positive Quellung reaction is produced when a serotype-specific antibody binds to the capsular polysaccharide and causes a change in the refractive index of the capsule so that it appears 'swollen' and more visible (Figure 3.2 (B)). The cell stains dark blue and is surrounded by a sharply demarcated halo, which represents the outer edge of the capsule. The light transmitted through the capsule appears brighter than either the cell or the background.

The optochin sensitivity test is routinely used to differentiate pneumococcus from other alpha streptococci species as *S. pneumoniae* are optochin-sensitive and therefore present a halo or zone of inhibition around the optochin disk on a BAP [116]. The optochin disrupts the structure of the bacterial cell membrane and causes optochin sensitive bacteria such as *S. pneumoniae* to lyse due to changes in surface tension.

Alpha hemolysis is also characteristic of the presence of *S. pneumoniae* as the bacteria display a greenish discoloration while growing aerobically on blood agar as shown in Figure 3.3. However, S. *pneumoniae* is not the only bacteria that displays this feature. In order to differentiate it from other alpha-haemolytic streptococci, the bile solubility test is employed.
S. pneumoniae is bile soluble which distinguishes it from other alpha-haemolytic streptococci. As a result, *S. pneumoniae* cells lyse in the presence of bile salts and the testing solution becomes clear in contrast to a negative control where the solution remains turbid [21].

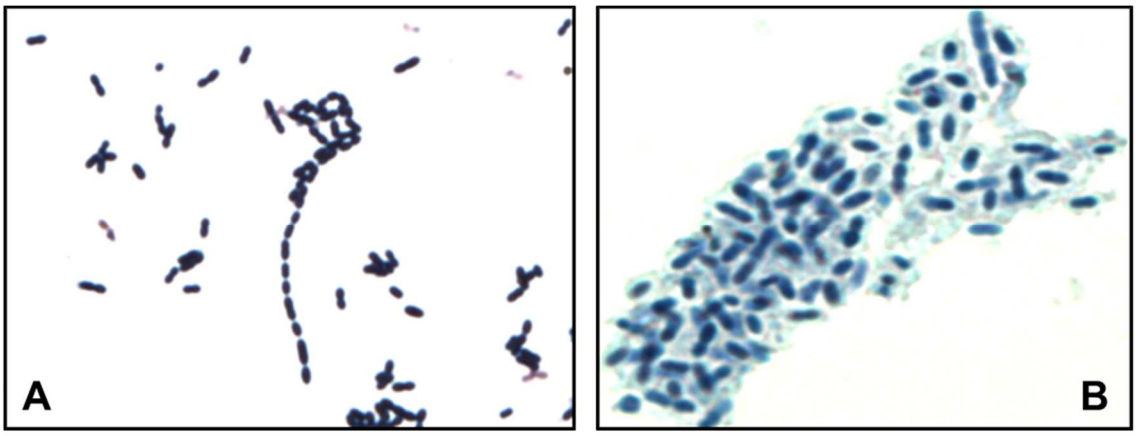

Figure 3.2: (A) Gram stain and (B) Quellung reaction of Pn19A bacteria. All images were viewed using oil-immersion lens (magnification x100) under a microscope (Olympus cx31).

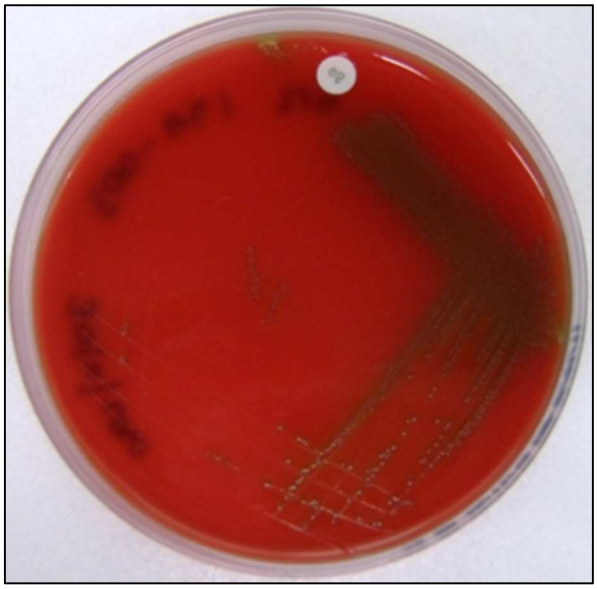

Figure 3.3: Optochin sensitivity and α-haemolysis of Pn19A bacteria.

Apart from bile solubility, these tests were used routinely during isolate and clonal selection as well as CPS production. Bile solubility was not performed routinely during this study as the remaining tests provided the necessary information to identify and evaluate isolate purity.

3.3 Medium Optimization

3.3.1 Introduction

Medium optimization is an essential part of fermentation-based process development influencing process efficiency (growth rate, cell viability, foaming and by-product formation), product yield (productivity) and quality (purity and product integrity) [65]. Bernheimer et al., [118, 119] (1942) coined the term “the pneumococcus medium” which refers to the medium initially developed for the cultivation of α-haemolytic Streptococci and later modified into a partially chemically defined medium suitable for pneumococcal cultivation. Cultivation of *S. pneumoniae*, a fastidious organism, was commonly performed using animal-sourced medium components, such as Chocolate Blood agar, Brain and Heart Infusion, Todd-Hewitt, and hydrolyzed casein derivatives, frequently supplemented with whole blood or serum [65, 120]. These medium recipes containing animal-derived components allow for high CPS production levels, but are unsuitable for vaccine production processes, due to the risk of prion-related diseases [120]. This follows since the emergence of Bovine Spongiform Encephalopathy (BSE) in the 1980s and subsequent concerns regarding transmissible spongiform encephalopathy (TSEs) in other species, there has been a growing concern over the use of meat and animal-derived products in the manufacturing of biological products [26, 121]. As such, a culture medium for the production of CPS from *S. pneumoniae* should be safe and free of animal and serum components thus reducing complexities in downstream processing and eliminating the need to show thorough analysis that all animal-derived products have been removed [65].

Culture media for bacterial growth provides a supply of nutrients that the bacteria needs for growth and survival. Nutrient components such as a carbon, nitrogen, phosphorus, sulfur and various minerals are

used as a source of energy. To achieve this, the medium components should contain supplements such as amino acids and vitamins which support the inoculum and cultivation development under cGMP production of pneumococcal CPS [121]. These requirements, however, result in the increased cost of medium components. Adams and Roe [119] (1945) discussed the emergence of media used for the cultivation of pneumococcus wherein the importance of the addition of amino acids (e.g. glutamic acid), reducing agents (e.g. thioglycolic acid) and meat infusion for improvement of growth was demonstrated by various research studies.

The pneumococcus medium was further modified by Hoeprich [73, 122] (1955) to an essentially defined medium in order to support growth. This medium was improved by modifying the salts and amino acid concentrations used in the chemically defined medium [73]. The culture medium used in this study for the growth of a facultative anaerobe was adapted from Gonçalves et al. [26] (2002) and Hoeprich [73] (1957) and was named modified Hoeprich's medium as a starting medium. Medium components used during this study are shown in Table 3.1.

Table 3.1: Medium components used in the final selected composition of modified Hoeprich's medium for cultivation of Pn19A.

Raw materials	Manufacturer/Supplier	Cat #	Concentration levels
$MgSO_4$	Sigma	63136	20 mg/L
Select soytone (15%)	Difco	212488	30 g/L
Yeast extract (13.3%)	Ohly	10-00179	20 g/L
Glucose (50%)	Merck	137048	18.8 g/L
Thioglycolic acid (10%)	Sigma	T3758	1 mL/L
HCl (33%)	Merck	100314	0.02 mg/mL
Catalase	Fluka	60634	500U/mL
Hoeprich's salts			
$NaHCO_3$	Merck	106323	1 g/L
K_2HPO_4	Merck	137010	5 g/L
$FeSO_4.7H_2O$	Sigma	44982	5 mg/mL
$ZnSO_4.7H_2O$	Sigma	96497	0.8 mg/mL
$MnSO_4.H_2O$	Sigma	13245	0.4 mg/mL
Hoeprich's amino acids			
L-Glutamine	Sigma	G8540	625 mg/L
L-Asparagine	Sigma	11149	100 mg/L
Choline. HCl	Sigma	26980	10 mg/L

S. pneumoniae has been grown on both blood agar surfaces and in broth under a 5% CO_2 atmosphere, with pH adjustment [123]. It is a facultative anaerobe that uses a variety of fermentable carbohydrates [124]. Its metabolic energy is obtained through fermentation of glucose, which leads to the production of lactic acid. The increase in lactic acid causes a decrease in pH, therefore, the media requires good buffering capacity and pH control. According to the literature, the optimum pH for growth of *S. pneumoniae* was found to be 7.8 with a pH control range of 6.5 - 8.3, ideally maintained at pH 6 or above [2, 125]. However, during this study, it was found that pH 7.2 was ideal for growth as well as

purification of the CPS. In fact, it was found that a pH of 7.8 would not facilitate the release of CPS upon inactivation of the bacteria.

The concentration levels of all the raw materials in this study were adopted from the literature. For example, the glucose levels of 18.8 g/L were taken from Gonçalves et al. [26] (2002) as it was observed that the concentration of glucose higher than 30 g/L resulted in bacterial growth inhibition due to the production of lactic acid. Salts such as monopotassium phosphate and magnesium sulfate, required for growth of bacteria were used in concentrations similar to those used by Gonçalves et al. [26]. Hoeprich's amino acids, namely L-glutamine, L-asparagine and choline were an important source of amino acids providing vital growth factors for this fastidious organism and Hoeprich's salts namely sodium, potassium, iron, zinc, and manganese were used to maintain buffering and osmolality of the medium, as well as supply a source of trace elements [26]. Thioglycolic acid with a concentration level of 1mL/L was used as an organic source of sulfur which supports uniform bacterial growth [65].

S. pneumoniae is an aerotolerant anaerobe indicating that it grows better under anaerobic conditions but still, survives in atmospheres containing molecular oxygen. *S. pneumoniae* is catalase deficient, which is commonly found in organisms exposed to oxygen. As a Gram-positive catalase-negative coccus that generates hydrogen peroxide (H_2O_2) via a flavoenzyme system, *S. pneumoniae* grows better in the presence of a source of catalase such as red blood cells. Pneumococci do not have the ability to break down H_2O_2 by itself. With the increase in bacterial growth, there is an increase in H_2O_2 production which increases the level of toxicity in the culture medium and limits further growth and CPS production. Thus a supplement that would break down H_2O_2 and allow optimal bacterial growth is required. Catalase catalyzes the decomposition of H_2O_2 to water and oxygen that is produced under both aerobic and anaerobic conditions. When bacterial cells are exposed to oxygen (e.g. upper respiratory tract), produce 2 to 3 fold more H_2O_2 via the pyruvate metabolism pathway in comparison to anaerobic conditions [126-128]. Details of this mechanism are unclear, but it has been linked to the expression of the SpxB gene, which is highest under aerobic conditions [128]. Previous studies performed at Biovac showed catalase as a medium component can influence the production of CPS. Therefore, the addition of catalase to Hoeprich's medium was evaluated on Pn1 cultures (Chapter 4) showed to increase CPS production.

In an endeavor to develop an industrial method for CPS production, a study by Gonçalves et al. [26, 129] (2003), evaluated the influence of medium composition and culture conditions on the cultivation of *S. pneumoniae* serotype 23F. The emphasis was on Acid Hydrolysed Casein (AHC) and dialyzed Enzymatically Hydrolysed Soybean meal (EHS) as nitrogen sources [130]. It was demonstrated that CPS production was more dependent on a higher initial concentration of nitrogen (30 g/L of AHC) than on the carbon source. From this experiment, an optimal carbon: nitrogen ratio of 1:2 was established (18.75 g/L and 30 g/L respectively) [129]. A study by Liberman et al. [120] (2008), later demonstrated that biomass production of an autolysin mutant strain of *S. pneumoniae* which was resistant to Kanamycin (Rx1A1-KanR) was 2.5-fold higher in EHC than in AHC. This demonstrates that a good

source of nitrogen is required for optimal CPS production. Therefore peptones were investigated as an optimal nitrogen source (Section 3.3.2).

Yeast extract is a key component used in culture media as it is a source of vitamins, minerals, digested nucleic acids, amino acids, growth factors and inorganic salts. The yeast extracts under investigation were highly purified by ultra-filtration to ensure purity that would meet pharmaceutical specifications for production. This highly pure yeast extract does not cause turbidity or precipitation during fermentation and downstream processing. The peptones were investigated as nitrogen sources of Hoeprich's medium (refer to Section 3.3.2). Soytone and yeast extract were used as sources of nitrogen and vitamins [131, 132].

The aim of this study was to evaluate yeast extracts and peptones that are salt-free or low in salt content as nitrogen sources in Hoeprich's medium. These nitrogen sources were acquired from easily obtainable and cost-effective suppliers for the growth and production of Pn1 CPS in different Hoeprich's medium compositions and later adapted to Pn19A.

- Yeast extracts: BD Bacto™ yeast extract (212750) and salt-free Ohly™ yeast extract (1095002),
- Peptones: Oxoid veggietone (VG0100B) and BD Difco™ select soytone (212489), both animal-free peptone sources.

3.3.2 Methods for medium optimization

3.3.2.1 Peptone and yeast extract optimization for Pn1 cultivation in Hoeprich's medium

In this study, Hoeprich's medium as published by Gonçalves et al. [26] (2002) and represented in Table 3.1, was used with different combinations of peptone and yeast extract suppliers to determine the best combination for Pn1 cultivation and CPS production. The different Hoeprich's medium combinations that were tested are summarized in Table 3.2. Hoeprich's salts, catalase, and amino acid combinations remained the same for all compositions. Catalase was added to all media at 500 units per milliliter (U/mL). All medium components were sterilized using a 0.22 µm filter and Falcon tubes (50 mL volume) were used for incubation studies. The study was carried out in two steps as illustrated in Figure 3.4.

Table 3.2: Different peptone and yeast extract combinations of Hoeprich's medium that were tested for Pn1 cultivation and CPS production.

Medium Name	Peptone	Cat #	Yeast Extract	Cat #
H1	BD Difco Select Soytone (BD Biosciences)	212489	BD Bacto Yeast Extract (BD Biosciences)	212750
H2	Veggietones (Oxoid Ltd.)	VG0100B	BD Bacto Yeast Extract (BD Biosciences)	212750
H3	BD Difco Select Soytone (BD Biosciences)	212489	Yeast Extract (Ohly)	10905002
H4	Veggietones (Oxoid)	VG0100B	Yeast Extract (Ohly)	10905002

3.3.2.2 *Pre-culture preparations*

Two Falcon tubes from each set containing 20 mL of pre-warmed H1 medium were each inoculated with 1 mL of Pn1 laboratory working seed lot (LWSL). Similarly, two Falcon tubes containing 20 mL of H2 medium were inoculated. All four inoculated cultures and one control of each medium (H1 and H2) were incubated at 10% CO_2, 36 ºC, 100 RPM, 70% relative humidity (rH) until the cultures reached an OD_{600nm} of approximately 1.0 as shown in Figure 3.4.

3.3.2.3 *Culture preparations*

The two 20 mL H1 pre-cultures were pooled and nine H1 and nine H3 media were each inoculated with 1 mL of the H1 pooled pre-culture. Similarly, the two H2 pre-cultures were pooled and used to inoculate nine H2 and nine H4 media (Figure 3.4). The initial OD_{600nm} (time 0 h) was measured for each culture and the tubes were incubated without agitation for a 4 h time period as per the pre-culture. Uninoculated controls were included for each medium type and incubated with the other cultures. Cultures were sampled for OD_{600nm} and CPS production by ELISA after 2, 3 and 4 h incubation periods. The optical density readings at 600 nm were determined in triplicate for each culture by preparing a 1:10 dilution with the appropriate Hoeprich's medium as diluent and blank. This tenfold dilution was achieved by mixing 100 µL of the sample with 900 µL of the appropriate sterile Hoeprich's medium.

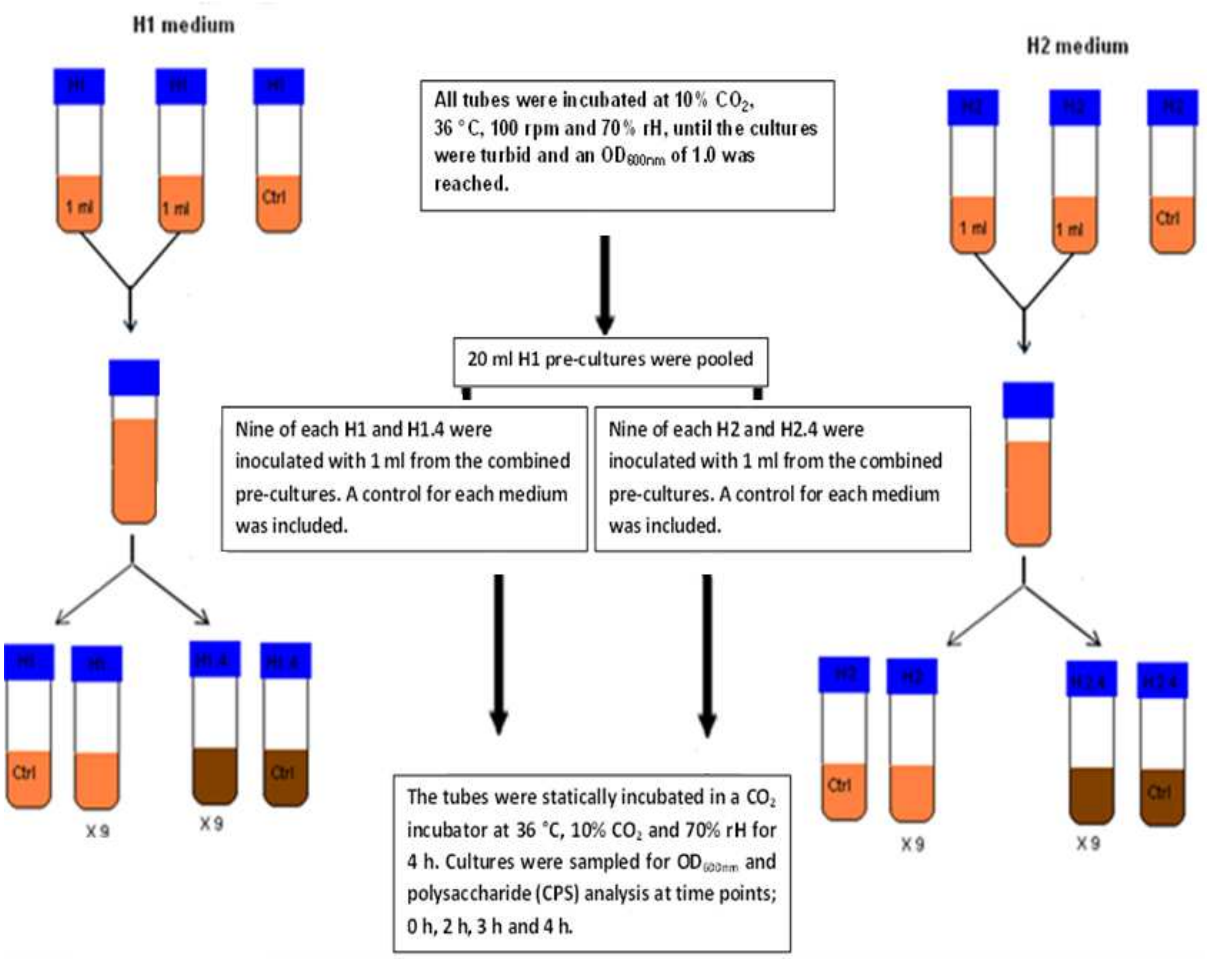

Figure 3.4: A flow diagram illustrating the Hoeprich's medium optimization process for the cultivation of *S. pneumoniae* serotype 1.

3.3.3 Results and discussion

Figure 3.5 shows the biomass for Pn1 growth comparisons for each Hoeprich's medium composition tested. Hoeprich's medium compositions with the salt-free yeast extract (Ohly) combined with veggietones as shown in H4, Figure 3.5 exhibited a marginal increase in growth for Pn1 as opposed to the medium with Bacto yeast extract as shown in H2, Figure 3.5. However, the use of different peptone and yeast extract combinations did not significantly influence the growth profiles of Pn1. Figure 3.6 shows the Pn1 CPS concentration levels for each Hoeprich's medium composition tested. In contrast to the growth profiles, better CPS yields were obtained with select soytone as a peptone source when compared with veggietones (H1/H3 and H2/H4 respectively, Figure 3.6).

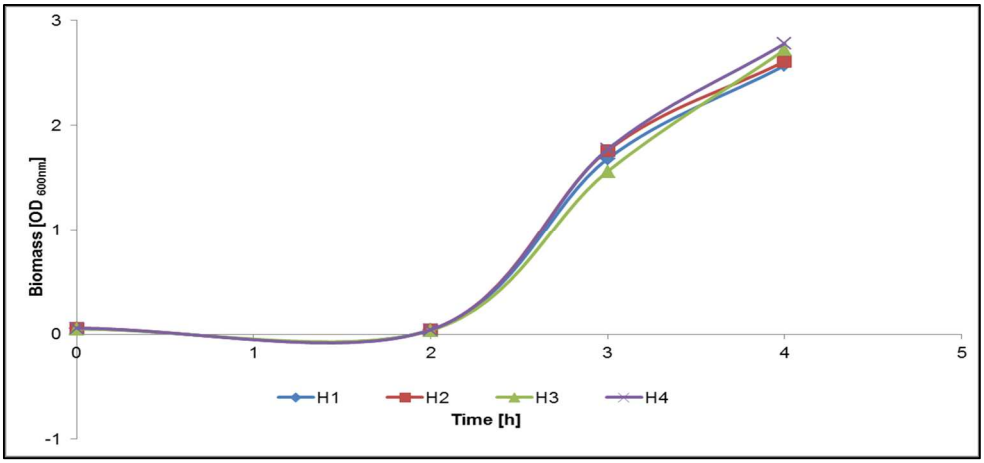

Figure 3.5: The biomass (OD_{600nm}) for Pn1 growth comparison for each Hoeprich's medium composition tested with a standard deviation of less than 10%.

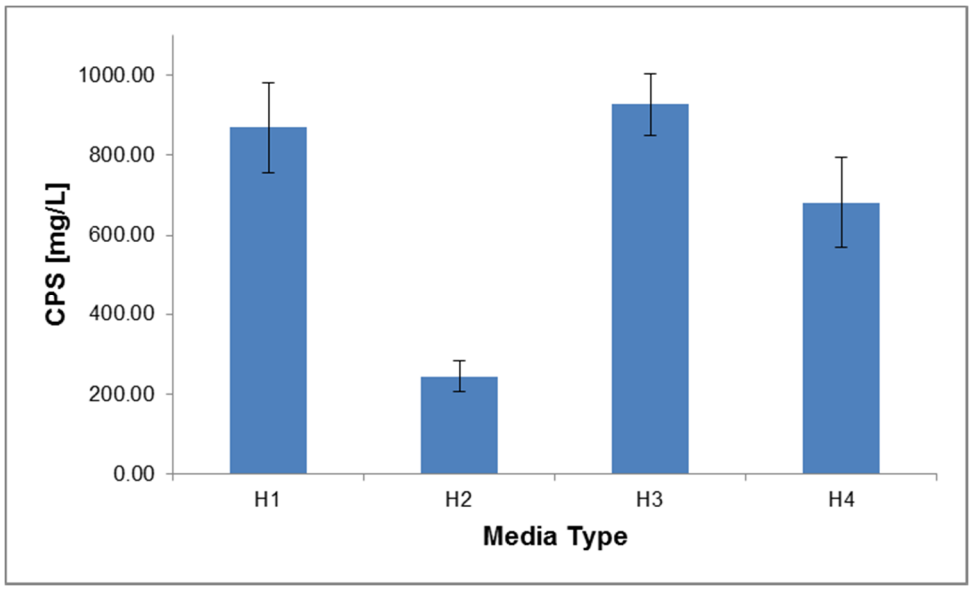

Figure 3.6: The CPS concentration levels produced by Pn1 determined by ELISA assay after 3 h post inoculation (p.i) in each Hoeprich's medium composition tested.

From these results, it was observed that the best Hoeprich's media combination for Pn1 CPS production was select soytone and salt-free yeast extract (H3, Figure 3.6) where the CPS production reached a maximum of 920 mg/mL after 3 h incubation. There was, however, no significant difference between the results obtained for H1 and H3 containing medium with the same peptone. Select soytone was

shown to be the preferred peptone source and yeast extract was based on availability and price. The data also indicated that the optimum time for CPS collection from Pn1 in shaker cultures was 3 h p.i as it is in the growing or exponential phase (log phase) of the bacterial growth cycle (growth cycle discussed further in Chapter 4). The time of harvest at this stage is important as the bacterial cells are still rapidly multiplying, at an earlier stage the number of cells would not be a true representative of the amount of CPS produced by these cells and a later stage the bacterial cells would not be viable and therefore would potentially lyse resulting in increased impurities. These data indicate that time to harvest is of importance and correlates with data provided by Avery, [133] (1924).

3.3.4 Conclusion

The CPS production levels but not the bacterial growth of Pn1 was influenced by the supplier of the medium components, peptone, and yeast extract. H1 and H3 containing select soytone (peptone from the same supplier) showed comparable production of CPS. H2 and H4 containing veggietone as a peptone source showed lower CPS production levels. This indicated that select soytone was a good peptone source as it influenced the CPS production regardless of the suppliers of the yeast extracts. Comparable yields in both bacterial growth and CPS production was achieved for select soytone. As it turns out, the H1 and H3 medium components were more cost effective and H1 medium components more readily available. Therefore the media of choice was modified Hoeprich's medium H1 and was thus referred to as Hoeprich's medium.

3.4 Isolate and clonal selection

An isolate and clonal selection method was developed and used to obtain a high Pn19A CPS producing clone from the clinical isolates supplied by the NICD. In summary, the clinical isolates were screened and *S. pneumoniae* serotype 19A identified. The selected clone was used to prepare the laboratory master seed lot (LMSL), which was subsequently used to manufacture a laboratory working seed lot (LWSL). This selection process ensured the removal of any trace components of animal origin that were found in the original media and was applicable to any serotype of *S. pneumoniae*.

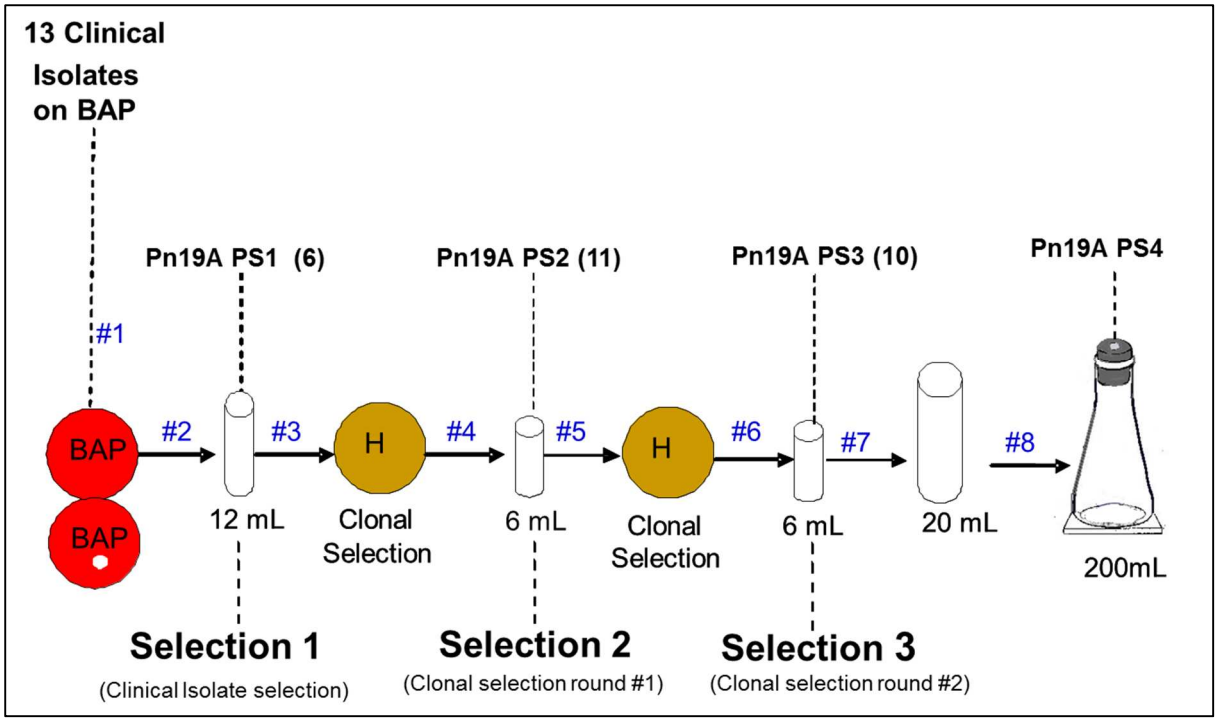

Figure 3.7: Process flow diagram of Pre-seed Pn19A PS4 preparation.

Due to its pathogenic nature, this organism presents a potential hazard in the laboratory if not manipulated with caution and as such is classified as a biosafety level 2 organism (BSL 2) [21]. In South Africa working with total *S. pneumoniae* culture volumes above 2 L require BSL 3 facilities. Clinical specimens isolated at the NICD from the cerebrospinal fluid of HIV-negative infants younger than 5 years old were selected for this study. Upon arrival at Biovac, the 13 isolates, cultured and stored on Dorset egg medium slants, were passaged onto blood agar plates (BAP) and cultivated. The selection strategy used during this study consisted of three steps which are explained and summarized in Figure 3.7. Each isolate was re-streaked on BAP and evaluated for growth, α-haemolysis, optochin sensitivity and Quellung. Phenotypic analysis of these clinical isolates was performed upon arrival the results of which are tabulated in Table 3.3. Isolates that failed any of these criteria were discarded and those that showed growth on BAP (without an optochin disc) were further passaged and stored at 2 - 8 ºC for later use. These seed isolates were labeled as Pn19A PS1 (1 to 13).

Table 3.3: Colony morphology of Pn19A isolates on BAP.

Identity	Growth characteristic	α-haemolysis	Optochin sensitivity
Pn19A (1)	Poor	Positive	No*
Pn19A (2)	Poor	Positive	Yes
Pn19A (3)	Good	Positive	Yes
Pn19A (4)	Good	Positive	Yes
Pn19A (5)	Good	Positive	Yes
Pn19A (6)	Good	Positive	Yes
Pn19A (7)	Good	Positive	Yes
Pn19A (8)	Good	Positive	Yes
Pn19A (9)	Good	Positive	Yes
Pn19A (10)	Good	Positive	Yes
Pn19A (11)	Good	Positive	Yes
Pn19A (12)	Good	Positive	Yes
Pn19A (13)	Good	Negative*	No*

*Unclear

Table 3.4: Summary of tests performed and results obtained during the Pn19A pre-seed preparation**.**

Pre-seed	Original isolate from NICD
Colony characteristics on BAP	Smooth, uniform α-haemolytic colonies
Growth on TSA	Pure culture
Optochin	Susceptible
Growth at 36˚C	Growth
Growth at 25˚C	No growth
Bile solubility	Soluble
Gram stain	ND
Quellung reaction	Positive for serotype 19A
Susceptible to antibiotics*	Susceptible

*Antibiotics include penicillin, ceftriaxone, chloramphenicol, tetracycline, erythromycin, clindamycin
ND – not done as was already performed

Table 3.4 presents a tabulated version of the identification tools used for identifying *S. pneumoniae* clinical isolates investigated during this study. Following selection 1, two further selection steps were performed (Pn19A PS2 and PS3). PS3 was further passaged to obtain the PS4 for the preparation of LMSL and LWSL. To note, a healthy active inoculum was required as it leads to minimizing the lag phase or the start of the bacterium growth cycle as shown in the literature and confirmed in this study [134]. An observation made during this study was that CPS production based on the ELISA assay was highest just before the stationary phase was reached. In addition, harvesting at the stationary phase resulted in increased impurities such as nucleic acids making purification (Chapter 4) more challenging.

3.4.1 Selection 1

One cryovial from each of the Pn19A PS1 isolates (1-13) was inoculated into 20 mL modified Hoeprich's medium and 6 mL from each was dispensed into 15 mL Falcon tubes in triplicate. The tubes (for each isolate) together with the control (20 mL un-inoculated Hoeprich's medium), were incubated in a CO_2 incubator with 5% CO_2, 70% rH and shaking at 50 RPM for 3 h,3.5 h, 4 h and 4.5 h (these set parameters are further discussed in Chapter 4). A loopful of the remaining original inoculate culture (20 mL Falcon tube) was streaked on a BAP with optochin and incubated in the stationary compartment of the CO_2

incubator, the conditions of which have been described. After the allotted time, the tubes were removed from the incubator and analyzed for growth using OD_{600nm} as well as CPS production using the competition ELISA assay which is serotype specific for Pn19A. Competition ELISA is a measurement of total antibody to CPS and aids in the determination of the total concentration of CPS providing an alternate method to the less sensitive direct ELISA method.

3.4.1.1 Results and discussion

All 13 isolates displayed a monoculture of pneumococcus on BAP with optochin disk as well as α-haemolysis and optochin sensitivity. Based on OD_{600nm} evaluations (Figure 3.8), certain clones and time points were selected for CPS analysis (Figure 3.9) performed using the ELISA assay.

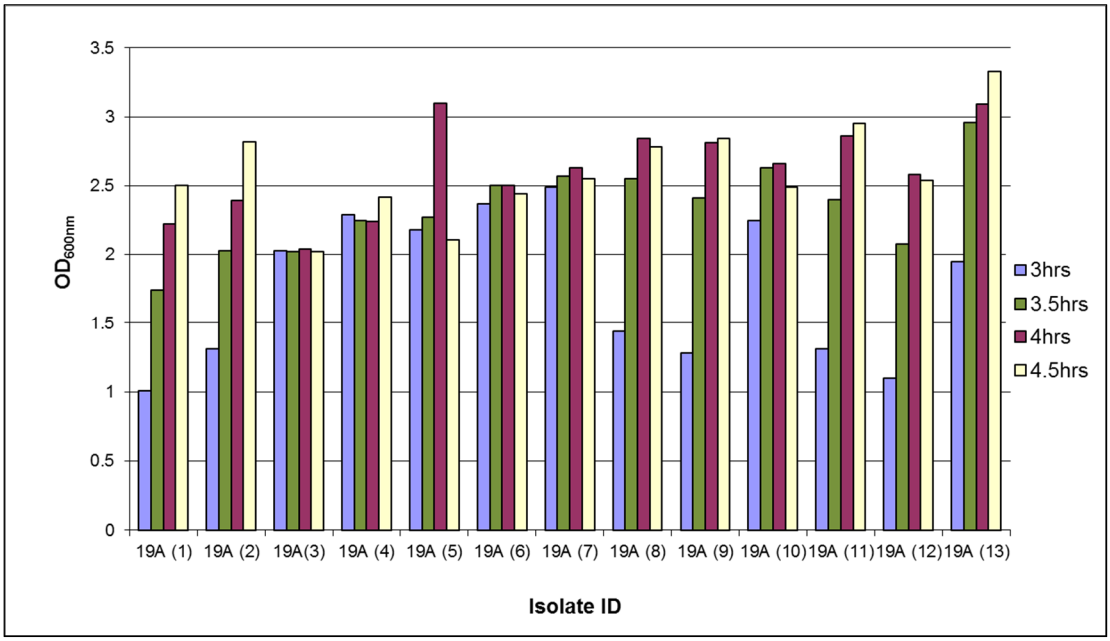

Figure 3.8: OD_{600nm} of Pn19A PS1 isolates during cultivation studies at 3, 3.5, 4 and 4.5 hours.

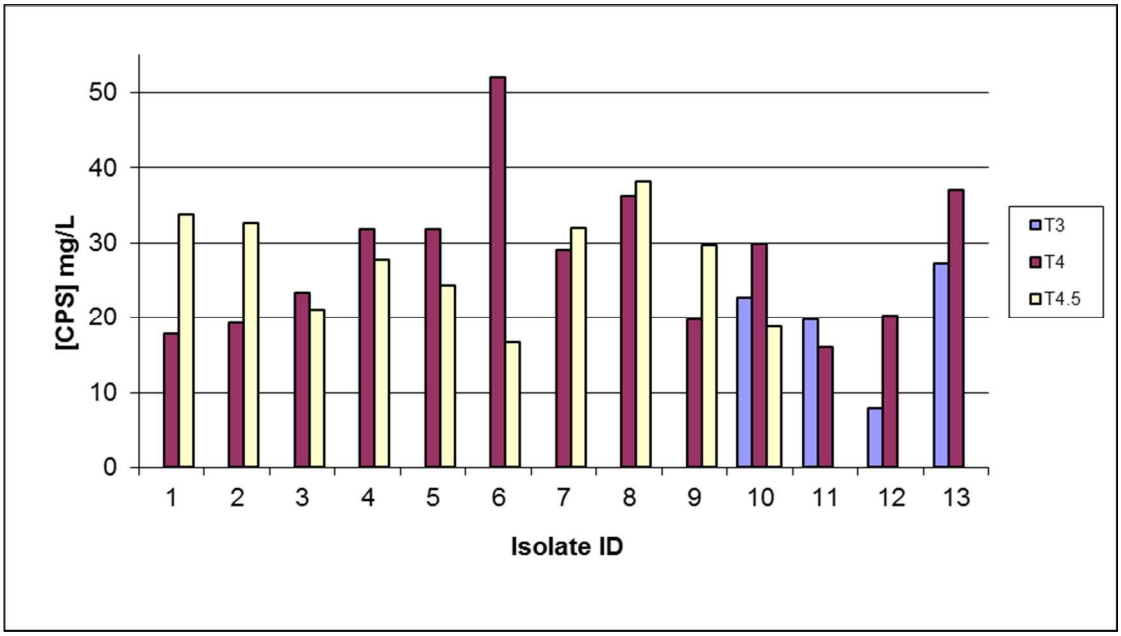

Figure 3.9: CPS concentration produced by Pn19A PS1 cultivation studies. T shows the time points in hours and the CPS concentration determined using the ELISA assay with ATCC standards.

The highest OD_{600nm} of 2.95 and 3.1 were reached at 4.5 and 4 h cultivation by Pn19A PS1 (11) and Pn19A PS1 (5), respectively shown in Figure 3.8. However, with respect to CPS production, Pn19A PS1 (6) showed the highest CPS production levels of 52.06 mg/L followed by Pn19A PS1 (8) as shown in Figure 3.9. As a result, Pn19A PS1 (6) and Pn19A PS1 (8) were selected for further passaging due to a combination of good growth and CPS production levels. Pn19A PS1 (13) was not considered as there was no defined zone of inhibition around the optochin disc to indicate α-haemolysis as listed in Table 3.3.

3.4.1 Selection 2

Having selected the Pn19A PS1 isolates 6 and 8 as high producers of CPS, one cryovial from Pn19A PS1 isolate 6 and 8 were thawed and incubated on Hoeprich's agar plates. Fifteen large opaque colonies were selected from each isolate (30 colonies in total). Each colony was used to inoculate 6 mL of pre-warmed Hoeprich's liquid medium in a 15 mL Falcon tube and incubated until turbid. Thereafter the cultures were immediately placed on ice to prevent further growth. The 15 mL Falcon tube cultures with colonies from Pn19A PS1 (6) were labeled as 6.1 to 6.15 and Falcon tube cultures with colonies from Pn19A PS1 (8) were labeled as 8.1 to 8.15. Six 1 mL culture aliquots containing 10% glycerol were frozen and stored at -80 ºC for each Falcon tube. This seed lot was labeled as Pn19A PS2 (6.1 & 8.1) to Pn19A PS2 (6.15 & 8.15). Cultures that had not grown after 10 h were left for a further 24 h. If growth was observed after 24 h, the cultures were frozen with glycerol. One cryovial from each of the above frozen lots was inoculated into 20 mL Hoeprich's medium of which 5 mL from each 20 mL inoculates were dispensed into 4 different Falcon tubes to account for 4 different incubation times. These tubes together with 20 mL un-inoculated Hoeprich's medium, as a control, were incubated for 2.5 h, 3 h, 3.5 h and 4 h. A loopful of each of the remaining 20 mL culture inoculate was streaked on BAP with optochin, and incubated in the CO_2 incubator as previously described. At the end of each incubation time (2.5 h, 3 h, 3.5 h and 4 h), the tubes were removed from the incubator and assessed for OD_{600nm} and CPS production by ELISA.

3.4.1.1 Results and discussion

Of the 15 colonies selected from Pn19A PS1 (6), all had grown after 8 h incubation and these were banked (seeded or stored in seed bank) as Pn19A PS2 (6.1 to 6.15). Out of 15 colonies selected from the seed bank Pn19A PS1 (8), only 13 grew after 8 h incubation. These were banked as Pn19A PS2 (8.1 to 8.13). Figures 3.10 and 3.11 show the growth profiles for clones 6 and 8 following the second passage. Based on previous experience with Pn1 an OD_{600nm} of above 2.5 was considered selection criteria for the suitable growth of the bacteria and was also an indication that the bacteria was in the exponential growth phase. The data analysis shows that isolate Pn19A PS1 (8.1 – 8.13) did not meet the specifications of an OD_{600nm} of above 2.5 and for this reason, it was not passaged further. However, this needed to be confirmed by CPS analysis. Based on the OD_{600nm} evaluations (Figures 3.10 and 3.11) clones were selected at different times of growth for CPS analysis, the results of which are displayed in Figures 3.12 and 3.13.

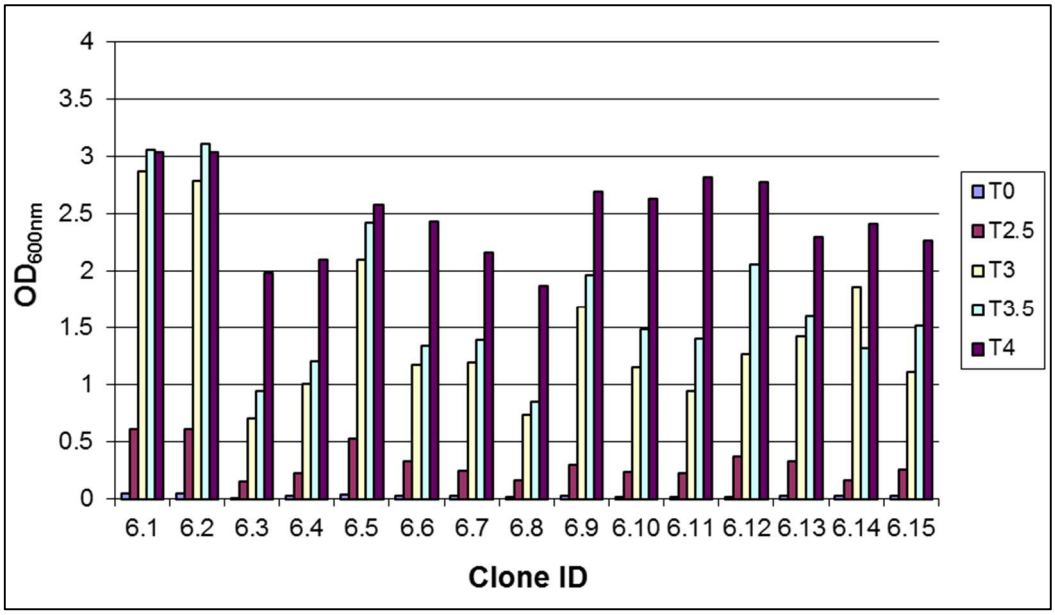

Figure 3.10: OD_{600nm} of Pn19A PS2 clones (number 6.1 to 6.15) during clonal selection studies. T shows the time points in hours.

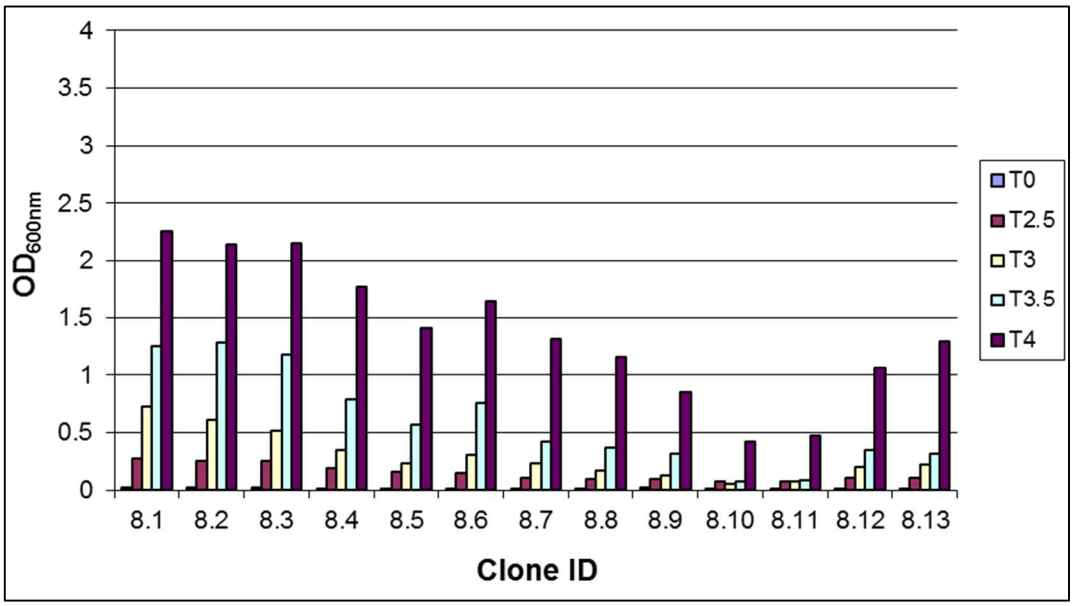

Figure 3.11 OD_{600nm} of Pn19A PS2 clones (number 8.1 to 8.13) during clonal selection studies. T shows the time points in hours.

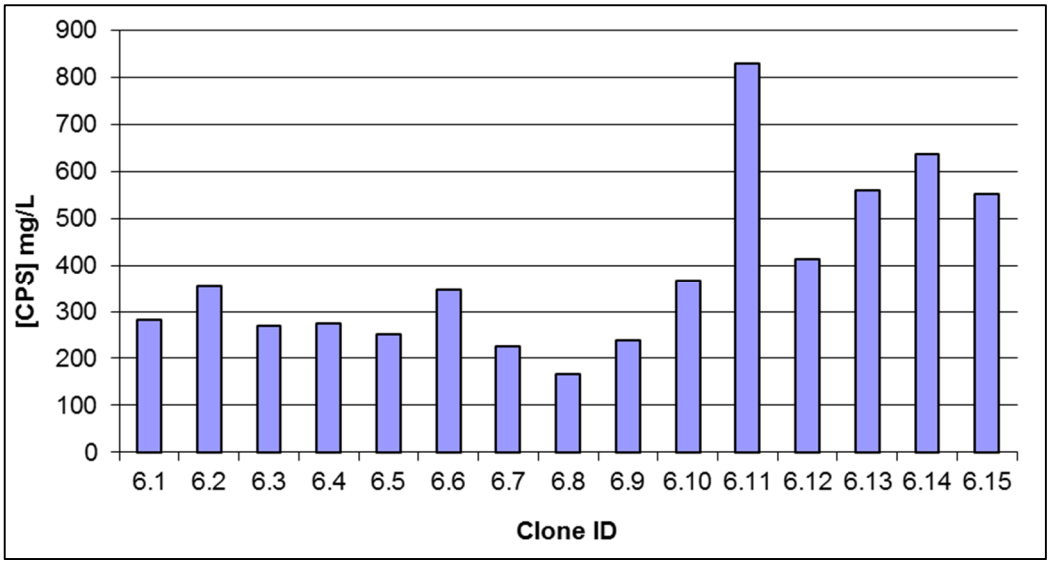

Figure 3.12: CPS concentration produced by Pn19A PS2 isolate 6 clones (1 to 15) during cultivation studies after 4 h determined by ELISA using ATCC standards.

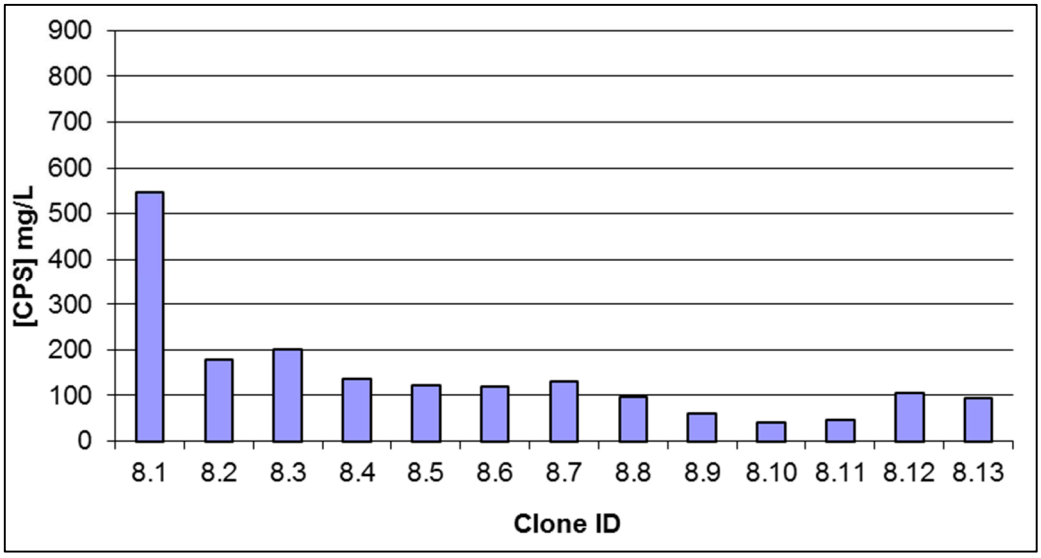

Figure 3.13: CPS concentration produced by Pn19A PS2 isolate 8 clones (1 to 13) during cultivation studies after 4 h determined by ELISA using ATCC standards.

The highest OD_{600nm} of 3.03 was observed after a 4 h cultivation for Pn19A PS2 (6.1 and 6.2). Pn19A PS2 (6.11) and Pn19A PS2 (8.1) produced the highest CPS of ±830 and ±550 mg/L respectively. Isolate 8.1, however, was not taken further because it did not reach an OD_{600nm} of 2.5 and isolate 6 produced significantly more CPS. Isolate 6 - Pn19A PS2 (6.11) was selected for further passaging based on an OD_{600nm} above 2.5 (or as close as possible to 2.5) and as a high CPS producer.

3.4.2 Selection 3

Having selected the isolates 6.11 as a high producer of CPS, one cryovial was thawed and streaked on Hoeprich's agar plates. The clonal selection strategy used for Pn19A PS3 was similar to Pn19A PS2 with a few exceptions. The incubation times increased from 4 h to 6.5 h and the amount of colonies selected decreased from 15 to 10 colonies. The frozen samples collected during the cultivation study were thawed and submitted for CPS analysis using ELISA.

3.4.2.1 Results and discussion

After 6 h incubation, all colonies selected from Pn19A PS3 (6.11) grew to OD_{600nm} levels above 2.5 and were labeled Pn19A PS3 (6.11.1) to Pn19A PS3 (6.11.10). Six aliquots of each isolate that grew were frozen with glycerol. The third passage shown in Figure 3.14 indicates the growth profiles for clone 6. An OD_{600nm} of above 2.5 was the selection criteria for the suitable growth of the bacteria and an indication that the bacteria was in the exponential growth phase. The ideal time to harvest was during the exponential growth phase just before stationary phase. Early stationary phase was seen to be suitable but with more of the culture proceeding into the stationary phase and ultimately into death phase more problems arose during the purification process. There was also a dramatic decrease in CPS levels as death phase approached. Samples were taken at various time points to get close to late exponential or early stationary phase. Sampling occurred often but due to the rapid doubling time of pneumococci determining the late exponential or early stationary phase proved difficult.

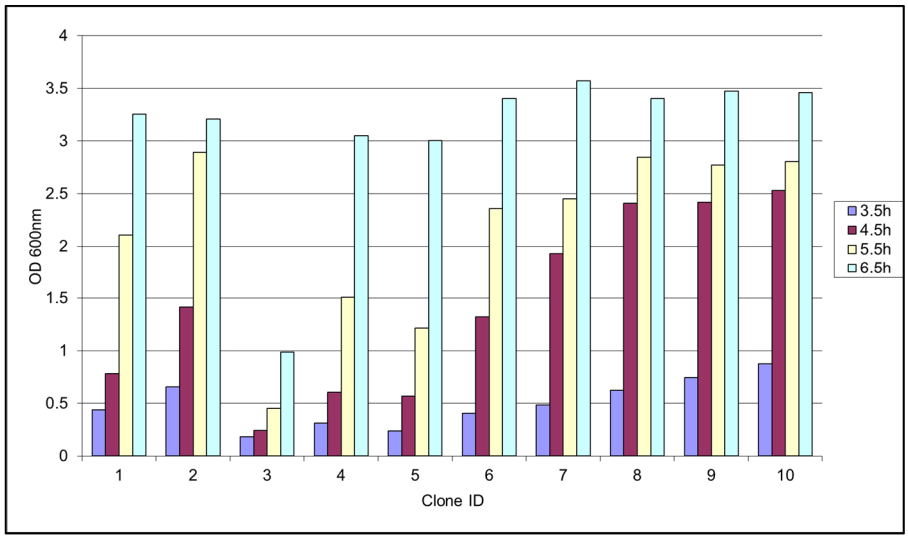

Figure 3.14: OD_{600nm} of Pn19A PS3 of clones (6.11) 1 to 10 during pre-seed 3 clonal selection studies. T shows the time points in hours.

Based on the OD_{600nm} evaluations, clones were sampled at different incubation times of growth i.e. 3.5 to 4.5 h or 5.5 to 6.5 h for CPS analysis, the results of which are shown in Figure 3.15.

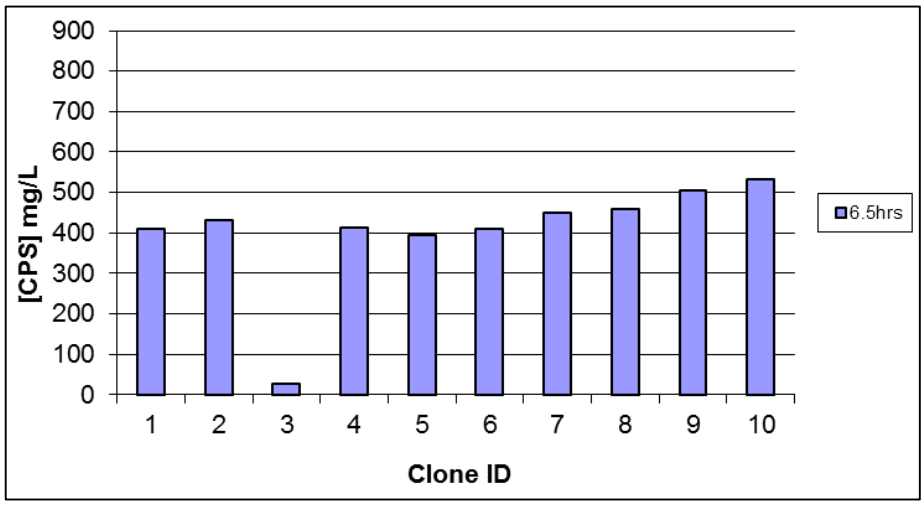

Figure 3.15: CPS concentration produced by Pn19A PS3 (6.11.1 – 6.11.10) cultivation studies after 6.5 h determined by ELISA using ATCC standards.

The highest CPS levels for Pn19A PS3 (6.11.10) was ± 530 mg/L (Figure 3.15) compared to PS2 that obtained levels of ± 830 mg/L. Sampling for CPS production was performed at 6.5 h and due to testing at this time bacteria could have been in or close to death phase hence the CPS production appears lower in PS3 than in PS2.

As Pn19A PS3 (6.11.10) was the highest producer, it was selected to prepare Pn19A PS4, the Pn19A pre-seed. Pn19A PS3 (6.11.3) was the slowest grower as the ODs obtained reached approximately 1 which resulted in the lowest producers of CPS for Pn19A. This is an indication of a correlation between biomass/growth of bacteria (as shown by OD levels) and the amount of CPS produced.

3.4.3 Conclusion

A Pn19A pre-seed (PS) was successfully prepared, based on clonal selection by growth and CPS production analysis. There was a three-step selection process with each step generating a PS. Upon comparing selection 3 with selection 1, there was a 10 fold increase in CPS levels of isolate 6.11.1 showing that with clonal selection the bacteria adapted to the medium and resulted in increased production of CPS. This justifies the clonal selection process. Pn19A PS4 was subsequently used for the production of a LMSL and a LWSL for the development of a Pn19A fermentation process and could potentially be further utilized to produce a cGMP LMSL for production purposes (Section 3.5). The results of the tests performed on each pre-seed is summarized in Table 3.5.

Table 3.5: Summary of tests performed and results obtained during the Pn19A pre-seed preparation.

Pre-seed	Original isolate from NICD	Pn19A PS1 (6)	Pn19A PS2 (11)	Pn19A PS3 (10)	Pn19A PS4
Colony characteristics on BAP	Smooth, uniform α-haemolytic colonies	Smooth, uniform α-haemolytic colonies	Smooth, uniform α-haemolytic colonies	Smooth, uniform α-haemolytic colonies	Smooth, uniform α-haemolytic colonies
Growth on TSA	Pure culture	Pure culture	Pure culture	Pure culture	Pure culture
Optochin	Susceptible	Susceptible	Susceptible	Susceptible	Susceptible
Growth at 36˚C	Growth	Growth	Growth	Growth	Growth
Growth at 25˚C	No Growth	ND	ND	ND	Poor growth
Bile solubility	Soluble	ND	ND	ND	Soluble
Gram stain	ND	ND	ND	ND	*Diplococcus* Gram-positive
Quellung reaction	Positive for serotype 19A	ND	ND	ND	Positive for Serotype 19A
Susceptible to antibiotics*	Susceptible	ND	ND	ND	ND

*Antibiotics include penicillin, ceftriaxone, chloramphenicol, tetracycline, erythromycin, clindamycin

ND – not done

Table 3.6: Passage summary of pre-seed Pn19A PS4 preparation.

Steps #	Description *
1	PS4 was streaked on fresh Blood Agar Plates (BAP) and incubated for ~24 h.
2	A loopful from BAP was transferred into 12 mL Hoeprich's liquid medium and incubated for 20 h at 36 ºC, 70% rH,10% CO_2 saturation, and an agitation rate of 100 RPM (**Pn19A PS1 isolate 6**).
3	A loopful from **Pn19A PS1 isolate 6** was streaked onto a fresh Hoeprich's agar and incubated for 48 h.
4	A single colony was transferred into 6 ml Hoeprich's medium. The culture was incubated for ~ 4 h in sterile 15 mL Falcon tubes (6 mL working volume) as indicated above (**Pn19A PS2 isolate 11**).
5	A loopful of cells from **Pn19A PS2 isolate 11** was streaked onto fresh Hoeprich's agar and incubated for 24 h.
6	A single colony was transferred into 6 mL Hoeprich's liquid medium and incubated for ~ 4 h in sterile 15 mL Falcon tubes as indicated above (**Pn19A PS3 isolate 10**).
7	One cryovial of **Pn19A PS3 isolate 10** was used to inoculate 20 mL Hoeprich's liquid medium in a 50 mL Falcon tube and incubated for ~4 h as indicated above until OD_{600nm} of 0.35 was obtained.
8	Twenty (20) mL of Passage 7 was used to inoculate 180 mL Hoeprich's liquid medium in a 500 mL disposable Erlenmeyer flask and incubated for 4 h as indicated above until an OD_{600nm} of 1.82 was obtained. Two hundred mL of culture containing 10% sterile glycerol (total volume) was cooled on ice and aliquoted into two hundred 1 mL cryovials and frozen at -80 ºC. This seed bank was designated **Pn19A PS4**.

*The selected isolates are represented in bold.

3.5 Preparation of laboratory master and working seeds

3.5.1 Introduction

Preparation of a laboratory seed was required to establish a master and working seed to be used during *S. pneumoniae* small and large scale cultivation. A summary of the methodology and passages used to obtain this seed is summarized in Table 3.6. The aim of this study was to prepare LMSL and LWSL for Pn19A from Pn19A PS4, the selected clonal isolate for process development and fermentation experiments. Culture integrity was confirmed by Gram stain morphology analysis, colony morphology and hemolysis, optochin susceptibility, bile solubility and Quellung (Figure 3.2 and 3.3 and Tables 3.1 and 3.2).

3.5.2 Methods

3.5.2.1 Confirmation of the pre-seed identity and purity

Pn19A PS4 cryovials (x2) were used to inoculate, 2 x 50mL Falcon tubes containing pre-warmed 20 mL modified Hoeprich's medium. The Falcon tubes were incubated at 50 RPM, 36 ºC, and 70% rH for 2.5 h. The optical density at a wavelength of 600 nm (OD_{600nm}) was measured in triplicate, at inoculation and at the termination of cultivation. Uninoculated Hoeprich's medium was incubated under the same conditions and used as a control. When the OD_{600nm} reached between 1.5 and 2.5, a loop-full of each culture was used to aseptically streak two pre-heated BAPs i.e. four plates in total. The streaked plates were incubated at 36 ºC, 70% rH and 10% CO_2 for 24 h. Two of the four plates were then sealed with parafilm, packed and shipped to the NICD for identity testing in order to confirm that the pre-seeds matched the original isolate supplied. (See Table 3.5 for a list of tests performed).

3.5.2.2 Preparation of the laboratory master seed lot (LMSL)

A cryovial of Pn19A PS4 was used for preparation and seeding of the Pn19A LMSL. One cryovial of Pn19A PS4 was inoculated into 20 mL Hoeprich's medium and placed in a CO_2 incubator (parameters

as per Section 3.4) for 2 – 3 h. The turbid culture was transferred to the Erlenmeyer flask containing 180 mL Hoeprich's medium and incubated in a CO_2 incubator (parameters as above) for 2 – 4 h. When an OD_{600nm} of between 1 and 1.5 was reached, it was immediately placed on ice to stop or slow down the growth of the bacteria. Glycerol (10%) was added to the culture and mixed by swirling. The LMS was aseptically dispensed (1 mL) into 200 cold cryovials and stored at -80 ºC until further use.

3.5.2.3 Preparation of the laboratory working seed lot (LWSL)

Following preparation of the LMSL, a cryovial of Pn19A LMSL was used for the preparation and seeding of Pn19A LWSL. One cryovial of LMSL was inoculated into 20 mL Hoeprich's medium and placed in a CO_2 incubator (parameters as section 3.4) for 2 – 3 h. The turbid culture was transferred to the Erlenmeyer flask containing 180 mL Hoeprich's medium and incubated in the CO_2 incubator (parameters as above) for 2 – 4 h. Once the culture reached an OD_{600nm} of between 1 and 1.5, it was placed on ice immediately to stop or slow down the growth of the bacteria. Glycerol (10%) was added to the culture and mixed by swirling. The LWS was aseptically seeded (1 mL) into cold cryovial and stored at -80 ºC until further use.

3.5.3 Results and discussion

The Pn19A PS4 was tested by NICD and the *S. pneumoniae* serotype 19A identity confirmed (Table 3.7). The serum antibodies used in performing the quellung reaction was based on antisera from different pools and serotypes in serogroup 19 to determine if the samples were serotype 19A.

Table 3.7: Identity confirmation tests and results (carried out by the NICD) of Pn19A PS4.

Sample	PS4 sample 1	PS4 sample 2	NICD Ref**
Purity	Pure growth	Pure growth	Pure growth
Gram stain	Positive diplococci	Positive diplococci	Positive diplococci
Optochin	10.5 mm	11 mm	11 mm
Bile solubility	Positive	Positive	Positive
Quellung*	Pool B+, Pool P+, 19b-, 19c+,19f-,19h-	Pool B+, Pool P+, 19b-, 19c+,19f-,19h-	Pool B+, Pool P+, 19b-, 19c+,19f-,19h-
Serotype	19A	19A	19A
Growth at 37 ºC	Yes	Yes	Yes
Growth at 25 ºC	No	No	No
lytA PCR	+	+	+
lytA PCR ct value	14	16	13
Genes	19A	19A	19A

* Positive reaction in accordance with the WHO TRS identification of Pn19A pneumococci. The serum antibodies used in performing the quellung reaction was based on antisera from different pools and serotypes in serogroup 19 to determine if the samples were serotype 19A.
** Reference of the original isolate obtained from GERMS-SA.

Based on these results, the Pn19A PS4 was released for use in the preparation of Pn19A LMSL and production of Pn19A LWSL. The stock cultures of Pn19A LMSL and LWSL were seeded at OD_{600nm} values of 2.75 and 3.21 respectively (Table 3.8). Seed viability on BAPs at a 10^{-7} dilution of Pn19A LMSL and LWSL were at approximately 18 and 11 colony forming units per mL (CFU/mL), respectively. Sterility plating on Tryptic Soy Agar (TSA) plates of Pn19A LMSL sample indicated that it was a monoculture. Further testing of Pn19A LWSL (Table 3.7) confirmed Pn19A identity. The Gram stain

showed these seeds were positive for bacteria containing a cell wall, confirmed by the Quellung reaction that presents the cell wall as a halo surrounding the bacteria. The growth on blood agar and the presence of hemolysis, as well as its sensitivity to optochin, again confirmed the presence of *S. pneumoniae*.

Table 3.8: Identity and viability confirmation of the Pn19A LMSL and LWSL prepared at Biovac.

Sample	Gram strain	Growth on BAP and hemolysis	Quellung	Optochin sensitivity Y/N	OD_{600nm}	CFUs/mL
LMSL	positive diplococci	+	19A positive	Y	2.75	1.8×10^8
LWSL	positive diplococci	+	19A positive	Y	3.21	1.1×10^8

+Positive reaction in accordance with the WHO TRS identification of Pneumococcus.

3.5.4 Conclusion

Testing of the Pn19A PS4 pre-seed by the NICD confirmed the purity and identity of *S. pneumoniae* serotype 19A. The Pn19A LMSL and LWSL were successfully prepared and also confirmed as a monoculture of *S. pneumoniae* serotype 19A.

3.6 Inoculum train development

3.6.1 Introduction

The inoculum train, also known as the seed expansion train, refers to the expansion of cells from the frozen seed lot to the inoculation of the production bioreactor/fermenter vessel. Results obtained during the inoculum train development can also be used to establish culture growth characteristics. The starting seed lot cell density and viability, as well as the starting volume of the production vessel and production time, are parameters that will influence the number of passages and final inoculum density required [135]. An additional factor was the requirement by the national regulatory authority of South Africa (Medicine Control Council (MCC)) that “the number of passages between the seed lot and finished product during pilot-scale should be consistent with the medicine registration dossier and scale up to production scale should not change this fundamental relationship” [136]. This means that the inoculum passages required for small scale cultivation and development should be the same as the intended scale for production.

For microbial processes, the inoculum train has a substantial impact on process performance in terms of productivity, profitability and process control [137]. A well-characterized and robust inoculum train is essential for passage consistency, scale-up and implementation of the process in a manufacturing setting [137].

Factors that need to be considered when developing an inoculum preparation strategy include [138]:

- Medium composition;
- Cultivation parameters;
- Microbial growth dynamics;
- Optimum transfer criteria (qualitative inoculum variable);
- Volume of inoculum on transfer (biomass concentration);

- Number of seed-stage passages;
- Reproducibility.

The generation of inoculum for large-scale production by fermentation generally necessitates a build-up of active biomass through multiple growth cycles. In developing the multiple-growth cycle seed train, several experimental objectives had to be met. The first of these was defining the seed medium to minimize nutrient shift effects while supporting good growth over a short time scale. The development of an optimum Pn19A inoculum train and inoculum size was performed to achieve the seed expansion phase, the growth characteristics and behavior of the Pn19A bacterium in shake flasks. The experiments were performed on Pn1 after which growth conditions were applied to Pn19A with modifications.

The second objective was to investigate the effect of the inoculum size on pneumococcal CPS production and growth. Various inoculum sizes have been used in different studies starting from 0.1% in small-scale cultivation of *S. pneumoniae* using strain Rx1 as reported by Liberman, (2008) [120, 139]. Another approach for standardizing the inoculation of the bioreactor was to obtain a constant initial OD. An initial OD of 0.1 at 625 nm was used in the cultivation of *S. pneumoniae* serotype 23F strain whilst an initial OD of 0.1 at 600 nm was preferred in the cultivation of *S. pneumoniae*, strain Rx1 [26, 120].

The aim of this study was to evaluate two inoculum sizes, whereby the growth kinetics of the pneumococcus LWSL, at different inoculum train passages in 200 mL shaker flask cultivation at both 5 and 10% inoculum ratios were compared. Trial studies were conducted on Pn1 as Pn19A was not available at this stage of the study. The findings for Pn1 were subsequently applied to Pn19A.

3.6.1 Methods

No significant difference on either biomass or CPS yields, (data not shown) were observed in either the Erlenmeyer flasks or Schott bottles for Pn1. It was therefore decided that Pn1 cultivations would be carried out in 50 mL Falcon tubes and Schott bottles. A 20 mL aliquot of Hoeprich's medium (supplemented with 500 U/mL catalase) was aseptically dispensed into 10 x 50 mL Falcon tubes, 190 mL into 6 x 250 mL Schott bottles and 180 mL into 6 x 250 mL Schott bottles. Each Falcon tube or Schott bottle was pre-warmed for 0.5 – 1 h at 36 ºC before inoculation. The inoculum train experiment is depicted in Figure 3.16.

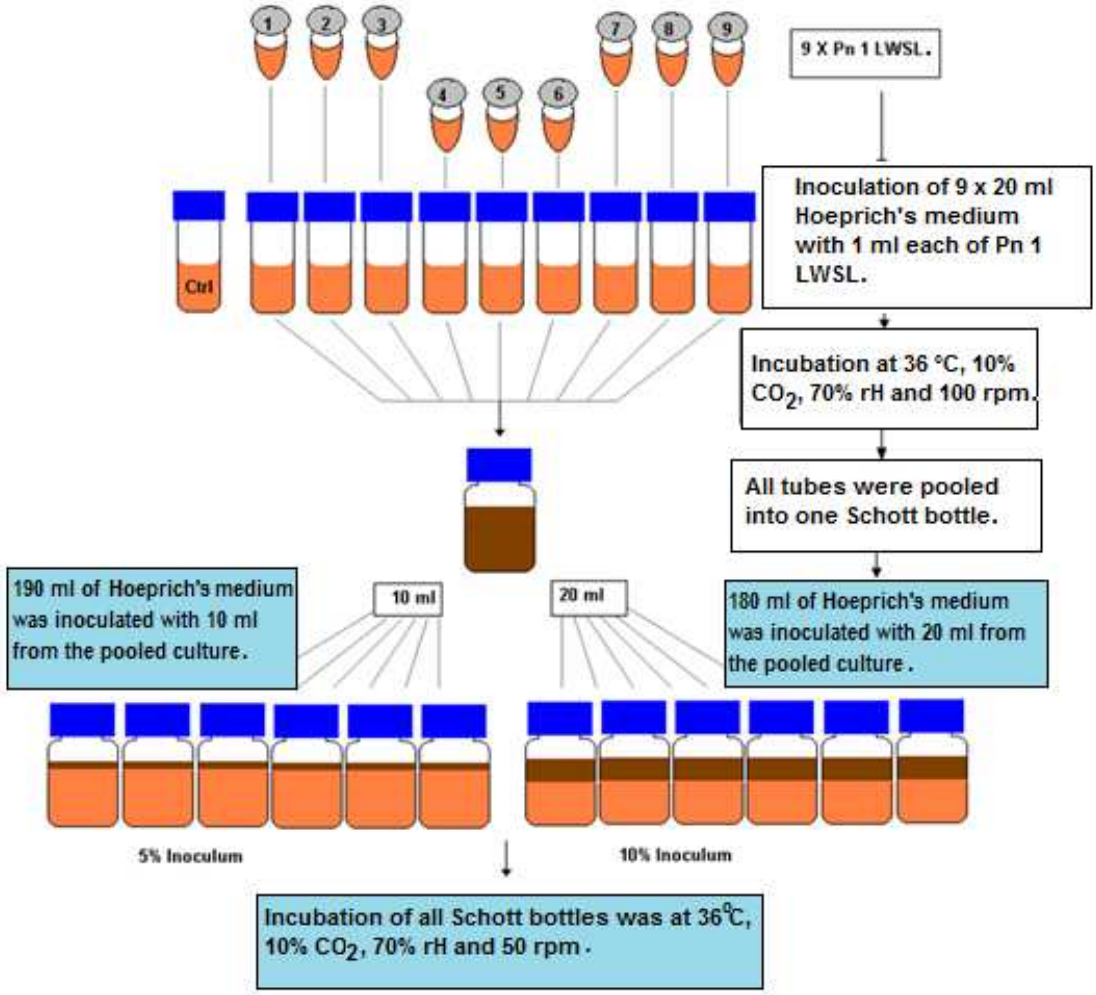

Figure 3.16: Schematic of the inoculum train experiment.

For Passage 1, nine cryovials of Pn1 LWSL were removed from the -80 ºC ultra-low freezer and thawed by rolling between the hands. Nine Falcon tubes with 20 mL of Hoeprich's medium were aseptically inoculated with 1 mL of Pn1 LWSL. An additional tube with uninoculated medium was used as a control. The initial OD_{600nm} was measured (in triplicate) for each Falcon tube followed by incubation of all tubes in a CO_2 incubator at 36 ºC, 10% CO_2 saturation, 70% rH, and 100 RPM. During incubation, the OD_{600nm} for each tube was measured at 30 min intervals in triplicate and upon reaching OD_{600nm} values of between 0.70 - 2.00 (~2.5 h), all tubes were pooled into a sterile 250 mL Schott bottle and a final OD_{600nm} reading of the mixture was measured (in triplicate).

For Passage 2, a 5% inoculation sample was prepared by aseptically inoculating 10 mL of culture from the pooled Passage 1 into each of six 250 mL Schott bottles, each containing 190 mL Hoeprich's medium supplemented with catalase (500 U/mL). Similarly, 20 mL of the pooled Passage 1 culture was aseptically inoculated into each of six 250 mL Schott bottles containing 180 mL media and catalase (500 U/mL) to produce a 10% inoculum. The initial OD_{600nm} was measured immediately after inoculation from one Schott bottle of each inoculum preparation. The two batches of six inoculated Schott bottles were incubated as described in Figure 3.16 at 50 RPM. Only one Schott bottle from each batch was sampled for OD_{600nm}, viability (Trypan blue stain), Gram stain and the optochin test to confirm

identification and purity, at 30 min intervals for 3 h. Glucose consumption, pH and CPS yields by ELISA assay were also measured for this passage.

3.6.2 Results and discussion

The OD_{600nm}, glucose consumption and pH measured at 30 min intervals, during Passage 2 of the four Passage inoculum train experiment are shown in Figure 3.17(A) for 5% and Figure 3.17(B) for a 10% inoculum. The development of a four Passage inoculum train was obtained using Pn1 to determine consistency and scalability of CPS production in a manufacturing setting. The data presented here shows an indication of which inoculum size would obtain the best results for manufacturing pneumococcal CPS.

From the data, it was seen that the OD_{600nm} increased exponentially for both the 5% and 10% Passage 2 inoculums. Glucose consumption, growth (OD_{600nm}) and pH levels followed a similar pattern for both inoculum sizes. The 5 % inoculum, however, showed a slightly better increase after 2.5 hours and there was still culture growth after 3 hours whereas the 10 % inoculum started to decrease after 3 hours. The data showed that the best transfer period between passages was during the logarithmic growth phase which was observed between 1.5 and 2 h for the 5% inoculum and between 1 and 1.5 h for the 10% inoculum.

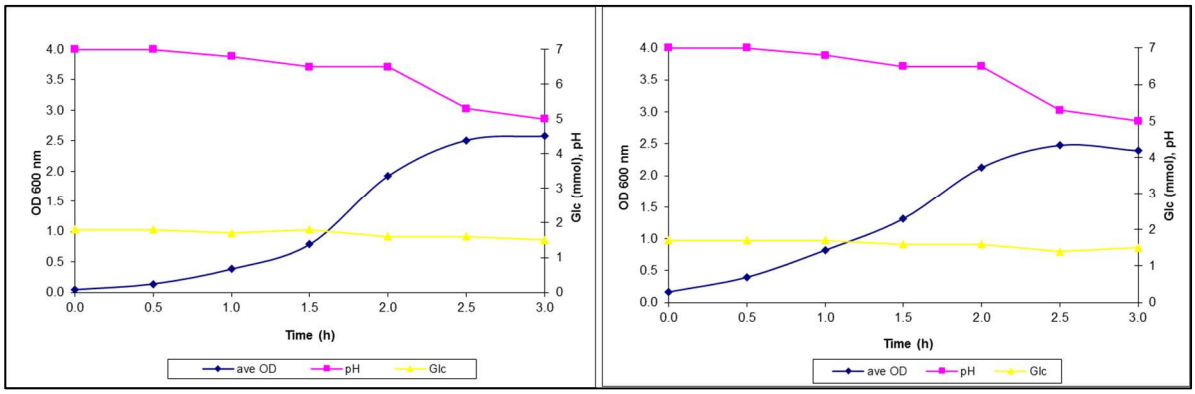

(A) **(B)**

Figure 3.17: Growth profile of Pn1 LWSL in Hoeprich's medium with 5% and 10% inocula (A) and (B) respectively**.**

The CPS production of the Passage 2 cultures at the indicated inoculum ratios was investigated as shown in Figure 3.18 at 3.5 h growth and showed that a 10% inoculum ratio had higher CPS yields. The higher CPS production could possibly be attributed to more competition towards nutrients earlier in the initial lag and early log phase of the culture growth, due to more active growing cells being available. This competition could induce the cells to undergo stress, forcing higher and earlier CPS production in 10% inoculum compared to 5% inoculum cultures. Further investigations would be required to understand the impact of this stress. When applying a statistical test such as the t-test it was observed that there was no significant difference in CPS production between the 5% and 10% inoculums (data not shown).

It is important to note that with extra time the 5% inoculum may certainly achieve higher CPS levels, especially in a manufacturing environment. However when developing a process for small scale analysis, time effectiveness which ultimately translates to cost effectiveness, is something to consider.

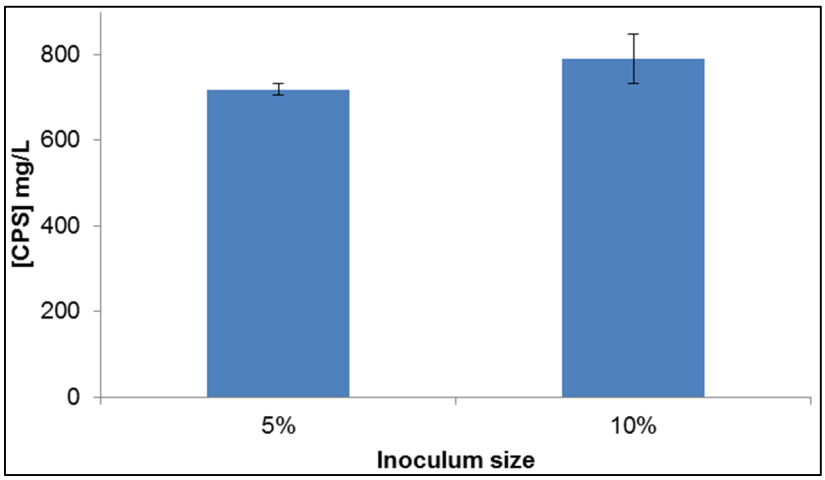

Figure 3.18: Passage 2 CPS levels determined by ELISA using ATCC standards of 5% inoculum and a 10% Pn1 inoculum batches obtained after 3.5 h.

These experiments show the necessity of the inoculum size and train studies in that the 10% inoculum showed a reduced lag phase in comparison to the 5% inoculum. The specific growth rate (μ) for the 10% culture was higher than 5% culture at $\mu = 1.8\ h^{-1}$ and $\mu = 1.4\ h^{-1}$ respectively. Both cultures (5% and 10%) reached an OD_{600nm} above 1 between 1 and 2 hours, the 10% culture reached an OD_{600nm} above 1, approximately 30 min faster than the 5% inoculum but this was not considered to be a significant difference as determined by the growth rate between these cultures. When performing a t-test the difference between the 5% and 10% inoculums were not considered statistically significant as the two-tailed p-value was high. Based on the scalability of a four passage inoculum train as shown in Figure 3.19, a 10% inoculum can be scaled up to 20 L, 8x less than what could be obtained with a 5% inoculum provided the whole inoculum was used. The 5% inoculum is scalable to 160 L, a factor to consider when choosing an inoculum size.

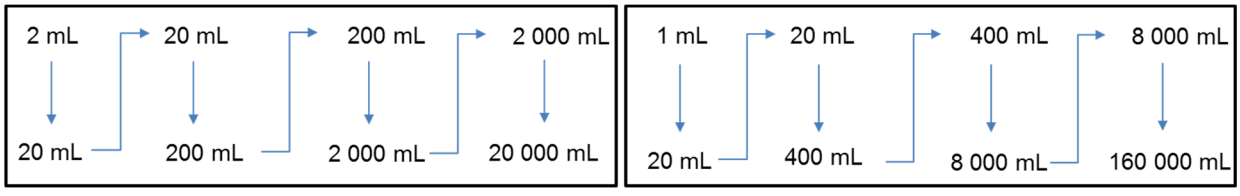

Figure 3.19: Illustrating the end product of a four Passage inoculum train using 10% (left) and 5% inoculum (right) sizes.

A 5% Pn1 fermentation inoculum train was used to prepare all 15 L Pn1 fermentation and a 7 L Wave bioreactor runs as detailed in Chapter 4. It is also recommended from studies performed at Biovac that a four passage train be used to ensure passage consistency to scale up pneumococci incubation.

3.6.3 Conclusion

In order to ensure passage consistency for scale up of Pn1 cultivation, these studies recommend a four-passage train to be followed. This follows the selection passaging of the isolate for LMSL and LWSL. For Pn1 a constant 5% transfer volume for each inoculum, passage was reproducible and allowed rapid growth upon transfer. A 10% CO_2 environment was successfully employed during the inoculum stages at a cultivation temperature of 36 ºC. A four-passage inoculum train using a 5% inoculum was used as it provided better scalability without loss of product when compared with the 10% inoculum for a manufacturing environment.

3.6.4 Pn19A cultivation

For Pn19A cultivation, as for Pn1, a four passage inoculum train was implemented as shown in Figure 3.20. Following selection of the Pn19A isolate at the Pre-seed 2, 3 and 4 levels, it was concluded that each passage in the inoculum train would be incubated between 2.5 and 3 h for all 4 – 5 L shaker culture and 7 L fermentation runs. From the aforementioned studies, it was recommended that a 5% inoculate be used during the Pn19A studies as there was no significant difference between the 5% and 10% inoculations. The inoculum train for Pn19A (Figure 3.20) comprised four passages incubated between 2.5 and 3 h to ensure that the final passage OD_{600nm} was above 1 (Figure 3.21). It was noted that the OD_{600nm} range for inoculation could be as low as 0.8. This range ensured that the bacteria were in the logarithmic growth phase during the transition to the next phase (Figure 3.22), which is the optimum transfer period.

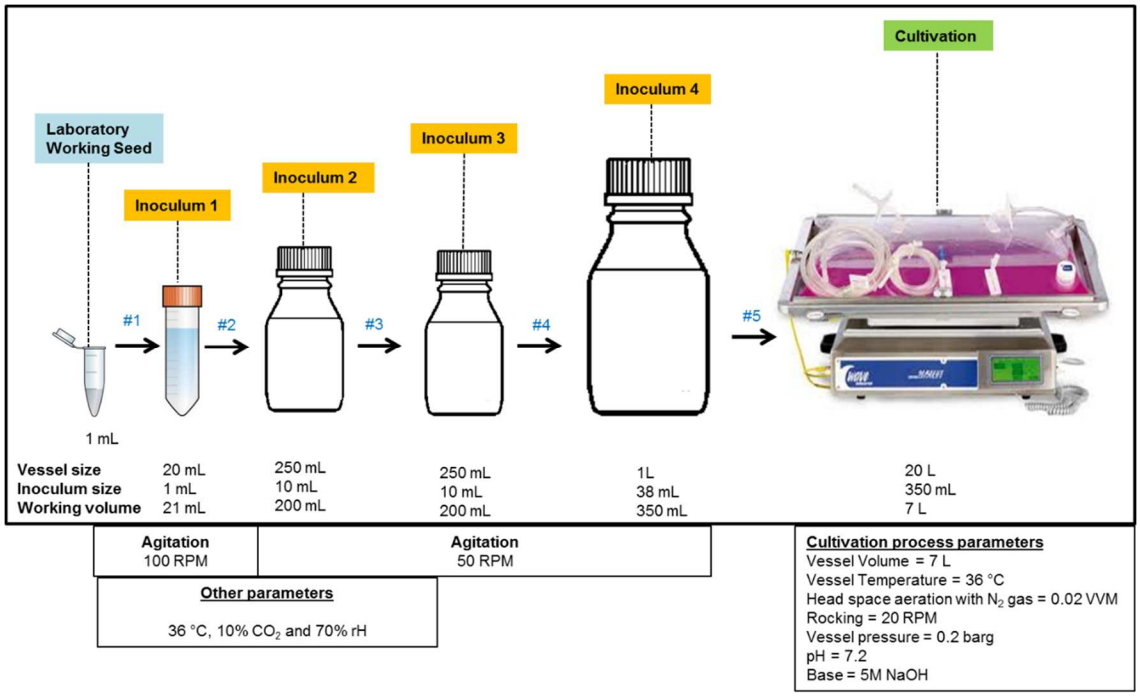

Figure 3.20: Process flow diagram of Pn19A fermentation at 7 L fermentation volume.

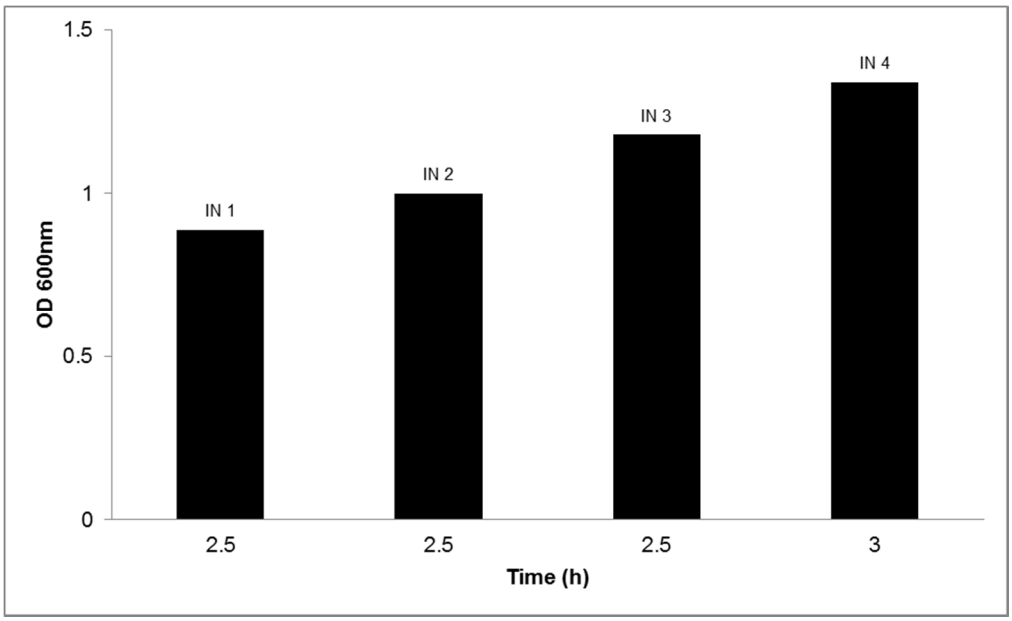

Figure 3.21: The inoculum train for Pn19A comprised four passages (IN 1, IN 2, IN 3 and IN 4) incubated between 2.5 and 3 h to ensure that the final passage OD_{600nm} was above 1.

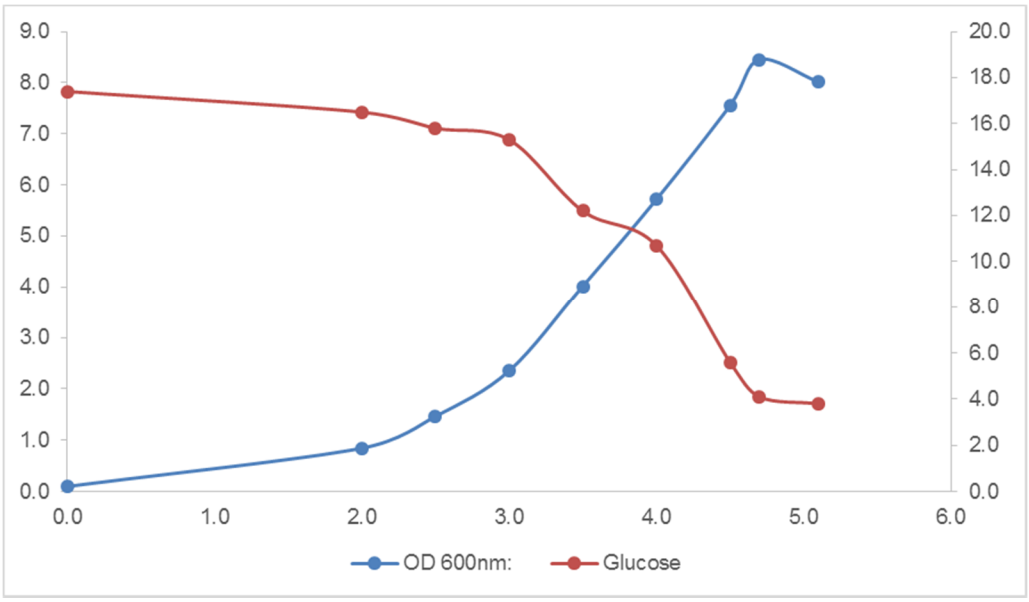

Figure 3.22: Logarithmic growth curve of *S. pneumoniae* serotype 19A after 5 h cultivation (blue) indicative of the depletion of glucose (red) upon completion of the batch cultivation.

3.7 Investigation of culture inactivation

3.7.1 Introduction

S. pneumoniae is a BSL 2 organism (WHO replacement of Annex 2, TRS 927) and BSL 3 when cultivated at volumes above 2.0 L. As such, care is required to ensure efficient inactivation of the fermentation culture before further processing [74]. The purpose of bacterial inactivation is two-fold, to kill the organism for further processing and to cleave CPS from the cell surface for release into the supernatant. A key component of the inactivation strategy is the maintenance of the integrity of the CPS post inactivation.

Generally, bacterial inactivation can be achieved using physical, enzymatic or chemical strategies. A physical approach of inactivating *S. pneumoniae* was through exposure to heat at approximately 60 ºC for 30 min. A study by Hvalbye et al. [140] (1999), demonstrated that inactivation of *S. pneumoniae* serotype 4 could be accomplished by heating in a water bath set at 56 ºC for 30 min. Chemicals employed in inactivation include formaldehyde or glutaraldehyde, β–propiolactone, phenol (carbolic acid) and sodium deoxycholate (DOC) [141]. The agent is chosen for effectiveness without destruction of antigenicity. Formaldehyde or glutaraldehyde causes inactivation by cross-linking and a condensate form of formaldehyde is commonly used as disinfectants. β–propiolactone is a highly reactive and bind with nucleic acids and proteins [142, 143]. These reagents are known to be carcinogenic and therefore were not considered for this study.

Phenol is known as a gross protoplasmic poison. Its mode of action is through penetration and disruption of the cell wall as well as precipitation of cell proteins [144]. In the 1950's, pyrogenic polysaccharides were isolated from bacteria by treatment with phenol and water extraction at 68 ºC [145]. Camacho et al. [146] (2013), further demonstrated that the use of phenol and heat inactivation of *Shigella flexneri* had a marked disruptive effect on the integrity of the cell when compared to 2-bromoethylamine hydrobromide (BEA). It was shown that the use of 0.5% phenol throughout this study causes both cell disruption and complete release of CPS [146].

Sodium deoxycholate (DOC) has also been shown to achieve the release of the CPS on killing of the bacteria [26]. Gonçalves et al. [26, 147] (2002), treated whole culture samples of *S. pneumoniae* serotype 23F strain St 99/95 with 1% DOC to achieve the release of CPS from the cell surface by releasing autolysin, an enzyme responsible for cleaving the cell wall polysaccharide (CWPS) containing peptidoglycan. The DOC process has been shown to reduce protein contamination while preserving the integrity of the CPS [148].

Two inactivation strategies phenol and sodium deoxycholate were compared and investigated as methods of inactivation. The goal was to obtain an effective release of CPS into the culture supernatant with as little contamination (CWPS (< 3% recommended), nucleic acid and total protein) as possible. Phenol and DOC have been used to inactivate *S. pneumoniae* for the production of conjugate vaccines. In this study, the phenol inactivation method was adapted from an expired patent by Liveyns, [145] (1989). The effectiveness of inactivation was evaluated at both room temperature (RT) (18 – 22 ºC) and 2 – 8 ºC. A concentration of at least 0.8 w/v% phenol and 0.12% DOC was added to *S. pneumoniae* culture for the preparation of the pneumococcal polyvalent vaccine [145]. Cell viability and both CPS and CWPS levels in the culture supernatant, after cell separation by centrifugation, were evaluated using the ELISA assay. The following Section details the establishment of Pn1 inactivation under small and large scale conditions and its subsequent application to Pn19A.

3.7.2 Small scale shaker culture inactivation

3.7.2.1 Introduction

In order to ascertain a chemical killing strategy all experiments were conducted at a 2 L scale. Shaker cultures were performed on Pn1 LWSL to establish an inactivation method on a small scale using both phenol and DOC solutions. According to the literature, a final concentration of 1% phenol and 0.12% DOC was used to lyse bacterial cells and release cell-associated polysaccharides.

3.7.2.2 Methods

Frozen Pn1 LWSL was used to initiate the inoculum train. All cultivations were carried out in Hoeprich's medium with 500 U/mL catalase. Liquid cultures were incubated in a CO_2 shaker incubator at 10% CO_2 saturation, 36 ºC, 100 RPM and 70% rH. BAPs from the National Health Laboratory Service (NHLS) were used as the substrate for solid-state cultivation in the CO_2 shaker incubator at 10% CO_2 saturation, 36 ºC, and 70% rH. The flow diagram for the small scale inactivation experiments is shown in Figure 3.23.

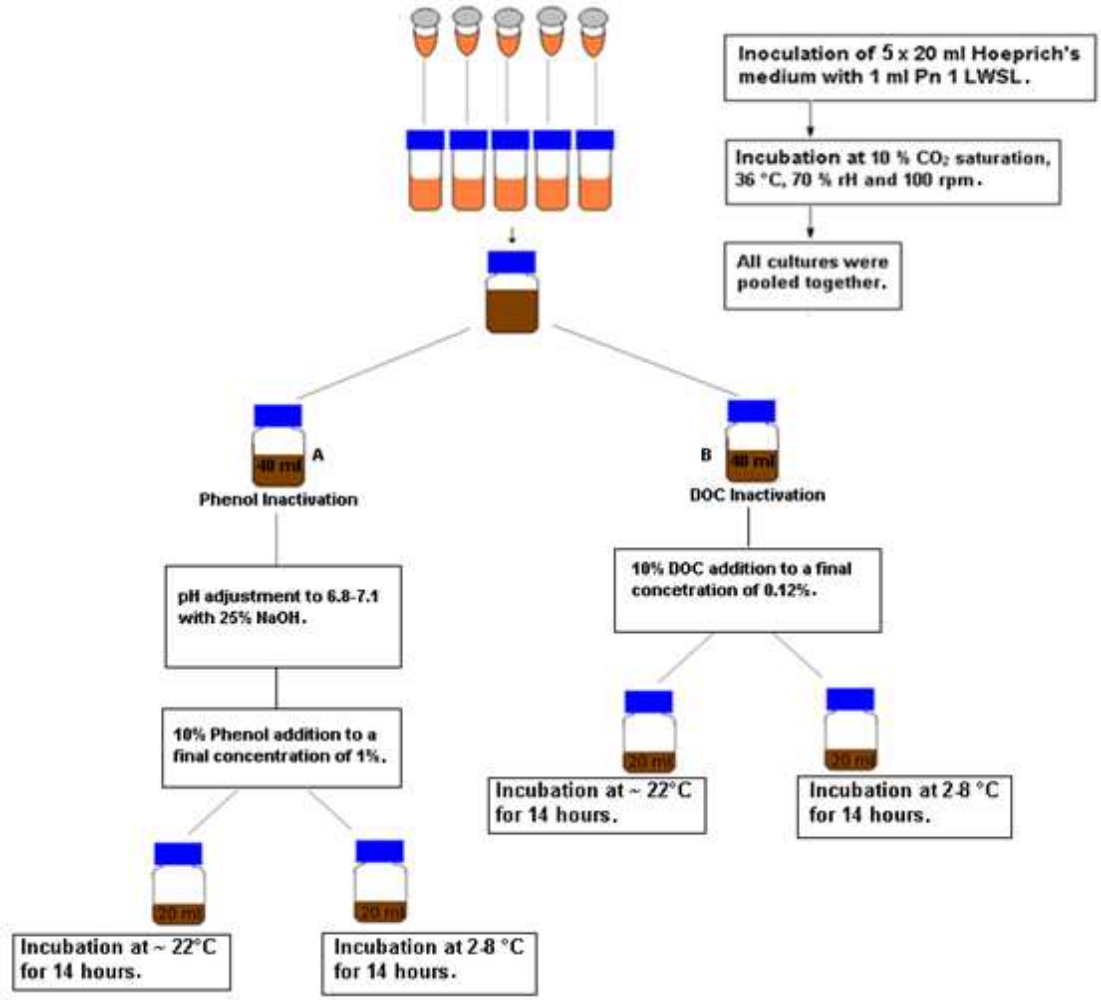

Figure 3.23 A schematic of the small scale Pn1 inactivation experiments performed at RT.

3.7.2.3 Cultivation

Five Pn1 LWSL vials were used to inoculate five 50 mL Falcon tubes, each containing 20 mL Hoeprich's medium. The tubes were incubated in a CO_2 shaker incubator at the standard conditions (10% CO_2

saturation, 36 ºC, 100 RPM and 70% rH) until an OD_{600nm} of above 1 was reached (~ 2.5 h of growth). The 20 mL cultures were then pooled together and OD_{600nm} and CPS levels were determined. A 10^{-6} dilution series of this pooled Pn1 culture was prepared by dilution in phosphate buffered saline (PBS). Three 50 µL of the diluted sample was spread evenly on BAPs to determine the initial amount of CFU/mL of the culture before executing the inactivation protocols. The 40 mL pooled culture (Figure 3.20) was aseptically aliquoted into two sterile Schott bottles labeled A for phenol inactivation and B for DOC inactivation. According to the literature a minimum of 14 h is required for the DOC and phenol inactivation time [145].

3.7.2.4 Phenol inactivation

The pH of the 40 mL culture in Schott bottle A was adjusted to 6.8 - 7.1 using 25% NaOH. Following pH adjustment, 10% phenol (dissolved in purified water, Merck, Cat. No. 100206) was added to the culture to give a final concentration of 1%. The culture was aseptically transferred into 2x 20 mL sterile Schott bottle. The two Schott bottles were incubated for 14 h at 2 - 8 ºC and RT.

3.7.2.5 DOC inactivation

A 10% DOC solution (dissolved in purified water, Merck, Cat. No. 264101) was added to 40 mL of culture in Schott bottle B to a final concentration of 0.12%. The culture was aseptically transferred into 2x 20 mL sterile Schott bottle. The two Schott bottles were incubated for 14 h at 2 - 8 ºC and RT.

3.7.2.6 Sampling

After 14 h incubation, 1 mL samples were aseptically taken from each of the four Schott bottles at 1 h intervals up to 22 h post inactivation. From each sample, two 50 µL volumes were evenly spread onto BAPs to determine the amount of CFUs. The BAPs were incubated in the CO_2 incubator at 36 ºC, 10% CO_2 saturation, and 70% rH for 24 h. The remaining 900 µL culture samples were stored at -80 ºC for Pn1 CPS and CWPS analysis.

3.7.3 Results and discussion

The viability plates (control) indicated that 5 colony-forming units (CFUs) were obtained per 50 µL of culture diluted to 10^{-6} (10^{8} CFU/mL). The pooled cultures after 2.5 hours of cultivation had average OD_{600nm} of 1.01. After 15 h inactivation no CFUs were observed in either the DOC or phenol inactivated cultures, irrespective of the inactivation temperature.

Figure 3.24 shows that upon inactivation with DOC and phenol at the two tested temperatures the Pn1 CPS production levels during fermentation were similar, ranging from 150 to 450 mg/L. Prolonging the inactivation time beyond 15 h (growth on BAP) revealed no bacterial growth at or beyond that time point (data not shown). The CWPS levels for both phenol and DOC were low (2.5 mg/L) and will not be further discussed as CPS production was the focus of this study.

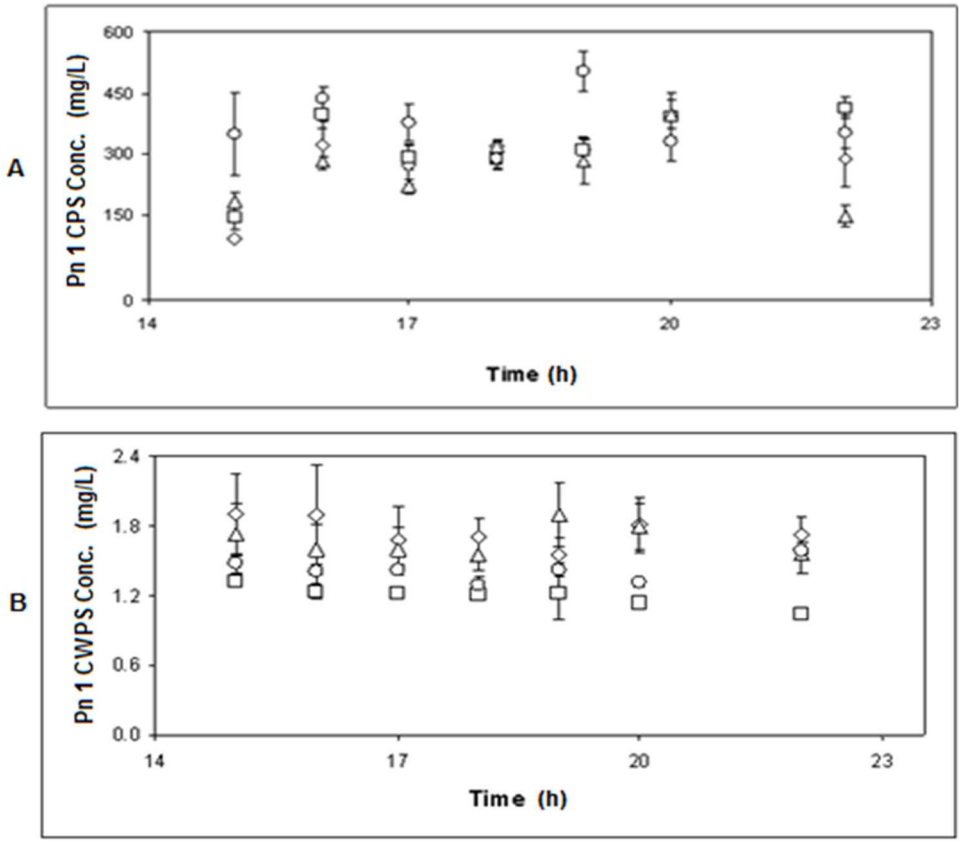

Figure 3.24: Time course data of Pn1 CPS (A) and CWPS (B) production during the small-scale inactivation experiment with (○) DOC inactivation at 2 - 8 ºC, (Δ) Phenol inactivation at 2 – 8 ºC, (□) DOC inactivation at RT and (◊) Phenol inactivation at RT. Error bars represent the standard deviation of the mean of replicate analysis (n = 5).

3.7.4 Conclusion

The CPS production based on ELISA and the biomass based on growth on BAP shows that a killing time of 15 h is required for inactivation of bacterial cells as no CFU were visible after 15 h at RT and 2 – 8 ºC. The CPS levels were comparable for both DOC and phenol. The CWPS for both methods were low with levels of less than 5% for CPS purification. These results require confirmation using a larger scale where detailed purification analysis of the CPS can be implemented and is more accurate than 1 mL CPS extractions for analysis of CPS purity and culture inactivation. This study, however not conclusive, does demonstrate that a total killing time of 15 h is required and align with the study by Liveyns. For manufacturing purposes a killing time of 16 h was preferred.

3.8 Large scale shaker culture inactivation

3.8.1 Introduction

With the inactivation strategy determined at small scale further process parameters were investigated. The effects of DOC and phenol were further evaluated at 4 L shaker cultivation volume. At a larger scale, the production of CPS was increased and hence the quantity and purity of the CPS was easier to evaluate. Large scale studies revealed that an additional step for DOC inactivation was required for media pH adjustment to ensure complete lysis and protein precipitation which could prevent Pn1 CPS O-deacetylation [108, 147].

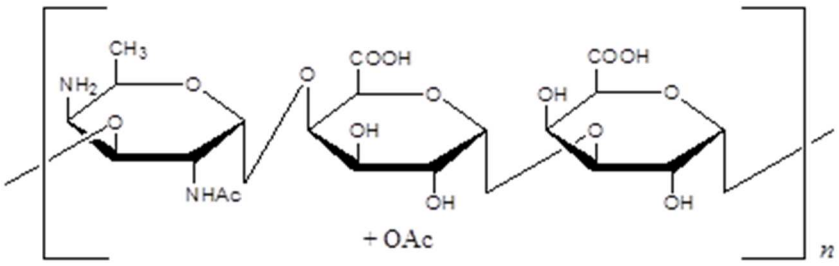

Figure 3.25: Structure of Pn1 repeating unit consisting of [3)-α-D-Sug1*p*-(1→4)-α-D-Gal*p*A-(1→3)-α-D-Gal*p*A-(1→]$_n$ + (OAc)

From studies performed on Pn1 (structure of Pn1 shown in Figure 3.25), it was demonstrated that DOC interfered with the rate nephelometry assay which was used to determine the amount of CPS present in a sample after CTAB addition in the purification step as there was co-precipitation between the CTA^+ and DOC salts [108]. After completion of the purification step using DOC-inactivation, no CPS was found in any fractions collected. This led to further investigation and to a publication by Gonçalves et al. [26] 2002, on medium optimisation for CPS production. This showed that for DOC inactivation, the fermentation broth needed to be diafiltered and concentrated using tangential filtration to remove excess sodium deoxycholate. Hence the need for the additional step as shown in Figure 3.26.

3.8.2 Methods

Three experiments with minor variations were carried out in duplicate (Figures 3.26 and 3.27) to compare phenol and DOC inactivation approaches. Four-litre shaker cultivations of Pn1 using Hoeprich's medium with 500 U/mL catalase and inoculated with a frozen stock culture of LWSL were prepared for the studies. Cultivation parameters were: 10% CO_2, 36 ºC, 70% rH. Agitation was set at 100 RPM for Falcon tubes and 50 RPM for Schott bottle cultivations (volumes above 20 mL). The procedure describing Experiment 1 is shown in the flow diagram in Figure 3.26 and Figure 3.27 illustrates the flow diagram for Experiments 2 and 3.

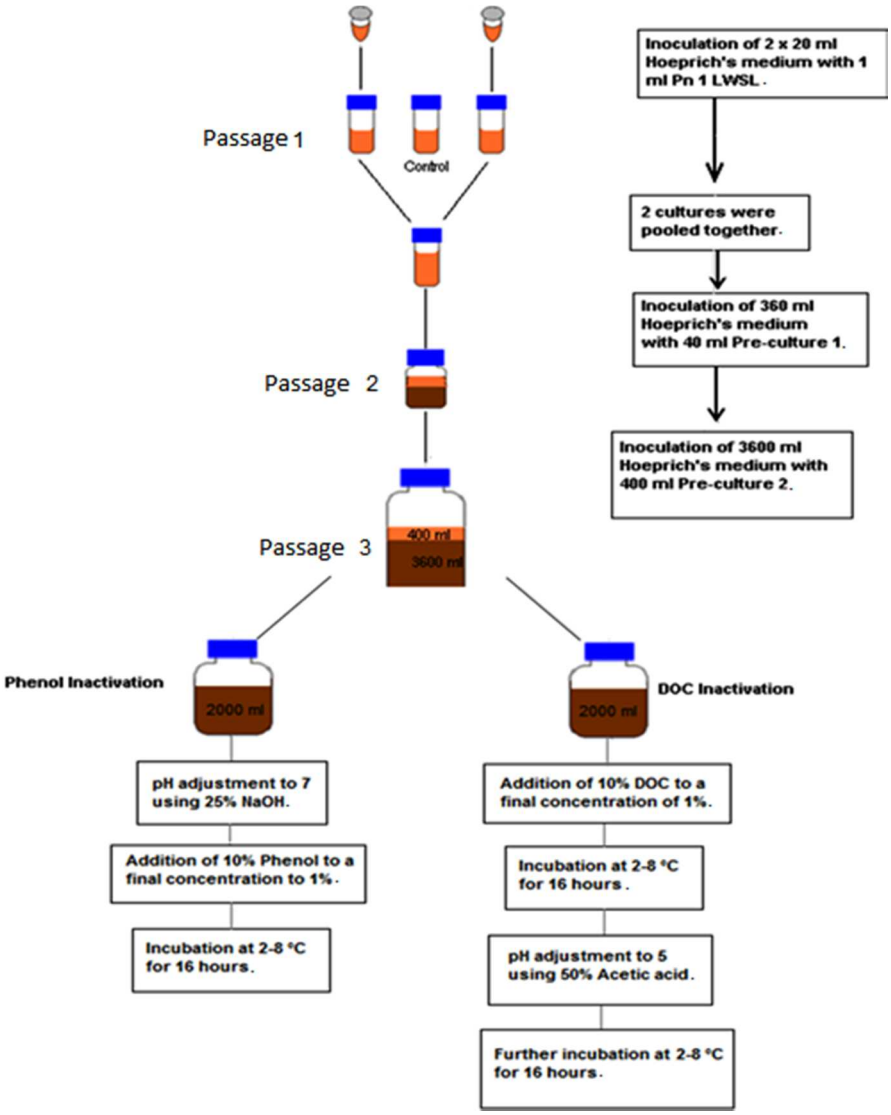

Figure 3.26: A schematic of the large scale inactivation Experiment 1. Passages 1 - 3 were carried out at 10% CO_2, 36 ºC, 50 RPM (100 RPM for Passage 1 only) and 70% rH.

3.8.2.1 Passage 1

Two 1 mL cryo-preserved Pn1 LWSL vials were defrosted and aseptically added to two 20 mL pre-warmed Hoeprich's medium aliquots in 50 mL Falcon tubes. A third un-inoculated 20 mL medium aliquot was used as the control. The initial OD_{600nm} of each of these Passage 1 cultures was measured. All tubes were then incubated until the inoculated medium turned turbid and the OD_{600nm} was between 0.9 and 1.8 (approximately 3 h incubation). This step was the same for all three experiments.

3.8.2.2 Passage 2

The Passage 1 cultures (2 x 20 mL) were used to inoculate two pre-warmed 380 mL Hoeprich's medium aliquots in 500 mL Schott bottles (Passage 2 cultures). The initial OD_{600nm} values of the Passage 2 cultures were measured and the tubes were incubated until turbidity had reached an OD_{600nm} between 1.4 and 2.2 (approximately 3 h incubation). This step was different in Experiment 1 wherein the two Passage 1 cultures were pooled together and the entire 40 mL was inoculated into 360 mL Hoeprich's medium as in Figure 3.25.

3.8.3 Large scale shaker cultivation

The Passage 2 cultures (Figure 3.24 & 3.25) were used to inoculate two pre-warmed 3800 mL Hoeprich's medium in 5 L Schott bottles for phenol and DOC inactivation. The OD_{600nm} of the cultures was measured until the cultures were turbid and the OD_{600nm} was between 2.0 and 2.5 (4 h incubation in Experiments 1 and 2 and 5 h incubation in Experiment 3).

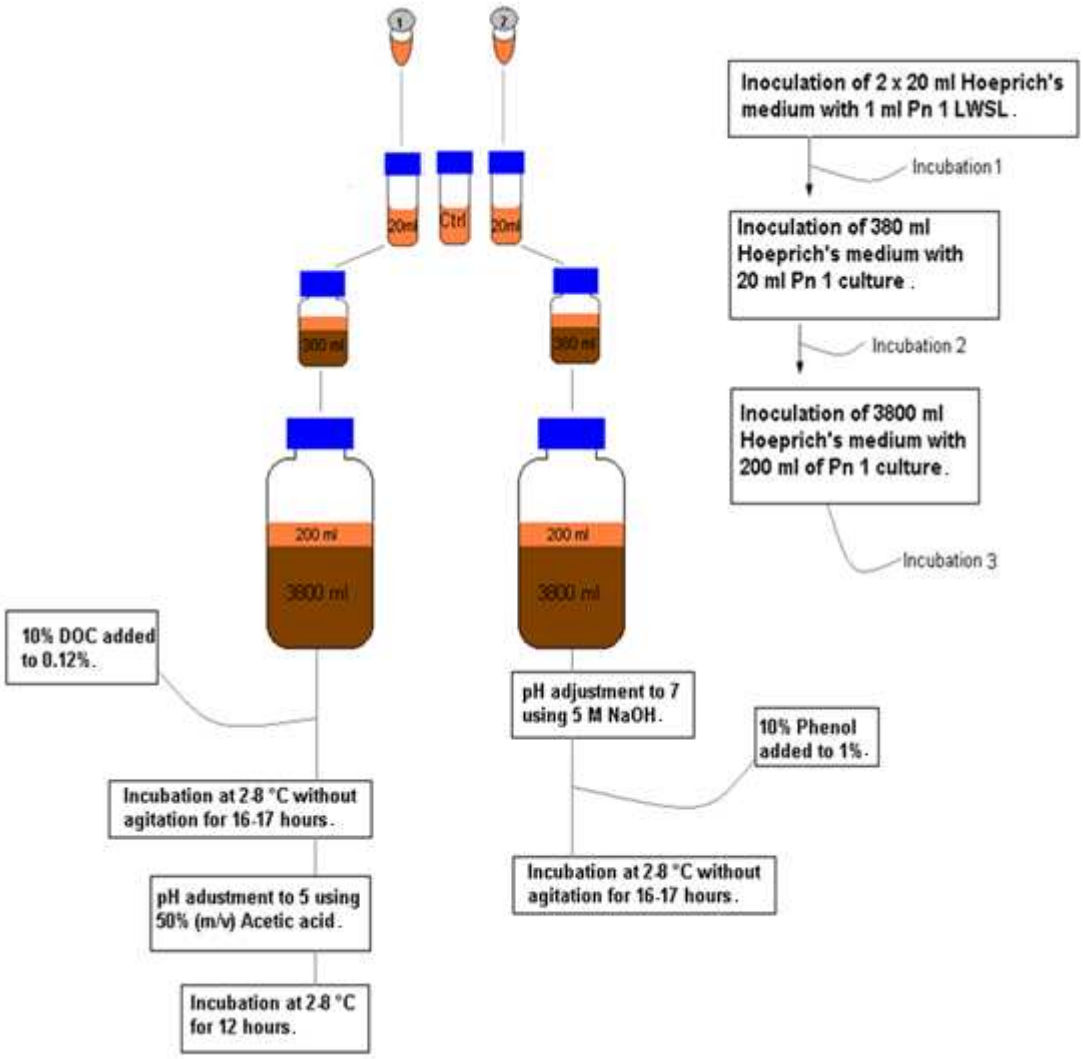

Figure 3.27: A schematic of the large scale inactivation Experiments 2 and 3. Passages 1 - 3 were carried out at 10% CO_2, 36 ºC, 50 RPM (100 RPM for Passage 1 only) and 70% rH.

3.8.3.1 Phenol inactivation

The pH of the 4 L culture labeled "phenol inactivation" was adjusted to pH 7 using 5 M NaOH. The pH-adjusted culture was then inactivated with the addition of 10% phenol to give a final concentration of 1% at pH 7. The phenol-treated culture was statically stored at 2 - 8 ºC overnight (16 h).

3.8.3.2 DOC inactivation

Ten percent (10%) DOC was added to the culture labeled "DOC inactivation" to give a final concentration of 0.12%. The DOC-treated culture was statically stored at 2 - 8 ºC overnight (16 h). After 16 h inactivation, the pH of the culture was adjusted to pH 5 with a 50% (m/v) acetic acid solution,

followed by a further static incubation at 2 - 8 ºC for 12 h (Experiment 1) and 16 h (Experiments 2 and 3).

3.8.3.3 Clarification

The inactivated cells were concentrated in a flow-through centrifuge (Laboratory – Centrifuge GLE, CEPA Biotech GmbH in Germany) at a set point 6 ºC, 40,000 x g, and a pump speed setting of 15 L/h for a single pass. Thereafter, the clarified supernatant was further processed for purification and evaluation studies.

3.8.4 Results and discussion

After inactivation, neither the phenol nor the DOC inactivated cultures showed visible growth on BAP, confirming that the bacteria had been killed. Figure 3.28 illustrates, by comparison, the CPS concentrations measured from the six phenol and DOC inactivated cultures. The CPS levels (Table 3.9) ranged between 350 and 750 µg/mL at the indicated time points for the three experiments. The inactivation of Pn1 bacteria with phenol (1%) and DOC (0.12%) at 2 – 8 ºC and RT (18 - 22 ºC) was performed with 100% inactivation efficiency for periods of 15 h or longer. Of note, during the purification process the excess DOC used during inactivation interfered with precipitation of the negatively charged CPS. Both CTAB and DOC are positively charged chemicals which would compete to bind the negatively charged CPS which could lead to poor CPS extraction. In order to confirm removal of CTAB and an interference free purification process, a further 12 – 16 h incubation was required for DOC inactivation [108].

No significant benefit was apparent when comparing inactivation temperatures in terms of Pn1 CPS release at 2 - 8 ºC or 18 - 22 ºC. As demonstrated on small scale at least 15 h is required for bacterial cell death on BAP but in order to ensure effective protein precipitation an additional 12 to 16 h was required for CTAB removal when using DOC inactivation for CPS purification. Therefore a major difference between these two chemical methods was observed when comparing the incubation time required for inactivation to be achieved for successful purification.

Table 3.9: Summarized results for six Pn1 shaker inactivation studies.

	Experiment 1		**Experiment 2**		**Experiment 3**	
Inactivation method	**1% Phenol**	**0.12% DOC**	**1% Phenol**	**0.12% DOC**	**1% Phenol**	**0.12% DOC**
Final OD_{600nm}	2.14	2.14	2.51	2.41	2.76	2.72
Age at start of Inactivation (h)	4	4	4	4	5	5
Inactivation time (h)	16	16 + 12*	16	16 + 16*	16	16 + 16*
Average CPS (µg/mL) as per ELISA (ATCC std)	364	424	665	667	739	653
Average CPS (µg/mL) as per ELISA (CDIBP std)	85	99	154	155	180	152
pH	7.29	5.3	6.44	5.31	6.84	5.30

* Further incubation at 2 - 8 ºC after adjusting the pH of DOC-treated culture to 5 with 50% (m/v) acetic acid.

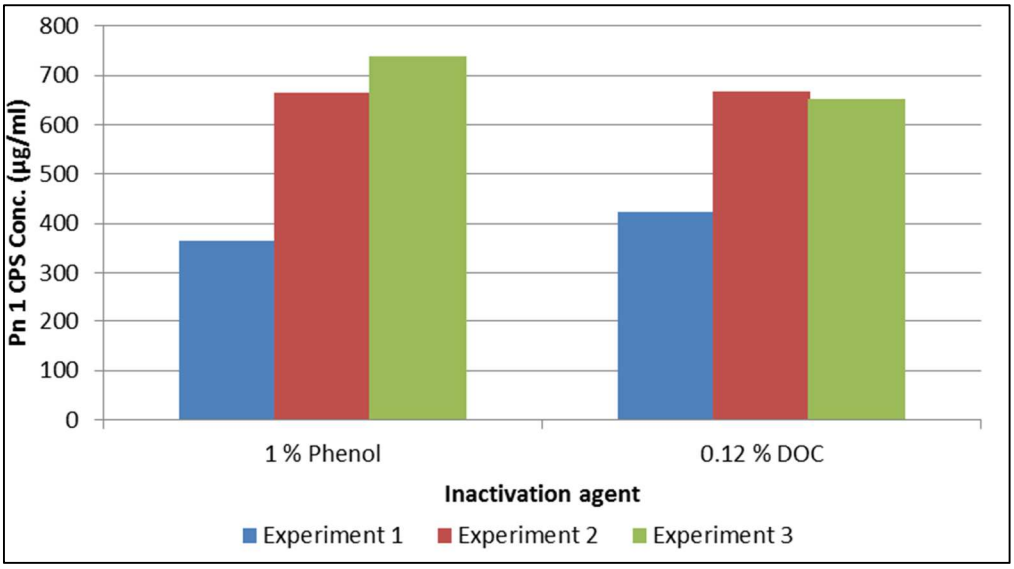

Figure 3.28: A graph of purified CPS concentrations in phenol (16 h) and DOC (up to 32 h) inactivated samples from the six 4 L Pn1 cultivations obtained from three experiments performed using the EISA assay. Also, see Table 3.9.

3.8.5 Conclusion

The inactivation of pneumococcal bacteria using chemical reagents such as phenol and DOC was evaluated. Both phenol and DOC achieved bacterial inactivation but the advantage of phenol over DOC was; (1) processing time for inactivation was shorter for phenol as an additional processing step was required for DOC post inactivation due to interference of DOC in the CTAB precipitation step and (2) the cost of phenol was cheaper than that for DOC. Studies conducted at Biovac on DOC inactivation showed that an additional 12 h to 16 h was required for the final killing time before effective protein precipitation was achieved (data not shown). Also, an additional diafiltration step was required to remove DOC-salt before CTAB precipitation (purification), as the DOC interferes with CTAB precipitation. The NMR results (data not shown) confirmed the identity of the purified structure as Pn1 CPS after both phenol and DOC inactivation and showed 100% integrity of the CPS following phenol inactivation. The contamination of concern, CWPS, and the acetylation levels were well within WHO specification.

3.9 Fermentation inactivation

3.9.1 Introduction

The shaker culture experiments showed that phenol inactivation was suitable for the killing of pneumococcal bacteria. A similar phenol-based strategy was evaluated in the fermentation studies, with the aim of identifying a robust and reproducible process that could be implemented at larger scale. The temperature of the inactivation process was investigated; (1) addition of phenol at RT to the culture at 36 ºC and (2) addition of cold phenol (2 – 8 ºC) to cooled culture (15 ºC). The addition of cold phenol to cooled culture was based on the hypothesis that cooling would aid in the release of CPS as the cooling would initiate a defense mechanism by the bacteria thus resulting in the release of pneumococcal CPS. All experiments were performed on Pn1 cultivations.

3.9.2 Methods

3.9.2.1 Inactivation without cooling

The inactivation strategy without a cooling step was performed in four 15 L fermentation runs. The inactivation step was initiated at the point of the harvest of the fermentation where a volume of 10% phenol solution (18 – 22 ºC) was pumped (1 L/min) into the fermentation broth in the fermentor to allow for a final concentration of 1% phenol. After 10 min of mixing at 50 RPM without temperature control, the fermentation broth (15 L) (containing 1% phenol) was pumped out of the fermenter (5 L/min) into a 20 L Schott bottle. The 20 L Schott bottle was then placed at 2 – 8 ºC for 16 h.

3.9.2.2 Inactivation with cooling

The inactivation strategy with a cooling step was performed in four 15 L fermentation runs. The inactivation step was initiated at the fermentation point of harvest by first cooling the fermentation broth to 15 ºC (with the pH controller turned off). A volume of 10% phenol solution chilled to 2 – 8 ºC was then pumped (at 1 L/min) into the fermenter to allow for a final concentration of 1% phenol. After 10 minutes of mixing at 50 RPM and the temperature controlled at 15 ºC, the fermentation broth (containing 1% phenol) was pumped out of the fermentor (at 5 L/min) into a 20 L Schott bottle. The 20 L Schott bottle was then placed at 2 – 8 ºC for 16 hours.

3.9.3 Results and discussion

Figure 3.29 shows the decrease in Pn1 CPS concentration after inactivation in all fermentation runs evaluated without the cooling step. This decrease could be attributed to the sudden change in the culture environment from 36 ºC to cool, with the addition of phenol at RT. This drop in temperature change could have caused cell death as the bacteria were not allowed to adjust to the change which in turn led to the decrease in CPS recovery. The inactivation strategy incorporated a cooling step in order to determine whether or not decreasing the temperature of the culture broth would have an effect on the CPS release. Samples were taken at the point of harvest before inactivation and again after inactivation and tested for CPS concentration using competition ELISA.

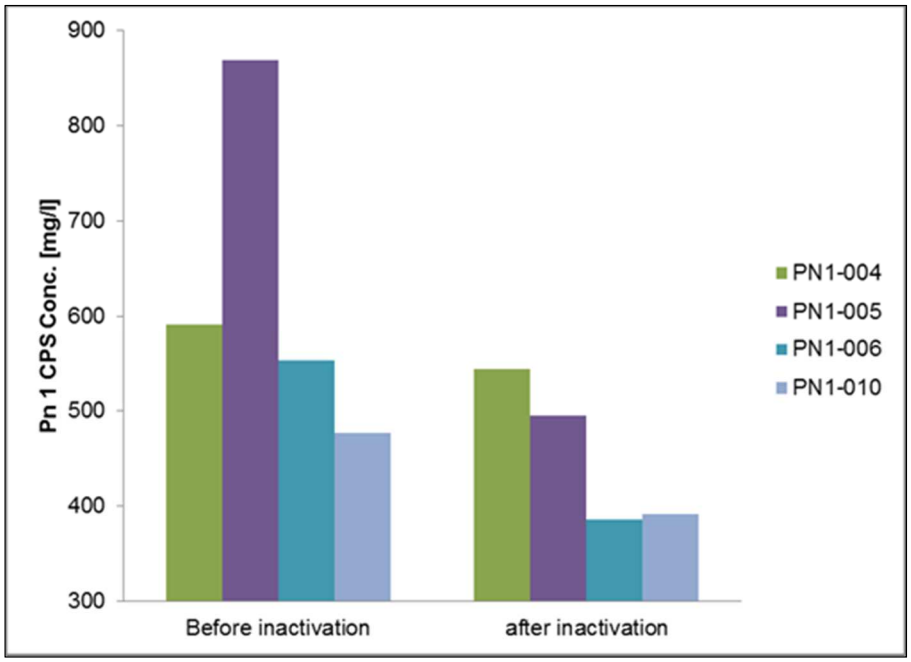

Figure 3.29: Inactivation strategy without cooling: evaluating CPS production levels determined by ELISA assay before and after inactivation for fermentation runs Pn1-004, Pn1-005, Pn1-006 and Pn1-010 in the fermentor.

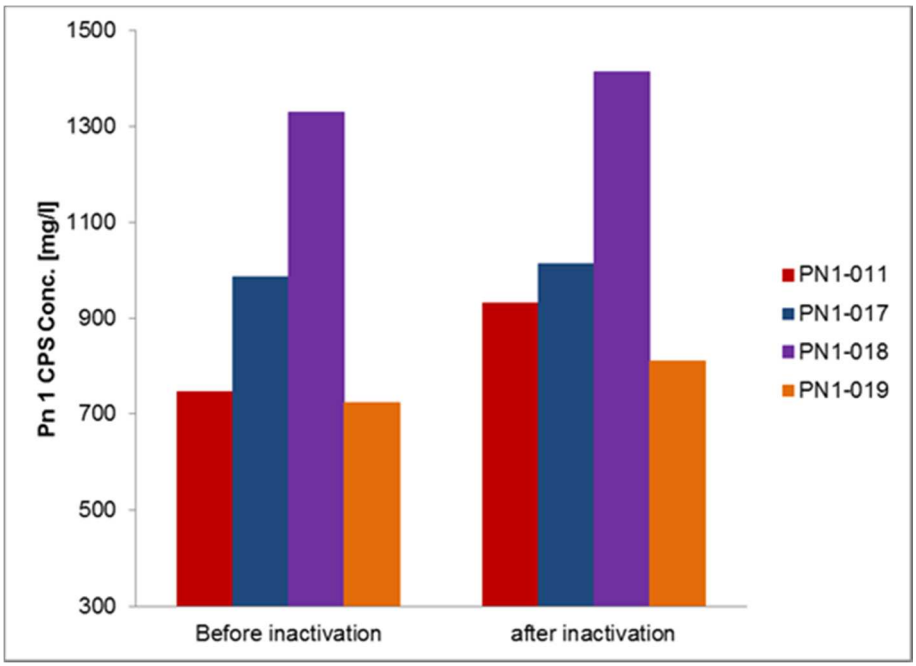

Figure 3.30: Inactivation strategy with cooling: evaluating CPS production levels determined by ELISA assay before and after inactivation for fermentation runs Pn1-011, Pn1-017, Pn1-018 and Pn1-019 in the fermentor.

However, implementation of the cooling step to the inactivation protocol resulted in an increase in Pn1 CPS after inactivation in all fermentation runs evaluated (Figure 3.30). The assumption was that the gradual reduction in culture temperate allows the bacteria to adjust to the change and thereby releasing more CPS as a defense mechanism to the changes in cultivation. This indicated that the inactivation step with cooling resulted in better cleavage of CPS from the whole cell. Without cooling the CPS levels were observed to decrease from harvest to final inactivation for all cultivations whereas with cooling all CPS levels increased with cultivations.

3.9.4 Conclusion

This section experimentally validated chemical inactivation of the bacteria *S. pneumoniae* cultivated in the fermentor. The implementation of a cooling step in the inactivation strategy was unique to this study and was applied in the Pn19A strategy which resulted in improved recovery of CPS based on the ELISA assay (Chapter 4). As a result of this, the inactivation temperature was identified as a key process parameter in the process. Control and monitoring of the inactivation temperature at 2 – 8 ºC was therefore recommended during the inactivation of Pn1 and was applied to Pn19A cultivations.

3.10 Clarification of the inactivated fermentation broth

3.10.1 Introduction

Clarification after cell inactivation is important in order to separate the cellular debris which contains the inactivated cells from the supernatant which contains CPS. To clarify the fermentation broth, a continuous tubular flow-through-centrifuge (FTC) was employed. FTCs are widely used in a variety of biological processes from cell harvest and clarification to the separation of chemicals, food, blood and pharmaceuticals. High performance is consistently achieved in continuous, semi-continuous or batch operations. Fluid mixtures are fed into the bottom of the rapidly rotating separating chamber.

With regards to critical process parameters during clarification, there are several factors to consider in relation to separation efficiency when using an FTC:

- Feed inlet rate: if too high, separation efficiency is also decreased and more than one pass may be required since breakage of the cells could lead to the release of the cell components such as nucleic acids and proteases into the supernatant. These contaminants are difficult to remove during purification [149].
- Low flow rates: may increase separation efficiency but can also increase the temperature of the feed, which may damage the product of interest [149].
- Temperature: can alter both the viscosity and the stability of the product. For every 1 ºC increase in temperature, the viscosity decreases by 2% [149]. The decreased viscosity of the fermentation broth significantly augments the efficiency of solid–liquid separation by centrifugation. Thus, increasing the temperature of the feed may lead to better clarification efficiency.

The aim of this experiment was to develop a clarification process that resulted in separation of cell debris from the supernatant without affecting the quantity or integrity of the CPS.

3.10.2 Methods

The CEPA bench top centrifuge Model GLE, used in this study, is able to process 2 to 30 L of culture per hour with a maximum rotation speed of ~ 40,000 x g and with cooling capacity [150]. This model was used to clarify the Pn1 inactivated fermentation broth at a feed inlet flow rate of ~15 L/h, a rotation speed of ~ 40,000 x g and cooling at 2 – 8 ºC. The inlet (inactivated fermentation broth) and outlet

(clarified broth) reservoir, as well as the tubular centrifuge, were temperature-controlled at 2 – 8 ºC. A semi-batch mode of operation was performed whereby the number of passes through the FTC depended on the OD_{600nm} of the inactivated fermentation broth. The reference OD_{600nm} of the clarified broth was predetermined (per batch) by spinning a 1 mL sample of the inactivated broth in an Eppendorf tube at 13000 RPM, for 10 minutes. The OD_{600nm} of the obtained supernatant was measured and used as a reference for the final clarified broth. For every pass of the fermentation broth through the FTC, the OD_{600nm} was measured and the process continued until the reference OD_{600nm} was less than or equal to the reference OD_{600nm} recorded.

3.10.3 Results and discussion

The described clarification process led to a significant reduction of inactivated cells from the fermentation broth as indicated by a decrease in OD_{600nm} of samples collected after each clarification pass (Table 3.10).

Table 3.10: The CPS levels of Pn1 fermentation broth collected after each pass of the clarification process.

	Final Fermentation Sample	FTC Pass 1	FTC Pass 2	FTC Pass 3
Biomass (OD_{600nm})	4.023	2.223	0.91	0.33
CPS (µg/mL)	1014	923	804	850
Standard Deviation	68	27	59	9

The CPS levels of the clarified broth after each pass was evaluated using the ELISA assay in comparison to that of the final fermentation broth post inactivation (Figure 3.31). There was no significant decrease in CPS concentration as observed by the standard deviation after 3 passes through the FTC indicating good CPS recovery post clarification.

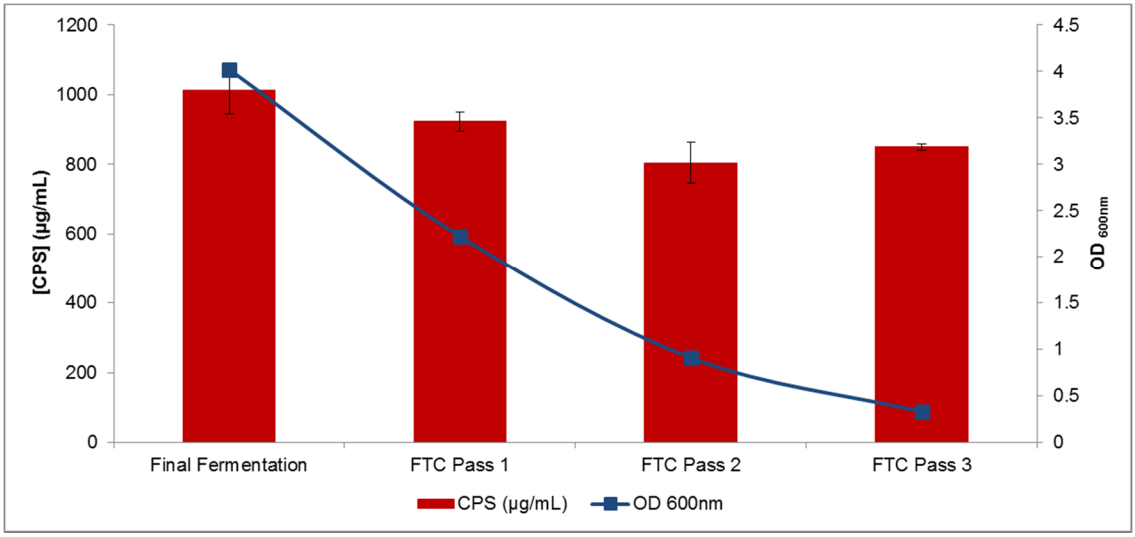

Figure 3.31: The CPS determined by ELISA assay and OD_{600nm} profiles of Pn1 during the clarification process.

3.10.4 Conclusion

The clarification process was successfully developed by ensuring that the final OD_{600nm} of the clarified broth was less than 0.35 and that the process was controlled at 2-8 ºC. CPS levels during this process remained fairly stable through the repeated passes, which makes this process very robust.

3.11 General conclusion

The clonal selection process was used to select a pure and high producing colony and adapt the cells to a new medium. Clonal selection consisted of four passages based on investigations performed on Pn1 and was successfully applied to Pn19A. The growth at each passage was consistent and showed that the seeds adapted to the medium and cultivation conditions with a 10 fold increase in biomass. Both Pn19A LMSL and LWSL were successfully prepared and confirmed in the laboratory as *S. pneumoniae* serotype 19A through the Quellung, Gram stains, optochin sensitivity tests and growth on BAP. The optimal conditions for the inoculum process was a 5% inoculum size throughout 4 passages and an incubation temperature of 36 ºC in the CO_2 shaker incubator with 70% rH and suitable for 15 L scale.

Medium optimization was based on Gonçalves and Hoeprich's [26, 73] methodology and with the addition of catalase was adapted for this study to allow for optimal medium conditions and adequate nutritional components for the growth and CPS production of Pn19A. Inactivation studies included DOC and phenol, performed on 2 L and 4 L scales before proceeding to larger scales using the fermentor/Wave bioreactor. These approaches revealed that both DOC and phenol produced similar Pn1 CPS yields. However due to the longer incubation times required for DOC inactivation (an additional 12 – 16 h) and interference with subsequent purification, the phenol inactivation method was preferable and was applied to Pn19A cultivations.

A cooling strategy involved cooling the culture (36 ºC) to 15 ºC followed by the addition of inactivation agent (cold phenol) and an overnight reaction time to allow for complete inactivation before the clarification process. CPS loss was observed in the inactivation strategy without cooling. Inactivation temperature was, therefore, a critical parameter in the process and novel to this study. This strategy improved recovery of CPS after termination of fermentation. The implementation of a cooling step in the inactivation strategy is novel to the studies conducted on Pn1 and applied to Pn19A confirming that it can be applied to more than one serotype of *S. pneumoniae*.

A high yielding CPS Pn19A isolate was selected and used for CPS production using the disposable Wave bioreactor technology detailed in Chapter 4.

CHAPTER 4. CULTIVATION AND PURIFICATION

This chapter describes the cultivation and CPS purification strategies (Figure 4.1) performed on *S. pneumoniae* serotype 19A based on the processes developed for Pn1. These strategies were successfully established for Pn1 and utilized for Pn19A for small and larger scale cultivations.

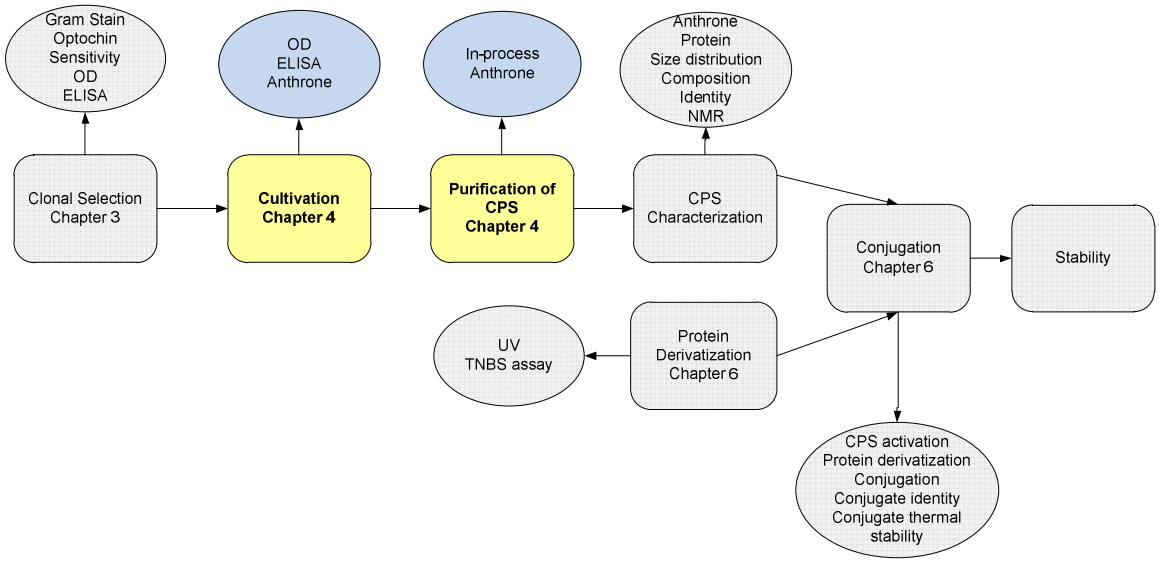

Figure 4.1: The process development steps for Pn19A conjugate vaccine production, highlighting the fermentation and purification procedures performed during this study.

4.1 General introduction

Bacterial cultivation is generally performed in a traditional stainless steel stirred tank fermentor or in a single use fermentor. Stirred tanks, or conventional fermentors, have been widely used for culturing suspension cells since the 1960s. The stirred tank bioreactors can be operated in batch, fed-batch, or continuous fermentation modes [151]. Batch cultivation is a closed system where no additional nutrients are added and the bacteria reaching stationary phase is an indication that all the nutrients have been depleted as shown in the schematic in Figure 4.2. With fed-batch cultivation, a semi-closed system, nutrients are strategically added during the fermentation process to allow for optimal growth and polysaccharide production [132]. Continuous cultivation, on the other hand, is an open system that allows the continuous flow of nutrients into and out of the fermentor at a fixed rate [152]. Fed-batch is the preferred mode of operation for the commercial process due to scalability but the batch mode was preferred during this study for reasons mentioned above.

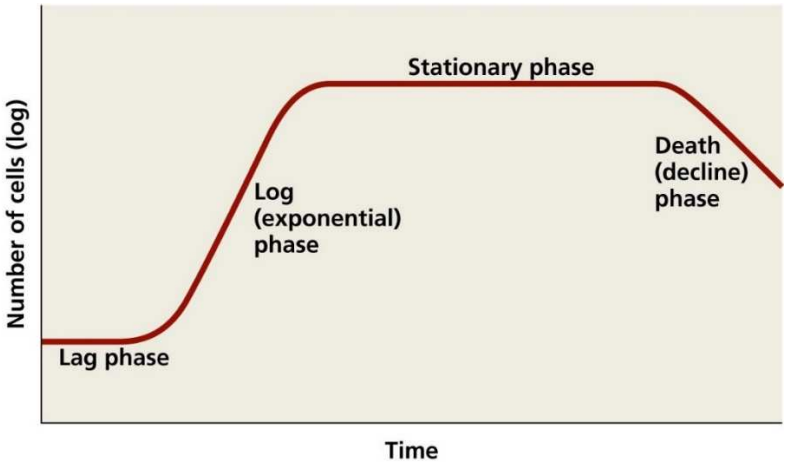

Figure 4.2: A typical bacterial growth curve showing bacterial growth in a closed system [70].

In contrast to a stirred tank such as a fermentor, the Wave bioreactor, introduced by Singh [67] in 1999, uses wave agitation which is induced by a rocking motion. According to Singh [153], this motion offers a less invasive mechanism of nutrient distribution and better gas transfer with reduced shear force and gas bubbles compared to stirred tank fermentors. These bioreactors have mainly been used for cell culture (e.g. insect and mammalian cells) but yeast and microbial cultivation have also been tested. It has been shown that Wave bioreactors are suitable for cells with low to medium oxygen demands that are cultivated in batch mode at small to medium scale [154]. *S. pneumoniae* bacteria are shear-sensitive, facultative anaerobes and therefore it was hypothesized that the wave-like motion of the Wave bioreactor would be suitable reactor for their cultivation [65, 123].

This bioreactor system utilizes an inflated disposable plastic bag as the cell cultivation chamber. These bags are made of biocompatible material and are delivered sterile, eliminating the need for cleaning and sterilization and hence eliminating the need for cleaning validation [67]. The Wave bioreactor is used in single-use bioprocesses which could be advantageous in the pharmaceutical industry, as it has the potential to eliminate cross-contamination between production batches or between batches of different products [154].

The cultivation bags are pre-sterilized and ready for use, thus increasing process efficiency and safety. The advantages and disadvantages of using the Wave bioreactor are summarized in Table 4.1. some advantages are significantly lower processing costs, reduced changeover times and reduced time-to-market for new products [155, 156] while disadvantages are that the plastic used in the manufacturing of the bags could contain leachables and could potentially be detrimental to bacterial growth [157, 158].

Table 4.1: The advantages and disadvantage of using disposable bag technology.

Advantages	Disadvantages
Smaller facility (HVAC demand lower)	HVAC requires bigger facility
Scalable to a certain volume	Above 1000 L is challenging
Robust	Reliance on external supply chain
Reliable	Does not always support cultures with high oxygen demands
No contamination risk	Bags could contain leachable
Reduced utility requirements (WFI, steam, and therefore costs)	High consumables (single use) vs high utility and maintenance requirements and cost

This cultivation in the Wave bioreactor, however, offers an alternative to conventional fermentation technologies, to achieve cGMP manufacturing requirements faster and was therefore considered worth investigation. Table 4.2 shows a comparison of the turnaround time between the stirred tank fermentor and Wave bioreactor.

Table 4.2: Turnaround time comparison: harvest to inoculation [159].

	Stainless steel stirred tank	Wave bioreactor
Working volume	100 L	100 L
Cleaning validation	Yes	Not required
Maintenance, O-rings	Yes	Not required
Sterilization procedures before use	Yes	Not required
Media sterility hold	Yes	Not required
Batch turnaround (same product)	6 – 10 h	1 – 2 h

The aim of this investigation was to cultivate Pn19A under conditions that produced CPS in high yields. To this end, both stirred tank and Wave bioreactors were used on the model serotype Pn1 to determine the most convenient and affordable approach. The aim of this study was to determine CPS production upon nutrient depletion and hence batch fermentation was utilized for Pn19A cultivation.

4.2 Key variables affecting the production process

Critical process parameters in pharmaceutical manufacturing are key variables that are monitored to detect deviations in production operations and product quality. These process parameters are adjustable parameters of the process that when maintained within a narrow range, ensures optimum process performance. Under cGMP conditions, these parameters can ensure that ideal cultivation conditions for optimal bacterial growth are met. Table 4.3 represents the process parameters examined in this thesis which is further discussed in Sections 4.3 and 4.5. For shake flask and Wave cultivations the medium and inoculum train are not considered control parameters as these can vary depending on the scale of the cultivations.

Table 4.3: Process parameters investigated at small and large scale**.**

Parameters	Control Set points	Literature Reference
Temp	36 ºC	In-house methods at Biovac
Agitation: shaker	100 RPM	In-house methods at Biovac
Agitation: Wave	20 RPM	[67, 160]
pH	7.2	[123, 125]
Humidity: rH	70%	In-house methods at Biovac
Gassing: CO_2	10%	In-house methods at Biovac
Gassing: N_2	0.02 VVM	[26, 161]
Medium	Hoeprich's	[26, 73, 122]
Inoculum train	4 passages	In-house methods at Biovac

4.3 Small scale cultivation development

4.3.1 Introduction

Pneumococcus was first isolated simultaneously and independently in 1881 by U.S Army physician George Sternberg and French chemist Louis Pasteur [9]. It has since been routinely cultured in laboratories at a small scale in submerged cultures. The studies discussed in the following sections were conducted on Pn1 due to the unavailability of Pn19A at the time the study was conducted. All successful methodologies were developed to Pn1 and then to Pn19A. In this section, the key process parameters in shaker cultures for Pn1 are presented and then applied to Pn19A. The impact that these process parameters has on the quality attributes such as biomass and structure of CPS is also discussed. Experiments were designed to evaluate the control parameters required to obtain optimum cultivation conditions for Pn1 biomass growth and CPS production. These control or process parameters were;

- Media: the effect of catalase addition to the cultivation medium.
- Gassing: the use of CO_2 in cultivation.
- Temperature: 36 ºC vs. 37 ºC.
- Agitation: static vs. shaking of the culture medium.

4.3.1.1 Vessel type

Small scale submerged cultivations have been cultured in vessels which include glass tubes [2, 119, 120, 162] and Erlenmeyer flasks [162, 163]. During the early development phase of this study, Pn1 was cultured in 50 mL Falcon tubes, Erlenmeyer flasks (250 mL to 5 L) and Schott bottles (250 mL to 5 L). In terms of CPS production levels, none of the above vessels had an effect on growth (data not shown), Falcon tubes and Schott bottles have low oxygen transfer compared to Erlenmeyer flasks. Pneumococci does not require high oxygen transfer for growth which would be provided when using Erlenmeyer flasks. It was therefore decided that a 50 mL Falcon tube and Schott bottles (2 x 250 mL Schott bottles and 1 x 1 L Schott bottle) would be used for the seed expansion studies during the inoculum train as they are more cost effective and practical for use compared to using Erlenmeyer flasks.

4.3.1.2 Gassing

Pneumococcus, being a facultative anaerobe, does not require oxygen, and clinical isolates have therefore been routinely cultivated in a CO_2 atmosphere [162]. Literature studies have utilized CO_2 concentrations ranging between 3% and 10% [120, 164]. Yavordios and Cousin, [165] (1983), observed that anaerobic cultivation of *S. pneumoniae* using N_2 in the fermentor produced three-fold more CPS compared to that stated previously with a higher biomass [165]. This was confirmed by Gonçalves et al. [166] (2006), who observed that although the biomass growth was achieved under both CO_2 and N_2 environments, higher specific growth rates, and CPS yields were reached under an N_2 atmosphere. The use of CO_2 was found to increase foam formation during cultivation as well as acidification of the medium, leading to increased NaOH consumption during pH control [162]. Based on this knowledge, in this study, N_2 was used for gassing in the fermentor and CO_2 was used during the inoculum train incubation and other shaker culture experiments.

4.3.1.3 Agitation

Agitation of small scale submerged pneumococcal cultivations is not a requirement as pneumococcus has been cultured under static conditions [120, 162], however, agitation levels have been evaluated [120, 139, 162, 163]. Agitation at high set points such as 180 RPM was shown to reduce growth and CPS yields of Pn23F, due to elevated shear stress [163]. In contrast, it was shown that agitation at a set point of 50 RPM or lower produced the highest CPS yields during Pn1 cultivation. During this study, an agitation rate between 50 and 180 RPMs was investigated and compared to static cultivation to determine the effects on Pn1 growth and CPS production.

4.3.1.4 Temperature

For the production of CPS, *S. pneumoniae* has generally been cultivated between 35 and 37 ºC [120, 124, 163]. In this study, two temperature settings, 36 ºC and 37 ºC were evaluated in shaker cultures. The effect of Pn1 cultivation at 35 ºC was investigated at a later stage (Section 4.5.2) in the fermentor and compared with 36 ºC.

4.3.2 Methods

4.3.2.1 Inoculum preparation

Three frozen 1 mL vials of Pn1 LWSL were used to aseptically inoculate three 50 mL Falcon tubes containing 20 mL Hoeprich's medium. The three inoculum cultures were incubated for 2.5 h in a CO_2 incubator at 36 ºC, 10% CO_2, 70 % rH and 100 RPM agitation.

4.3.2.2 Experimental cultures

When the three inoculum cultures reached OD_{600nm} values between 1 and 2, they were pooled and the OD_{600nm} was determined. Thereafter 1 mL of the pooled starter culture was used to aseptically inoculate each one of a set of 24 x 50 mL Falcon tubes containing 20 mL Hoeprich's medium with catalase at different concentrations. The second set of 20 mL Hoeprich's medium without catalase in 24 x 50 mL Falcon tubes was similarly inoculated with 1 mL of the starter culture. A loop full of the pooled starter culture was streaked onto BAPs with optochin for presumptive identity and purity testing. The 20 mL cultures were incubated for 4 h in a CO_2 incubator to evaluate temperature (36 ºC versus 37 ºC), CO_2

saturation (5% versus 10%) and agitation (150 RPM versus static). Humidity was controlled at 70% rH throughout the cultivation study. Cultivations were performed in triplicate for each combination of parameters (Table 4.4). After 4 h incubation, samples were taken for OD_{600nm} and CPS concentration, which was determined using an immunological technique, ELISA.

Table 4.4: Summary of the Pn1 cultivation optimization study conditions in 20 mL Hoeprich's medium using 50 mL Falcon tubes.

Experiment No.	Cultivation temperature	Agitation	CO_2 saturation	Catalase concentration (U/mL)				
1	36 ºC	Static	5%	0	500	1000	1500	2000
			10%	0	500	1000	1500	2000
		150 RPM	5%	0	500	1000	1500	2000
			10%	0	500	1000	1500	2000
2	37 ºC	Static	5%	0	500	1000	1500	2000
			10%	0	500	1000	1500	2000
		150 RPM	5%	0	500	1000	1500	2000
			10%	0	500	1000	1500	2000

4.3.3 Results and discussion

The study investigated 20 mL Pn1 cultivations in 50 mL Falcon tubes at two temperature set points (36 ºC and 37 ºC); five catalase concentrations (0, 500, 1000, 1500 and 2000 U/mL); two agitation points (static and at 150 RPM) and two CO_2 saturation values (5% and 10%). The biomass (OD_{600nm}) values and CPS yields are shown in Figures 4.3 and 4.4 respectively and showed that Pn1 cultivation at 36 ºC generally produced higher biomass and CPS yields than at 37 ºC. When comparing the CO_2 saturation at 36 ºC, it was observed that 5% CO_2 saturation gave slightly higher CPS yields than 10% CO_2 saturation for static incubation. However, when cultures were agitated at 150 RPM, incubation at 10% CO_2, produced slightly higher biomass than at 5% CO_2 incubations, which is in agreement with Howden [164] (1976), who observed growth comparisons on plates under anaerobic conditions gave higher CPS yields and larger colonies at 10% CO_2 incubations.

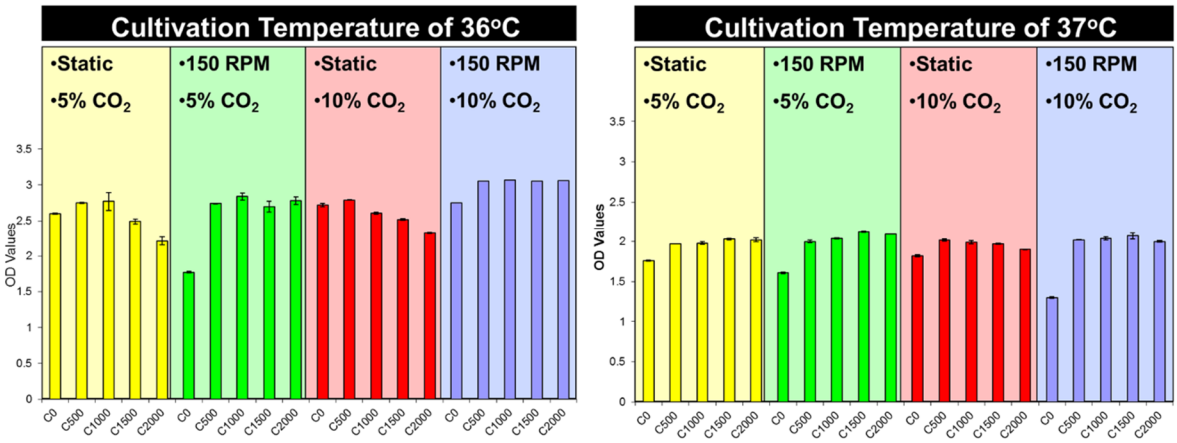

Figure 4.3: OD_{600nm} profiles of Pn1 after 4 h shaker cultivation at 36 ºC (A) and 37º ℃ (B) in varying concentrations of catalase, two CO_2 saturation levels (5 and 10%) with or without agitation at 150 RPM. The catalase concentrations are indicated on the x-axis, identified with C for concentration followed by the concentration used.

Referring specifically to the 36 ºC static incubation at 5% CO_2 it was observed that addition of 500 U/mL catalase to the medium significantly increased the CPS yields by 1.7-fold. A significant increase was observed between the static and agitated cultivation. Increasing the catalase concentration from 500 U/mL to 2000 U/mL in Hoeprich's medium did not further improve the CPS yields. Catalase concentration at 500 U/mL generally gave higher CPS yields across all experiments. It was therefore decided to add 500 U/mL of catalase to Hoeprich's medium for Pn1 cultivation and fermentation.

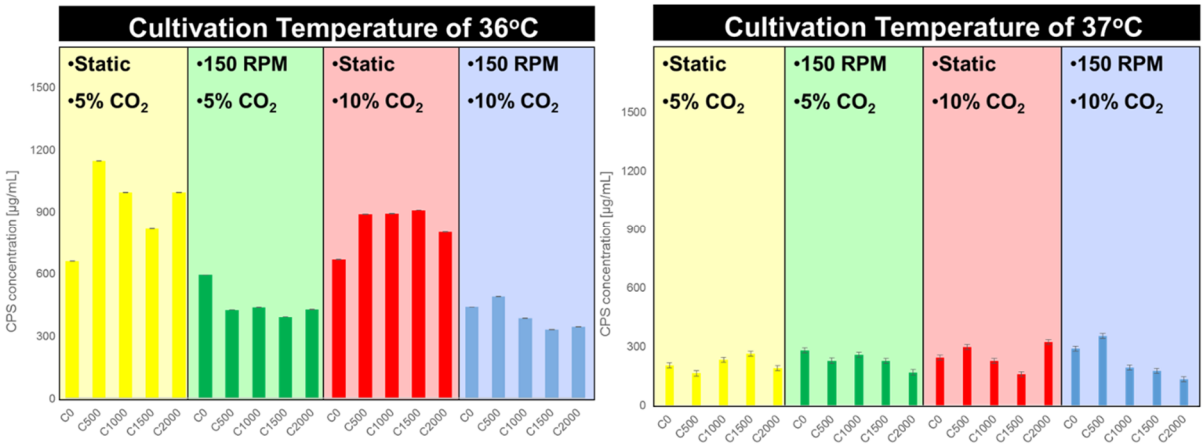

Figure 4.4: CPS yields produced by Pn1 after 4 h shaker cultivation at 36 ºC (A) and 37 ºC (B) in varying concentrations of catalase, two CO_2 saturation levels with or without agitation at 150 RPM. The catalase concentrations are indicated at the bottom of the graph, identified with C for concentration followed by the concentration used.

At 37 ºC (Figure 4.4) static and agitated cultivation were comparable as lower biomass and CPS production yields were obtained. The selection criteria (temperature, agitation, and CO_2 saturation) are summarized in Figure 4.5.

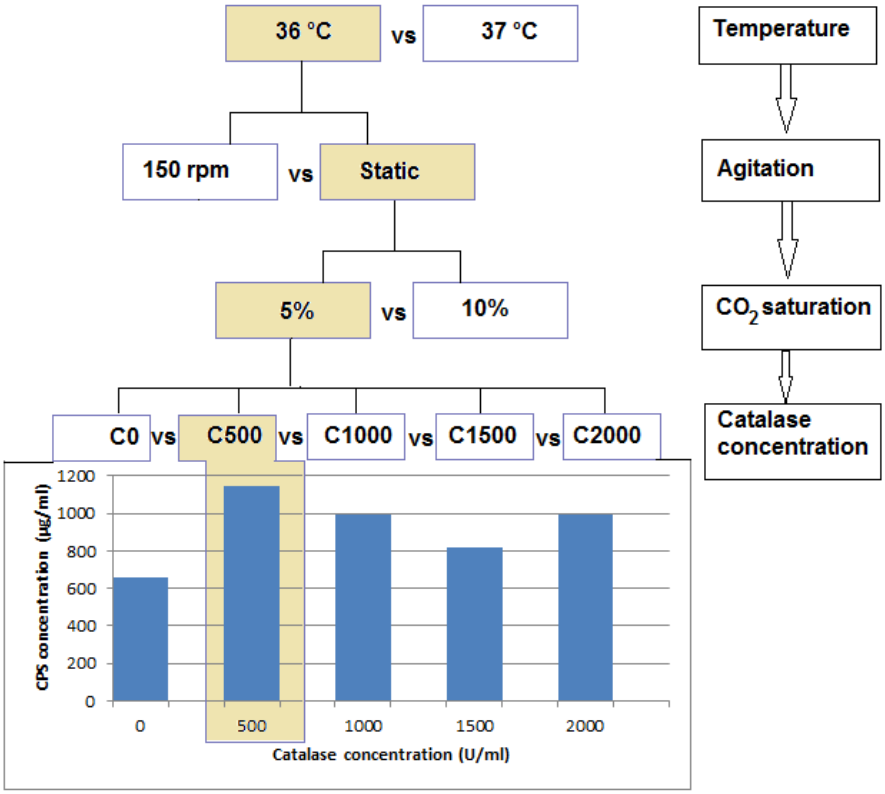

Figure 4.5: A summary of the selection of cultivation parameters based on Pn1 CPS yields performed using the ELISA assay after 4 h shaker culture incubation. The highlighted areas show the parameters observed to be the ideal condition in the cultivation of CPS. The CPS yields by Pn1 cultivation in various concentrations of catalase were compared at 36 ºC and 5% CO_2, under static incubation.

4.3.4 Conclusion

Based on CPS production, it was decided that 36 ºC should be the incubation temperature of choice for Pn1 cultivations and fermentations using 5% CO_2 saturation at static incubations with 500 U/mL catalase which in this experiment resulted in the highest CPS level obtained at 1.15 mg/mL. The static incubation was in agreement with previous findings by Klein [167] (1981), who demonstrated that *S. pneumoniae* serotype 1 CPS production was highest at stirring rates of 50 RPM or lower. Although 5% CO_2 incubation gave higher Pn1 CPS yields, it was decided to do small-scale incubation in 10% CO_2 saturation on the assumption that the CO_2 level will be reduced below 10% during the frequent opening and closing of the CO_2 incubator for sampling. On small scale cultivations, the difference in CPS production between 5% and 10% CO_2 was not significant and hence was tested again at a larger scale. The parameters followed were cultivation at 36 ºC with static incubation and a 5% CO_2 level with medium containing 500 U/mL catalase. These parameters were applied to Pn19A the results of which are discussed further in Section 4.4.

4.4 Pn19A cultivation in 5 L shaker culture

4.4.1 Introduction

The batch cultivation, clarification and inactivation techniques developed during the process development of Pn1 were applied to Pn19A. The aim of the procedures described in this section was

the evaluation of catalase on CPS production levels in 4 L shaker culture on Pn19A by implementing batch cultivation in the Wave bioreactor.

4.4.2 Materials and methods

All batches were cultivated either in Schott bottles (5 L) or the Wave bioreactor (10 L). Cultivation parameters utilized are summarized in Table 4.5 and included the following:

- Substrate: Modified Hoeprich's medium, pre-warmed (≥ 1 h) at 36 ºC.
- Preparation of the inoculum train as described in Chapter 3.
- Inactivation: 10% cold (2 - 8 ºC) phenol was added to the culture in Schott bottles to give a final concentration of 1% of the total fermentation broth. The phenol was stored to 2 - 8 ºC, for 4 h prior to use. During Wave bioreactor runs, the bag was first cooled by placing it on ice for ± 15 min or until the culture broth reached ~15 ºC (temperature monitored using a thermometer attached to the cell bag) after which 10% cold (2 - 8 ºC) phenol was added to the culture to give a final concentration of 1% of the fermentation broth.
- Broth clarification: After 16 h static inactivation in the bags/bottles at 2 – 8 ºC, clarification was performed using a bench-top centrifuge (3220 x g for 15 min) for the cultures cultivated in Schott bottles or the Flow-through Centrifuge (FTC) for broth from the Wave bioreactor. Thereafter, the supernatant was kept for further analysis.

Table 4.5: Cultivation parameters for Pn19A in Schott bottles or the Wave bioreactor.

Cultivation parameters	Schott bottle parameter set point	Parameter range	Wave bioreactor parameter set point	Parameter range
Substrate	Hoeprich's Medium	NA	Hoeprich's Medium	NA
Inoculum train	4 Passage (Fig. 3.20)	NA	4 Passage (Fig. 3.20)	NA
Temp	36 ºC	ND	36 ºC	± 0.5
rH	70 %	ND	NA	NA
Nitrogen gassing	NA	NA	0.02 VVM	± 0.01 VVM
CO_2 gassing	5%	ND	NA	NA
Agitation	50 RPM	NA	10 RPM	20 RPM just before sampling
pH	7.2	ND	7.2	7.0 - 7.3
Inactivation	10% phenol	2 – 8 ºC	10% phenol	Decrease cultivation temp for 15 min until 15 ºC is reached *prior* to cold phenol addition
Clarification	Bench top centrifuge	3220 x g, 15 min	Flow through centrifugation	40000 x g for 2 passes

4.4.2.1 5 L batch cultivation with and without catalase

In this study, the addition of catalase to a 4 L shaker liquid culture incubated at 5% CO_2 conditions was investigated for Pn19A growth and CPS production. The catalase concentration was previously established at 500 U/mL. Batch shaker cultures were carried out in two 5 L Schott bottles using Hoeprich's medium, in which catalase was added to one of the bottles. The initial volume was 4.5 - 5 L. The Schott bottles were inoculated when OD_{600nm} of the inoculum was above 0.8, cultivated for 4.5 - 5 hours and inactivated by cooling the cultures and adding 10% cold phenol to a final concentration of 1% phenol of the total fermentation broth. After 16 h, the broth was clarified using a bench top centrifuge

(3220 x g for 15 min), to remove cell debris and the clarified supernatant was kept for Pn19A CPS purification.

4.4.3 Results and discussion

Figure 4.6 shows the cultures grown with catalase (Pn19A-002) obtained the highest growth rate (μ) at 0.98 h^{-1} in comparison to cultures without catalase (Pn19A-001) which obtained a μ = 0.74 h^{-1} . The highest OD_{600nm} measurements were similar for both cultures, reaching levels of 2.5 after 5 (without catalase) and 2.7 after 3.7 h (with catalase) cultivation, showing that with the addition of catalase the time taken to reach an OD_{600nm} of 2.5 was faster.

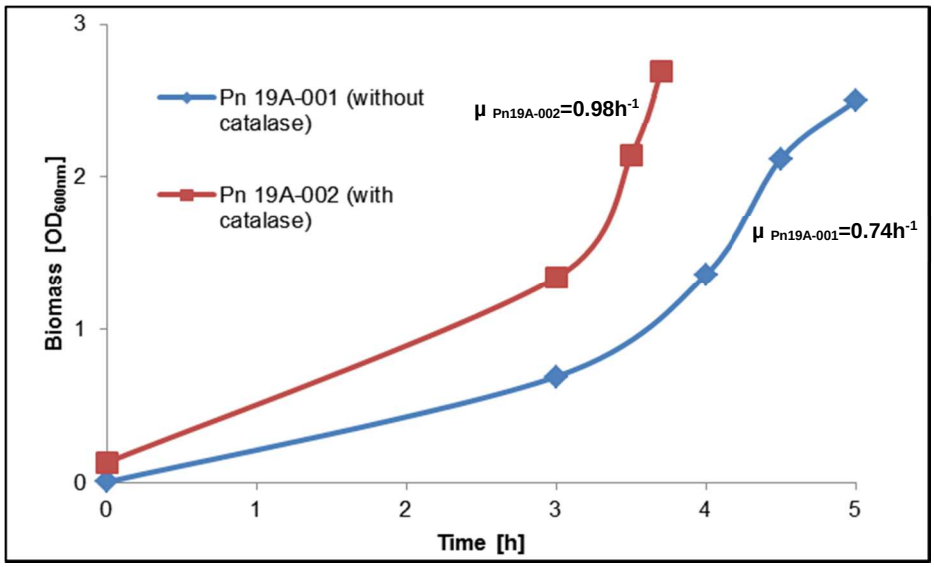

Figure 4.6: Time course and growth rate data profiles for shaker culture 1 (Pn19A-001) without catalase (blue graph) and 2 (Pn19A-002) with catalase (red graph) indicating Pn19A growth measured at OD_{600nm}. The final OD_{600nm} for culture 1 was 2.5 after 5 h and the final OD_{600nm} for culture 2 was 2.7 after 3.7 h. Data points represent triplicate analysis with a standard error less than 5%.

Figure 4.6 also shows that Pn19A-001 without catalase has a longer lag phase than Pn19A-002 with catalase. A longer lag phase could be due to the initial OD_{600nm} of the starting culture for Pn19A-001 without catalase being lower and therefore needing more time to adapt to the culture medium (Table 4.5).

Table 4.5: Batch cultivation parameters and results for Pn19A batches 1 & 2 cultivated in Schott bottles at 36 ºC.

Batch	1	2
OD_{600nm} [0 h]	0.03	0.13
Harvest Time [h]	5 h	4 h
+Initial Volume [L]	5 L	4.5 L
Additives	No Catalase	Catalase
Agitation [RPM]	50	50
Highest OD_{600nm} / (time)	2.5/ (5 h)	2.7/ (4 h)
Highest CPS [mg/L]	0.4	0.7
OD_{600nm} at collection	2.5	2.7
CPS at collection [g/L]	0.4	0.7

Table 4.5 shows the Pn19A CPS production level data of shaker cultures without catalase and with catalase to determine the CPS levels at harvest time were performed using the ELISA assay and resulted in ~400 mg/L after 5 h for culture without catalase and ~700 mg/L after 4.5 h for the culture with catalase. With the addition of catalase, it was observed that the CPS levels based on ELISA were approximately 1.7 fold higher in comparison to cultures without catalase. The residual glucose concentration at this point was ~0 mmol/L. The addition of cold phenol (2 - 8 ºC) had no effect on the CPS concentration (before and after inactivation) as the CPS concentrations remained unchanged.

4.4.4 Conclusion

The addition of catalase was observed to increase the rate of growth which led to an increase in CPS production. These experiments confirmed that the addition of catalase to the Hoeprich's medium when culturing *S. pneumoniae* increased bacterial growth as well as CPS production. In a manufacturing setting the fast turnaround time of bacterial growth with the result of increased CPS product is beneficial and cost effective.

4.5 Parameter selection for scale-up studies

4.5.1 Introduction

Complex interactions exist between the process conditions, the productivity and the morphology in microbial fermentations and thus considerable effort in understanding these process parameters to maximize product yield for a particular bioprocess must be performed. Process parameters that could influence product quality and yield include inoculum train, inactivation, and clarification have been discussed in Chapter 3 and in this section. While the feeding strategy is key to bacterial growth, all fermentations were performed using batch cultivation and hence the feeding strategies were not investigated.

4.5.1.1 Bioreactor design considerations

An efficient large-scale bioprocess relies on optimization of the abiotic phase, i.e. bioreactor design and performance. Generally, *S. pneumoniae* is cultured in stirred tank reactors also referred to as fermentors, for which highest CPS production levels have been observed to be highest at agitation rates below 180 RPM [133, 162, 163]. Exposure to high shear zone conditions in the fermentor may not cause immediate damage to the cells, but the damage may occur gradually due to shear as well as hydrodynamic stresses of certain *S. pneumoniae* serotypes; the main cause of damage due to stress and shearing is the high agitation rates of the impellors [163].

An alternative bioreactor to the fermentor is the Wave bioreactor, which makes use of disposable bag technology. The Wave bioreactor is suitable for shear-sensitive cultures, cultures that do not require vigorous mixing and which are sensitive to foam generation. The rocking of the bioreactor induces a wave-like motion in the culture bag which contains the medium and cells, and thus aids in a cell suspension, bulk mixing (sufficient nutrient and gas transfer to cells), as well as the reduction in shear forces and foam generation [67, 160, 168].

The Wave bioreactor facilitates the regulation of rocking angle, rocking rate, and the measurements of temperature, aeration rate as well as N_2 rate and pH.

The two bioreactors considered for the development of an *S. pneumoniae* fermentation process were;

- Conventional microbial fermentor (BIOSTAT C-plus, Sartorius Stedim Biotech, German) (used for Pn1 CPS production only).
- Disposable bag bioreactor (Wave Bioreactor Systems 20/50 with cell bag 20 L, BC10, DO (part no. 28412287)) (used for Pn1 and Pn19A CPS production), as shown in Figure 4.7. Only the Wave bioreactor was utilized for Pn19A CPS production and compared to the Pn1 Wave cultivation.

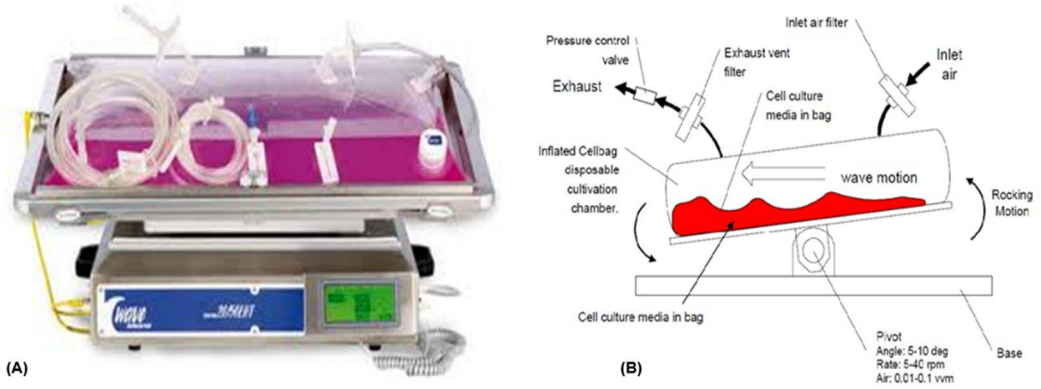

Figure 4.7: Disposable bioreactor (A) with an illustration (B) of a wave-induced agitation [157].

4.5.1.1 Mode of operation

A batch mode of operation, using Hoeprich's medium in the Wave bioreactor and the fermentor was investigated to establish the baseline growth profiles and CPS production levels of Pn1 and initiated by inoculating a working volume with a starter culture. No additional medium or inoculum is added during the fermentation process unless a titrant is required for pH control [169].

4.5.1.2 pH

The pH of the medium is a key environmental factor that can affect the transport of nutrients, the nutrient solubility as well as enzyme reactions or surface phenomena. The composition of the medium generally contributes significantly towards initial pH as well as the extent and direction of pH drifts during growth of the microorganisms. *Streptococcus pneumoniae* produces significant amounts of lactic acid during cultivation which affects the pH [170]. Since the optimum pH for growth was found to be 7.8 with a pH control range of 6.5 - 8.3 as previously described [2], pH control throughout the cultivation is required [125]. A pH set point of 7.2 was selected for Pn1 fermentation and extended to Pn19A cultivations and no further pH optimization studies were performed.

4.5.1.3 Agitation

In submerged fermentations, the purpose of agitation is to mix the cultivation broth in such a way that a uniform suspension of microbes is achieved. Generally, good mixing is of vital importance, ensuring good mass (gas and nutrient) and heat transfer thus providing a homogeneous, well-mixed cell

suspension. Exposure to a high shear zone in traditional stirred-tank fermentors may not cause instantaneous damage to the cells, but the damage may occur gradually due to shear as well as hydrodynamic stresses [171]. This implies that the microorganism has the ability to adapt to a certain level of mechanical stress. On the other hand, these effects may depend on the age of the cell. Potential cell damage can limit the impeller speed or power input. Consequently, the gas and nutrient transfer capability of a fermentor can be limited, ultimately reducing the volumetric productivity. The aforementioned factors demonstrate the effects of mechanical forces on biomass concentration. However, it must be emphasized that the superimposed effects of agitation on these variables are sometimes difficult to quantify and compare with one another. For instance, fermentor geometry and impeller type, diameter and area, (the greater the impeller area the greater the shear force), may differ from study to study. The disposable wave-like system allows for gentle agitation or wave-like motion for bacteria that do not require vigorous stirring. Bacteria such as *S. pneumoniae* require gentle agitation and no oxygen transfer for optimal growth and the Wave bioreactor can provide that kind of environment [67].

With respect to mixing of smaller volumes, for the purpose of Pn1 and Pn19A inoculum cultures (20 mL), agitation was kept at 100 RPM for IN1 Falcon tube (50 mL) and reduced to 50 RPM for IN2 to IN4 Schott bottles (250 mL) during the inoculum train (Chapter 3). The increased agitation at smaller volumes aid in the mixing of bacteria and media whereas at a larger volume a slower agitation is required, to obtain similar mixing.

4.5.1.4 Gas concentration

Literature suggests that fermentation of Pn1 in N_2 yields more CPS than in CO_2. It was observed that addition of oxygen to the anaerobic fermentation of Pn23F at the beginning of the stationary phase promoted the large increase of free CPS into the medium [129]. This was confirmed by a Pn1 fermentation run in the laboratory, wherein the accidental introduction of air increased the CPS yields. During the same study, Gonçalves [129] also implemented batch fermentation of Pn23F anaerobically by gassing with either CO_2 or N_2. Fermentation of Pn3 confirmed sparging air through a ring sparger ensures culture uniformity [163]. Although CO_2 was used in the inoculum preparation of Pn1 for fermentations, N_2 was used in the fermentor. Based on the above-mentioned literature, N_2 was supplied to the fermentor at a gas flow of 0.2 VVM through the head space, in order to avoid the formation of foam. This was applied to Pn19A cultivations in the Wave bioreactor as well. No further modifications or parameters were tested.

4.5.1.5 Temperature

Although it was demonstrated in Section 4.2 that the optimum temperature for the cultivation of Pn1 was 36 ºC in shaker flasks, in order to test the range of temperatures (35 – 37 ºC), 35 ºC was tested in the fermentor and compared to 37 ºC. The effect of bacterial cultivation at 35 ºC on Pn1 growth and CPS production was also investigated this time in the fermentor and compared to that of 36 ºC.

In summary, the key parameter that was further investigated was temperature. pH was maintained at a pH of 7.2 and further investigation of agitation was not required as a wave motion was utilized and N_2 was employed throughout the cultivation process.

4.5.2 The effect of temperature on growth of Pn1 and CPS yields

In this study, two batch fermentations were carried out to evaluate the effect of temperature on growth of Pn1 and Pn1 CPS yields at 36 ºC (Pn1-003) and 35 ºC (Pn1-004) respectively. Temperature evaluations were not performed on Pn19A but the methods and results obtained in this study were used as recommendations for the cultivation of Pn19A. An investigation to determine the effects of temperature on bacterial growth was undertaken in the Wave bioreactor.

4.5.2.1 Methods

Hoeprich's medium supplemented with 500 U/mL of catalase was used and the inoculum expansion was carried out as per Chapter 3. The Wave batch fermentations were controlled at pH 7.2, N_2 gassing through the headspace at 0.15 VVM, 50 RPM agitation. Temperatures were controlled at 36 ºC (Pn1-003) and 35 ºC (Pn1-004) respectively.

4.5.2.2 Results and discussion

In Table 4.6 at 36 ºC, the highest OD_{600nm} of 9.7 was reached after ~3.5h whereas at 35 ºC it took another half an hour to reach an OD_{600nm} of ~10. Upon collection, 550 mg/mL CPS at 36 ºC was collected and was 30 mg/mL more than that obtained at 35 ºC.

Table 4.6: Summary of Pn1 batch fermentation results for Pn1.

Batch (Run no.)	Temperature (ºC)	Highest OD_{600nm}	Age at high OD_{600nm} (h)	OD_{600nm} at collection	Age at collection (h)	CPS (mg/mL) at collection
003	36	9.7	3.5	9.2	3.75	550
004	35	10.2	4	9.2	5	520

Pn1 batch fermentation at 36 ºC resulted in a higher growth rate as observed by OD_{600nm} levels. The CPS yields was marginally higher whereas the biomass marginally lower than at 35 ºC. Cultivation time was also reduced by 1 h.

4.5.2.3 Conclusion

The use of 36 ºC as the temperature set point was implemented for all Pn1 fermentations. The results obtained for Pn1 regarding the temperature recommendation was applied to Pn19A.

4.6 Pn19A batch cultivations in the Wave bioreactor

4.6.1 Introduction

The cultivation, clarification and inactivation techniques developed during the process development of Pn1 were applied to Pn19A during the development process, with particular reference to Pn1 batch cultivation. The aim was to evaluate Pn19A growth and CPS production by implementing batch cultivation in shaker cultures and in the Wave bioreactor.

4.6.2 Methods

Six batch cultivations were carried out in a 20 L disposable wave bioreactor (GE Life sciences, USA) using Hoeprich's medium with catalase (500 U/mL) with an initial volume of 7 L. All cultivations were run under batch cultivation mode conditions and harvested after 4 to 5 hours when residual glucose levels in the culture medium were ≤ 5 mmol/L. The residual glucose level of ≤ 5 mmol/L was used as the indicator for harvesting the batch, shown during Pn1 fermentation a significant decrease in CPS production levels was observed when residual glucose levels were totally depleted. The six batches were inoculated as described in Section 4.5, in cell bags from different lots. The cultivations were inoculated into the cell bags once the inoculum train at passage four reached an OD_{600nm} of above 0.8.

4.6.3 Results and discussion

The highest OD_{600nm} measurements were similar for Batch cultures 3 and 8, reaching levels of 9.95 (culture 3) and 9.91 (culture 8) after 3.7 h and 4 h cultivation respectively (Table 4.7, Figure 4.8). The OD_{600nm} measurement for culture 6 reached approximately 8 after 5.2 h. For the successful cultures 3, 6 and 8, the OD_{600nm} levels in the Wave bioreactor increased significantly when compared to the two batch cultivations in Schott bottles (Pn19A-001 and Pn19A-002).

Table 4.7: Batch cultivation parameters for Pn19A cultivation in the Wave Bioreactor.

Batch/ Culture	**3**	**6**	**8**	**4**	**5**	**7**
OD_{600nm} at 0h	0.23	0.1	0.13	0.06	0.04	0.1
Harvest Time [h]	3.7 h	5.2 h	4 h	4 h	3.5 h	3.5 h
Agitation [RPM]	10 rocking angle 2.5º	20 rocking angle 2.5°	20 rocking angle 2.5°	20 rocking angle 2.5°	20 rocking angle 2.5°	20 rocking angle 2.5°
Highest OD_{600nm} / (time)	9.95 / (3.7 h)	8.02 / (5.2 h)	9.91 / (4 h)	0.23 / (2 h)	1.12 / (3.5 h)	0.29 / (3.5 h)
Highest CPS [g/L]	1.6	1.4	1.6	ND	ND	ND
OD_{600nm} at collection	9.95	8.02	9.91	NA	NA	NA
CPS at collection [g/L]	1.5	1.2	1.6	ND	ND	ND

Growth rates of cultures 3 and 8 were also similar, obtaining a μ of 1.09 h^{-1} and 1.0 h^{-1} respectively (Figure 4.8). Culture 6 obtained a μ of 0.85 h^{-1}. Residual glucose levels were measured periodically during the cultivation process and at the point of harvest, levels of 2.3 mmol/L (culture 3), 3.8 mmol/L (culture 6) and 0.8 mmol/L (culture 8) were measured after 3.7, 5.2 and 4 h cultivation respectively.

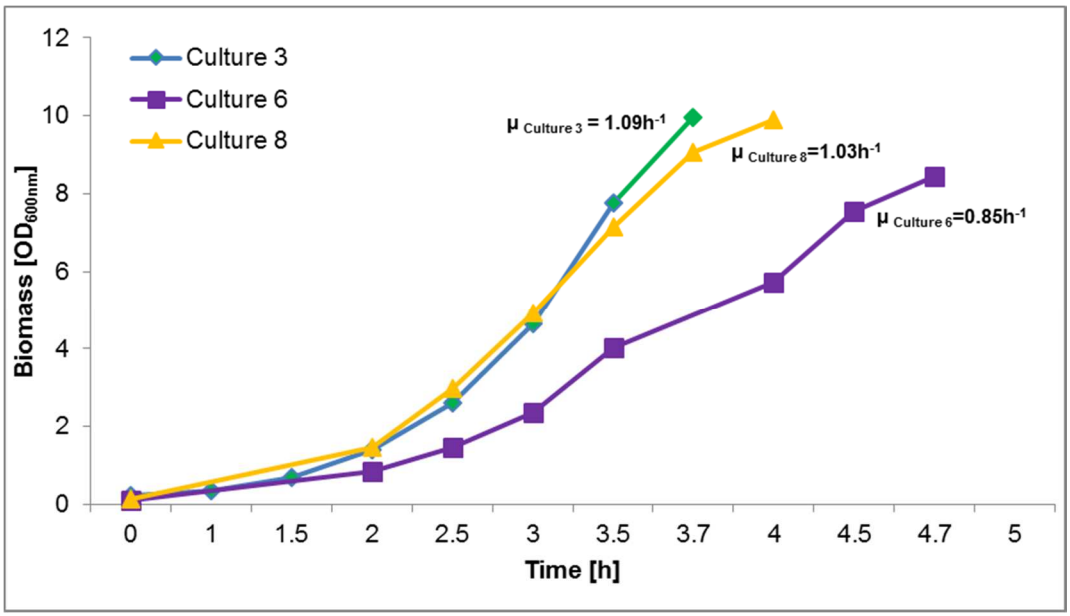

Figure 4.8: Time course growth rate data of Pn19A during Wave batch (3, 6 & 8) cultivation: indicating Pn19A growth measured at OD_{600nm}. Culture 3 shown in green grew for 3.7 h with a final OD_{600nm} of 9.95. Culture 6 shown in purple grew for 5.2 h to reach a final OD_{600nm} of 8.02. Culture 8 shown in orange grew for 4 h with a final OD_{600nm} of 9.91.

Out of the six batch cultivations, three were successful batches (Pn19A-003 (culture 3), 006 (culture 6) & 008 (culture 8)) and three batches (Pn19A-004 (culture 4), 005 (culture 5) and 007 (culture 7)) that failed. The principle difference between the failed and successful batches were the lot numbers of the bag.

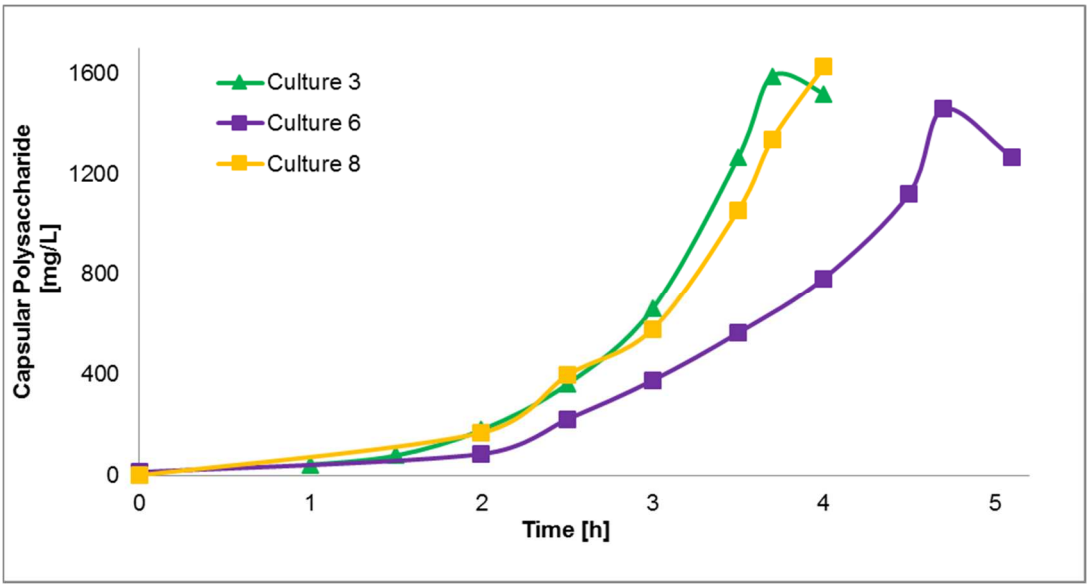

Figure 4.9: CPS data performed by ELISA assay of the three successful Wave cultivation batches: (Culture 3 (green line), Culture 6 (purple line) & Culture 8 (orange line)). Data points represent triplicate analysis with a standard error less than 5%.

Pn19A CPS production levels, as determined by ELISA, for cultures 3, 6 and 8 were 1.6, 1.4 and 1.63 g/L, respectively (Table 4.7, Figure 4.9). During the cooling step, Pn19A CPS production levels remained >1.4 g/L at 25 ºC, 15 ºC and after the addition of cold phenol (2 - 8 ºC) (Figure 4.10). No significant Pn19A CPS loss was observed between cultivation, inactivation, and clarification (Figure 4.10). The culture broth was clarified to a final OD_{600nm} of approximately 0.02. These results were

observed for all the successful batches and indicated that the cooling step was key in maintaining the integrity of the CPS.

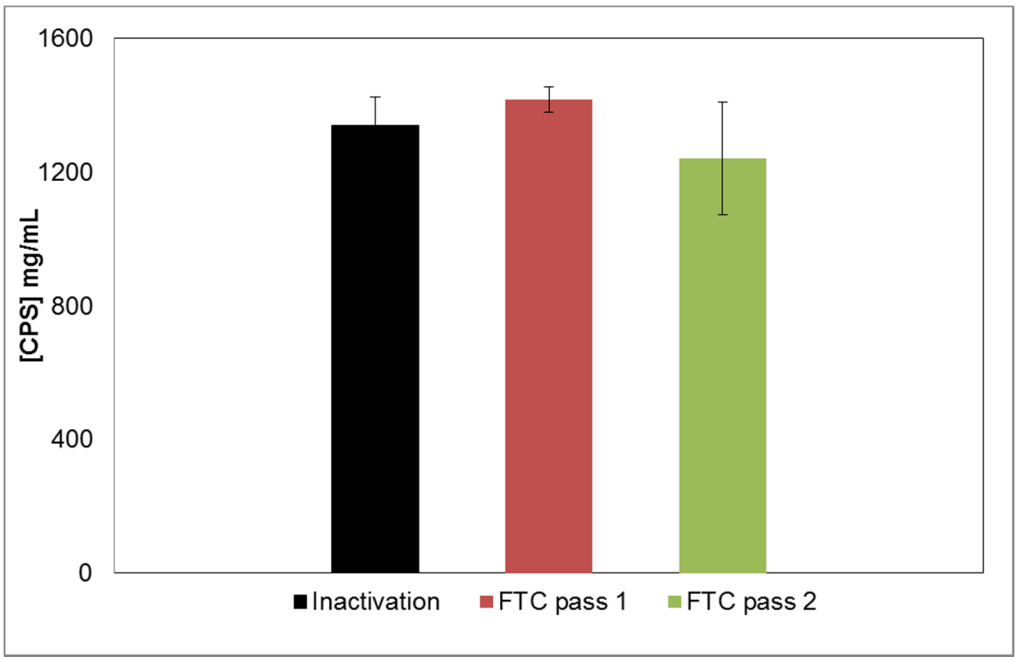

Figure 4.10: CPS production levels post fermentation for Culture 6, showing limited CPS degradation after cultivation in the Wave bioreactor. This was seen for the three successful batches in the Wave bioreactor. Data points represent triplicate analysis.

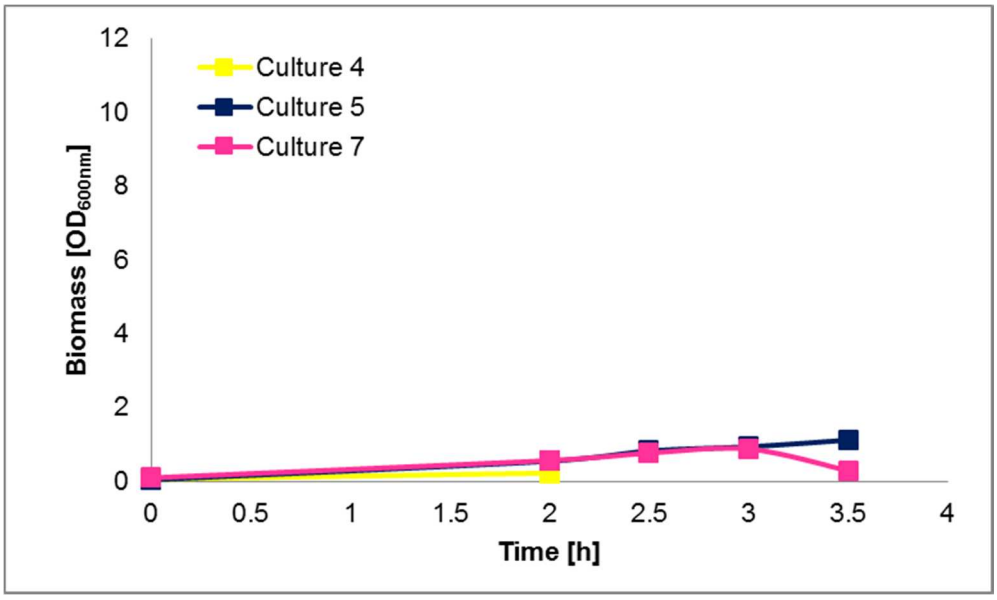

Figure 4.11: Time course data of cultivation batches (4, 5 & 7) indicating Pn19A growth measured at OD_{600nm}. Data points represent triplicate analysis with a standard error less than 5%.

For cultures 4, 5 and 7, maximum OD_{600nm} levels in the Wave bioreactor did not increase beyond 2 after 3.5 h of cultivation and because of the lack of growth as indicated by the OD_{600nm} the runs were aborted (Figure 4.11, Table 4.7). Culture 4 had an initial OD_{600nm} of 0.06 at the point of inoculation and after 2 h of cultivation, the run was aborted at an OD_{600nm} of 0.23. Culture 5 had an initial OD_{600nm} of 0.05 and after 3.5 h an OD_{600nm} of 1.12 led to the run being aborted. Culture 7 had an initial OD_{600nm} of 0.1 and after 3.5 h of cultivation, the run was aborted at an OD_{600nm} of 0.29. As a result of these low OD_{600nm} levels, no Pn19A CPS production levels were measured.

CPS production levels of Pn1 and Pn19A, as determined by ELISA using ATCC standards after 4 h cultivation (at the point of harvest), was compared to Pn1 and Pn19A under the same batch cultivation conditions in the Wave bioreactor. Pn19A produced more CPS (>1200 mg/L) than Pn1 (>400 mg/L) during cultivation in the Wave bioreactor. When compared to other serotypes namely 1, 3, 4, 5, 6A, 6B, 7F, 9V, 14, 18C, 19F, 19A, and 23F cultivated using fed-batch cultivation mode in stirred tank fermentor, Jain et al., 2011 showed CPS concentration levels of partially purified fermentation broth between 0.15 and 1.6 mg/L and for Pn19A concentration levels of between 0.45 and 0.70 mg/L [65]. It can, therefore, be concluded that the Pn19A fermentation process in the Wave bioreactor under batch cultivation conditions, developed at Biovac, delivered acceptable yields of CPS. However, as reported in Section 4.6.3, there was limited growth observed for three of the six Pn19A batches cultivated in the Wave bioreactor.

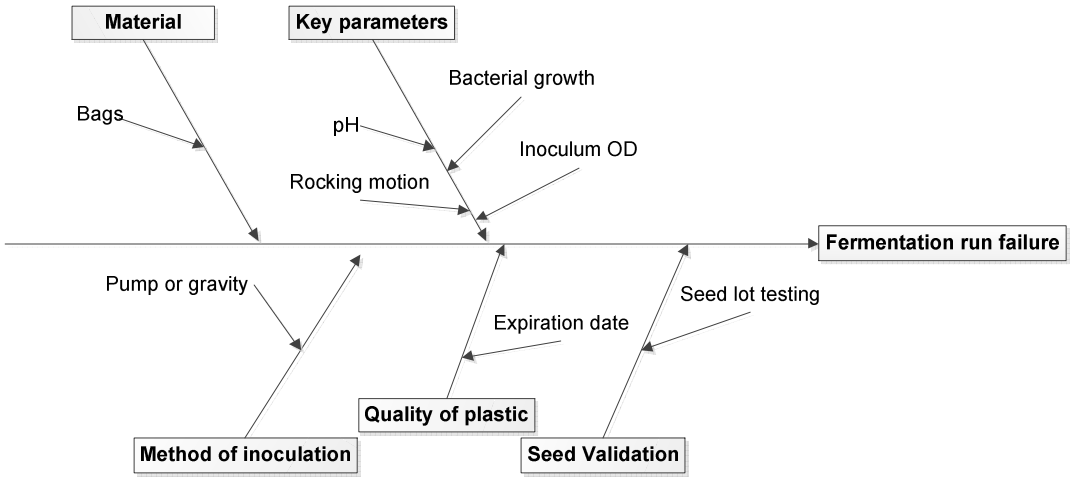

Figure 4.12: Root cause analysis to determine the cause of failure in batch fermentations.

Using a fishbone diagram as shown in Figure 4.12 to determine the root cause of failure the following factors were identified. Firstly, the cell bags were manufactured at different times as seen by the different lot number, they were then referred to as old and new cell bags. Batches 3, 6, and 8 were cultivated in “old bags” (manufactured at an early date) whereas batches 4, 5, and 7 were cultivated in “new cell bags” (manufactured at a later date). In order to determine if there was a difference between the lots, FTIR was performed on the lining on the inside and outside of the cell bags. It showed no difference in the bag lining indicating that these bags were composed of the same material (data not shown). This growth difference between the two lots of bags, however, was specific to Pn19A, as it was not observed for Pn1, 5 or 6B cultivations (other serotypes worked on at Biovac). Secondly, of the three successful batches, cultures 3 and 8 had similar growth and CPS profiles, while culture 6 had a slower growth rate (μ) and lower CPS production level at the point of harvest. The root cause for this slower growth rate is uncertain and requires further investigation. The failed batches did not obtain OD_{600nm} values of above 2, after cultivation times ranging between 2 and 3.5 h, and were therefore aborted as a result of a low initial OD_{600nm} levels of 0.1 or below, after inoculation into the culture bag.

Thirdly, cultures 4 and 5 had initial OD_{600nm} levels of 0.06 and 0.04, respectively, which were lower than that of culture 7 and all the other successful batches. These results may explain why the cultures were

never able to proceed into the exponential phase. However, culture 7, which also failed, had an initial OD_{600nm} level of 0.1 similar to the successful batch culture 6, after inoculation into the culture bag. This led to the hypothesis that perhaps there was another factor contributing to the lack of growth observed in the failed batches. After further investigation, it was observed that the three successful batches coincided with the use of the old bags, while the failed batches coincided with the use of the new bags. Whether the cell bags used for the failed batches contained leachables or not, that could have led to growth inhibition as was observed in the study of Hammond et al. [172] (2013), requires further investigation.

The inoculum train was compared across all batches and it is clear from Figure 4.13 that Passage 4 (IN 4) growth for the failed batches had a lower OD_{600nm} when compared to the successful ones. Investigations regarding the medium pH, cultivation temperature, mode of inoculation and viability and purity of the LWSL indicated that the inoculum train and LWSL conformed to growth specifications. Therefore further investigations looking at the root cause should be performed to determine whether it was the bags or if Pn19A strain is very sensitive to changes in growth parameter changes if minor.

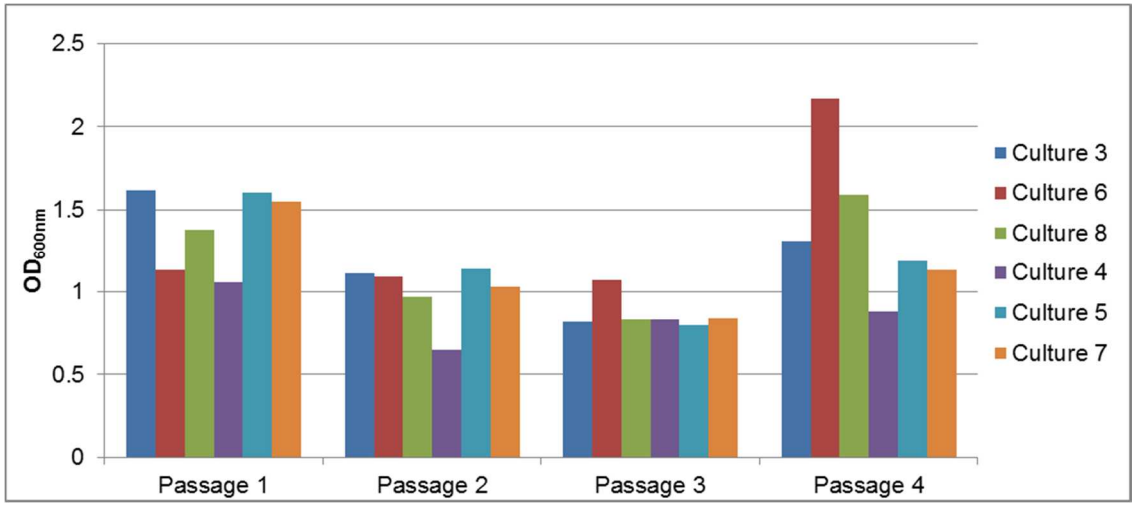

Figure 4.13: Final OD_{600nm} values of the inoculum trains of all the Pn19A batches cultivated in the Wave bioreactor. Batches 4, 5 and 7 failed to grow in the Wave. Data points represent triplicate analyses with a standard error less than 5%.

4.6.4 Conclusion

From the six Pn19A batch cultivations in the Wave bioreactor, three batches were successful (cultures 3, 6 and 8) while three batches failed (cultures 4, 5 and 7). For the successful Wave batches an average of 1.4 g/L as determined by competition ELISA was achieved under batch cultivation conditions (cultures 3, 6 and 8) post 16 h bulk inactivation. Pn19A CPS levels based on immunoassays were higher in the Wave bioreactor in comparison to *S. pneumonia* serotype 1 (Pn1) CPS produced at Biovac in the stirred tank bioreactors under batch and fed-batch cultivation conditions. The Wave bioreactor for pneumococcal bacterial cultivation demonstrated by this thesis was found to be novel and applicable to Pn1 as well as Pn19A. The Wave process was easily adapted from one serotype to another.

4.6.5 General cultivation conclusion

The cultivation, inactivation and clarification techniques developed for Pn1 were applied to eight Pn19A cultivations: two shaker batch cultivations in Schott bottles (Pn19A-001 and Pn19A-002), and six batch cultivations (cultures 3 to 8) in the Wave bioreactor. During the shaker culture cultivation study, the addition of catalase to the medium was investigated and results indicated a significant increase in growth rate and in CPS production (1.7-fold). This supported the hypothesis that catalase, by breaking down H_2O_2 produced during cultivation has a positive effect on the growth of the bacteria as well as on the production of CPS.

The implementation of a culture broth cooling step, prior to phenol addition as used for Pn1 inactivation was applied to the Pn19A inactivation step and resulted in improved of CPS recovery and is therefore recommended. The cultures were fermented until a final OD_{600nm} of approximately 10, and residual glucose of less than 2 mmol/L were obtained. It was noted during Pn1 fermentations that if the glucose levels dropped below 5 mmol/L the CPS levels would decrease and thus it was introduced as a cultivation harvesting point.

No fermentations were performed on Pn19A in a conventional stirred tank fermentor. The wave-based fermentation development results for Pn19A showed that the growth profiles and CPS production levels were similar, if not better than Pn1 in shaker and Wave bioreactor cultivations. The benefits of using the Wave bioreactor and cell bags are that they are convenient to use because cell bags are pre-sterilized and disposable and therefore do not require cleaning and validation thereby eliminating the chances of cross-contamination. Single use stirred tank fermentors are available but stirred tank fermentors culture bags are more costly than Wave culture bags. The CPS levels for Pn1 in the stirred tank fermentors are comparable to Pn19A in the Wave bioreactor suggesting that the manner of mixing in the Wave is able to deliver sufficient nutrient mixing and heat transfer to ensure high CPS production when culturing this fastidious facultative anaerobe. The production of CPS in the cell bags allows for more fermentation runs with faster turnaround times. The Wave bioreactor and cell bags are a convenient way to cultivate anaerobic bacteria but *S. pneumoniae* serotype 19A is a fastidious organism [10, 65] that seems to be very sensitive as only 50% of the cultivations in the bag were successful. FTIR experiments were performed on the inner and outer coatings but these results were inconclusive. FTIR only identifies the type or grade of plastic used but does not account for that leachable or extractable were being released by the plastic under the cultivation conditions [172].

A novel system for culturing pneumococcal bacteria using the rocking motion mixing of the Wave bioreactor to obtain a high yielding CPS producing bacterium was developed. There are many advantages and disadvantages of using single-use technology but for Pn19A the advantages outweighed the disadvantages namely: the environment of the bioreactor is ideal for a shear sensitive bacterium, as well as the production of CPS is fast, with satisfactory results for different serotypes of the same bacteria.

4.7 Purification

Purification of the polysaccharide from bacterial cells for polysaccharide and conjugate vaccines involves separating the polysaccharide from the bacteria itself as well as removal of contaminants such as proteins, nucleic acids, cell wall polysaccharide and other debris. The separation is dependent on the physical and chemical properties of the polysaccharide and the impurities present in the fermentation slurry [120, 129, 173]. Figure 4.14 outlines the basic process steps of Pn19A purification, the key steps being extrapolated directly from the Hib purification process previously developed at Biovac and based on an expired patent [145]. To test this process, the protocol was applied to Pn1 CPS and Pn19A CPS.

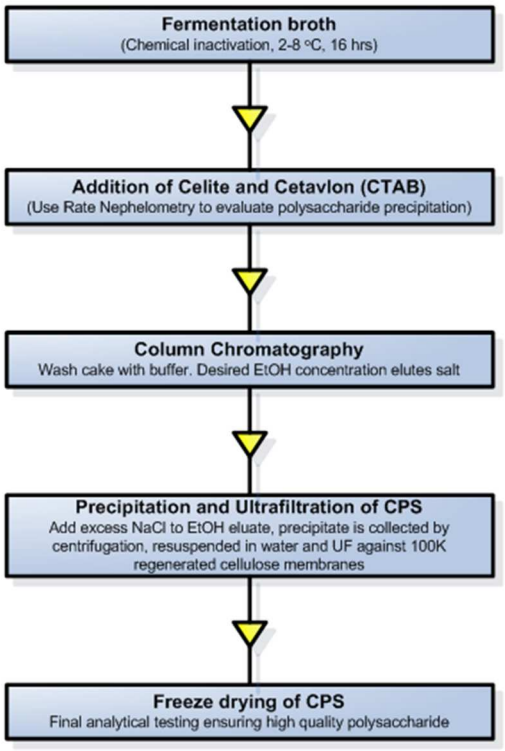

Figure 4.14: Overview of the process flow of purification of the polysaccharide.

The first step in the fermentation process is a clarification of the fermentation broth to separate bacterial cells and particles from the supernatant [174]. Two types of centrifugation methods were employed for the clarification of the fermentation broth: batch and flow through centrifugation (FTC as illustrated in Figure 4.15 (A)). The illustrations represented in Section 4.7 is of the work performed during this study and demonstrates the processes in action. Batch centrifugation was used for the shaker cultures as the volumes were low, while FTC was used for the higher volume cultivations as the processing times were faster and the process itself was less labor intensive. Optical density was employed as an indicator of the presence of debris in the supernatant and used to determine the end point or a number of centrifugation cycles required to remove all contaminants. The outcome in terms of $OD_{600\ nm}$ values for the two centrifugation methods was the same. For the batch centrifugation, it was observed that 3220 x g resulted in the best clarification. Figure 4.15(B) shows the Pn19A culture media after FTC clarification.

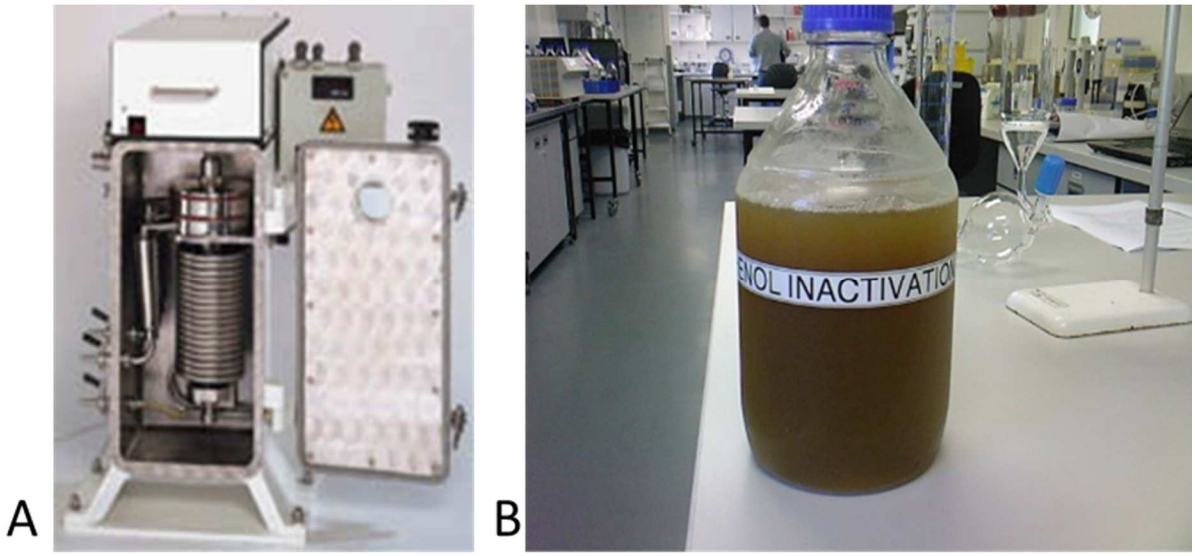

Figure 4.15: A representation of phenol inactivated Pn19A culture (A) using the FTC for clarification in the picture and (B) after clarification and before purification.

The purification method discussed in this thesis was based on the differential precipitation process first introduced by E. Gotschlich [175] which employs the cationic detergent *N*-Cetyl-*N, N, N*-trimethylammonium bromide (CTAB also known as Cetavlon) to precipitate anionic polysaccharides from the whole culture. This method was further modified, by Gonçalves et al. [129] by including tangential microfiltration and ultrafiltration, fractionated ethanol precipitation and enzyme treatments. The CTAB precipitation methodology has been applied successfully to the purification of polyribosylribitol phosphate (PRP) produced from the *Haemophilus influenzae* type b (Hib) and further employed for specific pneumococcal polysaccharides. Negatively-charged polysaccharides, such as Pn19A (due to the phosphodiester group), (Figure 4.16) are precipitated together with nucleic acids and proteins, by the addition of the positively charged cationic detergent CTA^+, (Figure 4.17) to form a CTA^+:Pn19A CPS salt that is insoluble in water and soluble in ethanol.

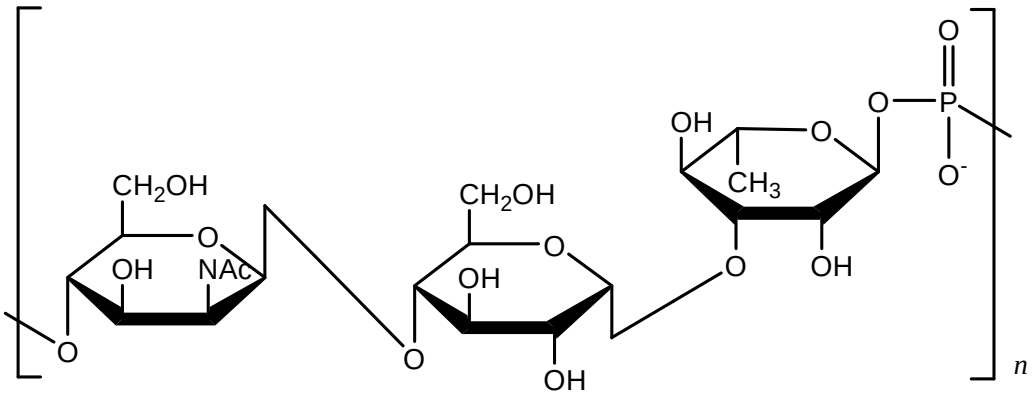

Figure 4.16: Structure of Pn19A CPS repeating unit showing the phosphodiester group responsible for the negative charge of the CPS [176].

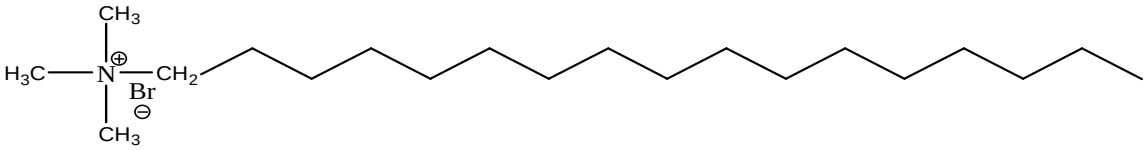

Figure 4.17: The structure of *N*-Cetyl-*N, N, N*-trimethylammonium bromide (also known as Cetavlon or CTA^+).

Figure 4.18: A representation of the filter trap caused by celite addition to the inactivated culture.

Celite, a filter aid is then added to trap the CTA^+:Pn19A polysaccharide precipitate as well as retaining most insoluble impurities and residual cells. The solution is homogenized after celite is added to ensure complete mixing and trapping of the polysaccharide (Figure 4.18). The celite: CTA^+:Pn19A polysaccharide slurry is loaded onto a chromatographic column and allowed to settle (Figure 4.19 (A)).

Figure 4.19: A representation of the (A) chromatography and (B) colorimetric testing using the anthrone assay performed during the purification process to track the CPS.

This is followed by the sequential washing and elution buffers:

- 0.05% CTA^+ in 0.05 M sodium acetate buffer, pH 6: wash solution to remove any media components, while maintaining a low level of CTA^+ to ensure CTA^+:Pn19A CPS salt remains intact.
- 20% ethanol (EtOH) in 0.05 M sodium acetate buffer, pH 6: wash solution to remove small quantities of nucleic acids and proteins
- 30% EtOH in 0.05 M sodium acetate buffer, pH 6: wash solution to further remove all nucleic acid and protein contaminants.
- 60% EtOH in 0.05 M sodium acetate buffer, pH 6: elution buffer to elute CPS. The Pn19A CPS: CTA^+ salt was then dissolved in the alcoholic solution and eluted from the column (Figure 4.21 (A)).

The elution of CPS is tracked using an in-process anthrone assay (Figure 4.19).

The eluted CPS collected from the column was further processed by the addition of saturated sodium chloride whereby sodium replaced CTA^+ to form a sodium: Pn19A polysaccharide salt (Figure 4.20 (A)). This sodium salt was insoluble in 60% ethanol and precipitates out thus facilitating separation by centrifugation. The supernatant is discarded, and the Pn19A polysaccharide was dissolved in water. This solution is diafiltered against a sodium salt solution followed by water, before being filtered through a 0.22 µm membrane and stored at -20 ºC (Figure 4.20 (B)).

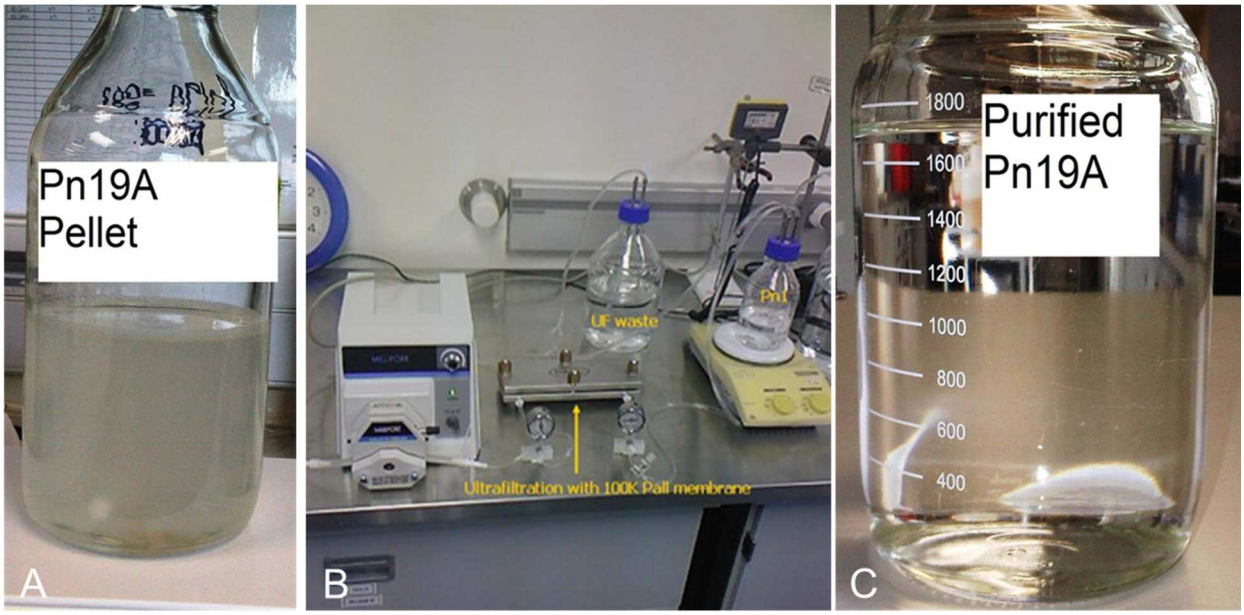

Figure 4.20: A representation of the CPS before and after ultrafiltration and ready for freeze drying for NMR analysis to determine identity and purity of the CPS extracted.(A) Pn19A CPS pellet, (B) diafiltration system using 100K Pall membrane and (C) Purified Pn19A CPS.

The ultrafiltration step using 100 kDa membrane is shown in Figure 4.20 (B) is necessary for the removal of buffers without affecting the CPS. Buffer removal is important as the purified CPS is required in the aqueous form for characterization using techniques such as NMR. The Pn19A polysaccharide was quantified, using (1) chemical colorimetric assays for concentration of polysaccharide, (2) Coomassie and nucleic acid assay to determine the amount of protein and DNA/RNA contamination, respectively

and (3) the molecular size distribution of the polysaccharide was determined using size exclusion high pressure liquid chromatography (SEC-HPLC). The purified Pn19A CPS solution is shown in Figure 4.20 (C).

The anionic nature of many pneumococcal bacterial polysaccharides can be attributed to the presence of the phosphodiester group of the repeating unit of the polysaccharide structure. This phosphodiester group is sensitive to pH and an alkaline range chemical treatment with a base such as NaOH should be avoided as it could cause hydrolysis or cleavage of the phosphodiester linkage between the phosphate group and the rest in the repeating unit. The phosphodiester linkage has been shown to be critical in the stability of the polysaccharide and even more so upon conjugation to a carrier protein [53] (discussed further in Chapter 6). The impact on the CPS should be monitored when establishing purification process parameters.

In this thesis, the objective of the purification procedure for pneumococcal serotype 19A CPS was to investigate the purification methodology using CTAB and its precipitation of negatively charged polymers (pneumococcal polysaccharides) and application to the negatively charged Pn19A.

4.8 Establishing the purification parameters

Parameters to be considered when developing a purification process are (1) pH of the medium for extraction of CPS, (2) amount of CTAB/Celite and (3) ethanol gradient for elution

4.8.1 Determination of optimal pH

Determining a suitable pH for the extraction of CPS from the supernatant was based on work previously conducted on Pn1. Figure 4.21 shows the difference in pH on CPS extraction for Pn19A. At a pH of 7.8 the CPS concentration was similar to that of the fermentation broth and was still present in solution, but once the pH of the fermentation broth was decreased to pH 6.2 the CPS concentration dropped dramatically indicating that there was no CPS left in solution and it was all trapped as in Figure 4.20 in the CTAB/Celite solution for further purification. At pH 7.8, 12% of CPS precipitated out at temperatures between 18 and 22 ºC, whereas, at pH 6.2 the Pn19A polysaccharide remaining in the supernatant was less than 2%. From the results, it was observed that the pH of the fermentation broth played a significant role in the precipitation of the Pn19A polysaccharide and thus a pH of 6.2 was employed.

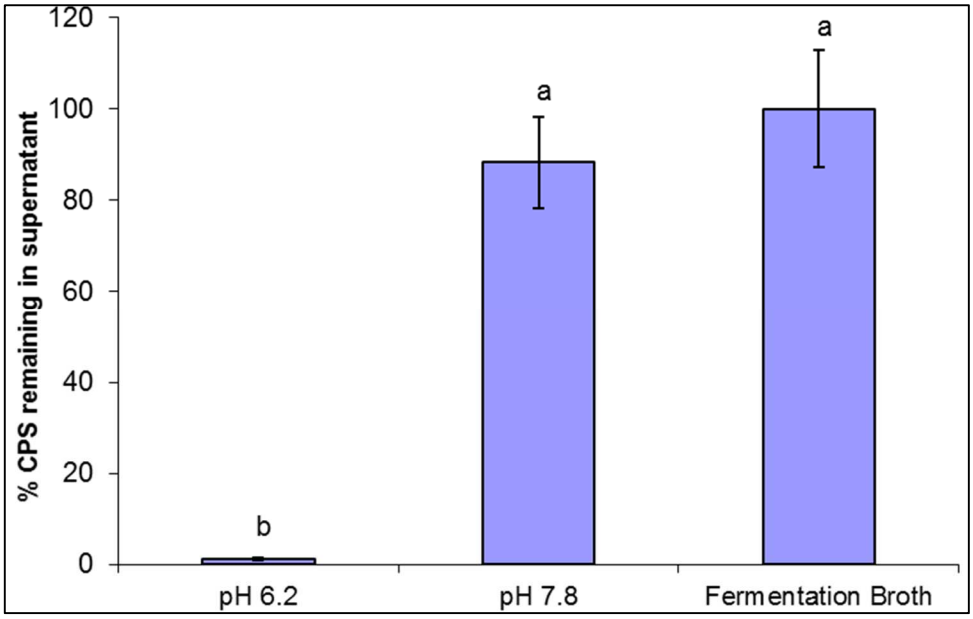

Figure 4.21: Percentage CPS remaining in supernatant upon pH determination for optimal Pn19A CPS extraction.

For Pn1 a pH of 7.8 was found to be suitable for CPS extraction as the functional groups, namely the O-acetyl, remained intact after exposure to these pH conditions. This pH was however not suitable for negatively charged CPS such as Pn19A as the CPS remained in solution at this pH. By making the environment more acidic it was found that the Pn19A CPS was more readily extracted from the supernatant. It was observed that lowering the pH of the broth allowed for the precipitation of proteins and nucleic acids from the supernatant thus making the CPS extraction process simpler. This study made use of rate nephelometry techniques to ensure that all the Pn19A CPS was precipitated from the supernatant, an important consideration when trying to optimize yields for any purification process.

4.8.2 CTAB/Celite precipitation step of the clarified supernatant

A study aimed to evaluate the amount of CTAB/celite used was performed to establish whether similar quantities used for Pn1 were applicable to Pn19A. The amounts of 5 g/L of CTAB and 15 g/L of celite based on studies performed on Pn1 were added to the phenol inactivated fermentation broth. The two experimental flasks were stirred vigorously for 30 min, then allowed to settle for at least one hour after which 2 mL of the supernatant were removed, centrifuged and analyzed for residual polysaccharide by rate nephelometry using the fermentation broth as a positive control. Rate nephelometry was then utilized to determine CPS concentration. Following the addition of the initial quantity of CTAB, further CTAB was then added if necessary until no CPS could be determined in the supernatant. From the Pn19A study with the aid of rate nephelometry, 5 g/L CTAB and 15 g/L m/v celite used for the fermentation slurry were sufficient to precipitate Pn19A polysaccharides in a solution at a pH of 6.2. Subsequent experiments showed these quantities were sufficient for CPS at a concentration of 700 - 1600 mg/L.

4.8.3 Column washing of CPS elution

All washes (see Section 4.7) were evaluated using UV spectroscopy at wavelengths of 260 and 280 nm for nucleic acid and protein content, respectively. Figure 4.22 shows a typical nucleic acid elution profile for Pn19A batch; the CTAB and 20% ethanol fractions contained large quantities of contaminants, while the 30% ethanol wash was able to selectively elute small quantities of nucleic acid. The Pn19A polysaccharide was selectively eluted in 60% EtOH. As soon as the 60% elution buffer was added to the column, the pressure increased and the flow rate decreased as a result of the viscosity of the Pn19A CPS.

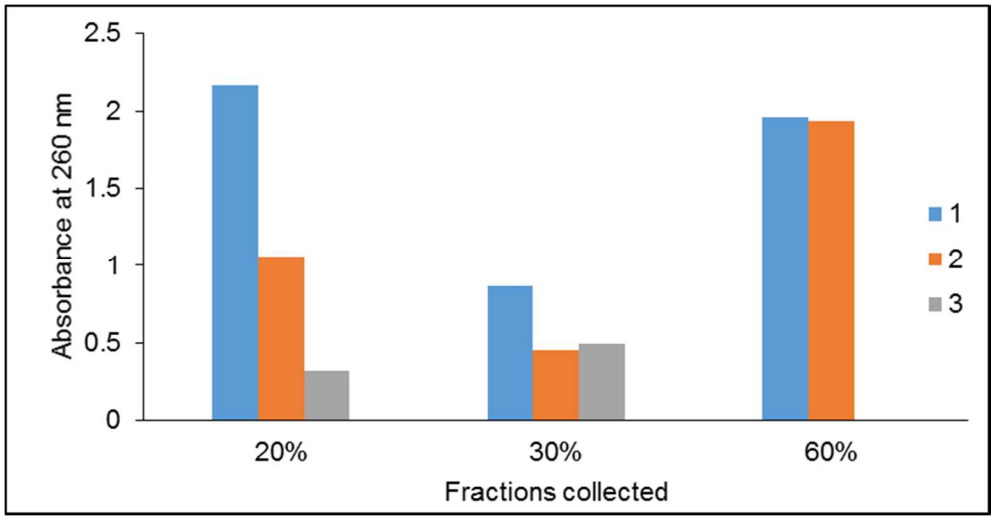

Figure 4.22: Batch Pn19A nucleic acid content per elution fraction captured in triplicate (1, 2 and 3) for 20%, 30% and 60% ethanol fractionation as monitored at 260 nm.

Figure 4.23 depicts the 60% elution profile of Pn19A upon purification washes with EtOH. The Pn19A CPS eluted as a clear viscous solution initially as a result of the high concentration, but viscosity decreased as the CPS concentrated decreased.

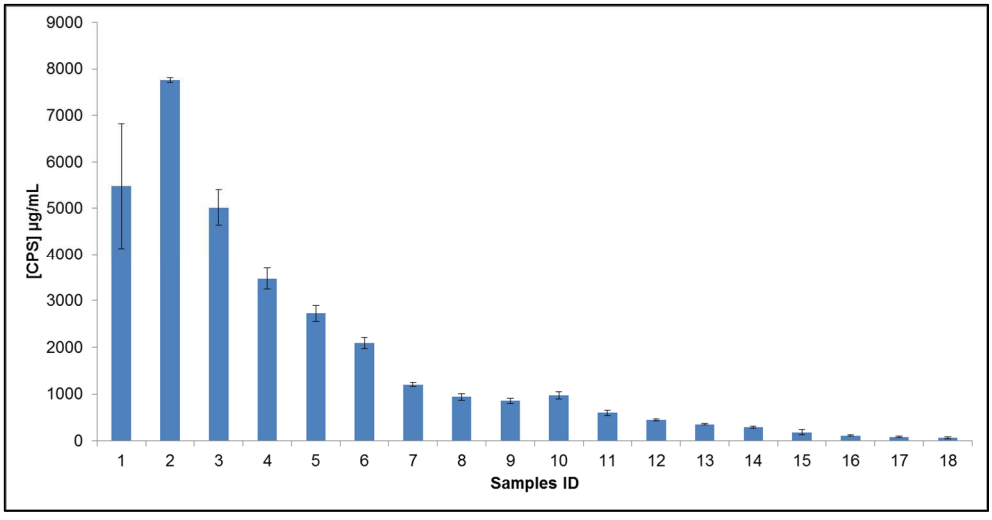

Figure 4.23: Elution profile of batch Pn19A CPS purification eluted during 60% EtOH in 0.05 M sodium acetate wash performed by the ELISA assay with ATCC standards. Fractions 1-8 (150 mL) and fractions 9-18 (250 mL).

The purification process presented here was based on modifications of previously reported methods by Gotschlich [175] and Gonçalves [129]. The outcome of the purification method was to obtain a good yield of CPS that was pure or met in-lab specifications. With the parameters investigated (as mentioned

above), it was found that a purification pH of 6.2 was determined to be the optimal pH for purification for allowing the CTA+ polysaccharide salt to form and precipitate out of solution. The ethanol fractionation range for adequate washing of the column was determined to be between 20% – 30% with low nucleic acid contamination. The CPS eluted during the 60% ethanol fractionation and provided a good yield of CPS before and after filtration. The purity of the CPS obtained meets the WHO specification provided in Table 4.8.

Table 4.8: Testing of purified Pn19A CPS from Wave cultivation.

		Anthrone	**Methyl pentose**	**Phosphorus**	**Protein concentration**	**Nucleic acid**
Batch1	CPS concentration	2.0 g/L	2.2 g/L	ND	NA	NA
	Assay Concentration	0.88 g/L	0.85 g/L	0.6 g/L	0.01 g/L	0.012 g/L
	Purity (%)	100 %	110 %	ND	NA	NA
	% composition	NA	42.5 %	4.1 %	< 1%	< 1%
Batch 2	CPS concentration	2.0 g/L	1.90 g/L	ND	NA	NA
	Assay Concentration	0.88 g/L	0.73 g/L	0.6 g/L	0 g/L	0 g/L
	Purity (%)	100 %	95 %	ND	NA	NA
	% composition	NA	36.5%	4.0 %	< 1%	< 1%
Batch 3	CPS concentration	1.8 g/L	2.0 g/L	ND	NA	NA
	Assay Concentration	0.80 g/L	0.78 g/L	0.59	0	0
	Purity (%)	90 %	100 %	ND	NA	NA
	% composition	NA	43.3%	4.0 %	< 0.05%	< 1%
Batch 8	CPS concentration	2.6 g/L	2.0 g/L	ND	NA	NA
	Assay Concentration	1.1 g/L	0.78 g/L	ND	0.07 g/L	0.01 g/L
	Purity (%)	130 %	100 %	ND	NA	NA
	% composition	NA	30.0 %	ND	< 1%	< 1%
WHO Specifications [145, 175]	% composition	NA	≥ 20%	3.0-5.5%	≤ 3%	≤ 2%

Note: Degree of moisture not determined on the freeze-dried sample.
ND Not done
NA Not applicable

Table 4.8 shows the tests performed on lyophilization batches. Despite the yields being low for all batches, the product that was isolated was pure and within the WHO specifications (Chapter 2). The CPS batches had above 20% recovery of methyl pentose, between 3.0% and 5.5% recovery of phosphorous, less than 1% protein and nucleic acid contamination. The mole percentage CWPS, as determined by NMR, was < 0.5% for all batches.

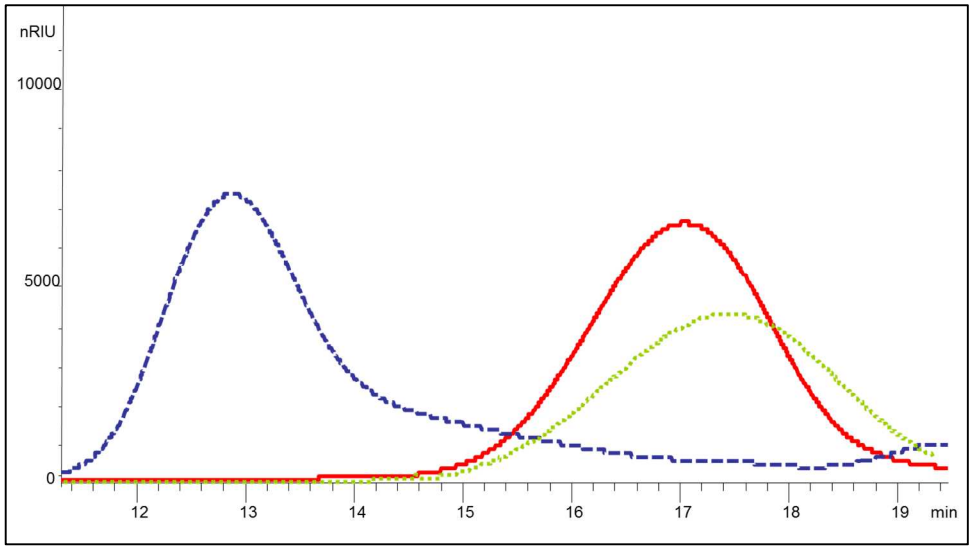

Figure 4.24: SEC-HPLC RID chromatograms of wave Culture 8.Full-length (blue) is sample before diafiltration with an MW of >1000kDa and the FD (red) and the diafiltered (green) are samples after diafiltration with MW of ~60kDa.

An anomaly observed with one of the purification runs as shown in Figure 4.24 showed that the size distribution of one of the batches before centrifugation to remove excess impurities had a molecular weight of about 1000 kDa but upon diafiltration with a 100 kDa membrane saw a decrease in size which then remained at this size after freeze drying and used as the product for conjugation. A theory for this once-off anomaly was that the membranes used during diafiltration were cleaned with base (NaOH), and not all the base was removed thus causing base hydrolysis and automatic reduction of CPS size. A reason for the inefficient cleaning of the membrane could be that the membrane underwent membrane folding and cause fouling.

A simple method was developed that could easily be scaled-up. The purified CPS met the WHO requirements for vaccine production and this method could be applied, with minor modification, to the purification of the CPS from the prevalent serotypes of *S. pneumoniae*; this was demonstrated for serotypes 5 and 6B at Biovac.

4.9 Conclusion

The knowledge acquired from the purification of PRP and Pn1 at Biovac greatly aided the experimental design of the Pn19A CPS purification. A pH of 6.2 was determined as the optimum condition for CTAB/celite precipitation of Pn19A. An ethanol elution gradient wash solution of 0.05% CTAB, 20% EtOH, 30% EtOH and 60% EtOH offered effective separation of Pn19A CPS from the fermentation slurry with the CPS eluting with the 60% EtOH fractions. The collection of the CTA^+:Pn19A CPS was dissolved in 2 M NaCl which allowed for full counter ion-exchange to Na^+:Pn19A CPS and the addition of 96% EtOH maintained a concentration of approximately 60% in order to achieve complete precipitation of Pn19A CPS, followed by centrifugation. The Pn19A CPS formed a relatively thick precipitate which allowed for simple separation through centrifugation. For the ultrafiltration step using 10 volumes of 0.5 M NaCl and water proved effective in removing residual impurities from the bulk Pn19A CPS solution, but significant losses were realized and further work is required to determine which MWCO membrane is suitable as well as optimal processing parameters. The purification process

using CTAB precipitation and chromatography yielded pure Pn19A with acceptable impurities level of nucleic acid and protein as recommended by the WHO. The analytical data showed that the purified Pn19A CPS was of acceptable WHO standards and the NMR analysis (described in Chapter 5) showed that the designed experimental approach was successful in purifying Pn19A CPS. A summary of the purification process is shown in Figure 4.25.

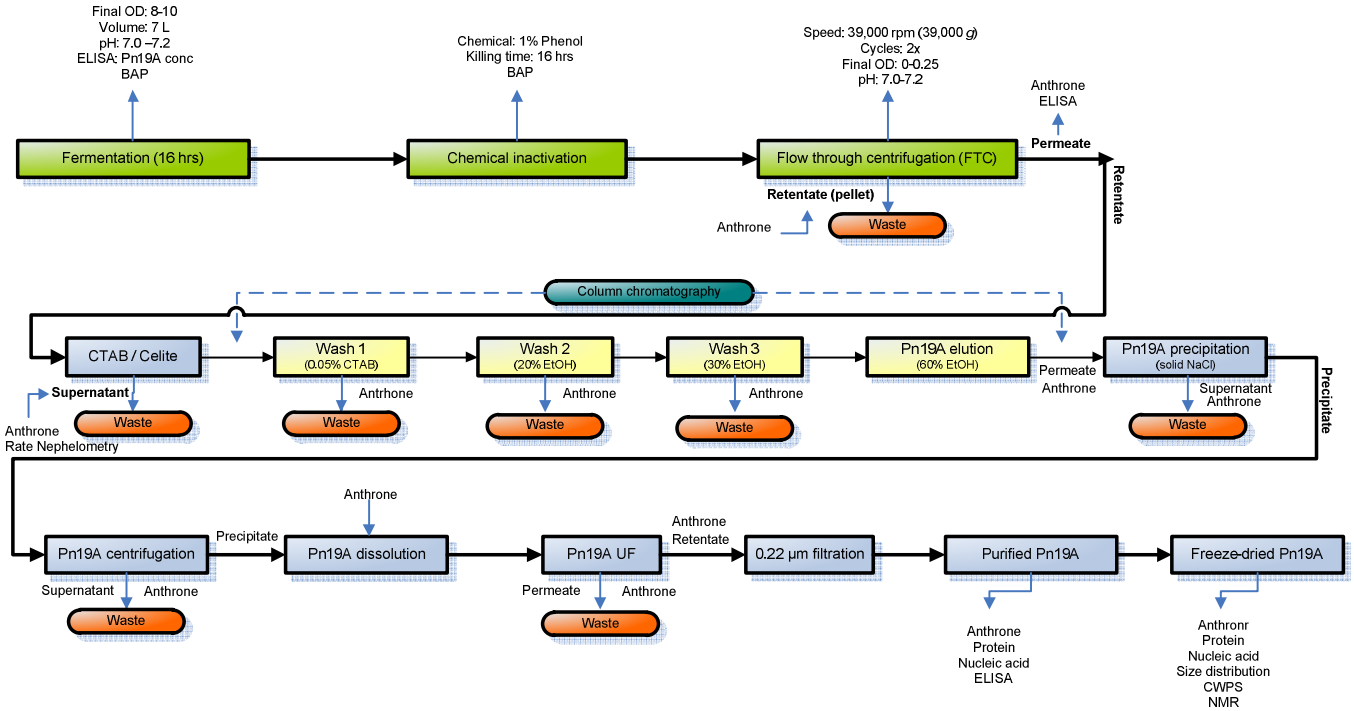

Figure 4.25: Final process flow for the purification of Pn19A CPS.

CHAPTER 5. CHARACTERIZATION OF Pn19F AND Pn19A CAPSULAR POLYSACCHARIDES

This chapter details the characterization of Pn19F and Pn19A CPS. Figure 5.1 outlines the methods applied to the purified CPS extracted from *S. pneumoniae* serogroup 19 for structural composition. The determination of the CPS repeating unit for each serotype of *S. pneumoniae* was required for the full structural identity and characterization [177]. There are numerous ways to fully characterize the polysaccharide with guidance provided by the WHO outlined in the TRS on polysaccharide vaccine characterization [74]. The three key aspects of characterization covered in the TRS include; (1) chemical characterization by colorimetric assays that determine the percentage of each component (qualitative assessment of the polysaccharide repeating units), (2) immunological assays (for determination of polysaccharide identity and antigenicity) and (3) chromatography methods using HPLC/GC (for monosaccharide composition) and NMR (for confirmation of structural identity).

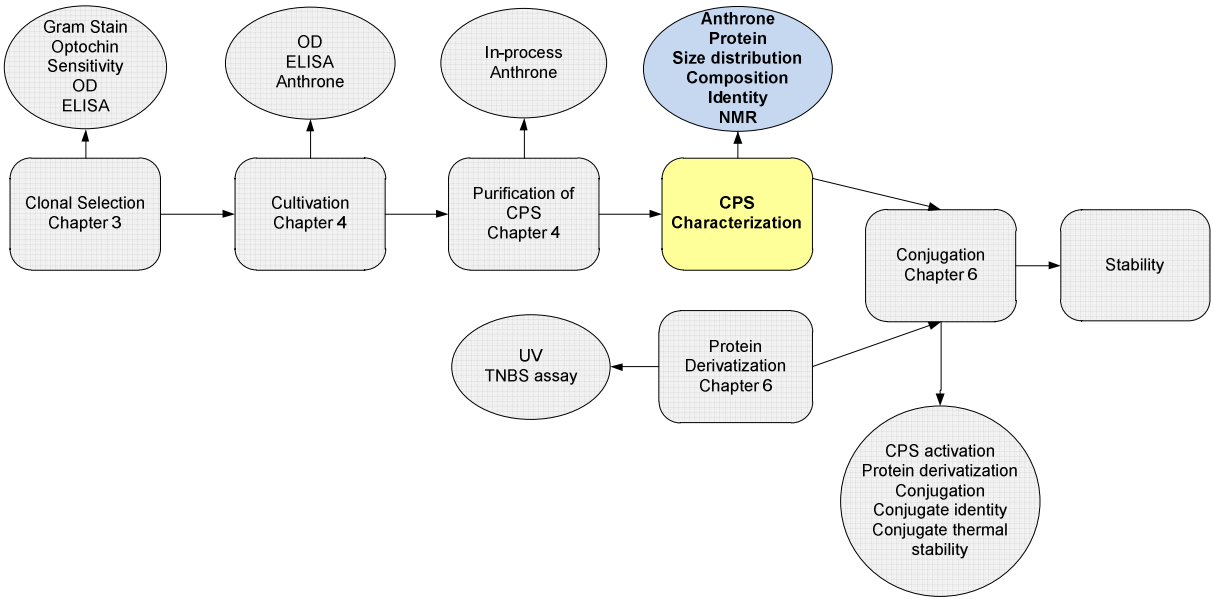

Figure 5.1: The process development steps for Pn19A conjugate vaccine production, focusing on characterizing the purified CPS after fermentation and purification processes.

5.1 The structure of Pn19F and Pn19A capsular polysaccharide

The CPS of *S. pneumoniae* plays a critical role in bacterial survival with more than 90 serologically defined CPS serotypes of which many are related. Two of these serotypes stem from serogroup 19, namely, serotypes 19F and 19A. These CPS are isomeric as their polysaccharide repeating units are identical with the exception of the linkage between glucose and rhamnose monosaccharide residues: C1 to C2 in the case of 19F (Figure 5.2) and C1 to C3 in the case of 19A (Figure 5.3) [53].

The specific CPS repeating units of *S. pneumoniae* serotype 19F and 19A are composed of a repeating trisaccharide unit containing N-acetyl-D-mannosamine, D-glucose, L-rhamnose and phosphate as shown in Figure 5.2 and 5.3 [176, 178].

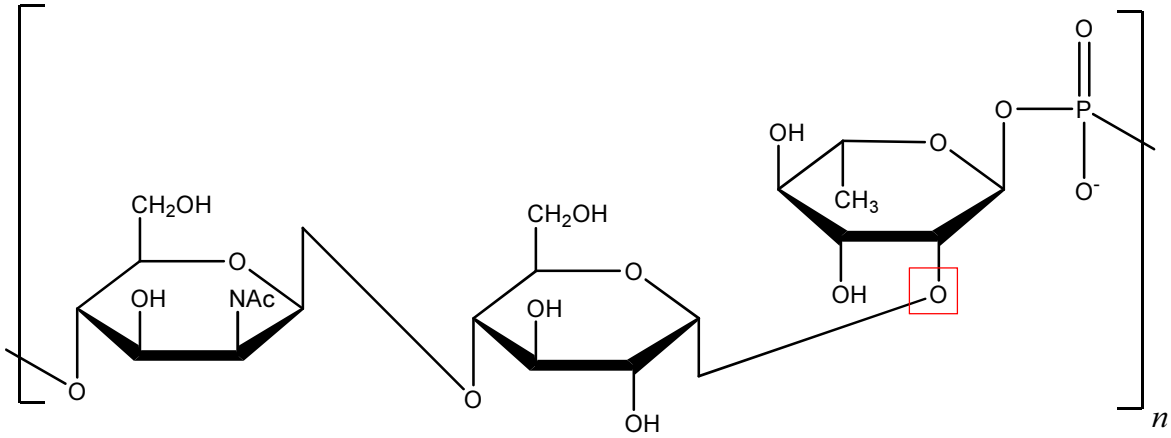

Figure 5.2: Pn19F trisaccharide phosphate repeating unit with a 1-2 linkage between glucose and rhamnose [178].

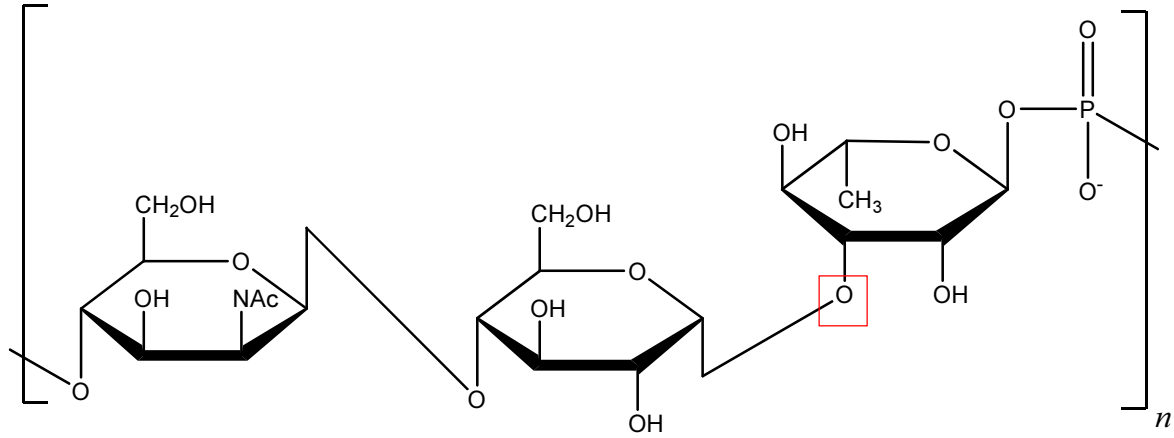

Figure 5.3: Pn19A trisaccharide phosphate repeating unit with a 1-3 linkage between glucose and rhamnose [176].

This structural similarity has led to the assumption that there would be cross-protection between these polysaccharides as was observed for serotypes 6B and 6A (Pn6B and Pn6A) [32]. Pn6B was shown to be more stable and induce functional antibodies to Pn6A and was therefore included in pneumococcal conjugate vaccines. With this understanding, it was believed that Pn19F would provide the same effect that Pn6B had with Pn6A and cross-protect the host against serogroup 19. This assumption was however contradicted by clinical studies which showed a very low and poor cross-protection against Pn19A by Pn19F [179]. According to Jakobsen (2003), it is the difference in this single linkage position between Pn19F and Pn19A that is responsible for the observed lack of cross-protection between the serotypes in children and adults [33]. Both Pn19F and Pn19A also contain a phosphodiester bond connecting the repeating units in these polymers. The phosphodiester bond is susceptible to hydrolysis under basic conditions resulting in an unstable linkage with the positioning of C1→C3 in Pn19A making this bond more susceptible to cleavage when compared to Pn19F [53]. As a result, Pn19A is considered less stable than Pn19F. However, cross-protection has not been shown between Pn19F and Pn19A so both would need to be included in the vaccine [61]. Pn19F CPS was used as a model comparator and therefore it was important to structurally characterize both these serotypes.

5.2 Colorimetric assays

Chemical assays are utilized to selectively quantify a known polysaccharide repeating unit in an unknown sample. According to the WHO TRS 927, the composition of pneumococcal polysaccharides

can be chemically defined by the percentage of functional groups present in the repeating units of these CPS namely total nitrogen, phosphorus, uronic acid, hexosamine, methyl pentose and acetyl groups as shown in Table 5.1. During this study, total nitrogen was not routinely performed and the uronic acid and O-acetyl assays were not applicable for serogroup 19 as these functional group are not present on the CPS. For serogroup 19, of the six assays presented in Table 5.1, only three were used routinely to comply with WHO TRS 927 specifications.

Table 5.1: Theoretical composition of pneumococcal polysaccharides for serotypes 19F and 19A*.

Total Nitrogen (%) (range)	Phosphorus (%) (range)	Uronic acid (%)	Methyl pentose (%)	Hexosamines (%)	O-acetyl groups (%)
2.27 (0.6-3.5)	5.04 (3.0-7.0)	0	26.32 (≥20)	32.98 (≥12.5)	0

*theoretical value with suggested range in parenthesis, based on published structures and dry weight [74].

The estimation of monosaccharides in pneumococcal vaccines had been carried out with many different techniques and these determinations are associated with numerous difficulties [83]. Some of the limitations associated with these colorimetric assays are (1) moisture (which was not accounted for), (2) some are only specific for one or two monosaccharides present on the repeating units of the CPS and (3) some assays are very time-consuming which could lead to the increase in experimental and human errors which in turn leads to calculation errors and false reading and findings. These assays are however appropriate for qualifying the presence of the monosaccharide under investigation.

In order to determine reproducibility and repeatability of these colorimetric assays, assessments were performed to qualify these assays for use in analysis of CPS production. The purity limits provided in Table 5.1 were expressed with reference to the CPS in its salt form, corrected for moisture content. To note, the CPS used during this study is in its salt form but was not corrected for moisture content and rather a combination of simple wet chemical tests was performed which could, therefore, lead to some discrepancy in the results when compared to the literature [74]. A fourth assay, anthrone was used as a generic colorimetric test for the quantitative estimation of CPS. Although this assay was not specific it was employed to quantify the total amount of CPS present in solution at various stages of CPS production and conjugate manufacture. This method was quicker than those previously used and well-suited for the determination of saccharides in pneumococcal vaccines.

Spectrophotometric polysaccharide and protein quantitation assays are methods that use UV/Vis spectroscopy to rapidly determine the concentration of polysaccharide and protein, relative to a standard and sample of known concentration (gold standard) present in a solution [85]. During these colorimetric assays, the polysaccharides are dehydrated upon the addition of acid and form furfurals which condenses with the chromophore to form a color complex that can be detected in the UV/Vis range of the spectrum. Some of these chromophores are L-cysteine, phenol, dimethylaminobenzaldehyde (DMAB) and anthrone to give colored products [180]. The mechanisms of these colorimetric assays are provided in Chapter 2. The colorimetric assays were assessed in terms of their linearity and working range, the precision of the assay, the assay's accuracy and its specificity.

Protein determination was also conducted using UV methods. These colorimetric assays were performed as a first step to identify the components present in these polysaccharides.

5.2.1 Methyl pentose assay

The European Pharmacopoeia protocol (the methyl pentose assay) to determine the rhamnose content in the solution of pneumococcal polysaccharides was followed. Under strongly acidic conditions the concentrated acid depolymerizes the polysaccharide chains and further dehydrates the monomers to form furfurals, which then chelates with cysteine hydrochloride to yield a pale yellow colored complex with an absorption maximum at 396 nm (maximum for methyl pentoses) and 430 nm (maximum for hexoses). The hexose presents as a yellow color but rapidly decreases in intensity in contrast to the reaction with methyl pentose [181]. Besides the yellow color, the reaction of hexose differs from that produced by methyl pentose in its absorption spectrum at 430 nm. Therefore to correct for both the pentoses and hexoses in solution, the OD 396 nm – OD 430 nm difference quantitatively measures the amount of the reaction product of methyl pentose with cysteine [181]. The theoretical methyl pentose composition (according to the WHO TRS) of pneumococcal polysaccharide serotype 19F and 19A is 26.32% (≥ 20) (Table 5.1) [74].

5.2.1.1 Assay verification

The purpose of this procedure was to establish in which range the assay elicited a linear response. A standard curve range from 0 – 1000 µg/mL was tested with a working concentration range for the L-rhamnose standards of 0 – 50 µg/mL (Figure 5.5).

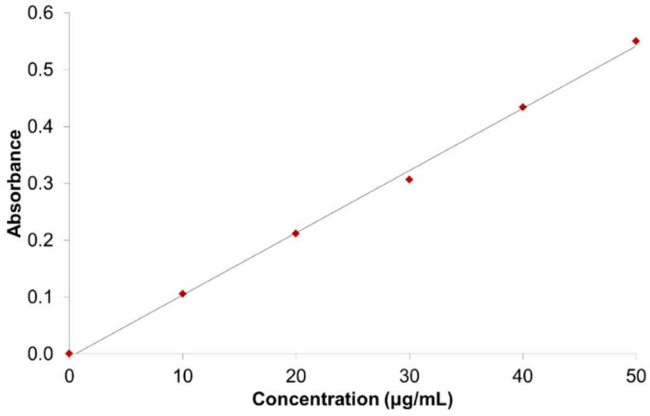

Figure 5.5: Straight line curve to illustrate the linearity absorbance response to working concentration ranges (between 0 – 50 µg/mL) for the L-rhamnose standards.

This assay was linear up to 100 µg/mL but the standard 100 µg/mL was excluded from the standard curve because the respective OD's were above 1.00.

Qualification of an assay involves documenting, through the use of specific laboratory investigations, the performance characteristics of a method that is suitable and reliable for the intended analytical applications [91].

The data generated and presented in Table 5.2 suggests that the methyl pentose contribution to the total CPS is 20.44% (average methyl pentose concentration is 10.22 µg/mL for an accurately prepared 50 µg/mL solution of Pn19F). Hence, the correction factor for the assay was experimentally calculated by dividing this contribution by 100 which gave 4.89, a higher correction factor compared to the

theoretical correction factor of 4.19. A reason for this was that the moisture content was not accounted for however, this result was satisfactory as the aim was to obtain above 20% recovery of rhamnose which was achieved for the methyl pentose assay.

Table 5.2: Precision of the methyl pentose assay.

Sample	Dilution	Absorbamce 396 nm		Absorbance 430 nm		396-440 nm		Corrected OD Value		Calculated methyl pentose concentration (ug) x=(y-c)/m		average methyl pentose concentration (µg/mL)	% methyl pentose content
		tube1	tube2	tube2	tube3	tube1	tube2	tube 1	tube2				
GS 50µg (1)	1	0.245	0.246	0.022	0.020	0.223	0.224	0.22	0.22	10.21	10.26	10.24	20.47
GS 50µg (2)	1	0.248	0.249	0.028	0.017	0.220	0.221	0.21	0.22	10.07	10.12	10.09	20.18
GS 50µg (3)	1	0.234	0.238	0.015	0.019	0.219	0.223	0.21	0.22	10.02	10.21	10.12	20.23
GS 50µg (4)	1	0.265	0.255	0.040	0.035	0.225	0.215	0.22	0.21	10.31	9.83	10.07	20.14
GS 50µg (5)	1	0.250	0.253	0.028	0.023	0.222	0.225	0.22	0.22	10.16	10.31	10.24	20.47
GS 50µg (6)	1	0.247	0.245	0.022	0.021	0.225	0.223	0.22	0.22	10.31	10.21	10.26	20.52
GS 50µg (7)	1	0.247	0.249	0.027	0.025	0.220	0.222	0.21	0.22	10.07	10.16	10.12	20.23
GS 50µg (8)	1	0.240	0.243	0.014	0.021	0.226	0.229	0.22	0.22	10.36	10.50	10.43	20.86
GS 50µg (9)	1	0.287	0.288	0.062	0.063	0.225	0.226	0.22	0.22	10.31	10.36	10.33	20.66
GS 50µg (10)	1	0.260	0.260	0.035	0.050	0.225	0.225	0.22	0.22	10.31	10.31	10.31	20.62
											Average		20.44
											Std dev		0.231
											Range (±2 xSTD)		48.90-51.09
											% RSD		1.13

The accuracy of the assay was assessed by analyzing a sample of known concentration at low, middle and upper levels of the linearity curve. The percentage recovery was found to be within acceptable limits of 96 – 105%. Results depicted in Table 5.3, where the following calculation was employed:

$$\% \text{ Recovery} = \frac{\text{Calculated concentration}}{\text{Actual concentration}} \times 100$$

Table 5.3: Calculation to determine the accuracy of the CPS using different concentrations of Pn19F

µg/mL	Absobance 396 nm			Absorbance 430 nm			Average 396 nm	Average 430 nm	Change in OD	Corrected OD	Concentration from graph (x=(y-c)/m)	Corrected CPS (µg/mL)
	tube 1	tube 2	tube 3	tube 1	tube 2	tube 3						
12.5	0.074	0.072	0.057	0.011	0.006	0.001	0.068	0.006	0.062	0.056	2.48	12
25	0.118	0.131	0.131	0.004	0.013	0.014	0.127	0.010	0.116	0.110	5.10	25
50	0.259	0.258	0.239	0.036	0.032	0.020	0.252	0.029	0.223	0.217	10.20	50
100	0.501	0.530	0.505	0.049	0.063	0.047	0.512	0.053	0.459	0.453	21.52	105

Interfering substances such as PBS used during fermentation and purification, residual CTAB and ammonium sulfate used during purification were tested to determine their effect on the assay. There was no interference observed by the potential analytes presented in Table 5.4 on the methyl pentose assay.

Table 5.4: Analysis of potential interfering species in the methyl pentose assay for Pn19F and Pn19A analysis.

Blank/Analyte	Blank/Analyte
Gold standard	5% EtOH in 0.05% NaOAc
0.2 M NaCl	10% EtOH in 0.05% NaOAc
10 mM PBS	15% EtOH in 0.05% NaOAc
10% CTAB	30% EtOH in 0.05% NaOAc
Saturated Ammonium sulfate	60 mM MES

The methyl pentose method was found to be suitable for the quantitative analysis of polysaccharides containing rhamnose residues in solutions containing pneumococcal polysaccharide including Pn19F

and Pn19A. The optimum linearity region for the L-rhamnose standards was optimized between 0 – 40 µg/mL. An experimental correction factor of 4.89 was calculated for Pn19F and applied to Pn19A.

5.2.1.2 Saccharide quantification

As Pn19F (Pn19A) are not solely constructed of rhamnose, a correction factor for this assay which aims to correct for the difference in total mass of the CPS and is not accounted for by the specific assay is required. The correction factor was determined using Pn19F CPS (Figure 5.1). The estimation of the methyl pentose content, such as rhamnose was based on the European Pharmacopoeia method as described in Chapter 2. The example provided describes the correction factor for the methyl pentose assay and the principles thereof can be applied to the hexosamine assay (Section 5.2.2). Pn19F and Pn19A CPS comprises of a repeating unit of three monosaccharides with residual molecular weights of N-acetyl mannosamine of 202 g/mol, glucose of 162 g/mol and rhamnose of 146 g/mol and a phosphate of 79 g/mol moiety. An additional 23 g/mol was added as this ionic CPS in the sodium salt form.

The theoretical methyl pentose composition was determined using the following equation:

$$\%\text{Composition} = [(\sum \text{MW comp}) / (\sum \text{MW res})] \times 100;$$

Specifically, using Pn19F CPS as an example, the % composition = [(146/612)] × 100 = 23.85%,

The percentage methyl pentose composition (23.85%) differs slightly from the theoretical percentage composition of 26.32 suggested by the WHO. The theoretical correction factor for this assay does not correspond to the experimental correction factor. Therefore, to correct for the polysaccharide residue not accounted for by the methyl pentose assay (total composition is 100%), a correction factor is required. The theoretical correction factor was calculated by dividing the percentage composition (percentage polymer composition accounted by assay) by 100 which gave a theoretical correction factor of 4.19. The experimental correction factor for this assay was determined by dissolving 5 mg pure Pn19F CPS in 100 mL water (50 µg/mL) followed by a further two-fold serial dilution (from 50 µg/mL to 12.5 µg/mL). The CPS concentration was then determined by the methyl pentose assay.

The data presented in Table 5.2 shows that the average recovery of rhamnose (as determined by the methyl pentose assay) in the Pn19F gold standard was >20% which falls within the WHO recommendation for methyl pentose content of Pn19F polysaccharide to be that of 26.32 (≥ 20%). Applying the calculated correction factor, the average Pn19F concentration was determined to be 49.98 µg/mL. The calculated % RSD for samples were all within specification limits of ≤ 2%.

5.2.2 Hexosamine assay

The Elson-Morgan reaction (hexosamine assay) is the procedure used for the detection of hexosamines, this assay was reported to be adequately specific [182] but not very sensitive and for this reason was used to identify the presence of these amino sugars but not to quantify them. The hexosamine assay follows the European Pharmacopoeia protocol whereby samples containing hexosamines are hydrolyzed by hydrochloric acid to release the hexosamine monomers and then

neutralized with sodium hydroxide and hydrochloric acid. This neutralized sample complexes to acetylacetone and a DMAB solution yielding a pink color at a wavelength of 530 nm [183].

The theoretical hexosamine composition (according to the WHO TRS) of pneumococcal polysaccharide serotype 19F and 19A is 32.98% (and should be ≥ 12.5%) [74]. Preliminary work showed that this method consistently showed a low recovery of hexosamine when compared to WHO specifications. As such the European Pharmacopoeia method (described in Chapter 2) was modified to overcome this finding, the changes are summarized in Table 5.5 [76]

Table 5.5: Hexosamine assay and modifications

Parameters	European Pharma Method	Modified Method
Concentration (M)	8	10
Temperature (ºC)	90	100
Hydrolysis (CPS)	1 h	2 h
Hydrolysis (Std)	1 h	10 min

The changes include; (1) an increase in concentration of hydrochloric acid from 8 M to 10 M, (2) an increase in temperature from 90 ºC to 100 ºC and (3) an increased hydrolysis time from 1 hour to 2 hours for CPS and decreased from 1 hour to 10 minutes for the standards. These changes were based on constant monitoring of experiments performed in the laboratory to determine the optimum conditions for analysis of CPS. Even with these changes to the European Pharmacopoeia method, there were still major issues with this assay. The maintenance of concentration throughout the process was difficult due to re-suspension issues and volumes changes which could not be controlled due to the excessive heating for long periods of time. Increasing the temperature was performed to increase the intensity of the color produced but in return decreased the specificity of the reaction. Determining a correction factor for this assay was therefore very challenging and inconclusive as the assay was not reproducible. For this reason, the assay was not used further in the determination of CPS concentration of Pn19F or Pn19A but rather used to identify the presence of amino sugars in the repeating units of Pn19F and Pn19A CPS.

5.2.2.1 Assay verification

Linearity for the hexosamine assay was investigated from 0 – 20 µg/mL which was found to be a narrow range. Although the assay continued to provide a linear response at higher concentrations the standards at 10 µg/mL and 20 µg/mL was excluded from the standard curve because the respective OD's were above 1.00. The working concentration range for the glucosamine hydrochloride standard was 0 – 5 µg/mL (Figure 5.6).

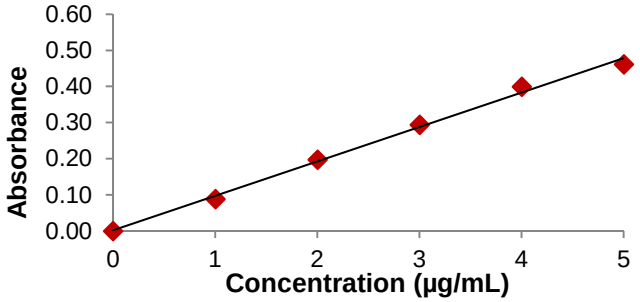

Figure 5.6: Straight line curve to illustrate the linear absorbance response to working concentration ranges (between 0 – 5 µg/mL) for the glucosamine hydrochloride standards.

Table 5.6: Assay precision table for hexosamine assay using Pn19F as a gold standard (GS).

Sample Name	Dilution 1	Dilution 2	OD values at 530 nm			Corrected OD value at 530 nm			Average OD at 530 nm	Concentration from graph (x=(y-c)/m)	Concentration (µg/mL)	% glucosamine content to total CPS
			tube1	tube2	tube3	tube1	tube 2	tube 3				
GS 50µg (1)	1	100	0.478	0.460	0.461	0.468	0.450	0.451	0.451	7.55	755.00	15.10
GS 50µg (2)	1	100	0.477	0.482	0.470	0.467	0.472	0.460	0.466	7.81	780.92	15.62
GS 50µg (3)	1	100	0.504	0.468	0.457	0.494	0.458	0.447	0.453	7.58	758.34	15.17
GS 50µg (4)	1	100	0.440	0.450	0.459	0.430	0.440	0.449	0.445	7.45	744.96	14.90
GS 50µg (5)	1	100	0.419	0.431	0.515	0.409	0.421	0.505	0.463	7.76	775.91	15.52
											Average	15.26
											std dev	0.30
											Range	14.96-15.56
											% RSD	1.96

The sensitivity of this assay was very low however, the presence of hexosamines was demonstrated and the WHO requirements of greater than or equal to 12.5% for Pn19F and Pn19A CPS was met. These requirements were met. Due to inconsistencies of this assay, poor reproducibility and time required in performing this assay; the hexosamine assay was abandoned and was not applied to any fermentation batches and only performed on model compounds and standards as shown above.

Table 5.7: Calculation of percentage recoveries to determine the accuracy of the polysaccharide using different concentrations of Pn19F CPS.

Sample Name	Dilution 1	Dilution 2	OD values at 530 nm			Corrected OD value at 530 nm			Average OD at 530 nm	Concentration from graph (x=(y-c)/m)	Concentration (µg/mL)	% glucosamine content to total CPS
12.5	1	400	0.129	0.124	0.126	0.119	0.114	0.116	0.115	1.94	775.31	15.51
25	1	200	0.241	0.238	0.235	0.231	0.228	0.225	0.227	3.80	760.65	15.21
37.5	1	150	0.342	0.340	0.343	0.332	0.330	0.333	0.332	5.56	833.93	16.68
50	1	100	0.515	0.440	0.459	0.505	0.430	0.449	0.440	7.37	736.60	14.73

5.2.3 Phosphorus assay

Samples containing phosphorus were mineralized by a sulfuric/perchloric acid cocktail and the resulting inorganic phosphate was released and formed a complex with ammonium molybdate (phosphomolybdate complex). Reduction of this phosphomolybdate complex by ascorbic acid resulted in a characteristically blue colored solution which was detected by measurement at 825 nm [81, 184]. The phosphorus assay is not specific to pneumococcal polysaccharides, as any samples containing phosphate salts or sugar phosphates would be expected to interfere. The CPS (Pn19F and Pn19A) phosphate concentration was determined from a standard curve using disodium phosphate as a standard.

5.2.3.1 Assay verification

The linearity of the assay was assessed by preparing and analyzing disodium phosphate (Na_2HPO_4) as a reference standard. The results were shown to be linear over the tested range of 0 – 60 µg/mL (Figure 5.7).

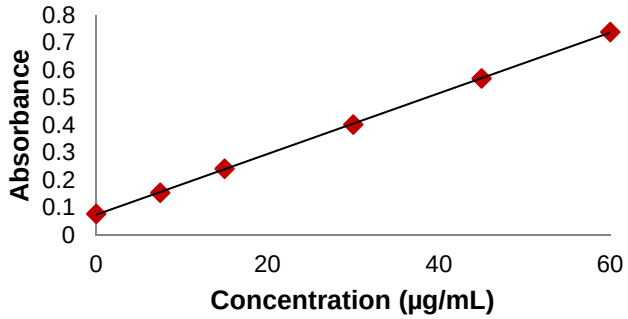

Figure 5.7: Straight line curve to illustrate the linear absorbance response to working concentration ranges (between 0 – 60 µg/mL) for Pn19F CPS.

The precision of the assay was assessed by analyzing ten replicates of the same sample and calculating the standard deviation, average, and relative standard deviation. This Pn19F gold standard (0.5 mg/mL) was prepared and used for the determination of free phosphorus present. The phosphorus content in a solution of pneumococcal polysaccharides met WHO specifications with a working range of 3 – 5% and Table 5.8 shows that the phosphorus content in Pn19F falls within that range. The calculated %RSD for samples were all within acceptable specification limits of ≤ 2%. However, this assay was not suitable for tracking CPS content as phosphates are found both in CPS and the cell wall polysaccharide (discussed in Section 5.3.4.3).

Table 5.8: Absorbance results for precision using Pn19F gold standard

Pn19F	OD values (825 nm)		Average OD	% Phosphorus content to total CPS	Calculated phosphorus content (µg) x=(y-c)/m	Actual phosphorus concentration (µg/mL)
	Tube 1	Tube 2				
1	0.312	0.313	0.313	4.42	22.076	22.08
2	0.310	0.311	0.311	4.38	21.893	21.89
3	0.312	0.313	0.313	4.42	22.076	22.08
4	0.308	0.311	0.310	4.36	21.801	21.80
5	0.305	0.304	0.305	4.48	22.400	22.40
6	0.304	0.306	0.305	4.49	22.448	22.45
7	0.304	0.304	0.304	4.47	22.352	22.35
8	0.301	0.302	0.302	4.42	22.111	22.11
9	0.297	0.303	0.300	4.39	21.967	21.97
10	0.314	0.313	0.314	4.43	22.167	22.17
					Average	22.13
					Std Dev	0.24
					Range	21.66-22.60
					%RSD	1.07

The accuracy of the assay was assessed by analyzing the Pn19F gold standard of known concentration at the low, middle and upper level of the linearity curve (Table 5.9). The percentage recovery was determined and found to be within acceptable limits of 90 – 110%. The European Pharmacopoeia methods (section 5.2.1 - 5.2.3) were adequate for quantification of pneumococcal polysaccharides and specifications according to WHO were met (Table 5.1).

Table 5.9: Calculation of percentage recoveries to determine the accuracy of the polysaccharide using different concentrations of Pn19F polysaccharide.

Theoretical concentration (µg/mL)	Experimental concentration (µg/mL)	Percentage recovery (%)
2.5	2.54	101
20	19.87	99
60	59.89	100

While this assay is specific for phosphorus, it is time-consuming and cannot distinguish between phosphorus found in CPS or the known contaminant CWPS found in trace amounts for Pn19A CPS. Thus a generic assay that was relatively quick, robust and non-interfering was required to quantify and track pneumococcal polysaccharide content at each stage of CPS production/manufacture.

5.2.4 Anthrone Assay

The use of anthrone for the analysis of carbohydrate material was first reported by Dreywood in 1946 [185]. The anthrone assay was used to determine the saccharide content in polysaccharides that contain neutral hexoses such as galactose, glucose, and rhamnose in their repeating units [82]. The polysaccharide undergo acid hydrolysis to depolymerize and release monosaccharides to form furfural derivatives followed by reaction with anthrone to yield a characteristic blue-green color with absorbance read spectrophotometrically at 625 nm [186]. The anthrone assay is a general assay used to detect and track the saccharide content in a sample. Anthrone reagent reacts with most saccharides, except for amino sugars, alditols and uronic acids [187, 188]. At the time of investigation of this assay both Pn19F CPS nor Pn19A CPS was available and therefore Pn6B CPS was used as a control as it contains the saccharides (glucose and rhamnose) and phosphate moiety similarly to Pn19F and Pn19A CPS. Sensitivity and simplicity without the need for extensive hydrolysis as in the case of the hexosamine assay were listed among the major advantages of this assay [189].

5.2.4.1 Assay verification

The linearity of the assay was assessed by preparing, the glucose standards from 0 – 400 µg/mL, analyzing in triplicate and plotting the mean absorbance against concentration (µg/mL). It was important to note that although linearity for this assay continued at concentrations greater than 40 µg/mL and up to 200 µg/mL (Figures 5.9), standards 75 µg/mL, 100 µg/mL and 200 µg/mL were excluded from the standard curve because the respective OD's were above 1.00. Thus, 0 – 40 µg/mL was the working concentration range for the D-glucose standards.

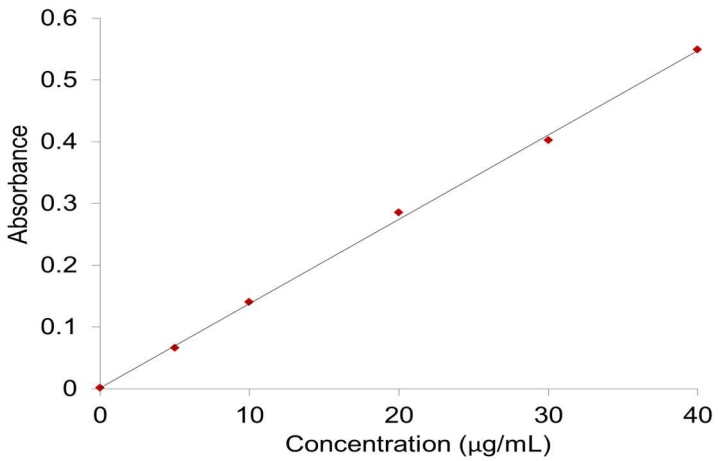

Figure 5.9: Straight line curve to illustrate the linear absorbance response to working concentration ranges (between 0 – 40 µg/mL) for the glucose standards.

The precision of the assay was assessed by analyzing ten replicates of the same sample (in this instance the known gold standard at 25 µg/mL) and calculating the standard deviation, average and relative standard deviation (Table 5.10). The calculated % RSD for samples were all within acceptable specification limits of ≤ 2%.

Table 5.10: Absorbance results for precision of Pn6B CPS

Sample Name	OD values			Corrected OD values			Average OD	Concentration from graph (x=(y-c)/m)	Actual concentration (µg/mL)
	tube 1	tube 2	tube 3	tube 1	tube 2	tube 3			
1	0.157	0.156	0.155	0.149	0.147	0.146	0.147	11.14	25.63
2	0.154	0.157	0.155	0.146	0.148	0.146	0.147	11.10	25.52
3	0.160	0.154	0.154	0.151	0.146	0.145	0.147	11.14	25.62
4	0.157	0.151	0.154	0.149	0.143	0.146	0.146	11.01	25.33
5	0.160	0.152	0.157	0.151	0.144	0.149	0.148	11.18	25.70
6	0.150	0.155	0.153	0.141	0.146	0.144	0.144	10.88	25.02
7	0.157	0.148	0.153	0.149	0.14	0.144	0.144	10.89	25.06
8	0.160	0.155	0.151	0.151	0.146	0.142	0.147	11.08	25.48
9	0.159	0.150	0.156	0.150	0.141	0.147	0.146	11.06	25.43
10	0.160	0.144	0.156	0.151	0.135	0.148	0.145	10.93	25.15
								Average	25.39
								Std Dev	0.25
								Range (±2xSTD)	24.90-25.89
								&RSD	0.97

The accuracy of the assay was assessed by analyzing a sample of known concentration at lower, middle and upper level of the linearity curve performed in triplicate. The percentage recovery was determined and found to be within acceptable limits of 90 – 110%. An average of the results is depicted below in Table 5.11, where the following calculation was employed:

$$\% \text{ Recovery} = \frac{\text{Calculated concentration}}{\text{Actual concentration}} \times 100$$

Table 5.11: Calculation of percentage recoveries to determine the accuracy of the polysaccharides using different concentrations of Pn6B polysaccharide.

Concentration (µg/mL)	OD values			Corrected OD values			Average OD	Concentration from graph (x=(y-c)/m)	% Recovery
5	0.074	0.071	0.073	0.066	0.063	0.065	0.064	4.95	99
20	0.270	0.306	0.261	0.261	0.298	0.293	0.284	21.29	106
30	0.385	0.391	0.377	0.377	0.351	0.382	0.370	27.70	92
50	0.741	0.701	0.733	0.733	0.635	0.693	0.704	52.51	105

The specificity of the test method was evaluated by analyzing for matrix interferences including buffers, reagents, and water. To this end, a reference standard was prepared by diluting 333 µL of the 25 µg/mL gold standard Pn6B with 167 µL of purified water to yield a final sample volume of 500 µL (1:3 dilution; 20 µg/mL final concentration). Testing samples were prepared with 167 µL of the interfering substance (analyte) and 333 µL of 25 µg/mL gold standard. The acceptance criterion is that no optical difference should be observed between the reference sample and the testing samples.

Table 5.12: Analysis of potential interfering species in the anthrone assay

Blank/Analyte	Blank/Analyte
Gold standard	5% EtOH in 0.05% NaOAc
0.2 M NaCl	10% EtOH in 0.05% NaOAc
10 mM PBS	15% EtOH in 0.05% NaOAc
10% CTAB	30% EtOH in 0.05% NaOAc
*Saturated Ammonium sulfate	60 mM MES

*interfering substance

It should be noted that only saturated ammonium sulfate was found to interfere with the anthrone assay. Therefore, if saturated ammonium sulfate was used during any processing, it would have to be completely removed in order to ensure no interference when assaying for saccharide content. The method was found to be suitable for the quantitative analysis of glucose residues in solutions containing pneumococcal polysaccharide including Pn19F and Pn19A [77]. Linearity for the D-glucose standards was optimized between 0 – 40 µg/mL.

5.2.4.2 Saccharide quantification

To calculate a correction factor for use of the anthrone assay Pn6B, shown in Figure 5.8 was used as it comprises of four sugars including galactose, glucose, rhamnose and a ribitol phosphate moiety. The glucose and the phosphate moiety can also be found in Pn19F and Pn19A CPS and since these CPS were unavailable at the time of investigation Pn6B was deemed a suitable substitute for these CPS.

Since the anthrone assay does not elicit a response from alditols (ribitol phosphate moiety in the case of Pn6B and rhamnose phosphate moiety in the case of Pn19F and 19A) and gives a low colour intensity for rhamnose, these two sugars are not experimentally accounted for by the assay and hence must be corrected for from the theoretical composition [77]. The theoretical carbohydrate composition is determined using the following equation:

$$\%\text{Composition} = [(\sum \text{MW comp}) / (\sum \text{MW res})] \times 100;$$

Hence, using Pn6B as an example, the % composition = [(162.145 + 162.145)/706.2] × 100 = 45.9%. And using Pn19F/ Pn19A, the % composition = [(162 + 146)/612] x 100 = 50.33 % (values as shown in Section 5.2.1.3).

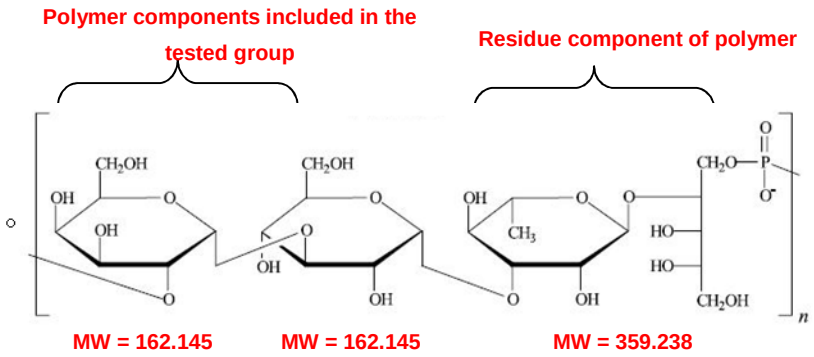

Figure 5.8: Structure of Pn6B repeating unit consisting of [2)-α-D-Galp-(1→3)-α-D-Glcp-(1→3)-α-L-Rhap-(1→4)-D-ribitol-5-P-(O→]n in the sodium salt form with residual molecular weights recorded.

To correct for the repeating unit components not accounted for by the anthrone assay (total composition is 100%), a correction factor was required. The theoretical correction factor is calculated by dividing % polymer composition accounted by assay by 100 which gave a theoretical correction factor of 2.17 for Pn6B and ~2 for Pn19F/ Pn19A. The theoretical correction factor using the anthrone assay for Pn6B and Pn19F/ 19A are comparable.

The experimentally determined correction factor for this assay was established by dissolving 5 mg pure Pn6B polysaccharide in 200 mL water (25 µg/mL) and then performing a further two-fold serial dilution (from 25 µg/mL to 1.56 µg/mL) of this solution. The polysaccharide concentration was then determined by the anthrone assay. The data generated suggest that the positive response from sugars to the total polysaccharide is 43.50% (average sugar concentration is 10.99 µg/mL, and this is for an accurately prepared 25 µg/mL solution of Pn6B). Hence, the correction factor (= 100/43.5) for the assay was experimentally calculated to be 2.30. While there is no WHO recommendation for the anthrone assay, this experimental determination of the correction factor was close to the theoretically determined one. Applying this calculated correction factor, the average Pn6B gold standard concentration was found to be 25.29 µg/mL. The calculated % RSD for samples were all within specification limits of ≤ 2%.

5.2.5 Quantification and application of assays

The two assays, methyl pentose, and anthrone were compared in Table 5.13 as they were suitable for determining the presence of the saccharides in the repeating units of Pn19F and Pn19A. A correction factor for the methyl pentose assay was determined experimentally. The data generated (Table 5.13) suggest that the positive response from methyl pentose sugars to the total polysaccharide 20.44%. Hence, the correction factor for the assay was experimentally calculated to be 4.89. The correction factor for the two assays differed because the methyl pentose assay was more specific in determining the presence of polysaccharides containing methyl pentoses such as rhamnose and compensates for the presence of hexoses such as glucose and mannose upon acid hydrolysis and complex development [77].

An experimental correction factor of 2.30 was calculated for Pn6B and applied to Pn19F and Pn19A using the anthrone assay because these pneumococcal polysaccharides both contain glucose and

phosphodiester groups. Applying the same principles to the methyl pentose assay, an experimental correction factor of 4.89 was calculated.

Table 5.13: Concentration of CPS determined by the anthrone and methyl pentose assays

Experiment number	Anthrone µg/mL	Methyl pentose µg/mL
1	11.05	10.24
2	11.13	10.09
3	10.41	10.12
4	11.12	10.07
5	11.17	10.24
6	11.22	10.26
7	11.43	10.12
8	10.79	10.43
9	10.25	10.33
10	10.42	10.31
Average	10.90	10.24
[Total CPS]	43.59 %	20.44%
CF	**2.30**	**4.89**

The anthrone assay is a method which detects the presence of hexoses and can be used as an alternative to the methyl pentose assay to quantify the amount of CPS produced. The anthrone assay was utilized to determine the presence of CPS during the purification process from culture broth to purified CPS. Due to its broad range of specificity, this method was applied to the stages of purification where the interference of contaminants had been substantially reduced (Chapter 4).

Table 5.14: Application of colorimetric assays on the fermentation broth of Pn19A

	Fermentation slurry volume	[Pn19A] ELISA*	Total mass ELISA*	[Pn19A] Anthrone	Total mass Anthrone	[Pn19A] methyl pentose	Total mass methyl pentose
Pn19A batch	7 L	1.6 g/L	11.2 g	1.3 g/L	9.1 g	1.6 g/L	11.2 g

* ATCC reference standards were used in the quantification of the Pn19A CPS.

The chemical assays (anthrone and methyl pentose assay) were used in conjunction with immunoassay and analytical tools to quantify the amount of CPS present during the fermentation, purification and conjugation processes. The anthrone and the immunoassays results were comparable and could be performed independently or simultaneously. Table 5.14 demonstrates the application of these assays on products generated by the manufacture of CPS. Some of the recoveries obtained when comparing chemical and immunological assays on a fermentation batch before purification were similar in determining the concentration of the CPS. The anthrone assay was used as a tracking tool to track the presence and amount of CPS produced at the different stages of CPS manufacture. Further description and identification of these pneumococcal polysaccharides by hydrolysis and compositional assays was required and discussed in Section 5.3. Colorimetric assays provided useful preliminary data on the

quantity and type of carbohydrates present. In this study, the identity of the monosaccharides present in the repeating unit of the Pn19F and Pn19A CPS was identified.

5.2.6 Summary of colorimetric assay development

The first step in characterizing a polysaccharide is the determination of its purity. This is reflected by its chemical composition which includes total sugar content, proteins and moisture [190]. Colorimetric methods described in Chapter 2 are suitable for estimating the amount of sugar types present. These assays were performed as semi-qualitative analysis for the identification of pneumococcal polysaccharides. Three colorimetric assays, in particular, were optimized from the European Pharmacopoeia methods to enable the accurate determination of the monosaccharides present in the repeating units of Pn19F and Pn19A polysaccharide. These colorimetric assays requires the construction of standardized assay conditions in order to generate a standard curve to achieve precision for quantitative purposes [191]. The colorimetric assays were qualified in terms of linearity, precision, accuracy and specificity and a correction factor for quantification of saccharide content because the CPS was stored in liquid and not lyophilized form was determined experimentally for each assay and corrected for moisture content. Due to time constraints of these WHO recommended assays, it was only used for initial and final stage testing whereas the anthrone assay which is fast and reliable was used as an in-house assay to determine the concentration of CPS at each stage of the manufacturing process.

5.3 Physiochemical techniques

Determination of the molecular size distribution of vaccine products by high performance size exclusion chromatography coupled to refractive index detection is important during the manufacturing process [192]. While colorimetric assays give an indication of the identification of functional groups such as methyl pentose, phosphate and hexosamines present on the repeating unit of the CPS, they are not specific to the monosaccharides present in the repeating units. For this reason, more sensitive and specific detection methods are required. For monosaccharide composition analysis of polysaccharides, HPLC and gas-liquid chromatography in combination with mass spectroscopy (GC-MS) can be applied.

5.3.1 Molecular size distribution

High-performance liquid chromatography (HPLC) is an analytical technique used to separate a mixture of compounds with the purpose of identifying, quantifying or purifying individual components in the mixture [193]. Size exclusion chromatography (SEC-HPLC) is a useful tool employed for the fractionation of carbohydrates that are separated according to their molecular size and the ratio of their molecular dimensions to the average diameter of the pores of the stationary phase [194]. SEC-HPLC was used to determine the size of full-length CPS and size-reduced CPS after size reduction. The molecular size of the purified CPS provides information relating to manufacturing consistency of purified CPS batches [74]. The molecular weight (MW) of polysaccharides is determined based on the use of Pullulan standards. When polysaccharides are eluted through a SEC column the chains are separated according to differences in hydrodynamic volume by the column packing material. The larger polysaccharides flow through the column more quickly than the smaller ones thus the smaller ones

have a longer retention time. The retention volume or time of an eluted peak provides a measure of the molecular size [193].

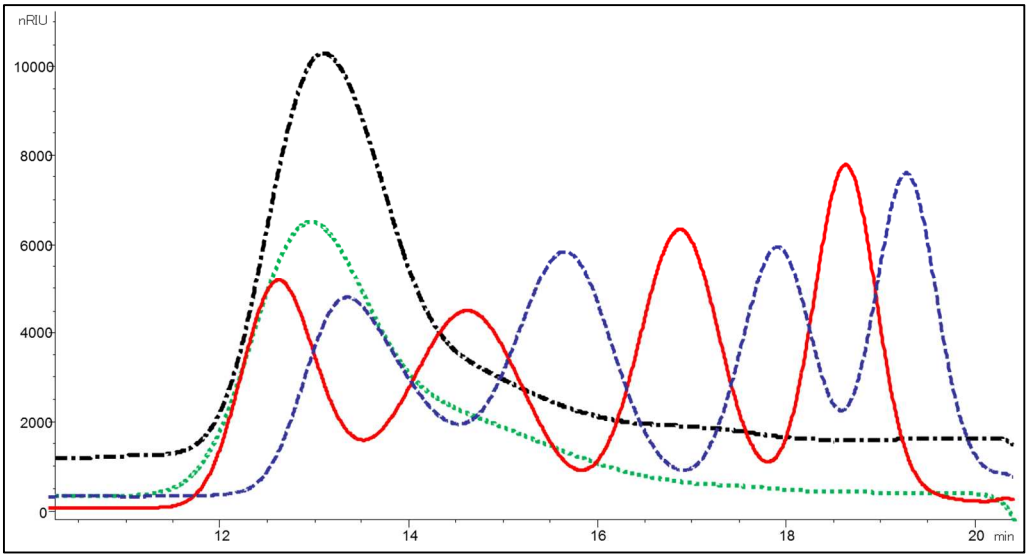

Figure 5.10: Typical SEC-HPLC with an RI detector showing the molecular size distribution of full-length Pn19F (black) and Pn19A (green) CPS. The polysaccharide eluted between 12.5 and 13.2 min with section Pullulan standard (red and blue) to represent the size of the fractions eluted.

The calibration of the column is critical in qualifying this methodology and was performed using Pullulan standards on Shodex 804 and Shodex 805 columns in series (as described in Chapter 2). The Shodex OH Pak SB -805 HQ will separate polysaccharides in the molecular weight range of 100 - 1,000 kDa while the SB -804 HQ has a molecular weight range of 5 – 400 kDa, both ranges based on Pullulan standards. As these two columns were run in series, the fractionation range for both columns is between 5 and 400 kDa. Any polysaccharide with a molecular weight greater than 400 kDa will elute in the void volume (10 min) while any saccharide with a molecular weight smaller than 5 kDa will elute in the total volume (20 min). Calibration curves were constructed with Pullulan standards and molecular weights of the polysaccharides of interest calculated based on the relationship between the Pullulan retention times and relative MW's. Figure 5.10 shows the chromatogram for the Pullulan standards (represented in blue and red). Included in the chromatogram are the profiles for full length Pn19F and Pn19A CPS.

After purification of the CPS, SEC-HPLC was performed to determine its size distribution at a known concentration of CPS in mg/mL. The CPS was then size-reduced and the subsequent molecular weights determined. Figures 5.11 – 5.13 shows purified Pn19F CPS and Pn19A CPS in its full-length form as well as its size-reduced form. Referring to Figure 5.11, it can be seen that the full length (native form) of Pn19F shown in black elutes at about 13 min, while the size-reduced Pn19F elutes at about 15.4 min. As size-reduced Pn19F is smaller in size it elutes later as it is retained on the column, compared with the full-length polysaccharide which is less retained. Similar results are shown for Pn19A (Figure 5.12). Figure 5.13 shows the similiarities in retention times for full length Pn19A and Pn19F.

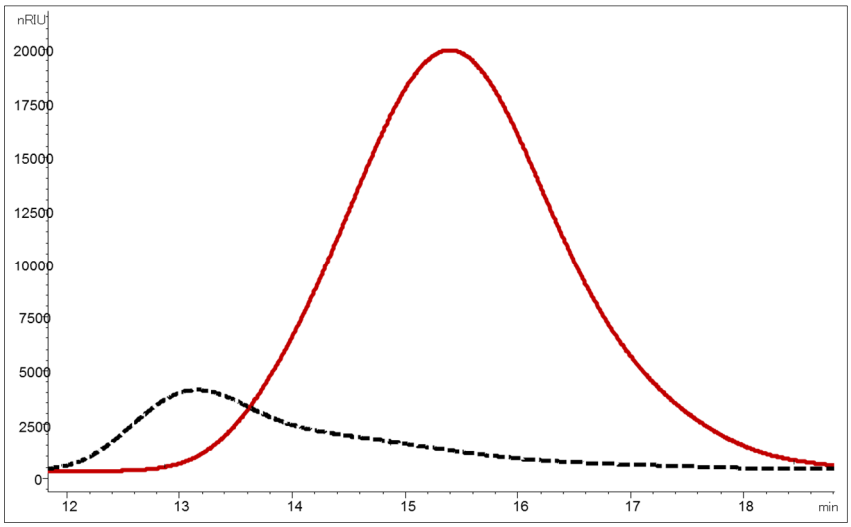

Figure 5.11: SEC- HPLC profile of Pn19F CPS full length (827 kDa) (black) and Pn19F size reduced (104 kDa) (red) CPS.

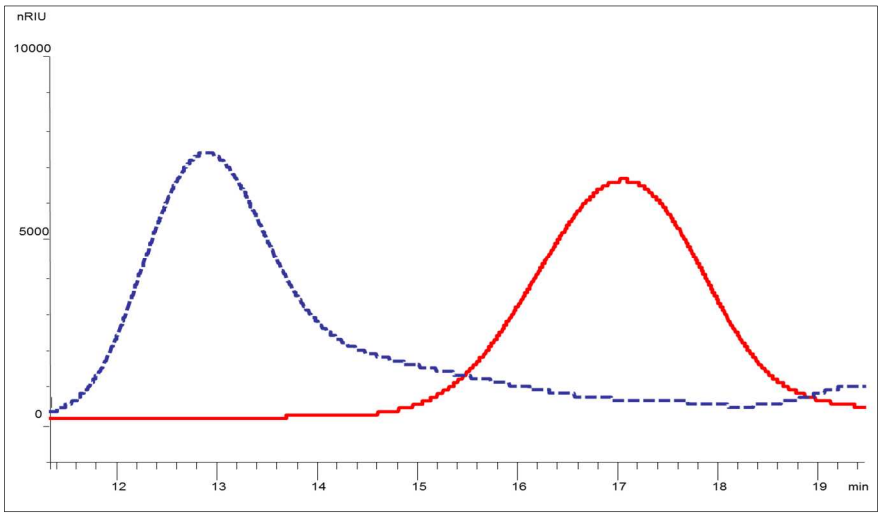

Figure 5.12: SEC- HPLC profile of Pn19A CPS (1129 kDa) (blue) and size reduced (61 kDa) (red) CPS.

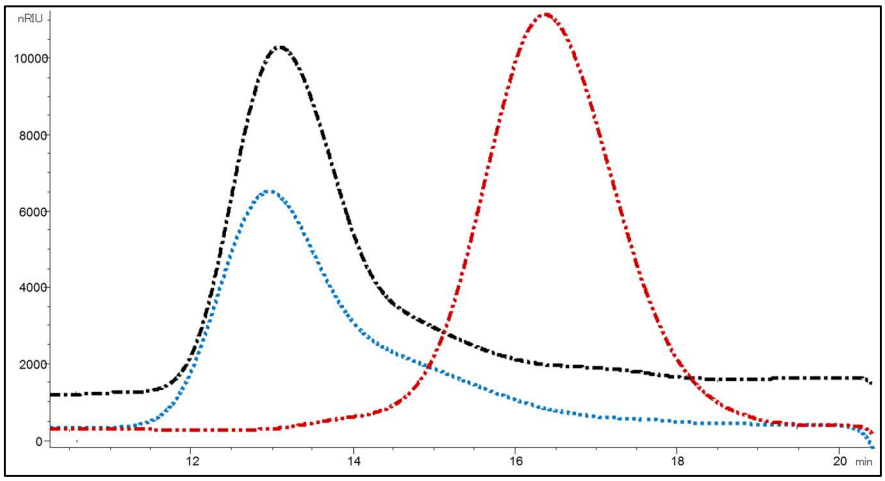

Figure 5.13: Purified full-length Pn19F CPS (black) compared to Pn19A CPS (blue) and sized Pn19A CPS (red).

5.3.2 Compositional analysis

The determination of monosaccharide composition, linkage, and branching patterns are essential for elucidating the structure of polysaccharides [191]. In order to carry out this analysis the CPS needs to

be hydrolyzed to its individual monomers and then derivatized for ease of analysis. Hydrolysis is achieved with the use of a strong acid.

5.3.2.1 Polysaccharide hydrolysis

Acid hydrolysis using TFA or HCl at various concentrations was used during this study. On addition to this, polysaccharides were also subjected to methanolysis, an alternate method of cleavage of the glycosidic bonds to produce O-methyl glycosides.

5.3.2.2 Polysaccharide derivatization

The preparation of derivatives of carbohydrates assist analysis by either increasing volatility as is required for gas chromatography or enhancing sensitivity [194]. The classical method for converting carbohydrates into volatile compounds before gas chromatography (GC) analysis is the replacement of all active hydroxyls with non-polar substituents such as methyl ethers [194]. Methyl derivatives allow GC analysis of up to 5 monosaccharides.

5.3.3 Chromatographic methods

Various chromatographic techniques are used to determine the composition of polysaccharides. High-performance anion-exchange (HPAEC) coupled with pulse amperometric detection (PAD) and GC are the most commonly employed techniques [102].

5.3.3.1 High-performance anion-exchange with pulse amperometric detection

In the eighties, a novel methodology was developed that provided a highly sensitive detection and efficient separation tool for carbohydrate analysis [195]. HPAEC at high pH coupled with PAD is one of the most useful techniques for carbohydrate determination either for routine monitoring or research application [132]. HPAEC separates all classes of alditols, aminosugars, mono-, oligo- and polysaccharides, according to structural features such as size, composition, anomeric and linkage isomerism [132]. The major advantage of this technique is that no derivatization of the CPS is required. Table 5.14 summarizes the reference methodology used during this study [102].

Table 5.14: Summary of acid hydrolysis methods performed by Talaga, (2002) on pneumococcal polysaccharides [102].

Method	Acid	Hydrolysis conditions		
		Concentration	Temperature (°C)	Time (h)
1	TFA	2N	121	2
2	HCl in methanol	2N	80	24
	TFA	2N	121	2
3	HF	48% (v/v)	65	2
	TFA	2N	121	2

For Pn19F and Pn19A CPS, the use of a model mixture of the monosaccharide components (Rha, Glc, and GlcNAc) to construct the standard chromatograms represents a starting point for the analysis of the polysaccharides. The monosaccharides of Pn19F and Pn19A CPS were released by hydrolysis with 2 N TFA followed by the use of an internal standard for quantitative analysis of the monosaccharides by HPAEC-PAD. A known amount of standard is added to the sample at the beginning of analysis so that any subsequent loss affects both sample and standard to an equal extent. The ratio of sample

(monosaccharide) to internal standard at the end of analysis is then the direct measure of the amount of monosaccharide in the sample. The choice of internal standard is critical and should satisfy certain requirements [196]. Fucose was used as an internal standard for the model mixes as well as the pneumococcal CPS as it is stable under the defined hydrolysis conditions. Experiments performed by Talaga's group using the Pn19F CPS (Figure 5.14) were carried out on the pneumococcal polysaccharides repeating units (Rha, Glc, and ManNAc) and using fucose as the internal standard.

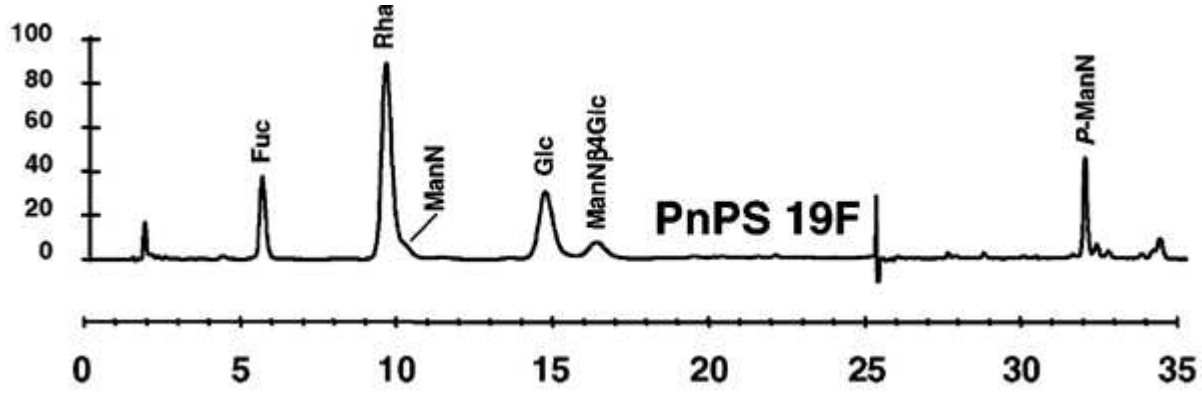

Figure 5.14: HPAEC-PAD chromatogram of TFA hydrolysis of serotype 19F. Fucose (Fuc) used as the internal standard [102].

This experimental method was implemented on the monosaccharides on Pn19F and Pn19A pneumococcal repeating units and were refered to as model mixes as represented in Figure 5.15.

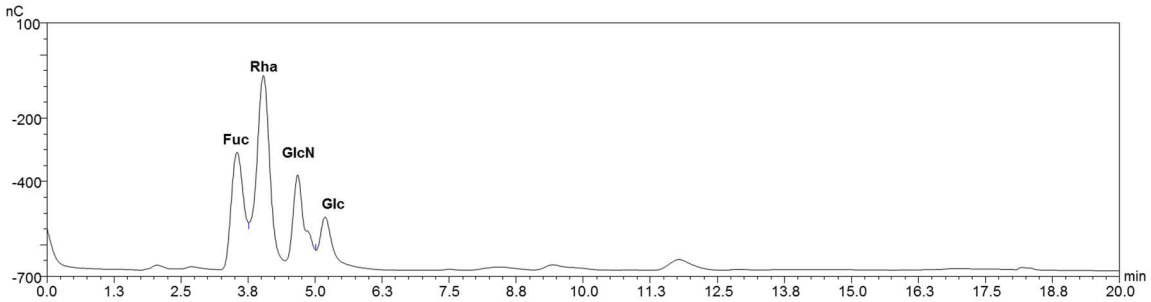

Figure 5.15: HPAEC-PAD chromatogram of Pn19A model mix displays the order of elution of the monosaccharides present in the repeating unit used as a control to determine where the sugars would be eluted between 3 and 6 minutes. Fuc was used as an internal standard.

Pn19A showed similar results for Pn19F (Figure 5.14) in that the Rha and Glc were easier to elute compared to the amino sugar (GlcNAc inplace of ManNAc due to availability) which created a GlcN disaccharide which was also observed by Talaga for the ManNAc component [102] (Figure 5.14). The glucose unit according to the literature has an elution time of 14.4 min (Figure 5.14) whereas in this study it was eluted at 5.2 min (Figure 5.15). The elution times when compared to Talaga are different but importantly the order of elution was the same. The acetyl group is lost upon hydrolysis and so is detected as mannosamine or ManN as a shoulder of the Rha peak (Figure 5.16). The phosphates and the amino sugars, however, were resistant to acid hydrolysis as seen by the peaks observed after 30 min which to the *P*-ManN which according to Talaga was clearly observed at about 31.7 min (Figure 5.14) and observed at 8.8 min for the Pn19A (Figure 5.16). The glucose peak also has a tail which according to the literature is ManNß4Glc.

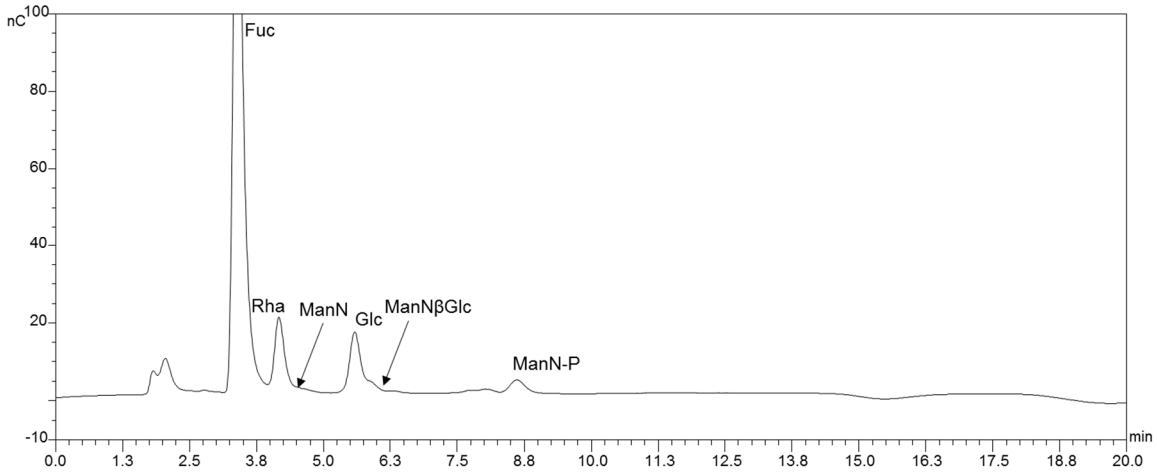

Figure 5.16: HPAEC-PAD chromatogram of Pn19A displays the order of elution of the monosaccharides present in the repeating unit. Fuc was used as an internal standard.

The HPAEC-PAD experiments performed on the Pn19F and Pn19A CPS showed the elution and release of the monosaccharide composition than compared to the literature. Factors affecting these results could be the age of the column used which led to the unresolved peaks that are indistinguishable between standards and sample. The experiments performed on the Pn19F and Pn19A CPS using HPAEC-PAD methodology demonstrated the presence of Rha and Glc and possibly ManNAc. Many factors could have impacted on these results; the use of 2N TFA for hydrolysis could have led to incomplete hydrolysis and release of ManNAc and the age of the column used could have resulted in the unresolved peaks. The use of hydrofluoric acid (HF) to facilitate the cleavage of the phosphodiester linkages was not possible and therefore methanolysis was employed as an alternative method of hydrolysis together with GC and GCMS analysis. TFA hydrolyzes the glycosidic bonds of phosphate containing CPS such as Pn19F and Pn19A and methanolysis followed by TFA hydrolysis lead to improved recovery of CPS containing amino sugars [102]. The HPAEC-PAD data was used as a baseline experiment for the identification of the monosaccharides present in Pn19F and Pn19A but GC and GC-MS were suitable for more detailed studies and identification.

5.3.3.2 Gas chromatography (GC)

GC and GC-MS are analytical tools used for structural and quantitative determination studies of polysaccharides. It involves the chemical conversion of molecules of interest into volatile derivatives that can be easily isolated using GC prior to MS analysis. GC identifies the retention times of the monosaccharides, the identity of which is confirmed by the MS fragmentation pattern. These techniques have been shown to be applicable for a wide range of monosaccharides and provide two separate dimensions of information about the monosaccharides in the sample [197]. A classical derivatization method consists of the substitution of the polar groups of monosaccharides in order to increase their volatility. The methodologies used during these experiments were outlined in Chapter 2. The monosaccharide standards included Rha, Glc, and ManNAc at concentrations of 20 µg/mL while the pneumococcal CPS was assayed at concentrations of 10 µg/mL. The spectrum of the CPS at concentration of 10 µg/mL as it showed indistinguishable peaks so a split method was utilized resulting in a final concentration of 4 µg/mL. The conversion of the anomeric hydroxyl groups to methyl glycosides

resulted in four isomers namely furanose ring, pyranose and anomeric alpha (α) and anomeric beta (β) forms of the furanoside and pyranoside glycosides in different proportions depending on the monosaccharides. The GC-flame ionization detector (FID) and mass spectroscopy (MS) fragmentation patterns of the Pn19F and Pn19A CPS are shown in Figure 5.17.The retention times for Rha was between 11-15 min, for Glc 15-20 min and for ManNAc 20-25 min. Kim et al. [103] (2005), showed that even under extensive treatment with acid only trace amounts of ManNAc could be detected for both serotype 19F and 19A CPS.

With respect to the mass spectroscopy, the base peaks that are significant for pyranoside and furanoside were observed at a mass/charge ratio (m/z) of 204 for the pyranosides and 217 for the furanosides forms. This correlates to the mass spectra illustrated in the literature [198]. With the aid of GC, retention times and MS fragmentation pattern the assignments of each methyl glycoside could be determined and assigned. The fragmentation patterns with an ion at m/z 173 corresponds with the amino sugar ManNAc (203Da) and the ion at m/z 204 is consistent with the pyranose ring on the Rha (146Da) and Glc (162Da) residues on the repeating units of both Pn19F and Pn19A CPS. The separation of each peak is clear and represents the glycosidic forms which corresponding to the retention times of the pyranose (α, β), as the furanose (α, β) forms are rarely observed except for galactose. The total ion chromatograms of Pn19F and Pn19A are labeled and shown in Figure 5.17. Both Pn19F and Pn19A contain phosphodiester bonds in their primary polysaccharide structure.

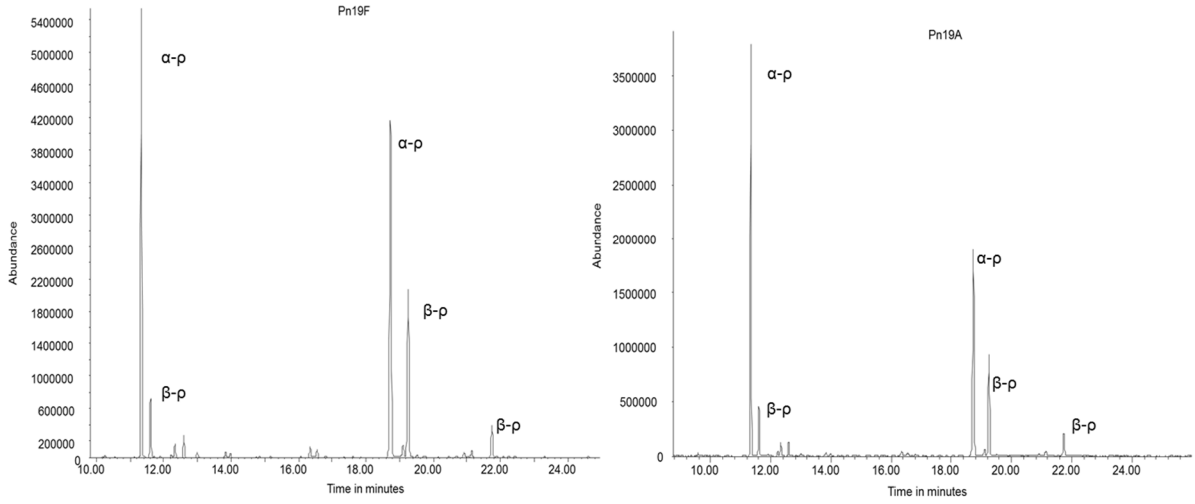

Figure 5.17: GC-MS total ion chromatographs of the trimethylsilyl (TMS) derivatives of the anomeric methyl glycosides present in serotype 19F and 19A CPS. Rha – rhamnose, Glc – glucose, ManNAc – N-acetyl mannosamine, P- pyranoside, F-furanoside

The monosaccharide composition analysis is not distinguishable between serotypes 19F CPS and 19A CPS as they both present with the monosaccharides Rha, Glc and ManNAc. For both the Pn19F and Pn19A CPS, only trace amounts of ManNAc was released as the phosphodiester linkage is acid-resistant, this could be due to incomplete hydrolysis of the ManNAc bond resulting in low recovery of ManNAc. As stated by Ravenscroft et al. (2015), the high efficiency of separation afforded by GC together with confirmation of peak assignment and peak purity by analysis of the mass spectra makes this technique superior to liquid chromatographic methods even though each monosaccharide resulted

in more than one peak [101]. Additional benefits to the field of carbohydrate analysis may be that these polysaccharides with the application of derivatization followed by NMR methods can provide detailed structural analysis.

5.3.4 Nuclear magnetic resonance (NMR)

NMR is used to characterize bacterial polysaccharides such as that of *S. pneumoniae* serotype 19F and 19A and is used as a complementary technique to characterize and test the identity of polysaccharides in the licensure of conjugate vaccines. NMR spectroscopy is a non-destructive method that allows for the determination of polysaccharide structures. Information such as composition, sequence, linkage, and substitution position of polysaccharides as well as anomeric configurations can be obtained [199]. NMR spectroscopy theory is based on the principle of nuclear spin, an intrinsic angular momentum every magnetic nucleus possesses [200]. There is a repertoire of experiments that are performed to obtain a fully characterized structure including 1-dimensional (1D) and 2-dimensional (2D) experiments. The 1-D spectra include experiments such as proton (^{1}H), carbon (^{13}C) and phosphorus (^{31}P) and the 2D spectra include experiments such as homonuclear correlation spectroscopy (COSY), total correlation spectroscopy (TOCSY) heteronuclear single-quantum correlation (HSQC) and heteronuclear multiple bond correlation (HMBC). NMR has shown to provide information on quantitation and possible location of the functional groups. NMR was used to elucidate the polysaccharide structure and determine the different linkage positions between Pn19F and Pn19A. NMR spectroscopy was also used to confirm the antigen structural identity and integrity of Pn19F and Pn19A during this study.

5.3.4.1 Structural characterization of serotype 19F CPS using NMR

Structural analysis of Pn19F has been extensively studied in the late 1970s, early 1980s. The structural analysis of Pn19F CPS by NMR has been performed by Jennings et al. [178] in 1980. They elucidated the trisaccharide repeating unit structure of Pn19F CPS by using both NMR and chemical methods [178]. Structural assignments of all proton, carbon, and phosphorus chemical shifts were performed using various NMR structures, 1D (^{1}H, ^{13}C and ^{31}P) spectra and 2D (^{1}H-^{1}H, ^{1}H-^{13}C and ^{1}H-^{31}P) spectra assigning all peaks and cross peaks. The sensitivity and selectivity of ^{1}H NMR permit differentiation between two closely related polysaccharides that differ due to a single linkage such as Pn6A (→3)-D-Rib-ol) and Pn6B (→4)-D-Rib-ol) and Pn19A (→3)-α-L-Rhap) and Pn19F (→2)-α-L-Rhap) [32, 178]. The ^{13}C NMR spectrum, on the other hand, is diagnostic for each residue present and its connectivity in the chain [96].

Chemical analysis of serotype 19F CPS demonstrated that it contains 2-acetamido-2-deoxy-D-mannose, D-glucose, L-rhamnose and phosphate moiety with a molar ratio of 1:1:1 thus indicating that it is composed of a trisaccharide repeating unit [178]. This study was performed to confirm Pn19F structure as provided by the literature and compare it to the Pn19A CPS structure extracted from *S. pneumoniae* cultivated during these investigations.

The number of signals in the anomeric region of the 1D proton spectrum is indicative of the number of monosaccharides contained in the CPS repeating unit and usually resonates in the region of about 4-6 ppm. The ^{1}H NMR (Figure 5.18) of Pn19F showed the three anomeric peaks (5.50, 5.02 and 4.91 ppm) of Rha, Glc, and ManNAc, respectively. Rha and Glc are α-linked and ManNAc is β-linked as indicated by the anomeric chemical shift values. The diagnostic H2 signal from the ManNAc (4.59 ppm) residue is also clearly noted as well as the methyl group of Rha (1.31 ppm) and the N-acetyl (NAc) group of ManNAc (2.09 ppm). Cell wall polysaccharide (CWPS) a well-known contaminant in the purified CPS was observed at 3.23 ppm and used as the calibration peak for all 1D proton spectra [96, 201].

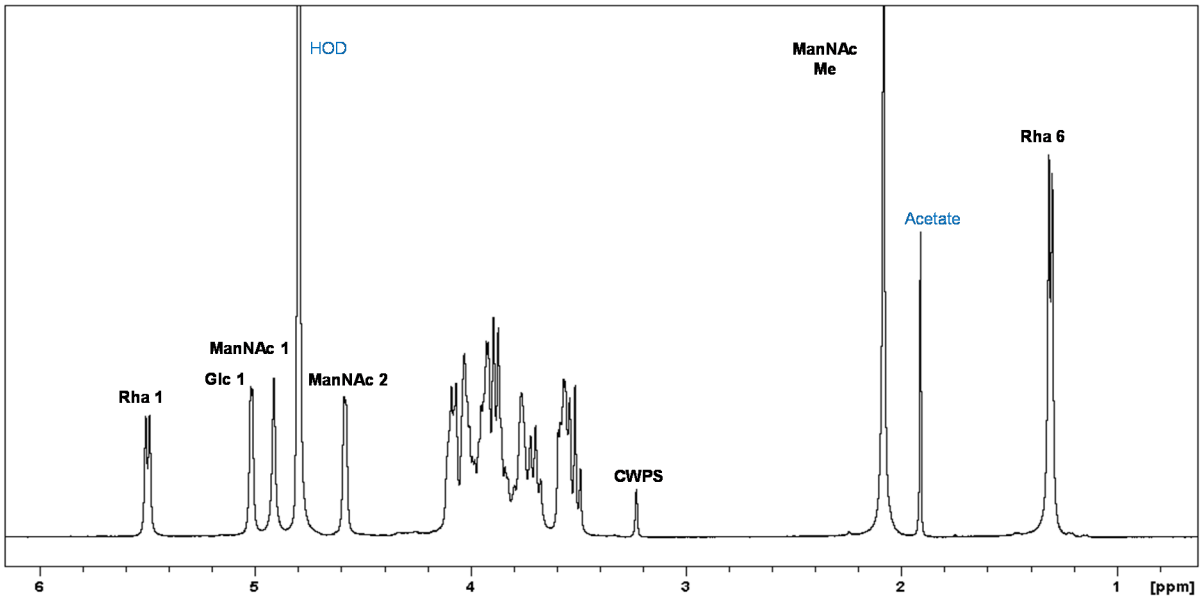

Figure 5.18: The ^{1}H NMR spectrum of Pn19F CPS with anomeric peaks and the diagnostic NAc and CH_3 of Rha peaks labeled.

The ring protons found in monosaccharides are often broad and overlap in the ^{1}H NMR ring region that is not easily distinguishable and are typically observed between 3.2 and 4.2 ppm (Figure 5.18). Due to this overlap, further experiments are required that would reveal the neighboring hydrogens in each ring structure and thereby allow for identification of the entire ring system of each monosaccharide component. Two-dimensional (2D) NMR methods provide this information. Firstly the simplest of the 2D experiments, the ^{1}H–^{1}H correlated spectroscopy (COSY) is analyzed. COSY is used to identify neighboring protons, however, cross peaks are only seen with correlations due to geminal and vicinal coupling. On the COSY spectrum starting from the anomeric and rhamnose methyl protons, it is possible to start assigning resonances, determining anomeric configuration, and identifying residues for all spin systems. The COSY spectrum (Figure 5.19) permits assignments of the neighboring connectivities in the sugar ring via a ^{1}H-^{1}H scalar coupling. The COSY spectrum correlates the anomeric proton to Rha H1 to H2 (5.50 to 4.03 ppm) and H5 to H6 (3.89 ppm to 1.31ppm), Glc H1 to H2 (5.02 ppm to 3.56), and ManNAc H1 to H2 (4.91 ppm to 4.59 ppm) and H2 to H3 (4.59 ppm to 4.02 ppm).

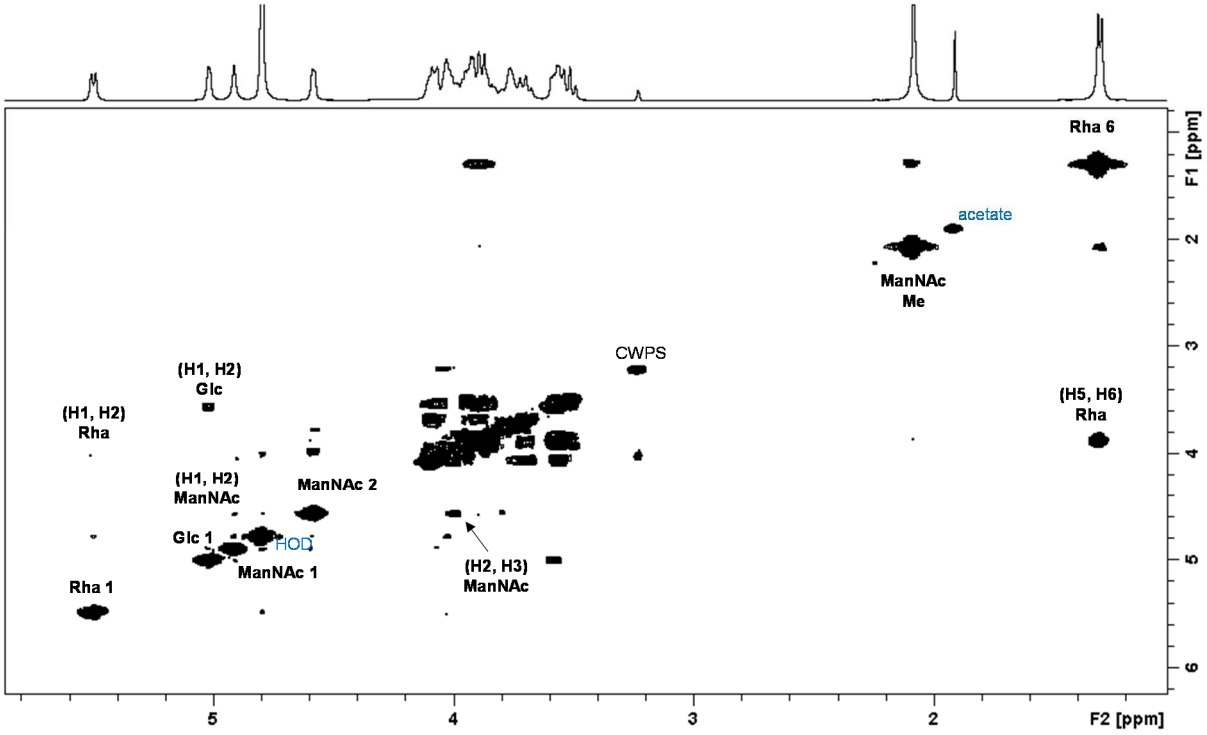

Figure 5.19: The COSY spectrum of Pn19F CPS in D_2O at 303K with the anomeric protons readily identified and the characteristic signals of the methyl protons of Rha and the acetyl methyl protons of ManNAc.

Along with COSY, 1D and 2D experiment provides identification of neighboring hydrogens but instead of the H1 to H2 for example 1D TOCSY provides more information by identifying the neighboring protons for the entire spin system of each monosaccharide. Figures 5.20 – 5.22 details chemical shifts assignments for each monosaccharide residue present on Pn19F repeating unit. Depending on the coupling constants the TOCSY spectrum reveals correlations between all protons within the same spin system. The expanded 2D TOCSY spectrum (Figure 5.20) was used to confirm the COSY assignments and show the addition of H5 ManNAc.

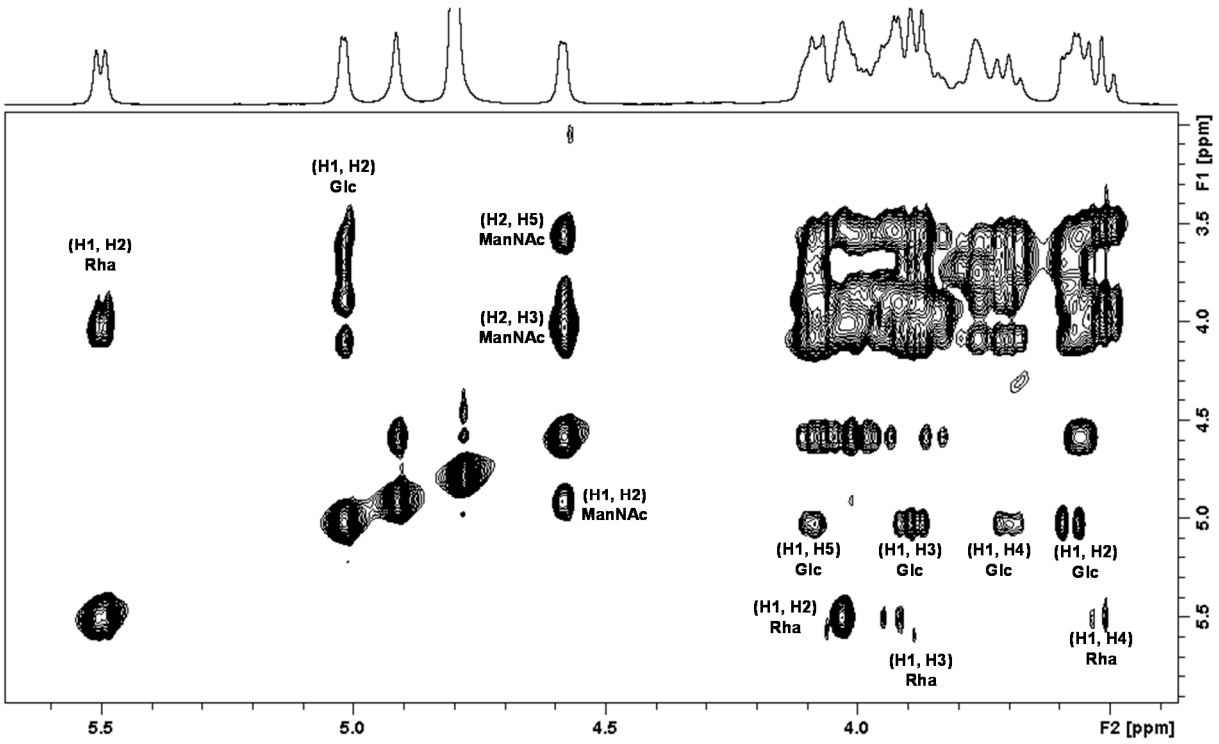

Figure 5.20: The expanded 2D TOCSY (120ms) spectrum of Pn19F CPS in D_2O at 303K.

From position 1 of the Rha spin system H1 is connected to H2 (Figure 5.21, bottom) whereas when analyzing the spin system from position 2 (Figure 5.21, top) it is possible to the follow the entire spin system around the ring to position 6. Thus the 1D spectra shows that it is possible to follow the spin system from position 1 to position 6.

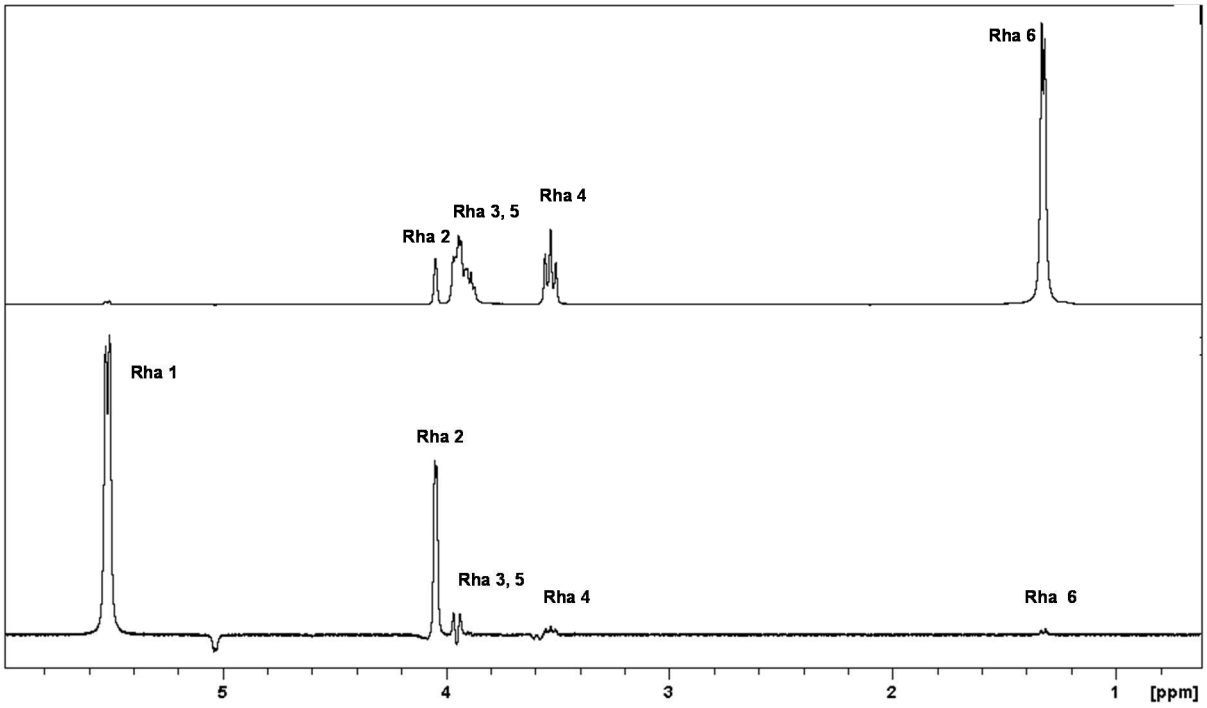

Figure 5.21: The 1D TOCSY (120ms) spectrum of Pn19F CPS in D_2O at 303K of Rha, top shows Rha spin system from proton 2 and bottom shows Rha spin system from the anomeric proton.

Figure 5.22 shows both Glc and ManNAc spin systems where Glc spin system starts at the anomeric proton and ManNAc spin system starts at the second proton. For ManNAc, the coupling constant at position 2 is large making analyzing the spin system with the addition of a longer mixing time easier to follow from position 2 as observed in Figure 5.22.

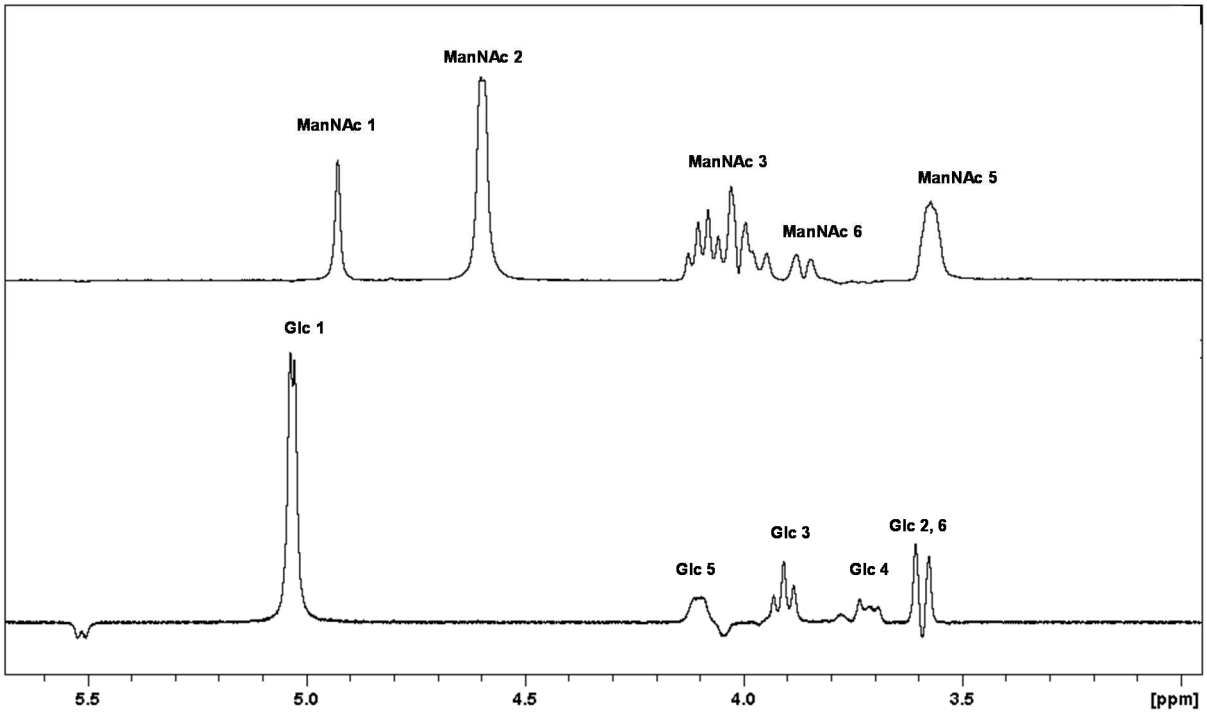

Figure 5.22: The 1D TOCSY (120ms) spectrum of Pn19FCPS in D_2O at 303K of Glc (bottom) and ManNAc (top).

To determine the positioning of the ring carbons 2D experiments are required. The Heteronuclear Single–Quantum Correlation (HSQC) spectrum is the heteronuclear equivalent of the COSY spectrum and consists of a plot of the 1D proton spectrum along one axis and the 1D carbon spectrum of the monosaccharide along the other axis and hence linkages between protons and carbons can be determined. The HSQC spectrum permits one bond correlation to be made between ^{1}H and ^{13}C (H/C) assignments. The HSQC spectrum indicates the carbon-proton linkage as shown in Figure 5.23 and Figure 5.24 indicating the anomeric protons and other diagnostic resonances used to confirm the presence of Pn19F. In the HSQC spectrum, the H/C cross peaks are labeled mainly using the fully assigned ^{1}H NMR spectrum. The chemical shifts for the carbons are confirmed and checked using the ^{13}C spectrum. There is overlap between the C2 Glc and the C5 Glc when analyzing the HSQC which can be resolved by using the ^{13}C spectrum to identify which signal corresponds to each carbon. The ManNAc (C4) is more deshielded as it has a phosphate group attached indicating that it is a linkage position (Glc1 – 4ManNAc) [202]. The position of the carbon also confirms where the ManNAc proton is positioned on the ^{1}H spectra.

Once the proton chemical shifts are known the corresponding carbon chemical shifts are assigned using HSQC, HSQC-TOCSY, and HSQC/HSQC-TOCSY overlay. These spectra are used to assign the major peaks (Figure 5.23), and to assign the ring region HSQC-TOCSY (Figure 5.24) was performed to

facilitate assignments of the different samples (monosaccharides presents on the RU of Pn19F CPS) as well as the anomeric regions (Figure 5.25).

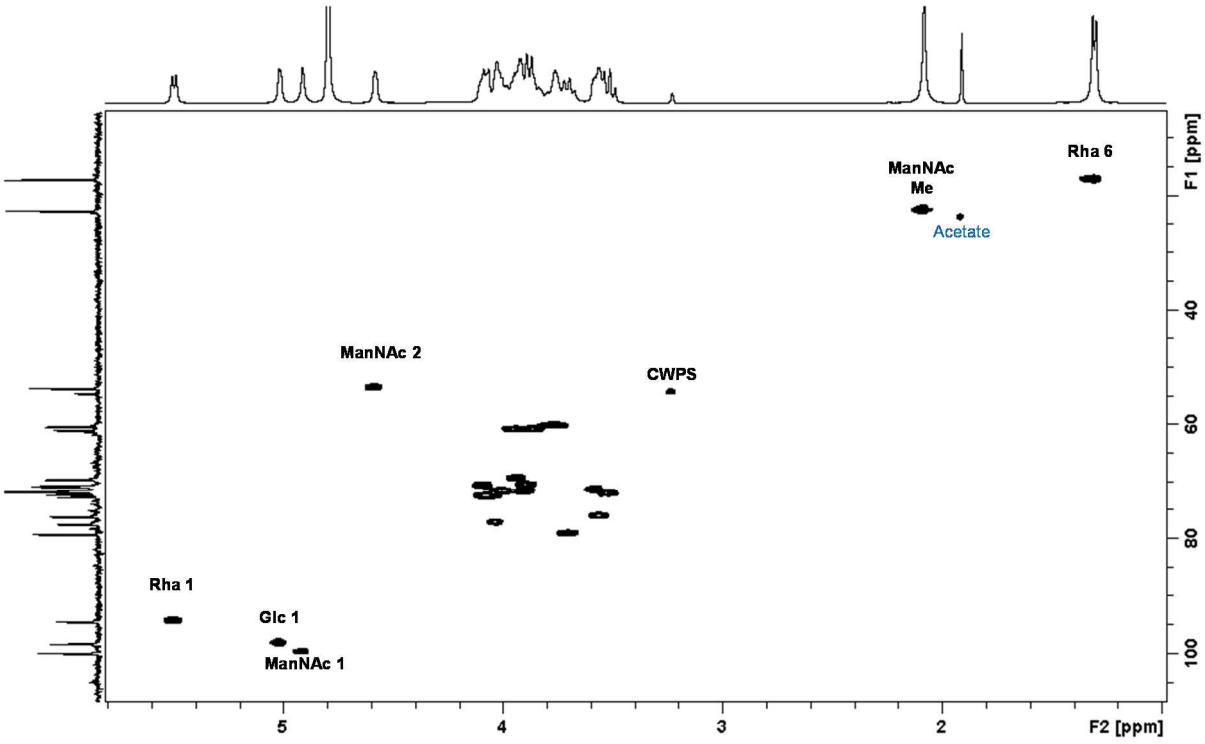

Figure 5.23: Full HSQC spectrum of Pn19F CPS in D2O at 303K with some cross-peaks labeled.

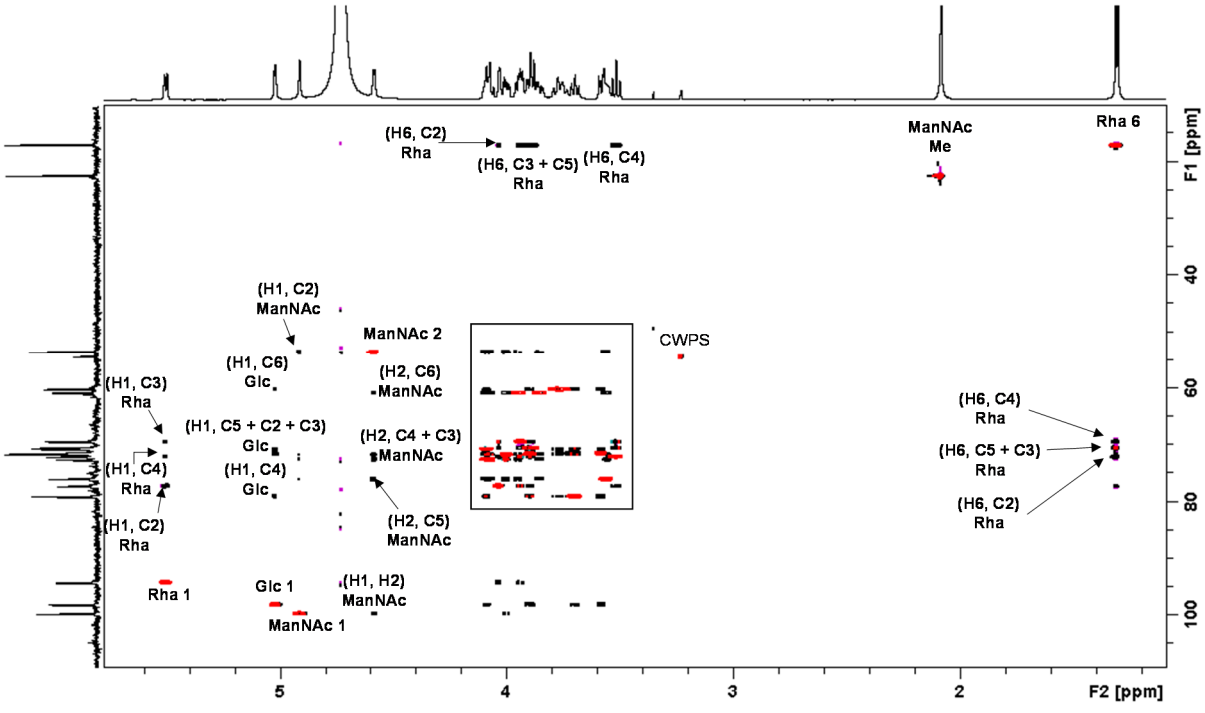

Figure 5.24: The full spectrum of HSQC (red) overlay with HSQC-TOCSY (black) to elucidate remaining correlations of the Rha saccharide.

These assignments are confirmed by 2D $^{1}H–^{13}C$ (HSQC) / $^{1}H–^{1}H$ (TOCSY) correlation experiments (Figure 5.24) and allowed for the full elucidation of the three spin systems. The Rha spin system was fully mapped and assigned. Following the spin system from the anomeric carbon as well as carbon 6

details the positioning of the neighboring protons and carbons with the aid the of the ^{1}H and ^{13}C spectra. The methyl to H5, H4 and H3 coupling of the Rha sugar is clearly visible in the 2D TOCSY spectrum. The ring region as indicated by the block in Figure 5.24 is the most challenging when mapping the spin systems. Figure 5.25 details the ring region and shows all assignments.

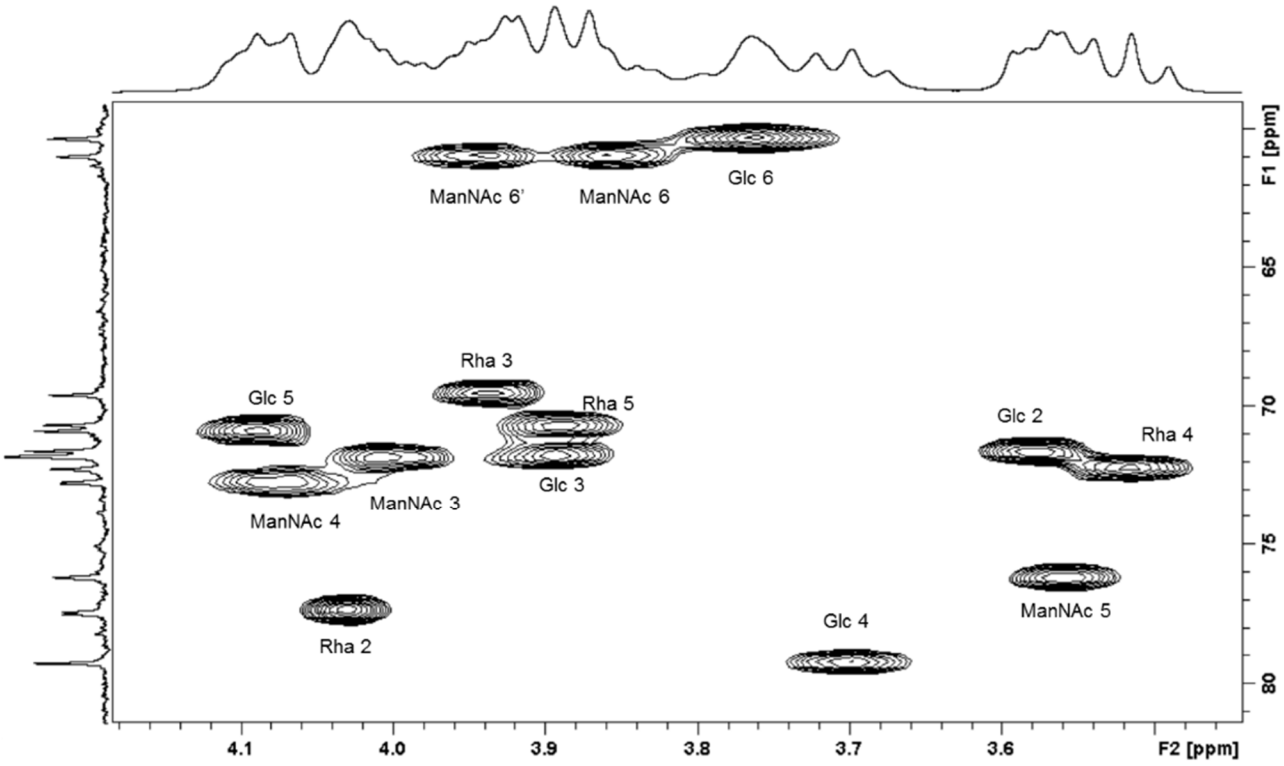

Figure 5.25: The ring region of the HSQC spectrum of Pn19F CPS in D_2O at 303K with cross-peaks labeled.

According to the published literature, the anomeric region in the unsubstituted monosaccharides when analyzing the ^{13}C spectrum is around 90 - 110ppm as shown in Figure 5.26. Jennings, et al. [178] (1980), reported that the ^{13}C NMR spectrum of Pn19F is composed of a trisaccharide phosphate repeating unit and that the three anomeric signals of the Pn19F CPS appear in the range of 94 – 100 ppm and were assigned by inspection to be ManNAc, Rha, and Glc, respectively. When analyzing the ^{13}C spectra the C6 of Rha (methyl group) and the methyl of NAc in the range 15 – 25 ppm, as well as the anomeric carbons, were assigned by inspection as their carbon signals are diagnostic for those functional groups and thus can be rapidly identified.

The ^{13}C NMR (Figure 5.26) of Pn19F showed the three anomeric peaks (94.39, 98.27 and 99.85 ppm) of Rha, Glc, and ManNAc, respectively. The correlation with the 2D HSQC spectrum and the assignments of the previously identified proton signals allows for the identification of the carbon signals and which monosaccharide it belongs to. The methyl carbons of NAc and Rha (carbon 6) is found at 22.55 and 17.15 ppm, respectively. Another peak at 175.96 ppm was observed and represents the carbonyl group present on NAc of ManNAc. These are easily assigned due to their positioning and chemical shifts.

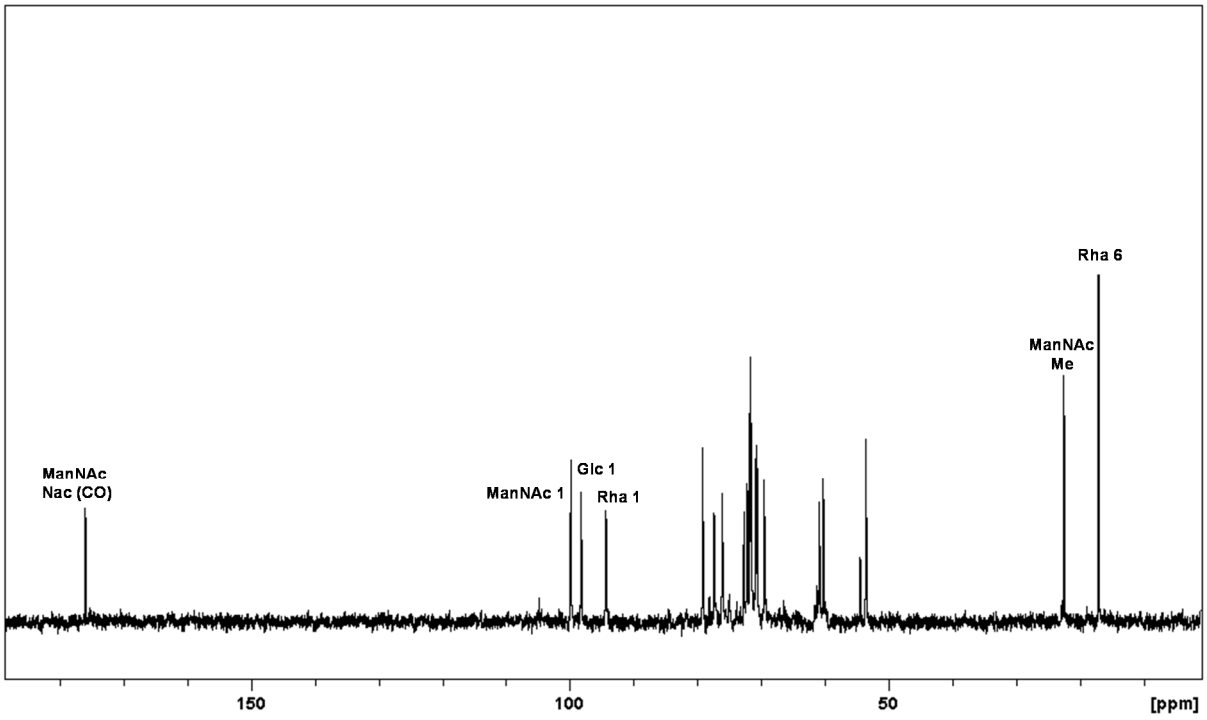

Figure 5.26: The full ^{13}C spectrum of Pn19F CPS in D_2O at 303K highlighting the anomeric carbons, the carboxyl group of the N-acetyl attached to Man and the methyl group of Rha.

Figure 5.27 shows the ring region of the ^{13}C spectrum of Pn19F CPS from region 50 ppm to 80 ppm. The ^{13}C spectrum confirms the chemical shifts and positioning of the carbons found when performing the HSQC experiments and correlates with the literature [152, 178].

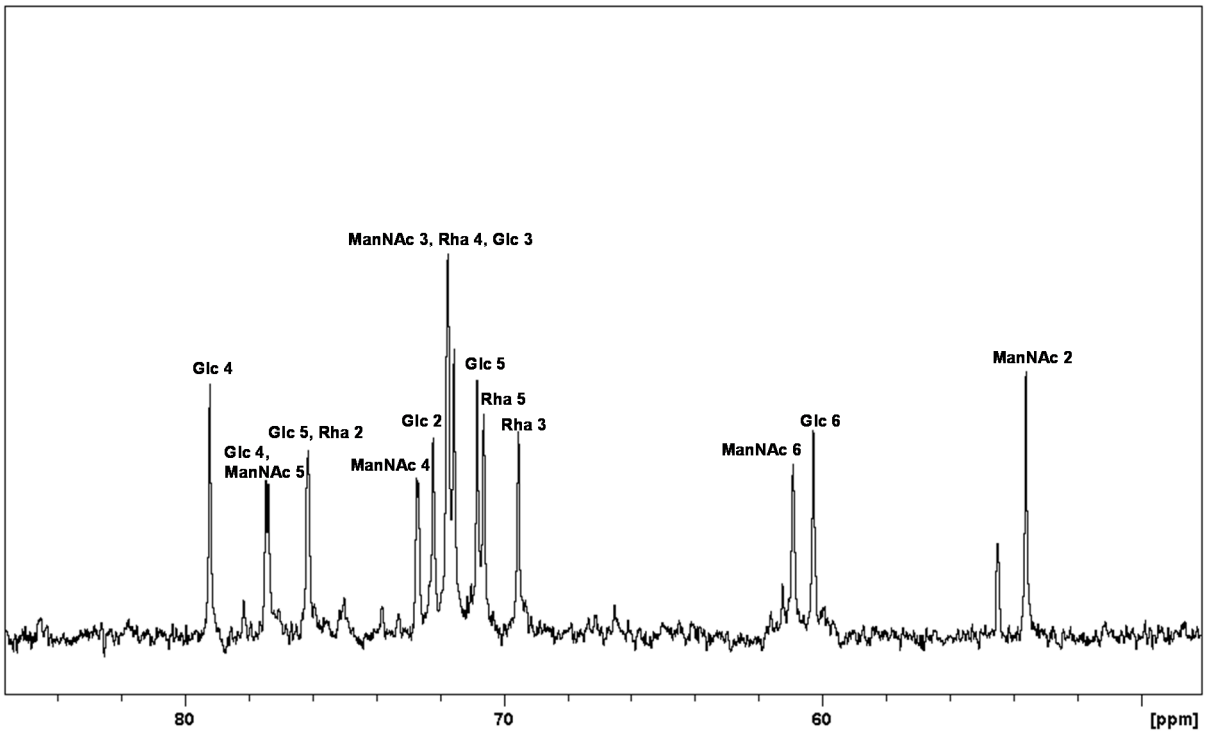

Figure 5.27: The expanded ^{13}C spectrum of Pn19F CPS in D_2O at 303K showing the ring region of the monosaccharides repeating units.

The HMBC experiment are used to elucidate the anomeric inter-residue linkage. Evaluating HMBC data will enable the determination at which positions the three monosaccharides are linked, confirm 1D TOCSY assignments and using the HSQC confirm the ^{13}C and ^{1}H NMR spectral assignments. This long range proton-carbon correlated HMBC experiment shows the correlations between the carbon and the protons that are separated by two or three bonds in a conjugated systems.

Figure 5.28 and 5.29 shows the full HMBC spectra with the assignments of the anomeric carbons provided as well as some linkages between the anomeric carbons to its neighboring monosaccharide. The presence of the methyl groups on the Rha and ManNAc as well as the carboxyl group is shown in Figure 5.28. The HMBC has a cross-peak for H1 ManNAc and C4 Glc (Figure 5.29), confirming it as a position of linkage, thus completing the structural assignments for 19F. From the HMBC H2/C2 Rha links to C1 Glc. The phosphodiester bond assignments were also attained by a ^{1}H - ^{31}P HMBC experiment as shown in Figure 5.31. The linkages are provided in Table 5.15 showing that due to the larger glycosylation shift at C1 and C4 of Glc, C2 Rha and C1 and C4 of ManNAc that these are linkage positions when compared to the published literature of each monosaccharide [152].

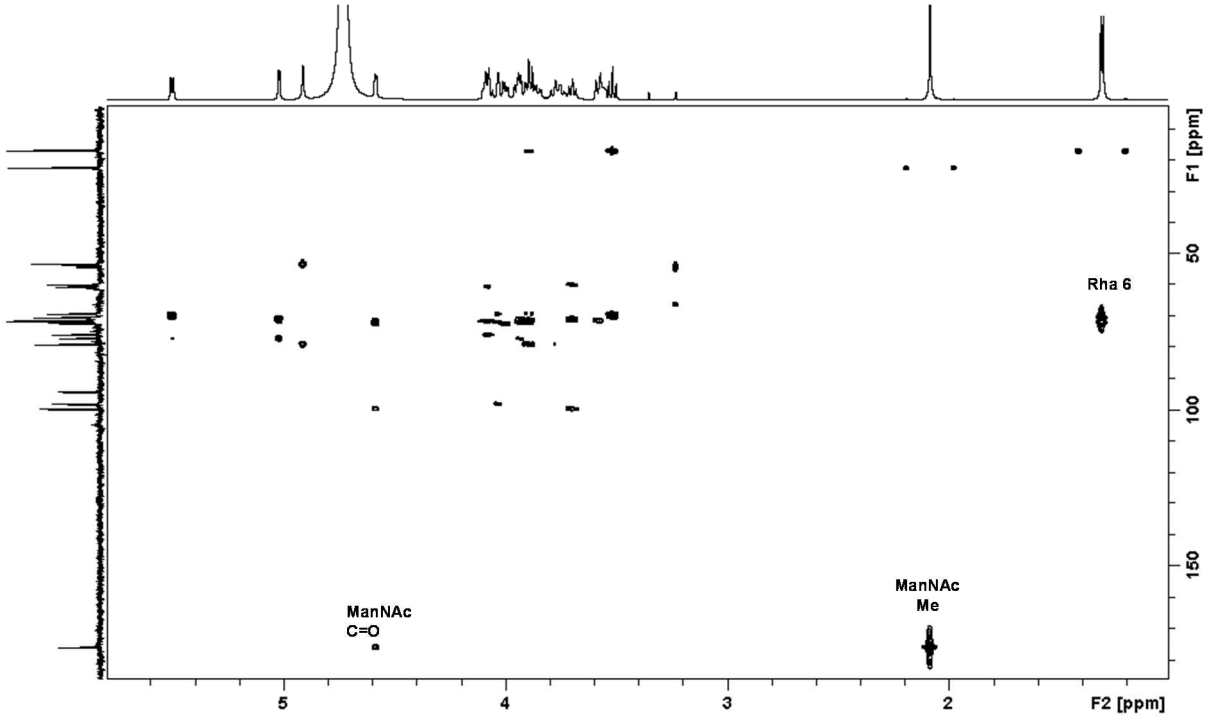

Figure 5.28: The full HMBC spectrum of Pn19F CPS in D_2O at 303K.

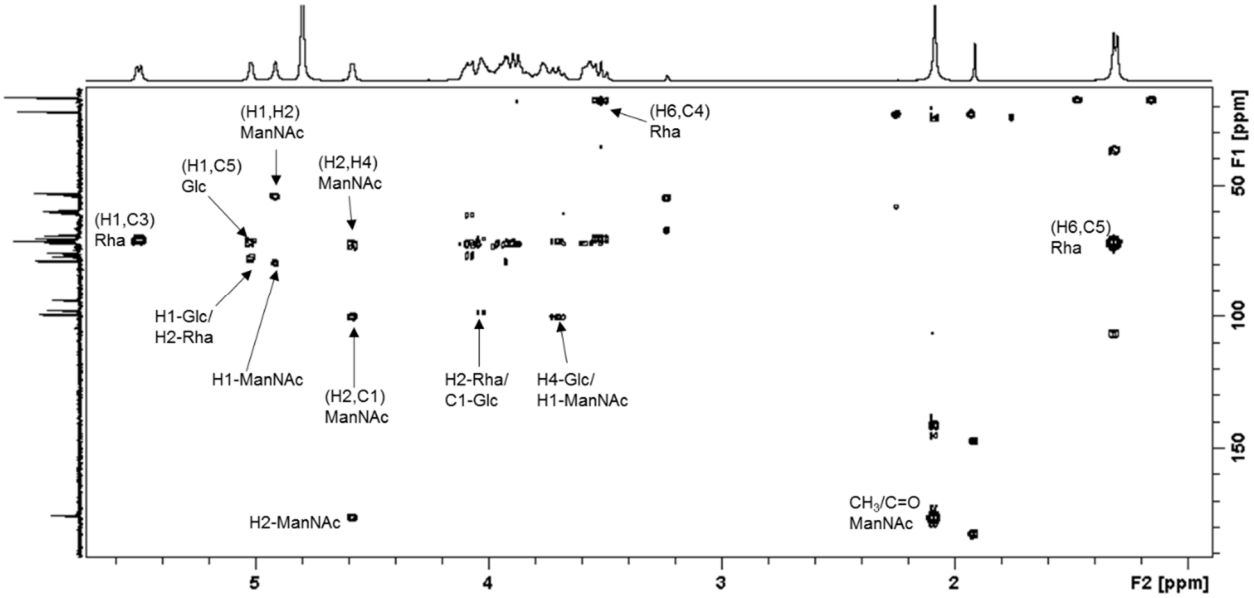

Figure 5.29: The full HMBC spectrum of Pn19F CPS in D_2O at 303K.

Figure 5.30 shows the ^{31}P spectrum and the presence of the phosphodiester in comparison to the presence of the CWPS, a known contaminant of purified CPS.

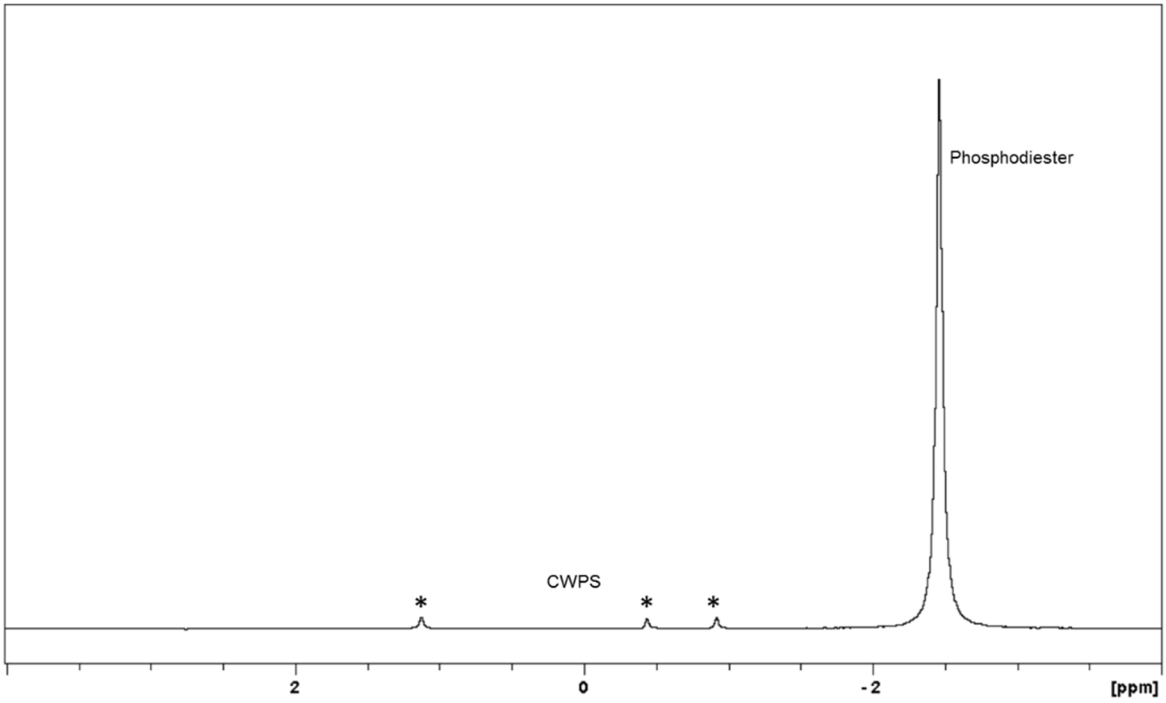

Figure 5.30: The ^{31}P NMR spectrum of Pn19F CPS indicating the amount of CWPS in comparison to the phosphodiester present on the repeating unit of Pn19F CPS. The resonance marked * arise from contamination by the CWPS.

Figure 5.31 showing the phosphodiester bond linkage correlation between H1 Rha/P and H4 ManNAc/P which confirms that the phosphate is linked to C4 of ManNAc monosaccharides on the Pn19F repeating unit. The positions of the phosphate groups were determined by correlations between the phosphorous and protons at the phosphorylation sites in a monosaccharide residue, which revealed by ^{1}H, ^{31}P HMBC spectra (Figure 5.31).

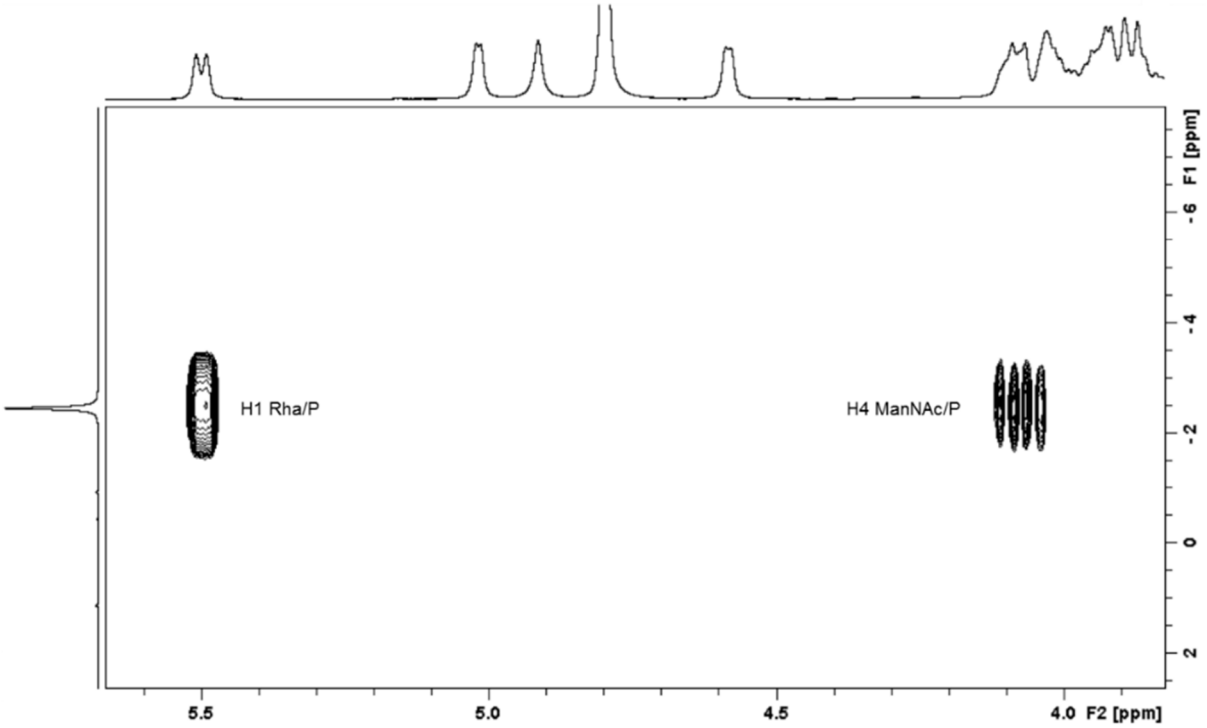

Figure 5.31: ^{1}H – ^{31}P HMBC spectrum of Pn19F CPS in D_2O at 303K with all cross peaks labeled.

The full assignments of Pn19F are summarized in Table 5.15 which were assigned and confirmed using a combination of the 1D (^{1}H and ^{13}C) and 2D (HSQC, HSQC-TOCSY, and HMBC) spectra.

Table 5.15: NMR assignments of Pn19F polysaccharide using ^{1}H-^{13}C spectra with a comparison to reported monosaccharide peak frequencies [152].

Residue Abbreviation	**$^{1}H/^{13}C$ ($J_{H1,H2}$ / $J_{C1,H1}$)**								
	1	**2**	**3**	**4**	**5**	**6/6`**		**Me[NAc]/ CO [NAc]**	
→ 2) – α – L - Rhap – (1 → P -	5.50 (0.38)	4.03 (0.11)	3.93 (0.12)	3.52 (0.07)	3.89 (0.03)	1.31			
	94.39 (-0.45)	77.41 **(5.6)**	69.54 (-1.46)	72.21 (-0.98)	71.74 (2.62)	17.15 (-0.52)			
→ 4) – α – D - Glcp – (1 →	5.02 (-0.21)	3.80 (0.02)	3.90 (0.15)	3.70 (0.28)	4.09 (0.23)	~3.77 (0.01)			
	98.27 (5.28)	71.56 (-0.91)	72.20 (-1.58)	79.21 **(8.5)**	70.68 (-1.69)	60.29 (-1.55)			
→ 4) – β – D - ManpNAc – (1 →	4.91 (-0.10)	4.59 (0.14)	4.02 (0.19)	4.07 (0.55)	3.56 (0.11)	3.84 (0.01)	3.95 (0.05)	2.09 (0.03)	
	99.85 (5.94)	53.62 (-1.32)	71.78 (-1.22)	72.75 **(5.10)**	76.13 (-1.12)	60.92 (-0.62)		22.55 (-0.43)	175.96 (-0.43)

The glycosylation shifts shown in brackets were calculated from the difference between the reported frequencies of the corresponding monosaccharides and the frequencies obtained for each residue in the polysaccharide repeating unit [152]. The signals with large glycosylation shifts represent the positions of linkage between the residues, shown in bold in Table 5.15.

The linkage position of each residue was assigned based on the carbon resonance induced by glycosylation or substitution with phosphate [203], and confirmed by the three-bond correlation between the anomeric proton and the linkage site carbon of the next monosaccharide residue observed in HMBC spectrum (Figure 5.31).

Spin systems for each sugar residue were identified based on the coupling constants estimated from the 2D NMR spectra and inferred relative configurations of the monosaccharides. The α configuration of rhamnose residues was deduced from the C-5 chemical shift of δ 71.74 (compare published data δ 69.12 and 72.83 for α-Rha*p* and β-Rha*p*, respectively) [152]. A comprehensive table of the chemical shifts and the linkages of the monosaccharides present in the trisaccharide repeating unit is provided in bold.

5.3.4.2 Structural characterisation of Pn19A CPS using NMR

Serotype 19F and 19A structures are virtually identical but for a single difference in the position of linkage between the Glc and Rha residue. With the information provided in Section 5.3.4.1 on serotype 19F and the use of the literature data as a guide, the linkage difference in Pn19A was determined using NMR analysis. Both 1D and 2D spectra were analyzed for the structural analysis of Pn19A. The proton NMR is a good reference point for the analysis of Pn19A as it presents the anomeric protons indicating the monosaccharides present.

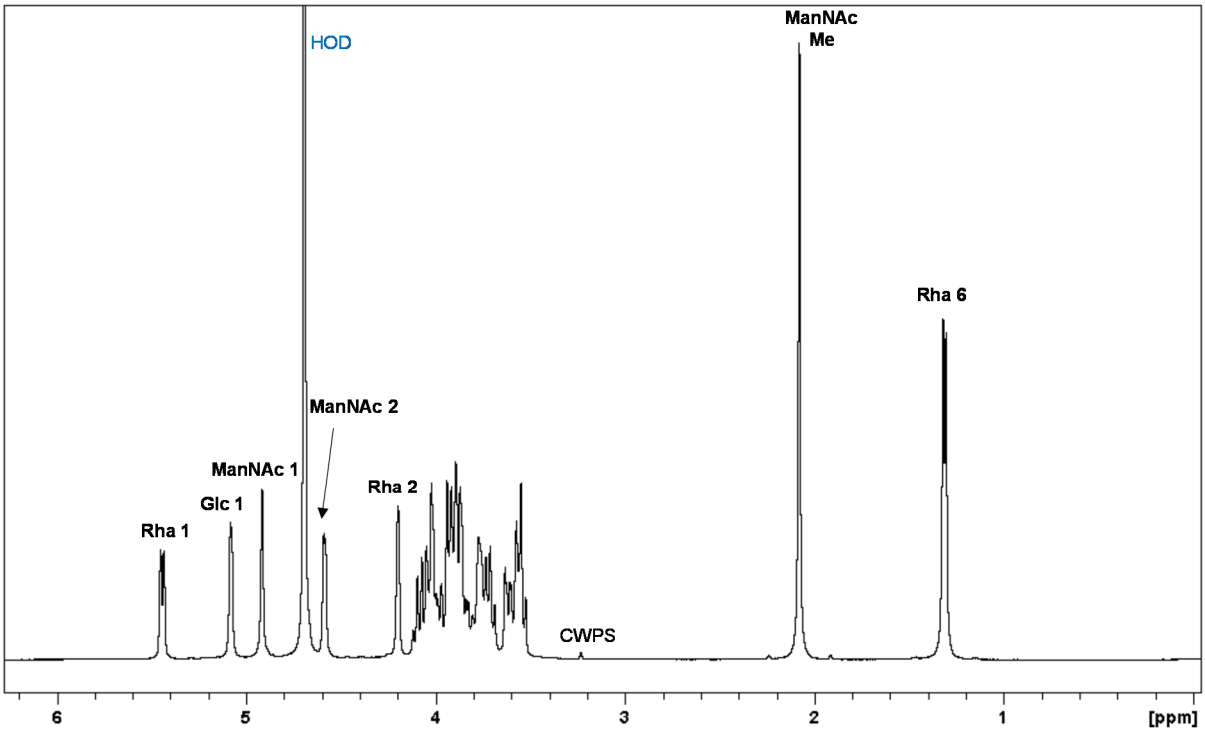

Figure 5.32: The ^{1}H NMR spectrum of Pn19A CPS in D_2O at 303K with anomeric peaks and some ring peaks labeled.

The ^{1}H NMR spectrum presented in Figure 5.32 is that of one of the fermented and purified batches of Pn19A CPS cultivated during this study. The anomeric protons are distinguishable peaks in the region

of 4 – 6 ppm namely α-L-Rha*p*, α-D-Glc*p* and β-D-Man*p*NAc consistent with the structure reported in the literature by Katzenellenbogen in 1983 [176]. The presence of three anomeric protons (5.44, 5.08 and 4.92 ppm) in the region of 4.9 – 5.5 ppm supports the presence of three monosaccharide residues. These anomeric signals are either a doublet of doublets, at 5.44 ppm or doublets at 5.08 ppm and 4.92 ppm which are assigned to L-rhamnose, D-glucose, and 2-acetamido-2-deoxy-D-mannose residues, respectively. The most up-field anomeric proton at 4.92 ppm, correlates to the most down-field carbon at 99.86 ppm on the ^{1}H and ^{13}C spectrum and was assigned as the H1 of N-acetyl mannosamine (ManNAc) [176]. The other two anomeric protons at 5.08 ppm and 5.44 ppm, correlating to carbon signals at 96.21 ppm and 96.41 ppm, were assigned to the anomeric protons of D-Glc and L-Rha respectively. A methyl (acetamido) singlet at 2.08 ppm and a methyl (rhamnose) doublet at 1.31 ppm was also detected and assigned to Man*p*NAc which is deshielded by the carbonyl group and H-6 Rha methyl being more shielded, respectively.

The proton NMR spectrum (Figure 5.32) highlights the anomeric protons that serve as a diagnostic tool and starting point for 2D NMR experiments. Further proton assignments were made by the use of COSY (Figure 5.33 - 5.34) and TOCSY (Figure 5.35 - 5.36) experiments which permitted identification of protons H2, H3 of Rha and ManNAc and the H5, H6 of Rha sugar residues. In the COSY spectrum of Pn19A (Figure 5.33) the most up-field anomeric proton H1 of the Rha (5.44 ppm) is correlated to the proton at H2 of Rha (4.20 ppm) which in turn is correlated to H3 (3.89 ppm). The H6 of Rha at 1.31ppm was easily correlated to its neighbor H5 of Rha.

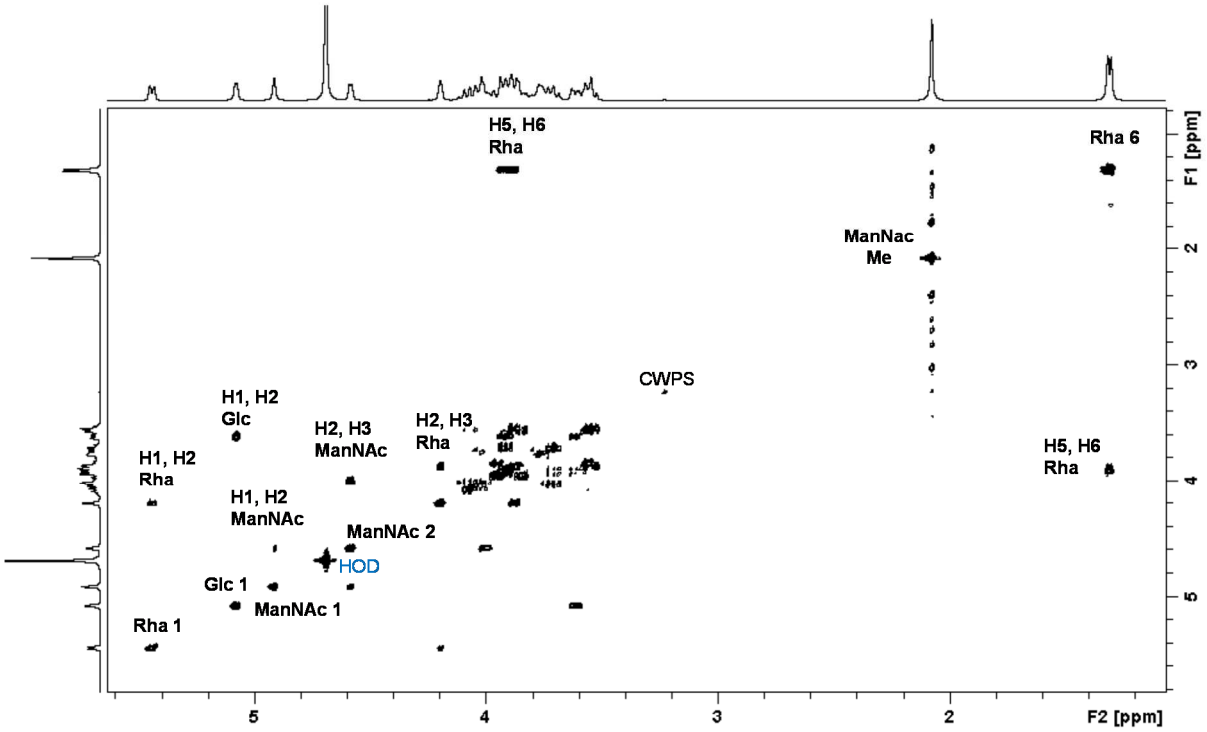

Figure 5.33: The full COSY spectrum of Pn19A CPS in D_2O at 303 K with some cross-peaks labeled.

In the expanded view shown in Figure 5.34, the anomeric protons connected to the H1, H2, and H3 proton correlations are shown.

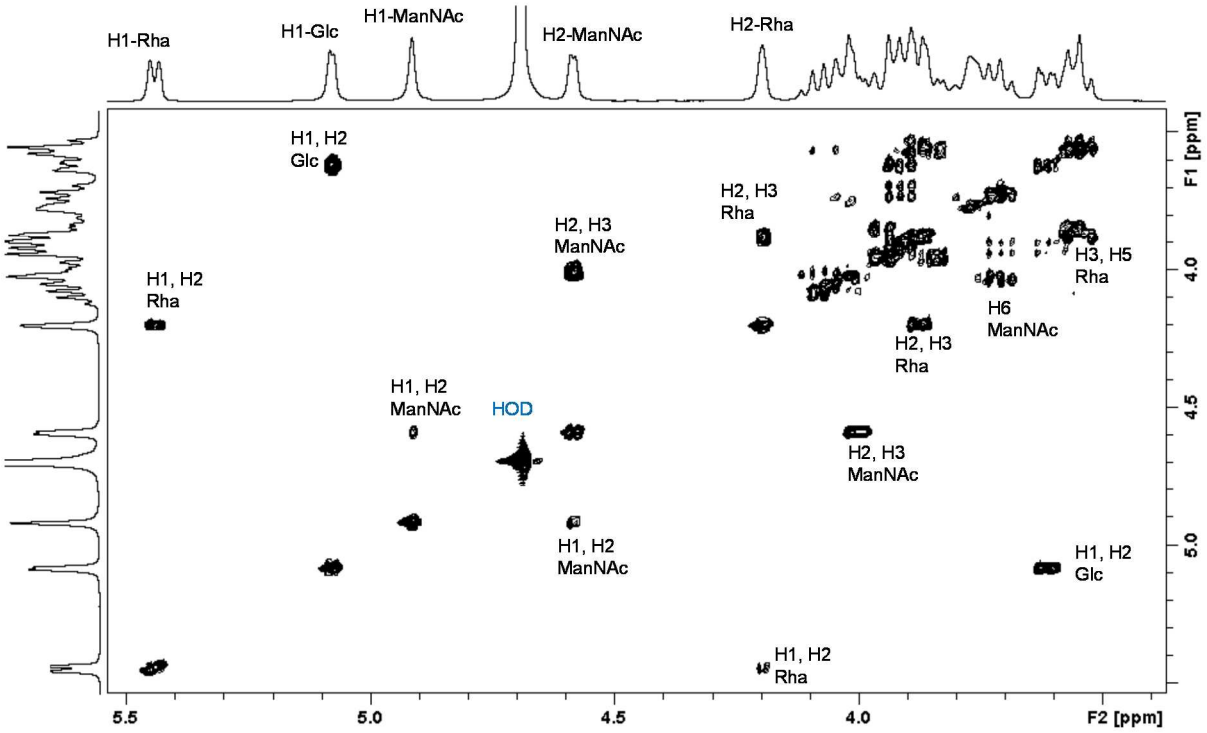

Figure 5.34: Expanded COSY spectrum of Pn19A CPS with some cross-peaks labeled. The anomeric and ring region of the COSY spectrum of Pn19A in D_2O at 303K. Not shown is the methyl region**.**

The TOCSY spectrum (Figure 5.35) reveals correlations between all protons within the same spin system not just in vicinal or geminal proton; however, this depends on the coupling constants. At this stage of analysis, the difference between the NMR spectra of Pn19F and Pn19A becomes apparent.

From the 2D TOCSY experiments, the correlations in the Rha spin system can be mapped from the H6 Rha to the H5, H4, and H3 of Rha and to some extend to the H2 of Rha.

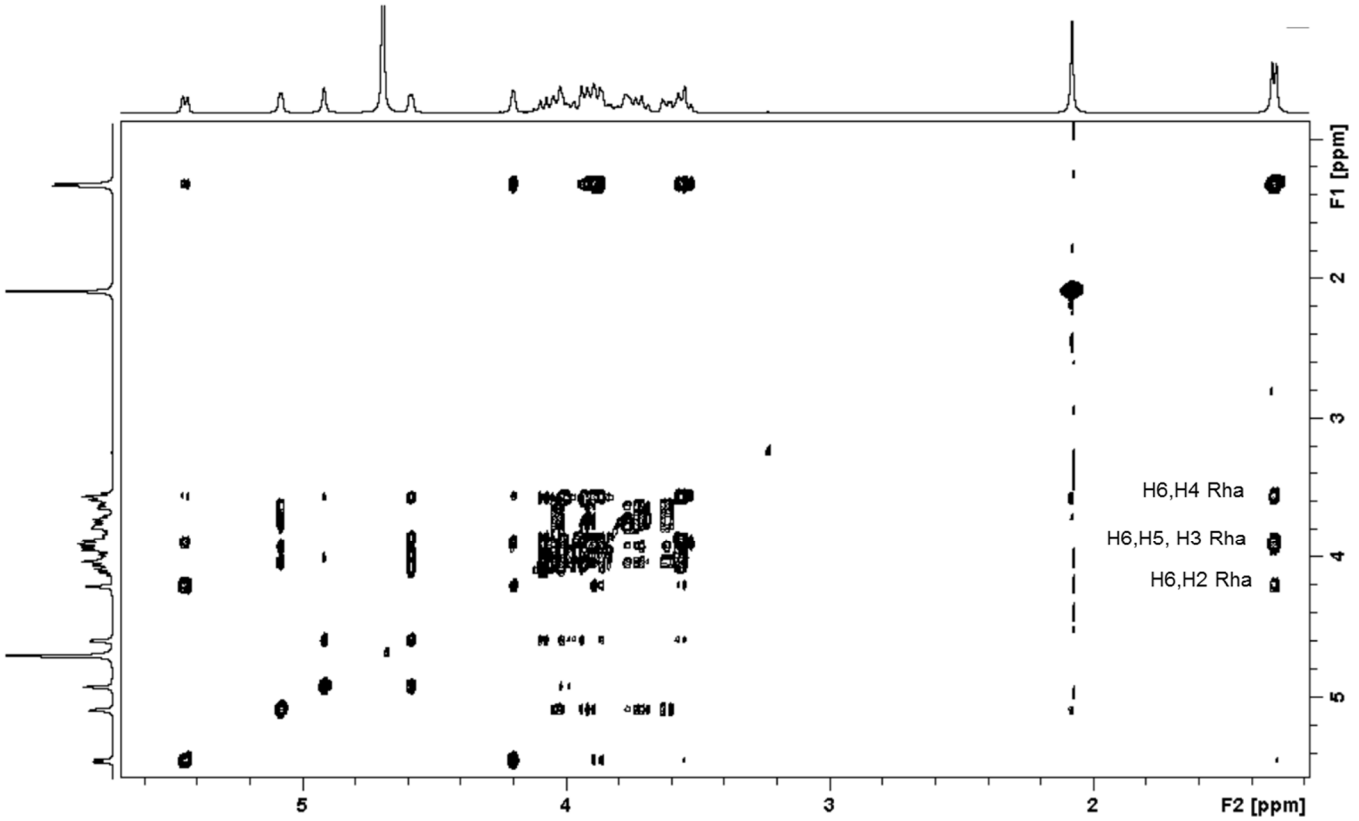

Figure 5.35: The full 2D TOCSY (180s) spectrum of Pn19A CPS in D_2O at 303K.

With the expanded version shown in Figure 5.36, the Rha spin system can also be mapped from the anomeric proton H1 to H5. The same is observed for Glc and ManNAc spin systems, mapping each spin system from the anomeric proton H1 to H5.

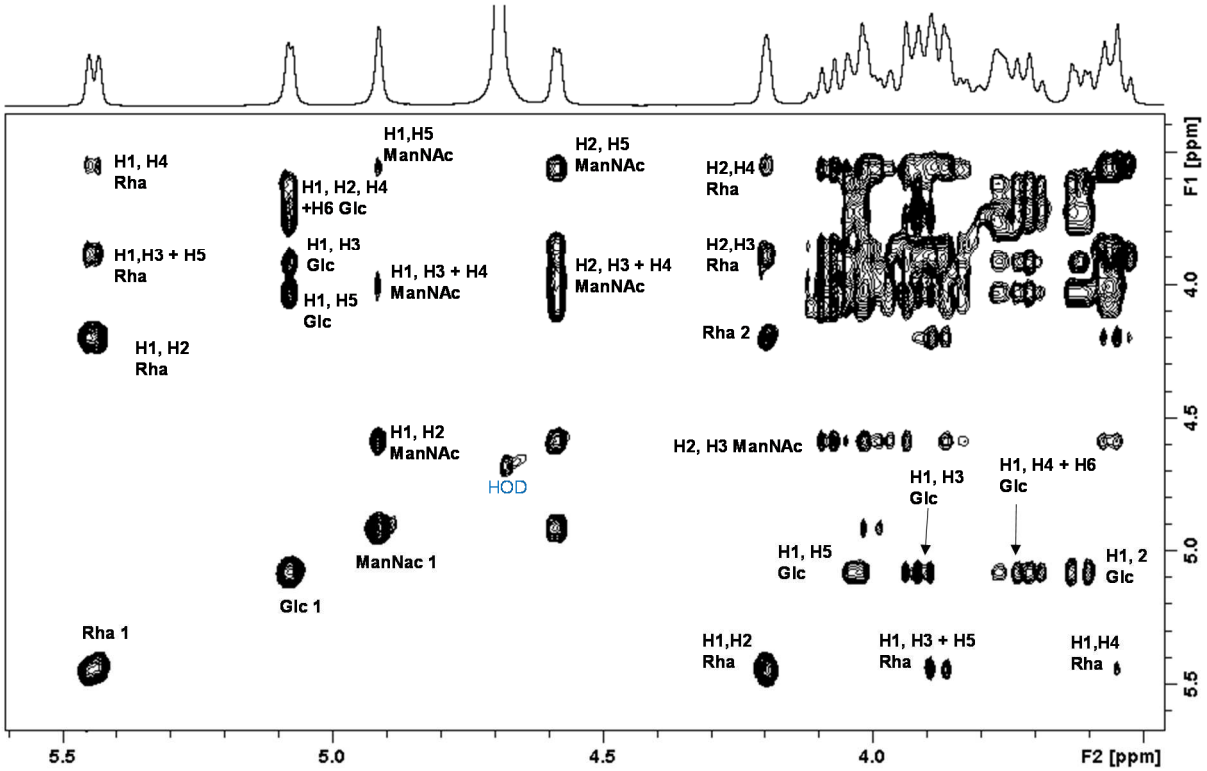

Figure 5.36: The expansion of the anomeric and ring regions of 2D TOCSY (180 s) in D_2O at 303K. Some peaks are labeled.

With the aid of the 1D TOCSY experiments, the Rha proton spin system can be fully assigned (Figure 5.37) as well as Glc and ManNAc proton spin systems (Figure 5.38) and confirm the 2D TOCSY assignments. For ManNAc it is easier to map the spin system from H2 as it has a large coupling constant and can see around the monosaccharide ring more easily than from the H1 position. With the 1D TOCSY experiments, a longer mixing time before conducting the experiment is usually performed which allows for better correlations around the spin system when compared to 2D TOCSY experiments.

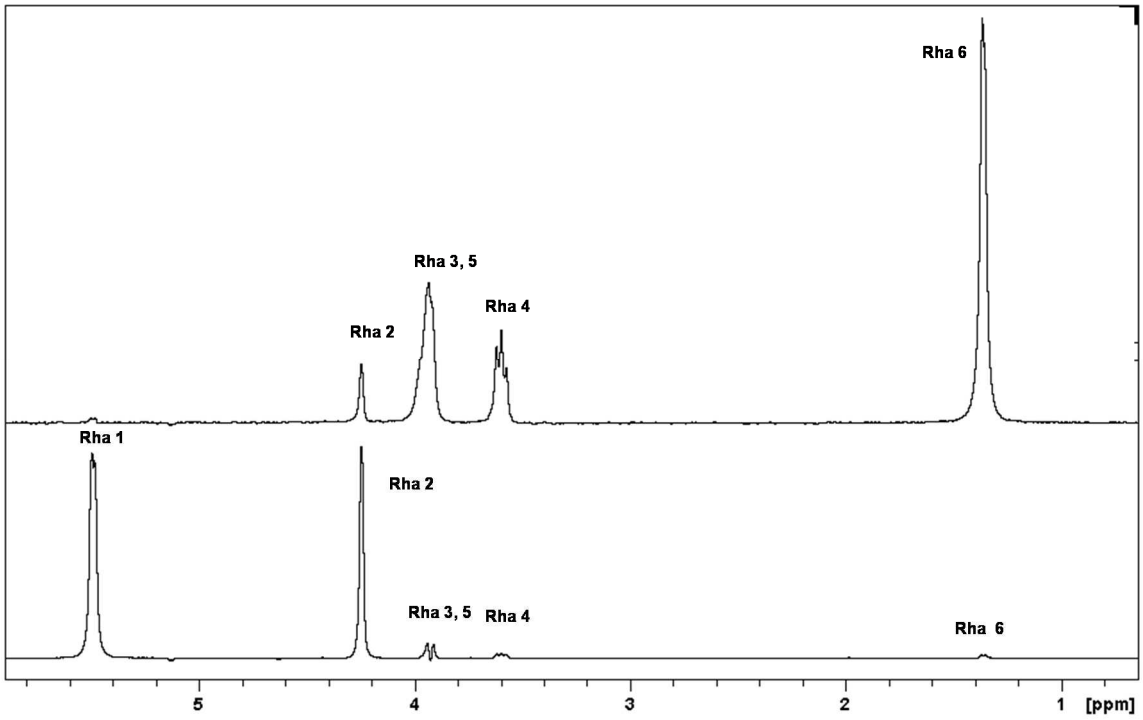

Figure 5.37: The 1D TOCSY (120ms) spectrum of Pn19A CPS in D_2O at 303K of Rha, top shows Rha spin system from proton 2 and bottom shows Rha spin system from the anomeric proton.

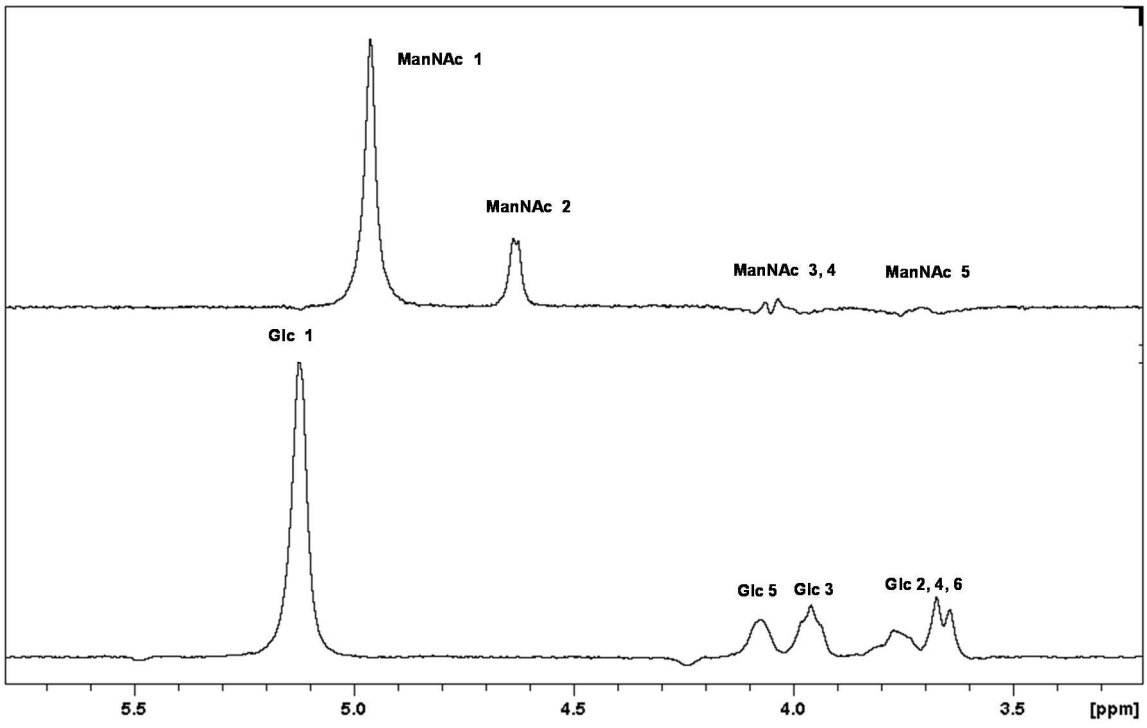

Figure 5.38: The 1D TOCSY (120ms) spectrum of Pn19A CPS in D_2O at 303K of Glc (bottom) and ManNAc (top).

The ^{1}H shifts and ^{13}C resonance were assigned using HSQC spectrum presented in Figure 5.39 shows diagnostic signals of the monosaccharides present on the repeating unit of 19A CPS, the anomeric carbons as well as the methyl and amino residues of Rha and ManNAc, respectively.

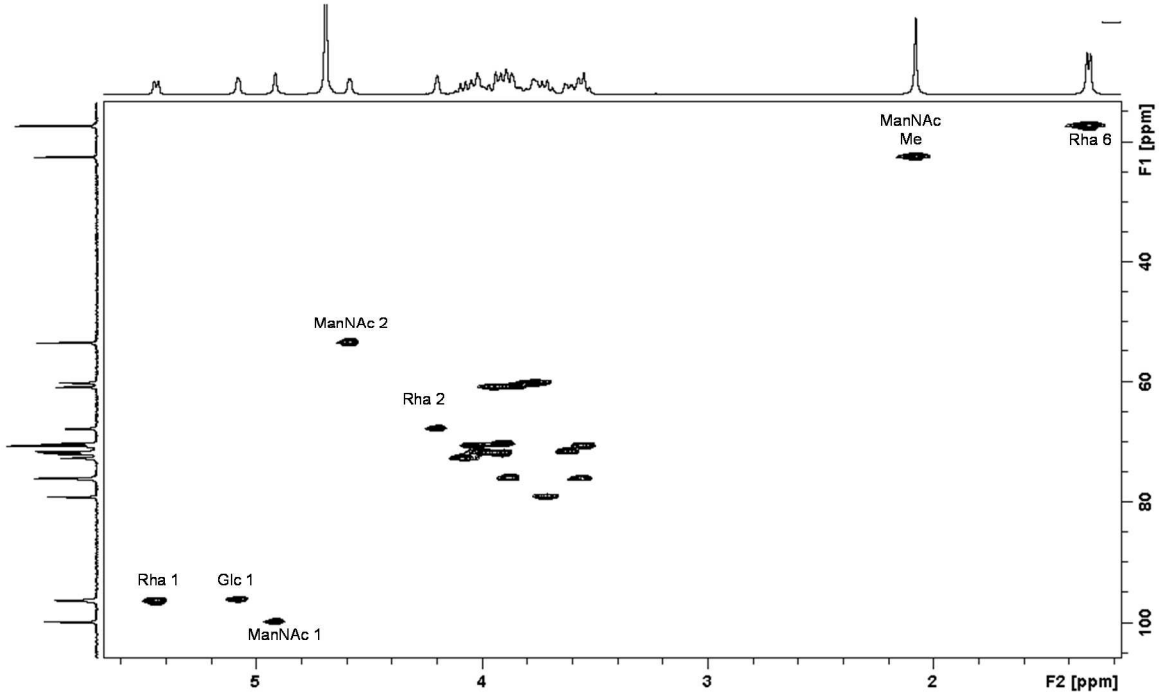

Figure 5.39: The full HSQC spectrum of serotype Pn19A CPS in D_2O at 303K.

The expansion of the HSQC spectrum of Pn19A shown in Figure 5.40 shows the proton-carbon present on the repeating unit of the CPS which forms the ring carbons and details the assignments of the carbons present. These assignments are confirmed by the use of the proton spectra.

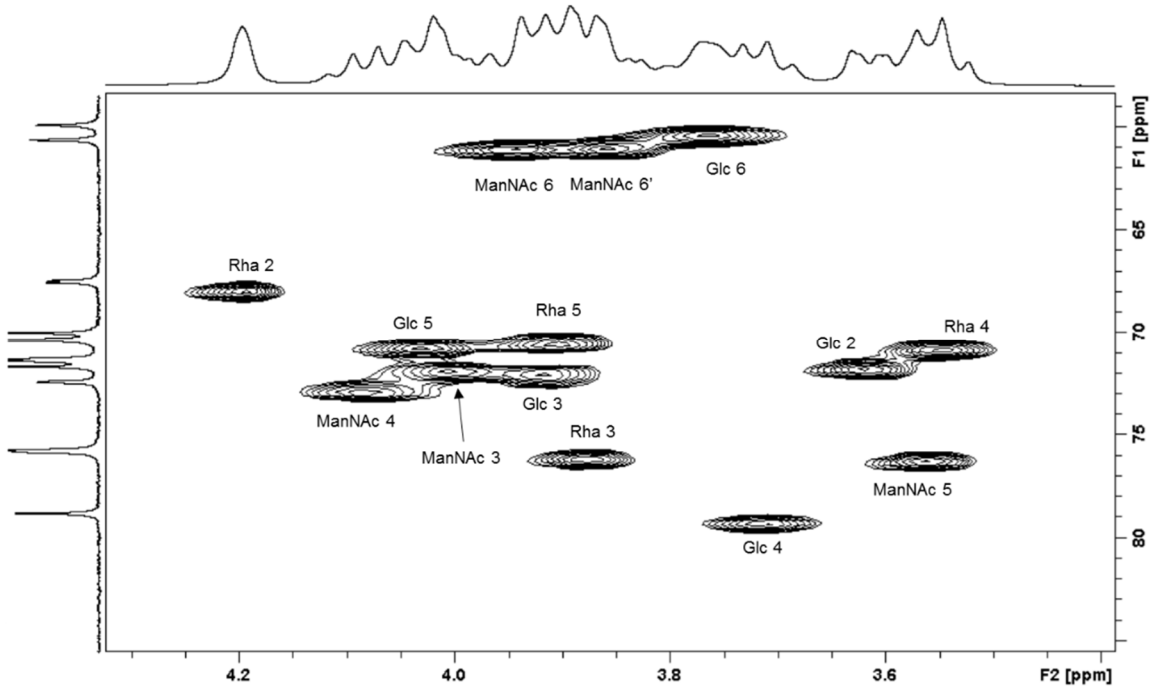

Figure 5.40: The expansion of ring region of HSQC spectrum of Pn19A CPS in D_2O at 303K.

The ^{13}C NMR spectrum of serotype 19A shown in Figure 5.41 confirms the presence of a trisaccharide repeating unit. In accordance with the ^{13}C NMR spectrum signals three anomeric carbons (δ 95 – 100

ppm), a signal at 17.34 ppm signaling the methyl group in L-rhamnose and a signal at 22.53 ppm indicating the presence of the acetyl group of N-acetyl-ManNAc. The three anomeric signals were assigned by inspection to ManNAc (99.86 ppm), Rha (96.41 ppm) and Glc (96.21 ppm) and compared to the literature [152, 176].

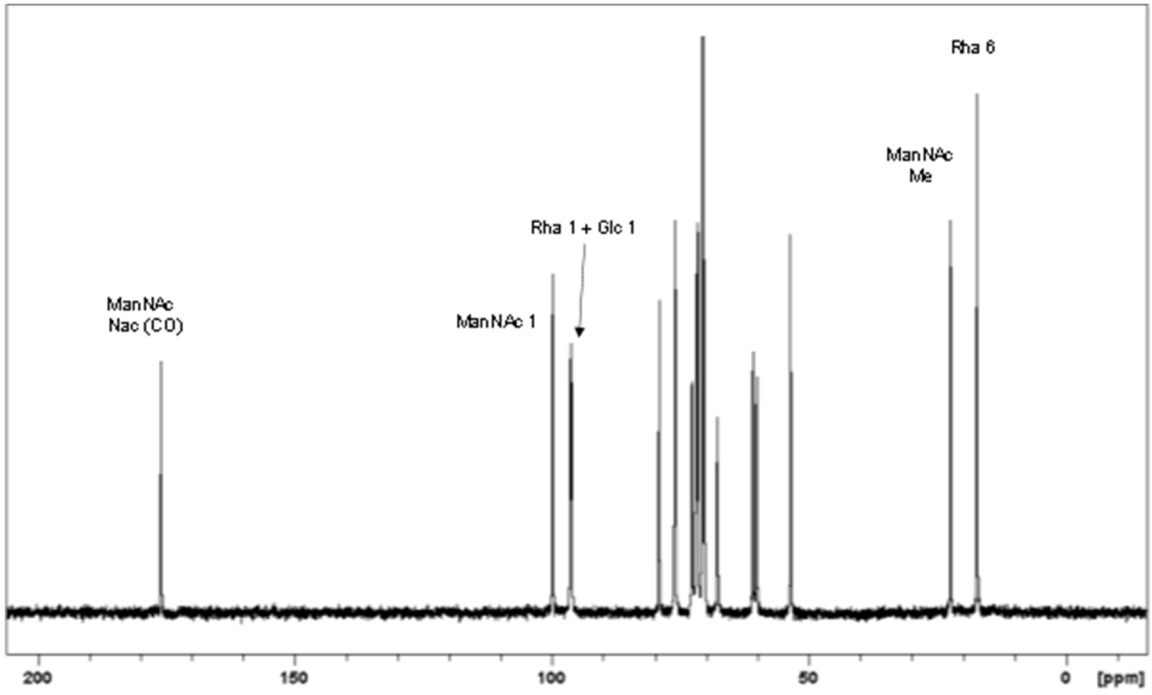

Figure 5.41: The ^{13}C NMR spectrum of one of the Pn19A CPS batches fermented and purified during this study.

Figure 5.42 details the carbons present in the ring region between 50 – 80 ppm. By comparing the literature assignments as well as the HSQC spectra, these assignments were made.

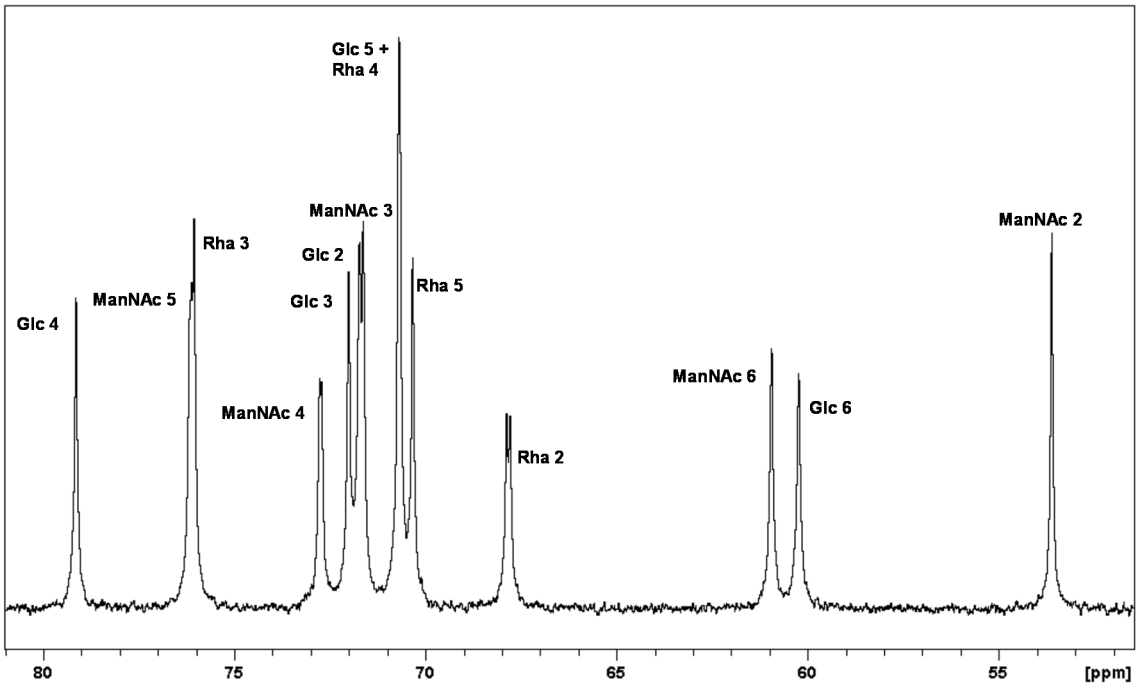

Figure 5.42: The ring region of the ^{13}C NMR spectrum of Pn19A CPS in D_2O at 303K.

The HMBC experiment detects long range coupling between proton and carbon with linkages up to two or three bonds away. The HMBC spectrum in Figure 5.43 shows two cross-peaks from the acetyl (NAc) carbonyl carbon at 175.96 ppm to the methyl NAc at 2.08 ppm and to H2 ManNAc confirming the position of the NAc, thus completing the structural assignments for Pn19A.

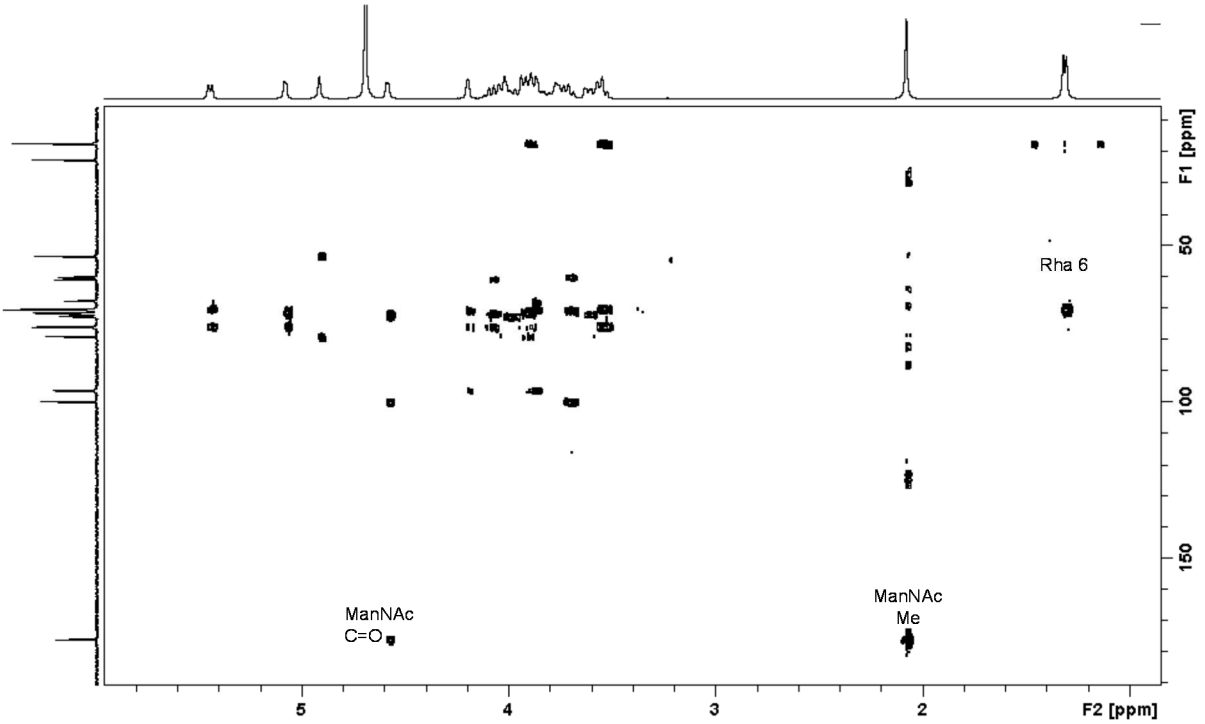

Figure 5.43: The full HMBC spectrum of the anomeric and ring region of Pn19A CPS.

The expansion HMBC spectrum (Figure 5.44) provides linkage information showing that for example C1 of ManNAc is linked to H1 of ManNAc. It also shows that the C1 of Glc is linked to the H3 of Rha which is the link that distinguishes between Pn19F and Pn19A. The anomeric proton of Rha appears as a doublet due to coupling to the phosphorus with $J_{H1\text{-}P}$ = 7.13 Hz. The ^{1}H-^{31}P HMBC in Figure 5.46 shows the linkage of the phosphate to H4 of ManNAc.

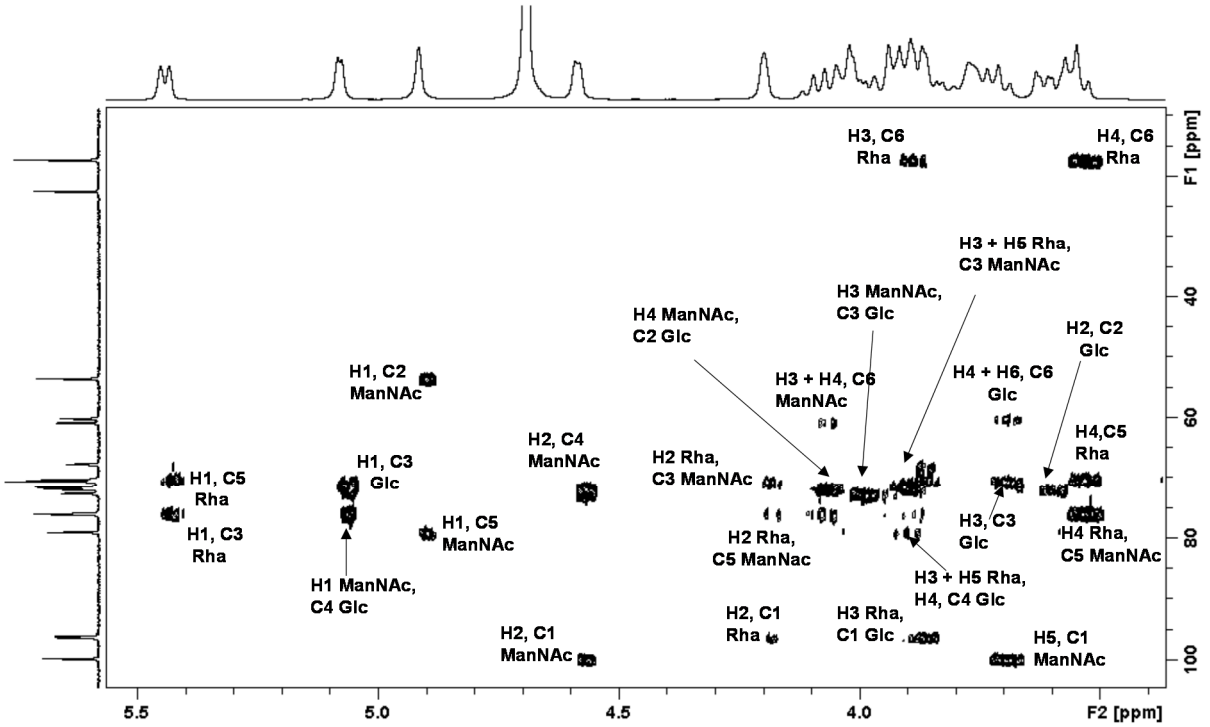

Figure 5.44: The HMBC expansion spectrum of the anomeric and ring region of Pn19A CPS.

The ^{1}D ^{31}P NMR spectrum in Figure 5.45 showed an intense resonance at -2.27 ppm indicating the presence of a phosphate group, one of the residues found in the repeating unit of Pn19A CPS. This phosphate group forms a phosphodiester linkage with rhamnose and is used to calculate the mole percent cell wall polysaccharide present in the sample as it contains phosphocholine substituents (phosphate groups) [201]; calculation shown in section 5.3.4.1 and was used to differentiate between the CWPS to the CPS in order to determine the purity of the CPS as CWPS is a contaminant and is picked up NMR and shows the intense resonance of the phosphate group present in this CPS (Figure 5.45) was used to calculate the percentage of contamination [201]. The presence of three minor resonances of approximately equal intensity assigned as arising from C-substance contamination as indicated by the CWPS for Pn19F was not visible in Figure 5.45 for Pn19A indicating that the contamination of CWPS for Pn19A CPS was very low.

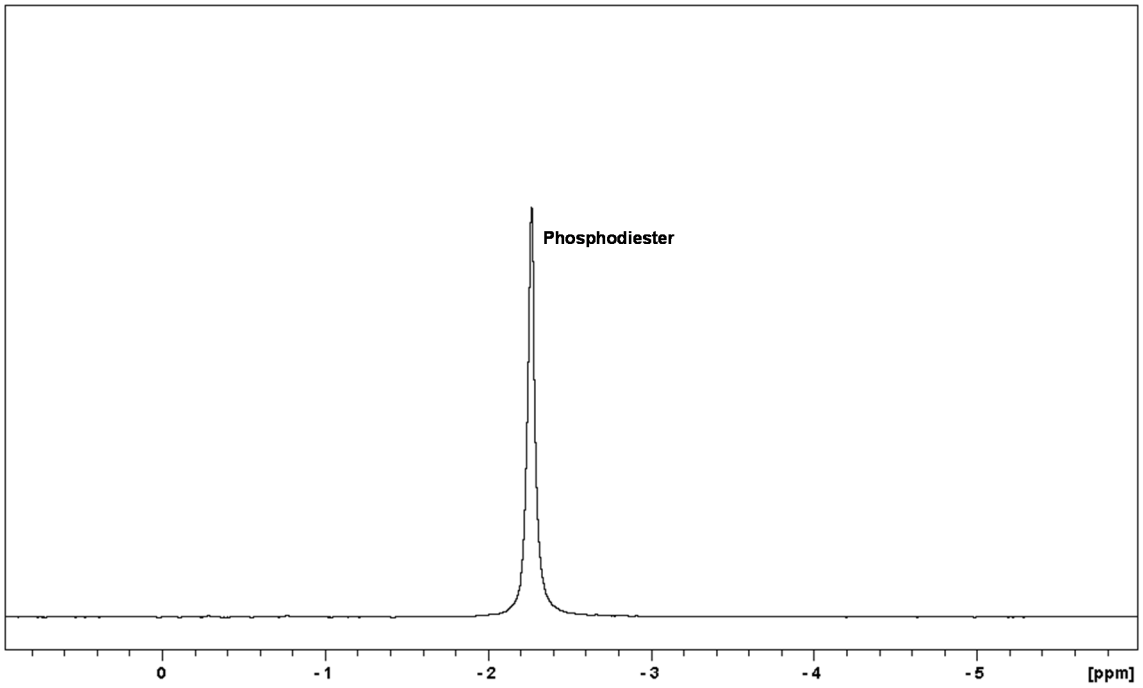

Figure 5.45: ^{31}P NMR spectrum of one of the Pn19A CPS batches fermented and purified during this study. Showing the presence of minimal contamination in the form of CWPS.

The position of the phosphate group is determined by the correlation between the phosphorous and protons at the phosphorylation sites between the Rha and the ManNAc residues, which were revealed by ^{1}H,^{31}P HMBC spectra as shown in Figure 5.46. The ^{1}H-^{31}P HMBC showed linkage of the phosphate to H-1 of Rha. Coupling of the phosphate to C-1 gave a $J_{H1\text{-}P}$ = 4.41 Hz and also gave a large coupling to C-4 ($J_{H2\text{-}P}$ = 5.15 Hz).

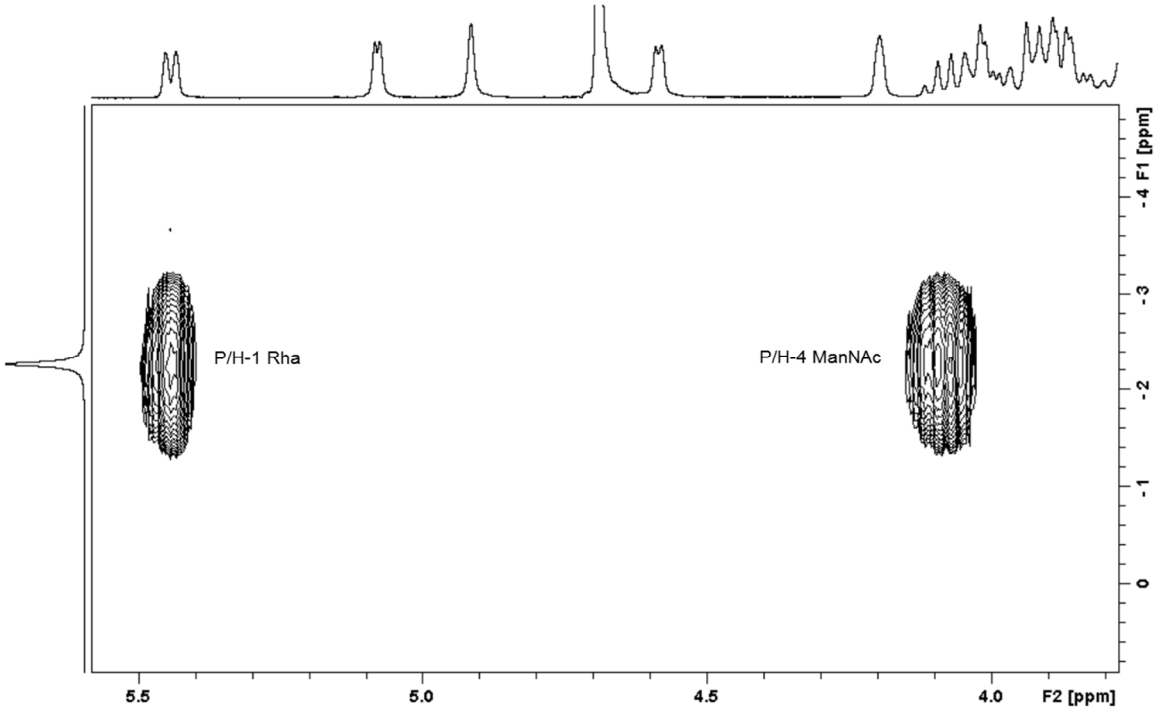

Figure 5.46: The ^{1}H-^{31}P HMBC spectrum of Pn19A CPS in D_2O at 303 K with all the cross-peaks labeled.

By overlaying spectra such as HSQC-TOCSY, HSQC and HMBC mapping of the spin systems for each residue was possible (Figure 5.47). The TOCSY spectrum showed a correlation from H-6 to a cross-peak corresponding to only one of the carbon shifts assignable to either H-5 or H-3. The 4-bond coupling between H-6 and C-3 would be too long range compared to the 2-bond coupling between H-6 and C-5 in the HMBC. The carbon shift of the cross-peak was thus assigned to C-5 and the corresponding proton shift. The H-1 Glc to H-3 Rha linkage position was confirmed by HMBC. Determining the inter-residue linkage between sites of the sugar is performed using HMBC spectrum and added information can be obtained with the overlay of the HSQC of that sugar.

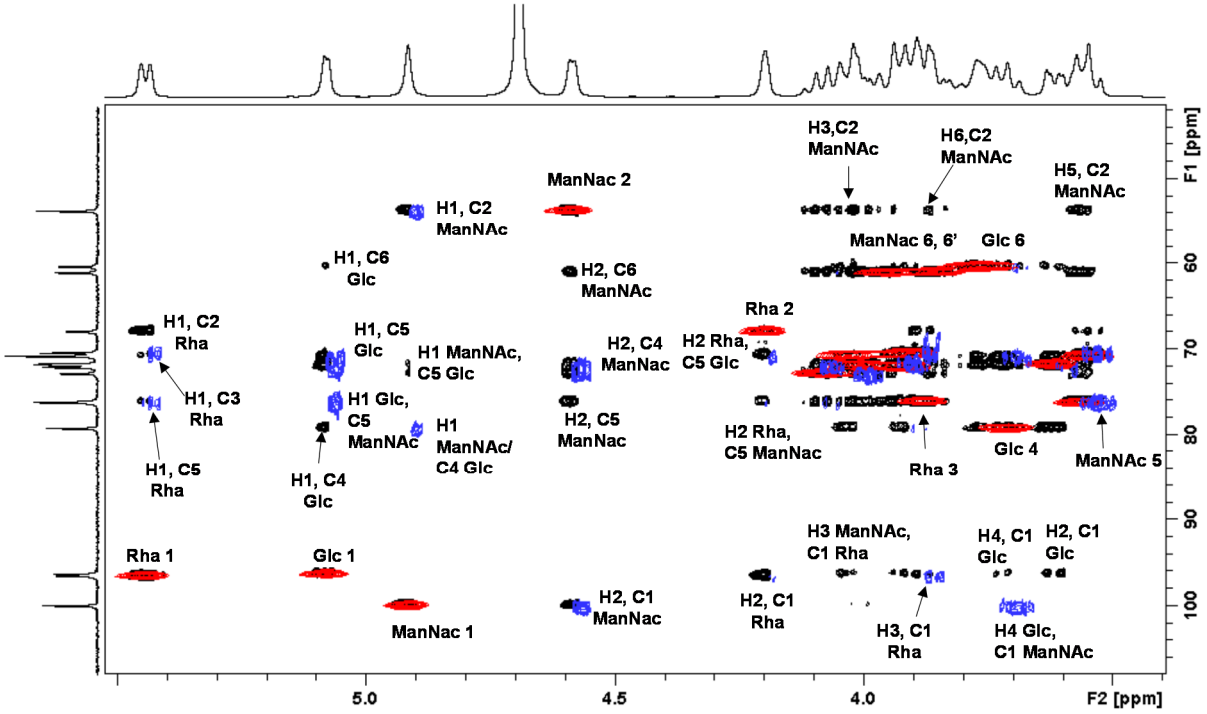

Figure 5.47: Expansion of HSQC-TOCSY (black) overlaid with HSQC (red) and HMBC (blue).

Table 5.16: ^{1}H and ^{13}C NMR chemical shifts (ppm) at 303 K of the sized Pn19A CPS repeating unit with inter-residue correlations from ^{1}H-^{13}C-HMBC spectra [152].

Residue Abbreviation	$^{1}H/^{13}C$ ($J_{H1,H2}$ / $J_{C1,H1}$)								
	1	**2**	**3**	**4**	**5**	**6/6`**		**Me[NAc]/ CO [NAc]**	
→ 3) – α – L - Rhap – (1 → P -	5.44 (0.32)	4.20 (0.28)	3.89 (0.08)	3.55 (0.10)	3.87 (0.01)	1.31 (0.03)			
	96.41 (1.57)	67.83 (-3.98)	**76.05 (5.05)**	70.68 (-2.51)	70.33 (1.21)	17.34			
→ 4) – α – D - Glcp – (1 →	5.08 (-0.15)	3.62 (0.08)	3.92 (0.20)	3.73 (0.31)	4.05 (0.21)	~3.77			
	96.21 (3.22)	71.63 (-0.84)	72.02 (-1.76)	79.14 **(8.34)**	70.69 (-1.68)	60.24 (-1.60)			
→ 4) – β – D - ManpNAc – (1 →	4.92 (-0.09)	4.59 (0.14)	4.02 (0.19)	4.09 (0.57)	3.57 (0.12)	3.94 (0.13)	3.86 (-0.04)	2.08 (0.02)	
	99.86 (5.95)	53.61 (-1.33)	71.73 (-1.27)	72.74 **(5.09)**	76.13 (-1.12)	60.95 (-0.59)		22.53 (-0.45)	175.96 (-0.43)

With the combination of 1D and 2D experiments, the full characterization of the structure of the Pn19A CPS repeating unit was obtained.

The NMR assignments of Pn19F CPS and Pn19A CPS is useful for NMR fingerprinting and as identity test methods (antigen identity and bacterial identity) and quality control method in research and industrial laboratories working on polysaccharide conjugates for vaccine development [203]. Tables 5.15 and 5.16 shows the NMR assignment for Pn19F CPS and Pn19A CPS, respectively.

A comparative analysis of the observable peaks in the ^{1}H NMR spectra (Figure 5.48) shows that there is a dramatic change in the anomeric region. These structural differences are reflected in distinctly different chemical shifts for the Glc H-1 and for the Rha H-1 and H-2 resonances. The spectra are centered on the HOD (water) signal and were both referenced according to the CWPS resonance at ^{1}H 3.23 ppm and ^{13}C 54.50 ppm. Rha anomeric resonance for Pn19F (5.51 ppm) is more deshielded than that of Pn19A (5.44 ppm). An indication of linkage position as the anomeric proton moved closer to the only other H2 Rha. H1 Glc is shielded in Pn19F but is not shielded enough to imply a β anomeric configuration.

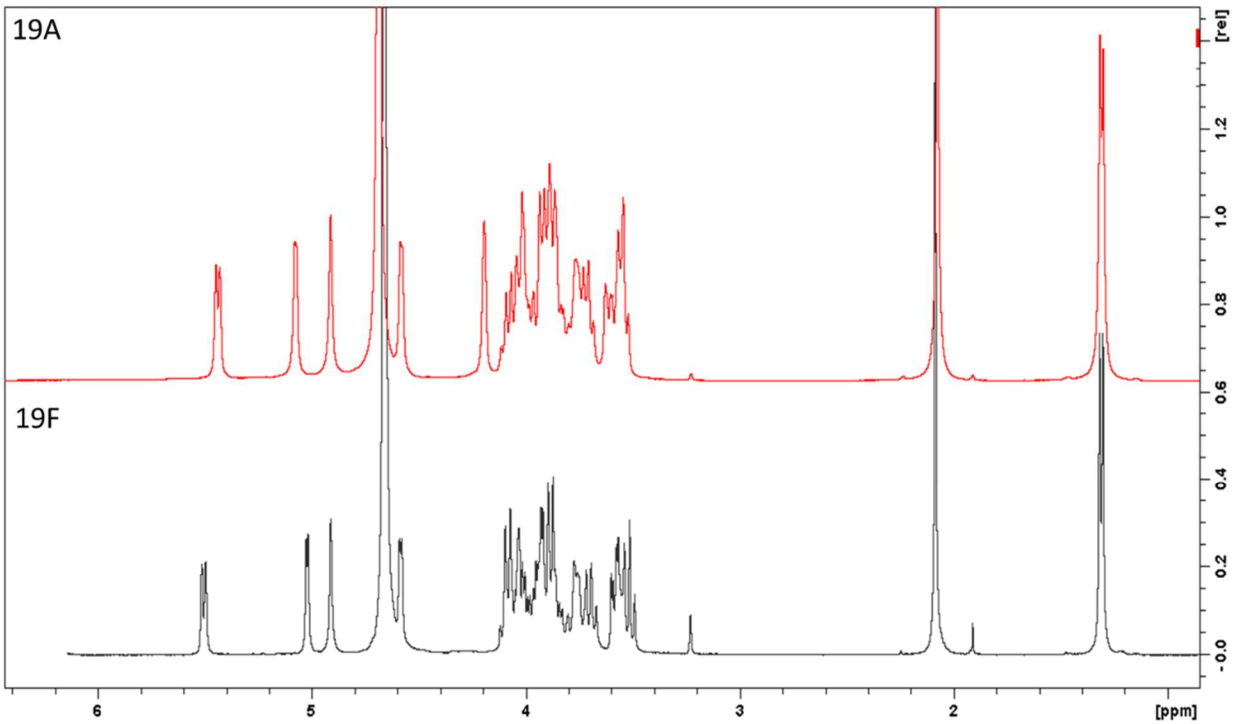

Figure 5.48: A ^{1}H NMR spectral comparison overlay of Pn19F CPS (black) and Pn19A CPS (red). The ^{1}H NMR spectrum of Pn19F overlaid with that of Pn19A both samples in D_2O at 303K.

The HSQC overlay of Pn19F in red and Pn19A in black in Figure 5.49 shows the anomeric carbons of the trisaccharide repeating unit, the H2 Rha (67.83 ppm) and the diagnostic rhamnose methyl group (1.31 ppm). It also indicates that the acetyl group of ManNAc (2.08 ppm) is attached to H2 (175.96 ppm) of ManNAc. Another difference between the two serotypes was that the presence of CWPS was much less in 19A than in 19F.

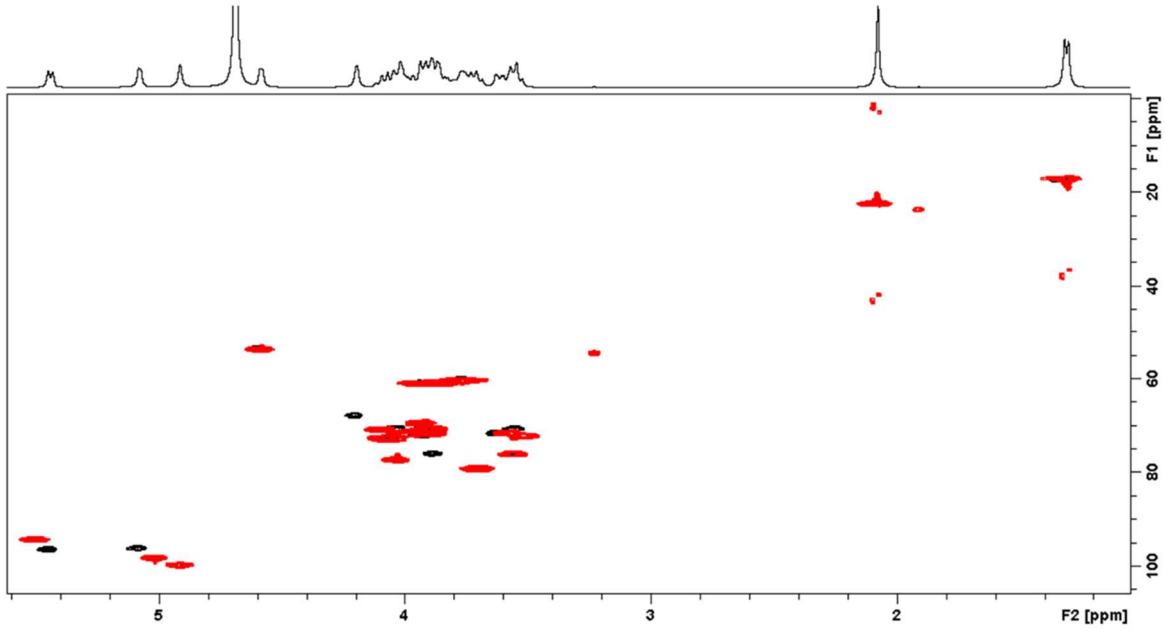

Figure 5.49: A spectral comparison of HSQC overlay of Pn19F CPS (red) and Pn19A CPS (black).

The structure of the CPS from *S. pneumoniae* 19F and 19A has been determined using NMR spectroscopy. The structures of both 19F and 19A CPS has been identified in the literature [176, 178] and confirmed in this study. It can be concluded that the CPS is composed of a trisaccharide repeating unit. The trisaccharide backbone of 19F is identical to 19A with the exception of a single linkage position between the Rha and Glc monosaccharides present of the trisaccharide repeating unit. Both 1D and 2D NMR techniques were employed to fully assign the proton and carbon spectra for the serogroup 19 CPS.

5.3.4.3 Cell Wall Polysaccharide (CWPS) contaminant

All pneumococci, both virulent and avirulent strains possess a common polysaccharide, Cell Wall Polysaccharide (CWPS, teichoic acid). The structure of CWPS (Figure 5.50) consists of a phosphodiester-linked linear tetrasaccharide-ribitol repeating units that are linked through a phosphodiester linkage between position 5 of the D-ribitol and position 6 of a β–D-glucopyranosyl residue [201]. The pneumococcal cell wall contains several different polysaccharides which are expressed by all pneumococci. CWPS and CPS are covalently linked to the cell wall peptidoglycan, which in the purification of the CPS makes it impossible to remove the bound CWPS [204]. The removal of the CWPS is important as it is highly immunogenic and can elicit universal protection against *S. pneumoniae* or any interference in the immune response to CPS and is thus considered as a contaminant and has to be quantified. The presence of CWPS can be estimated by NMR (^{1}H and ^{31}P NMR).

In order to determine the degree of CWPS present the equation shown here is used to determine the mole percentage (mol%) present from the proton NMR of the CWPS. NMR uses the ratio of the choline signal to the rhamnose methyl signal for calculating the CWPS content.

$$\%\text{CWPS} = \frac{\text{IPCho}/18}{\text{INAc}/3} \times 10 \qquad [205]$$

Where I_{PCH_0} is the peak integration of the phosphocholine peak and I_{NAc} is the integration of the N-acetyl peak.

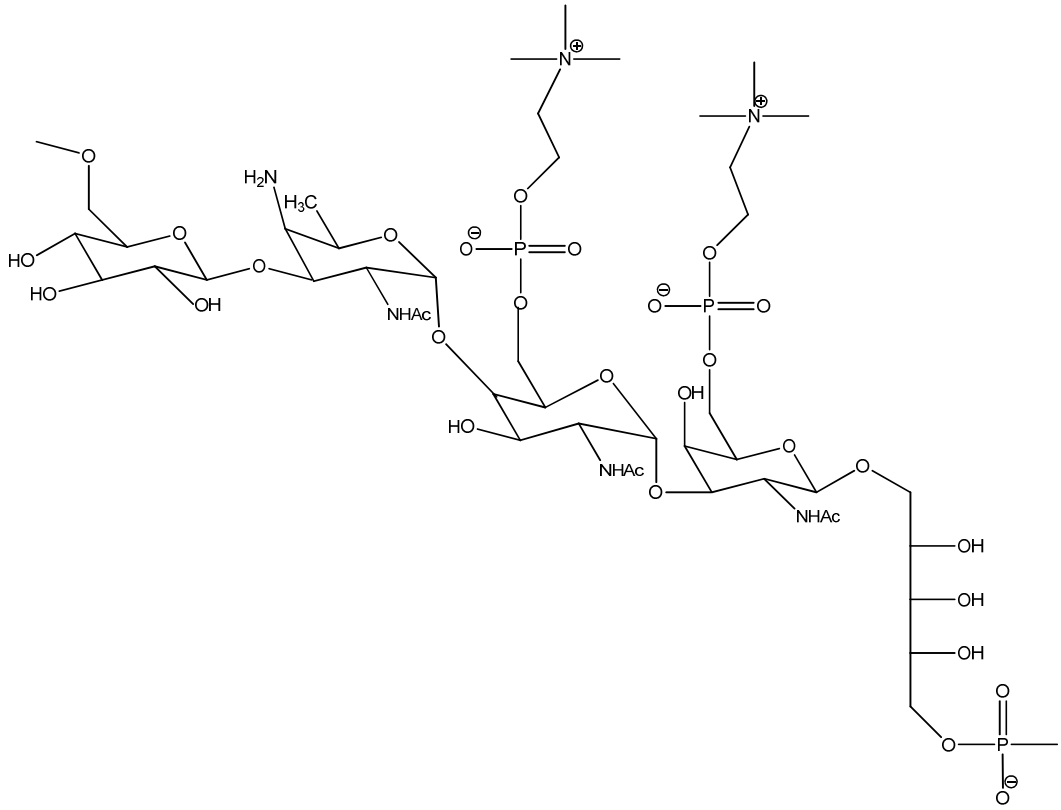

Figure 5.50: Structure of the pneumococcal cell wall polysaccharide (CWPS) containing two phosphocholine groups [96, 108].

In the case of Pn19F and Pn19A, the anomeric signal of the CPS represents one proton which is set at 1 and taken as the reference signal when compared the phosphocholine methyl group signal which represents 18 protons. An example of this is shown in Figure 5.51 where the value of the integral for one equivalent proton is 0.03 and therefore represents 3% contamination. With the preparation of CPS cultivation and purification, the end result of CWPS contamination should be no more than 3% [206]. The WHO has not released guidelines for the amount of CWPS contamination allowed in a purified batch of polysaccharide, however, Marburg et al. suggested a value of less than 3% (w/w) [148]. Both Pn19F and Pn19A showed very low levels of CWPS contamination and kept to the guidelines suggested by Biovac to be below 3.5% (Figure 5.51).

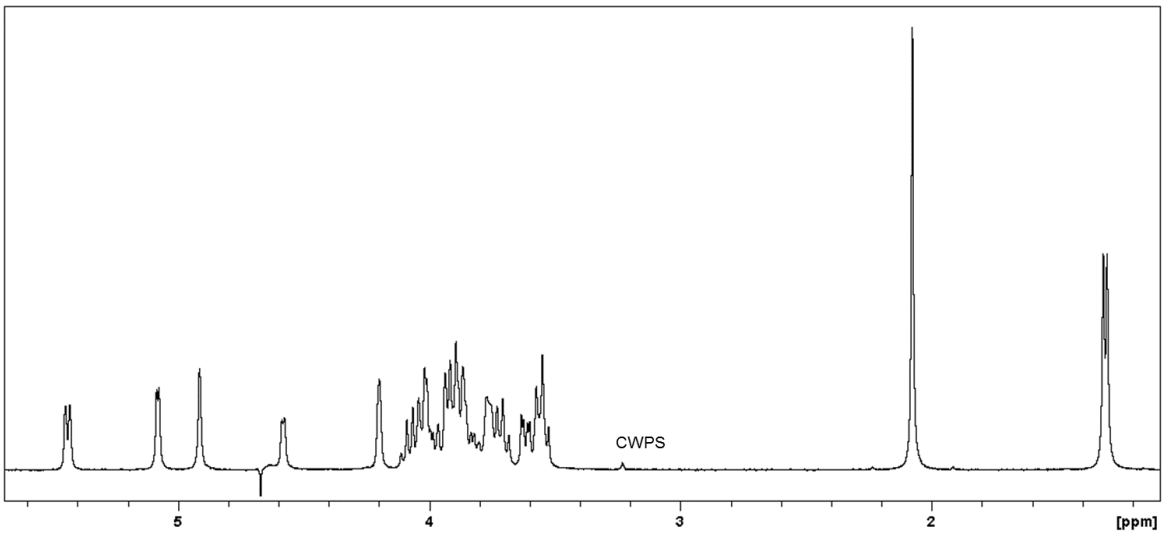

Figure 5.51: The pre-saturated ^{1}H NMR chromatogram suppressing the HOD peak depicts trace amounts of CWPS contamination present in Pn19A CPS repeating units.

The mole % CWPS present in the lyophilized samples of batches purified during this study ranged from 0.14 – 1.8 mol% which, according to the in-house guidelines of below 3.5% corresponds to suggestions in the literature [148]. The same was observed for the conjugates prepared and discussed in Chapter 6, that the percentage of CWPS was very low before and after conjugation and suitable for stability studies.

5.3.5 General conclusion

This chapter describes the colorimetric assays used for the qualification of pneumococcal polysaccharides achieved by size characterization of the respective monosaccharides by the use of physiochemical methods including liquid and gas chromatography, mass spectroscopy and NMR spectroscopy. When appropriate standards and controls were used, the colorimetric assays such as anthrone provided accurate quantitative measurements [103]. Although chromatographic assays provide quantitation of sugar-specific species present in a sample, these methods require hydrolysis of the sample prior to chromatographic separation. For characterization purposes, the GC-MS was preferred over HPAEC-PAD due to the additional information obtained from the peak purity and mass spectral analysis. GC composition analysis contributed to CPS characterization along with other physiochemical techniques such as NMR to identify the CPS. GC-MS is an analytical tool that can be utilized to analyze pneumococcal CPS at various stages of conjugate vaccine process. GC-MS provides absolute conformation of the peak identity. For specific serotypes such as 19F and 19A that only differ by a single linkage and have the same monosaccharides present, composition analysis cannot distinguish between the serotypes. Therefore structural tools such as NMR were performed to further analyze the CPS. NMR spectroscopy has been demonstrated to be the most powerful tool in the structural analysis of polysaccharides for vaccine production. The first step approach is always to have a simple ^{1}H and ^{13}C NMR spectra that can be compared against any literature data available [190]. The ^{31}P NMR spectrum also proved useful in identifying CPS such as Pn19F and Pn19A that contains phosphate or phosphodiester groups. The selectivity of 1D proton NMR permits differentiation between very closely related polysaccharides that differ by only a glycosidic linkage such as Pn19A/19F (→3)-

α-L-Rhap/ →2)-α-L-Rhap). Such differentiation is impossible to achieve with the traditional colorimetric tests [101]. The advantages of NMR approaches is that it is a non-destructive technique that requires small amounts of material for analysis and no reference standards if the sample contains a known reference peak like those of CWPS, although reference to the literature aids in confirming identification of the CPS under investigation. A combination of one- and two-dimensional NMR experiments together with component analysis are useful in a structural elucidation. A statement by Abeygunawardana, (2000) describes that “NMR can be used as a definitive measure of polysaccharide identity and that this method is both robust and rugged. For purposes of quality control of polysaccharides used in the manufacture of vaccines, this method provides a preferable alternative to the currently used elemental and colorimetric assays due to its simplicity, exquisite specificity, and inherent reproducibility” [177]. NMR spectroscopy has proven to be invaluable in demonstrating physiochemical equivalence of polysaccharide lots in order to structurally investigate the polysaccharides.

CHAPTER 6. CONJUGATION AND STABILITY OF Pn19F AND Pn19A BULK CONJUGATES

The chapter outlines, as displayed in yellow in Figure 6.1, the conjugation chemistry performed on serotypes 19F and 19A focusing on CDAP chemistry and determining, based on these results, the conjugate stability through thermal stability studies. The stability study was performed to determine whether there was a difference in stability between Pn19F or Pn19A bulk conjugates.

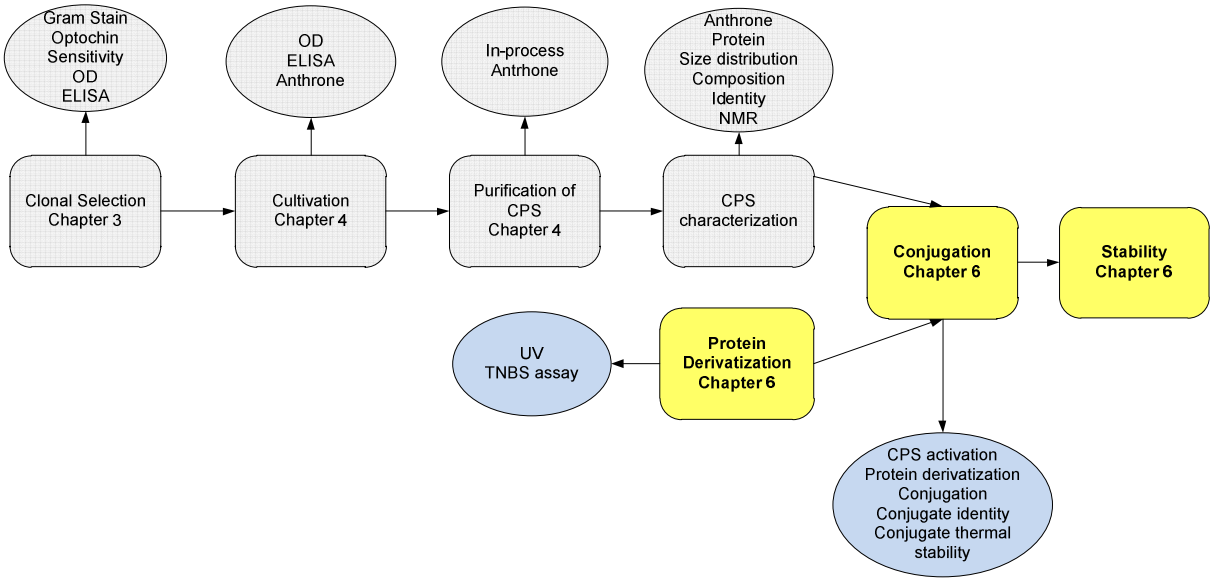

Figure 6.1: The process development steps for Pn19A conjugate vaccine production, highlighting the process flows for the preparation of Pn19F and Pn19A bulk conjugates.

6.1 Introduction

The manufacture of chemically complex conjugate vaccines involves four stages; (1) the preparation of antigen (CPS) and a carrier protein, (2) the activation of CPS and/or protein, (3) the coupling of activated components, and (4) the characterization of intermediates and conjugate drug substances. The chemistry used for conjugation is an important consideration to successfully produce an immunogenic vaccine. This chemistry must not; (1) modify the polysaccharide to void its immunogenicity, (2) cause cross-linking within the polysaccharide or protein and (3) cause cross-reaction between conjugates (if in a multivalent vaccine) or with the cross-linking bridge itself. A linker can be introduced onto either the polysaccharide and protein to assist these large macromolecules to bind chemically [107].

There are two main functional groups on the polysaccharides available for conjugation: the hydroxyl (OH) and carbonyl (COO^-) groups. These can be utilized directly or converted to reactive aldehydes via periodate oxidations and acid hydrolysis respectively. The two functional groups on the protein considered for conjugation were: (1) amino groups (lysine) which can be conjugated directly to the polysaccharide carbonyl groups through reductive amination, and (2) carbonyls (via aspartic or glutamic acid) which can be derivatized with adipic acid dihydrazide (ADH) to form reactive acid hydrazides which react with carbonyl groups on the polysaccharide through reductive amination [34].

Following conjugation, a key factor to be considered is the stability of the polysaccharide:protein conjugate. Hence, another aspect of this thesis was to compare Pn19F and Pn19A conjugate stability. These similarly structured CPS have an inherent instability due to the presence of phosphodiester bonds, however, it is hypothesized that Pn19A CPS is more labile towards hydrolysis than Pn19F CPS because the carbon at position 2 on the rhamnose on the repeating unit of serotype 19A can be depolymerized and cause phosphoric monoester formation faster than Pn19F CPS [207].

Two conjugation chemistries that were considered during this thesis: (1) periodate oxidation of the polysaccharide followed by reductive amination and (2) CDAP chemistry. The active /binding sites for each chemistry is shown in Figures 6.2 and 6.3 for Pn19F and Pn19A respectively where (1) represents the functional groups involved in periodate oxidation/reductive amination and (2) the functional groups involved in CDAP activation.

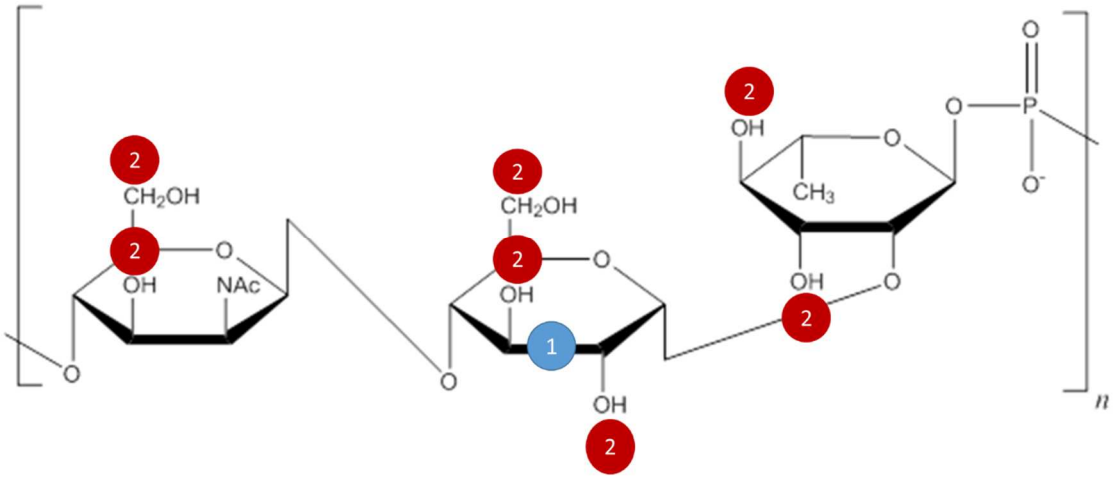

Figure 6.2: Pn19F trisaccharide phosphate repeating unit with a 1-2 linkage between glucose and rhamnose [178]. Representing the binding sites for (1) periodate oxidation followed by reductive amination and (2) CDAP chemistry.

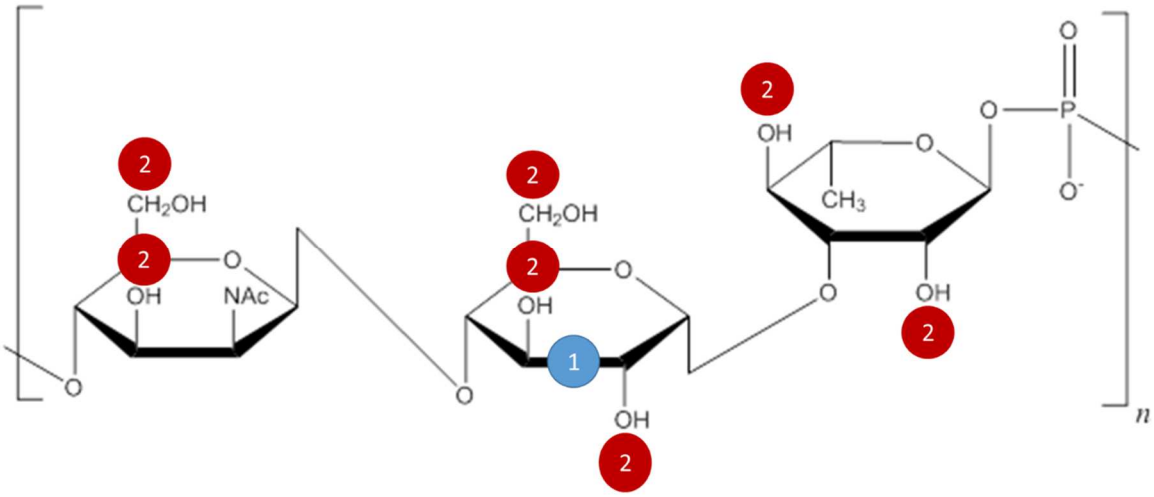

Figure 6.3: Pn19A trisaccharide phosphate repeating unit with a 1-3 linkage between glucose and rhamnose [176]. Representing the binding sites for (1) periodate oxidation followed by reductive amination and (2) CDAP chemistry.

6.1.1 Periodate oxidation and reductive amination

Reductive amination involves two steps, oxidation of the polysaccharide followed by reaction of the activated polysaccharide and a carrier protein to form a conjugate. CPS only have one naturally occurring aldehyde residue at the reducing terminus of the polysaccharide chain and however, in-change aldehydes through oxidation of adjacent diols with sodium periodate [107, 208]. The oxidation results either in ring opening if the diols form part of a ring or cleavage of the CPS repeating unit if the diol is terminal thus resulting in simultaneous size reduction. The mechanism for the periodate oxidation reaction is described in Figure 6.4 whereby the sodium periodate chelates in a hypervalent state to the vicinal diol resulting in ring-opening and the formation of aldehydes [107, 173]. The reactive aldehyde groups then undergo a reduction reaction with the free amino groups on the protein in the presence of a reducing agent such as sodium cyanoborohydride, which is selective for the reduction of double bonds in the presence of aldehydes, to form a stable secondary amine [64]. Sodium borohydride is then employed to reduce any unreacted aldehydes [107]. This is a slow process which can take up to several days to complete. The disadvantage of this method is that it physically alters the structure of the CPS which could potentially lead to loss of important epitopes and thus immunogenicity [34].

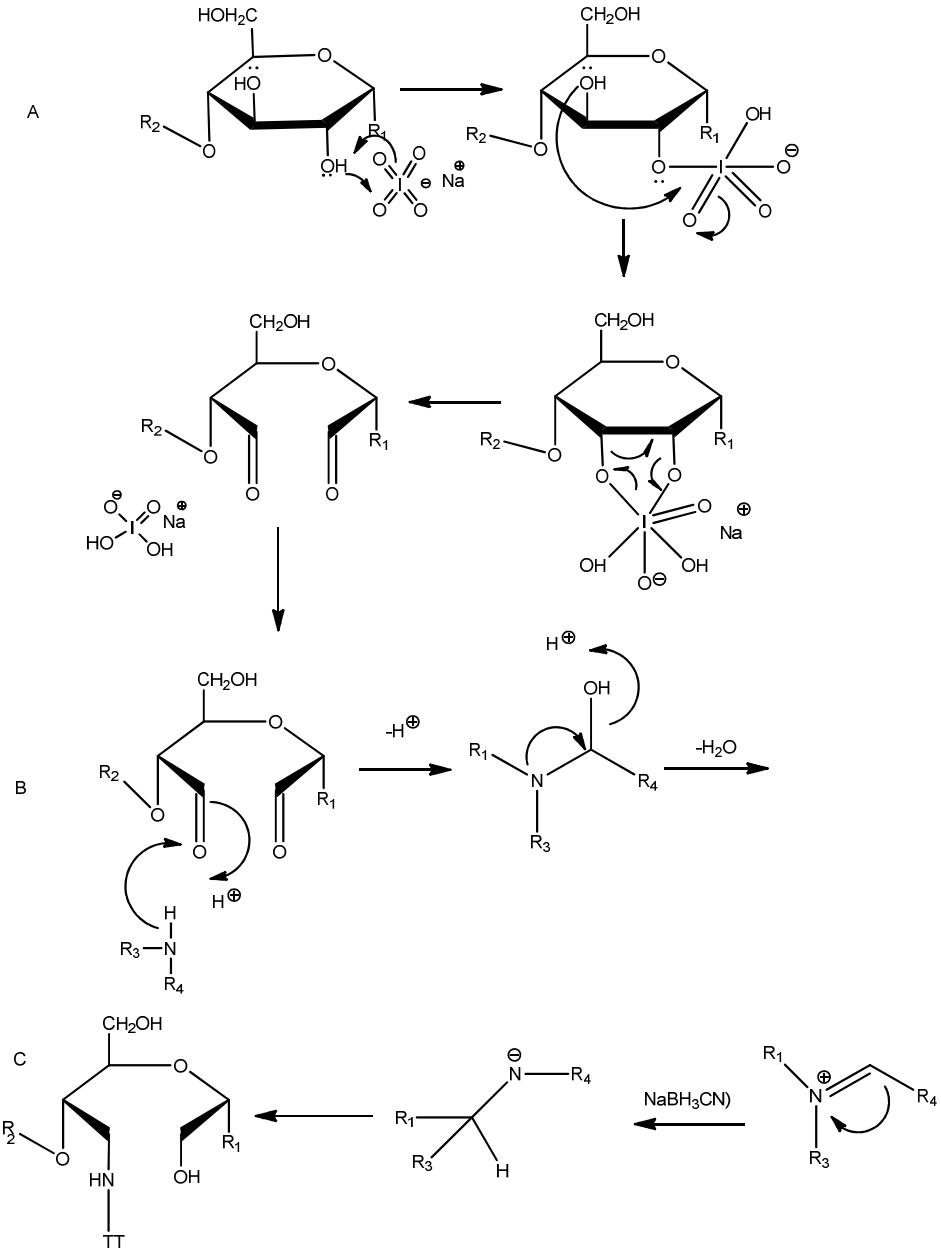

Figure 6.4: Conjugation method used for the production of PCV13. A) Periodate oxidation followed by the formation of a Schiff's base (B) and subsequent reduction (C) to an amine (reductive amination). R1, R2 = remainder of CPS and R3 = protein.

6.1.2 CDAP chemistry

Before the introduction of CDAP chemistry, cyanogen bromide (CNBr) a cyanylating agent, was used to activate hydroxyl groups to create reactive cyanate esters, which were subsequently conjugated to ligands containing amine functional groups to form isourea bond [209]. Hydroxyl groups (OH) have pKas of approximately 15-16 and do not react spontaneously with CNBr. As such, a strong base is required to transform the stable hydroxyl groups into more reactive alkoxide ions (O^-). These alkoxide ions are more nucleophilic and able to react with CNBr. However, strong base rapidly hydrolyzed both CNBr and the resulting active cyanate esters to inert carbamates, resulting in a lesser amount of active intermediates to efficiently form a conjugate.

In 1982 Kohn and Wilchek investigated the formation of cyanate esters on resins [210]. It was determined that instead of increasing the nucleophilicity of the hydroxyl groups on the resins, the electrophilicity of CNBr could be enhanced to react directly with the resin's hydroxyl groups to yield a "cyano-transfer" reagent. This could be achieved by introducing triethylamine (TEA) which reacts with CNBr to form *N*-cyanotriethylammonium (CTEA) which is more electrophilic than CNBr and is, therefore, more susceptible to attack by the hydroxyl functional groups reaction (Figure 6.5 and 6.6) [211]. In addition to this, the reaction can take place at neutral pH avoiding the inactivation of the active intermediates.

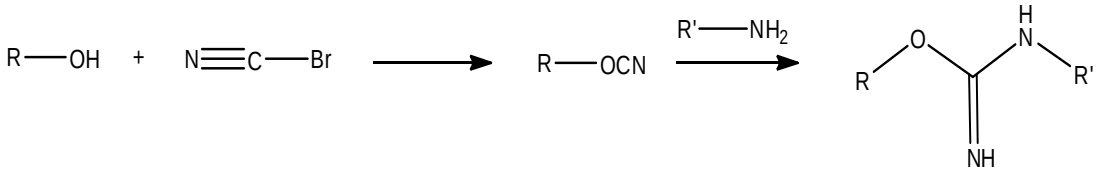

Figure 6.5: Schematic of the hydroxyl group reaction with CNBr and coupling with an amine group of the carrier protein [209].

Figure 6.6: Formation of an N-cyanotriethylammonium bromide (CTEA) intermediate [210].

Although the *N*-cyanotriethylammonium bromide intermediate, in Figure 6.6 was shown to be a suitable alternative to CNBr, it was found to be hazardous, unstable and decayed at -10 ºC [210]. However, replacing the bromide counter ion with a non-nucleophilic ion such as perchlorate (ClO^{-4}) or tetrafluoroborate (BF^{-4}), allowed the intermediates obtained to remain as a stable, crystalline compound. A tetrafluoroborate such as 1-cyano-4-methylaminopyridinium tetrafluoroborate (CDAP) salt, Figure 6.7, was first synthesized by Wakselman and Guibe-Jampel in 1976 [212], however, it was not considered until 1983 when Kohn et al. used the salt to activate a resin consisting of galactose and anhydrogalactose repeating units [210]. Substituting CNBr for CDAP showed an increase in the activation levels of the resin from 15% with CTEA to over 50% with CDAP, compared to between 1 - 2% using the traditional CNBr activation process with NaOH [210].

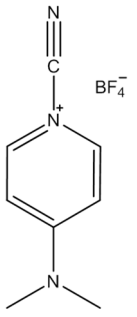

Figure 6.7: Molecular structure of CDAP [210].

The mechanism of CDAP activation in shown in Figure 6.8. The amino group on the protein reacts with the cyano-ester of CDAP-activated polysaccharides to form an unstable and reversible isourea which rearranges to a stable carbodiimide. Triethylamine is added to the reaction to quench the acid formed.

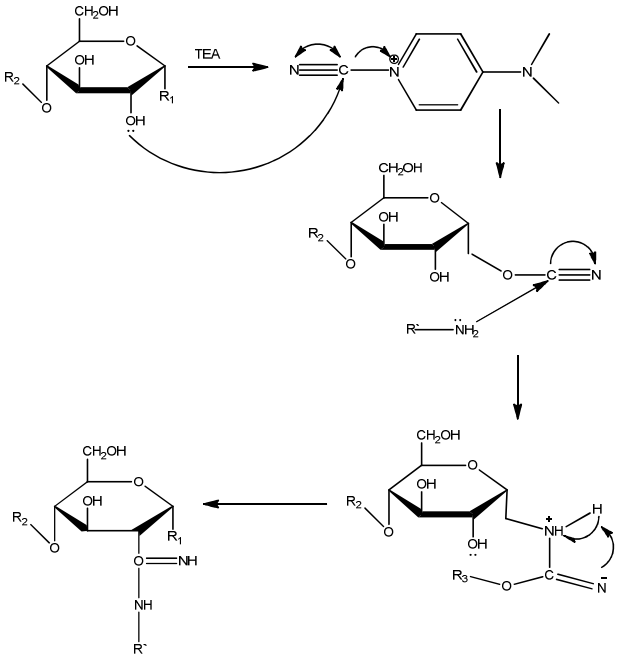

Figure 6.8: Activation of Pn19A hydroxyl group with CDAP and conjugated to TT as the carrier protein**.**

CDAP activation occurs at a much lower pH of 5.5 than that of the traditional CNBr-activation of pH 8.5, thus allowing polysaccharides sensitive to alkaline conditions to be activated. CDAP has been used to activate a broad range of polysaccharides that can either be used with or without a spacer molecule. The activation with CDAP is rapid, as 85% of the activation is achieved within 5 seconds and only 120 seconds is needed for the reaction to proceed to completion. In contrast activation with CNBr takes between 3 - 6 minutes. The lower pH and shorter reaction times have been thought to reduce the amount of inter- and intra- chain crosslinking of the polysaccharides hydroxyl groups [213]. The differences between the two cyanylating reagents are summarized in Table 6.1.

Table 6.1: Differences between CNBr and CDAP [213].

CNBr	**CDAP**
High pH (pH 11)	Low pH (pH 7-10)
Cheap but shipping issues	Expensive but no shipping issues
Toxic	Non-toxic
Forms cyanate esters on CPS hydroxyls	Forms cyanate esters on CPS hydroxyls – fewer modifications of CPS, ability to directly couple protein to CPS
Due to high pH unsuitable for alkaline-sensitive CPS	Ideal pH for alkaline-sensitive CPS
Longer reaction time	Shorter reaction time
Low activation yields	High activation yields

Andrew Lees et al. (1996) [213] examined various conditions for activating polysaccharides with CDAP and conjugating them to the carrier protein Bovine Serum Albumin (BSA), with or without a spacer

molecule. The activation of the polysaccharide in water or saline proceeded with the slow addition of CDAP in acetonitrile [213]. The slow addition was required as a rapid addition of an organic co-solvent would result in the polysaccharide precipitating out. The activation was complete within 30 seconds and the reaction pH was raised with 0.2 M TEA. Either the derivatization reagent or the protein was subsequently added 2 min 30 sec after the CDAP introduction. The reaction proceeded for at least an hour before ethanolamine was added to quench the reaction. Activations with and without the addition of TEA were examined and was shown that the degree of derivatization was reduced by 97% in the absence of TEA. Lees et al. also investigated whether the TEA was essential for the activation or whether it simply acted as a weak base [213]. Inorganic buffers, including sodium borate and carbonate, as well as NaOH were substituted for TEA to raise the pH after the CDAP activation and it was shown that as long as the pH was maintained in the basic region of the pH spectrum (pH 7 - 10), even a simple inorganic base could replace TEA [213].

Lees applied the CDAP approach to pneumococcal polysaccharide serotypes 6, 14, 19 and 23. All four of these serotypes had different pH optima for maximum activation levels. Pneumococcal type 6B with a phosphodiester linkage required the highest pH at pH 10. Lees et al. showed that the concentrations of CDAP and the polysaccharide, as well as pH, influential in the conjugation procedure [213]. This CDAP conjugation strategy was used in 2008 by Suarez et al. to conjugate pneumococcal type 14 to BSA [214]. The conjugate was first dissolved in a sodium borate buffer at pH 9.0, CDAP dissolved in a solution of acetone and water was then added and the activation was left to process for 5 min. The pH was decreased to 8.3 before the addition of protein. Three different carrier proteins: BSA, tetanus toxoid (TT) and pneumolysin (PLD) were each dissolved in a carbonate buffer at pH 8.3 before being added to the activated polysaccharide. An excess amount of TT and BSA were added to ensure sufficient nucleophilic groups were available for conjugation but a very small amount of PLD was used as it has a lower solubility than the other two proteins at the required pH. The reaction was left to proceed at room temperature for 8 hours before being quenched with a Tris-HCl buffer.

In summary, the purpose of this study was to establish a proof of concept that a conjugation method for anionic polysaccharides such as Pn19F and Pn19A was achievable and the relative stability of the Pn19F and Pn19A conjugates determined. To this end, CDAP chemistry was investigated further as the conjugate chemistry of choice. In addition, the conjugates prepared were stored at a specific temperature and tested at numerous time points to determine their relative stability.

6.2 Methods

6.2.1 In situ CPS activation

The first step in the CDAP conjugation process is the in situ activation of CPS with CDAP. The intermediate product is unstable and cannot be isolated. In order to measure the degree of activation, the activated intermediate was first coupled to ADH and monitored via SEC-HPLC. The degree of activation is confirmed by the TNBS assay which determines the presence of hydrazides in solution. The SEC-HPLC chromatogram shown in Figure 6.9 demonstrates a slight shift in retention time between the full length, unactivated Pn19F CPS (red) at 13.101 min and activated Pn19F

polysaccharide (blue) at 13.207 min. This shift indicates Pn19F is activated by CDAP to a spacer ADH (Figure 6.9) and confirmed by the TNBS assay (data not shown).

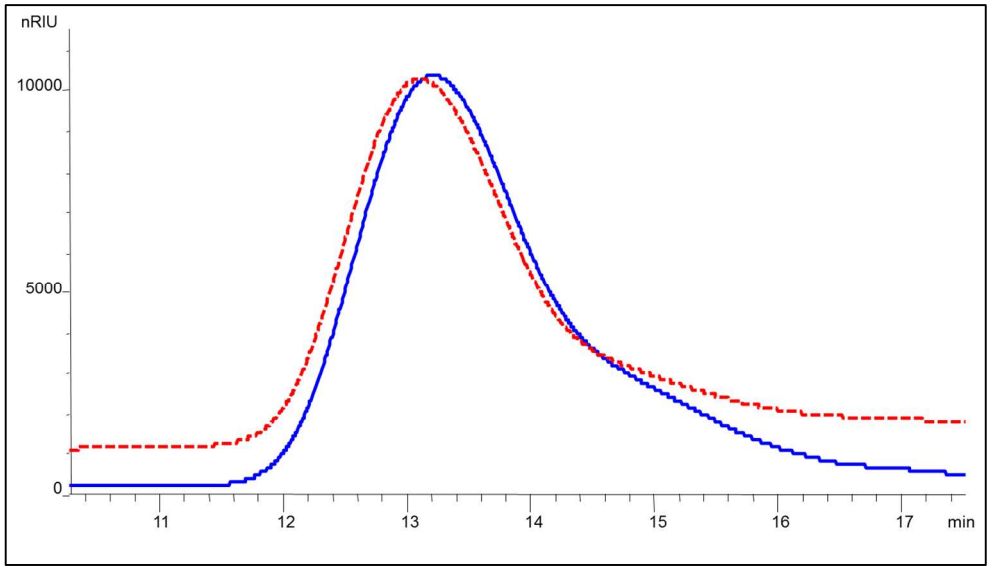

Figure 6.9: SEC-HPLC RID chromatograms of 2.5 mg/mL full length 19F (red) and 19F_CDAP_ADH (blue) using Shodex 805/804 in series, 10 mM PBS buffer pH 6.8, injection volume of 50 µL with flow rate of 1 mL/min.

6.2.2 Carrier proteins in conjugate vaccines and protein derivatization

To date there are at least five carrier proteins currently in use in the preparation of conjugates (Figure 6.10). These include TT, Diphtheria Toxoid (DT), cross-reacting material 197 (CRM_{197}), a non-toxic mutant of diphtheria toxin, protein D derived from non-typeable *H. influenzae* and the outer membrane protein complex (OMPC) derived from *N. meningitides* [215]. From a purely physicochemical perspective, size was a possible differentiating factor for most common carrier proteins. DT and CRM_{197} are diphtheria toxoid-based and are roughly the same size (62 kDa). TT is 150 kDa in size, 2.25 times larger than DT and CRM_{197} [216].

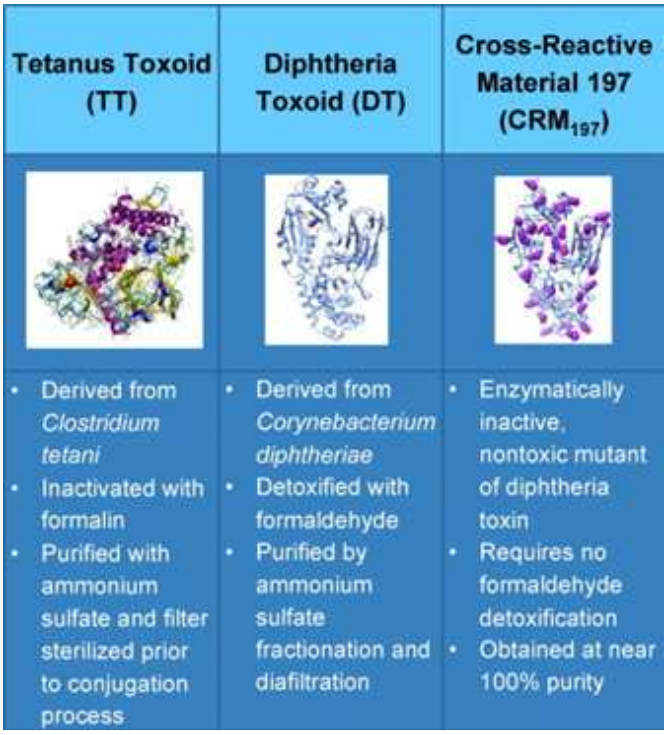

Figure 6.10: Carrier proteins used in *Haemophilus influenzae b*, *Neisseria meningitides*, and *Streptococcus pneumoniae* conjugate vaccines [216].

Carrier proteins that have been commonly used for *S. pneumoniae* include DT and TT and BSA. During this study BSA, which is readily available and cost-effective was used as a model carrier protein to develop a proof of concept before the chemistry was applied to TT.

6.2.2.1 Protein derivatization of BSA and TT

BSA has a molecular weight of 67 kDa and is a highly soluble protein containing numerous functional groups suitable for conjugation. BSA possesses a total of 59 lysine Ɛ-amine groups with only 30-35 of these available for derivatization [107]. TT (MW of 150 kDa) has 160 carboxyl groups, (from aspartic and glutamic acids) that are available for derivatization with ADH. Hydrazide derivatization is achieved by first activating the carboxyl groups with the water-soluble ethyl-dimethylaminopropyl-carbodiimide (EDC) and this activated complex undergoes nucleophilic attack by ADH to form an acid hydrazide (-$CONHNH_2$). To minimize reaction of the activated carboxyls with lysine residues on the protein resulting in internal cross-linking of the protein and denaturation, the reaction is conducted at a pH of 6.0, below the pKa for lysine, and with a large excess of ADH. BSA was used as a model protein for this proof of concept study to demonstrate the application of CDAP chemistry to the conjugation of CPS to a carrier protein.

The method used to derivatize BSA as described in Chapter 2, Section 2.9.7 involved the use of 0.5 g protein in 0.1 M MES at pH 6.0 to which 1.2 g ADH and 0.125 g EDC in water was added and incubated at room temperature (RT) for 4 h. Upon completion, the derivatized protein was diafiltered to remove excess ADH and unreacted EDC using a 10 kDa Pellicon membrane in 30 mM NaCl/ 5 mM Na_2CO_3 buffer and then concentrated to a working volume of 100 mL, at a concentration of approximately 5

mg/mL. An in-process TNBS assay (as described in Chapter 2, Section 2.9.7.1) was performed to track the removal of excess ADH in solution. With a hydrazide concentration of 0.0672, a 9% carboxylic acid substitution (9% activation of protein) was observed for the derivatized BSA. The SEC-HPLC chromatogram (Figure 6.11) showed a shift in retention time for the derivatized BSA from 18.036 min for the underivatized protein to 18.776 min. It is noted that the shift in retention time indicates the presence of a smaller molecular weight molecule compared to the starting material. It is hypothesized that the free hydrazide group from the ADH molecule interacted with the polyhydroxymethacrylate stationary phase of the column, resulting in prolonged interaction and retention on the column, and hence a shift in apparent lower molecular weight was observed [108].

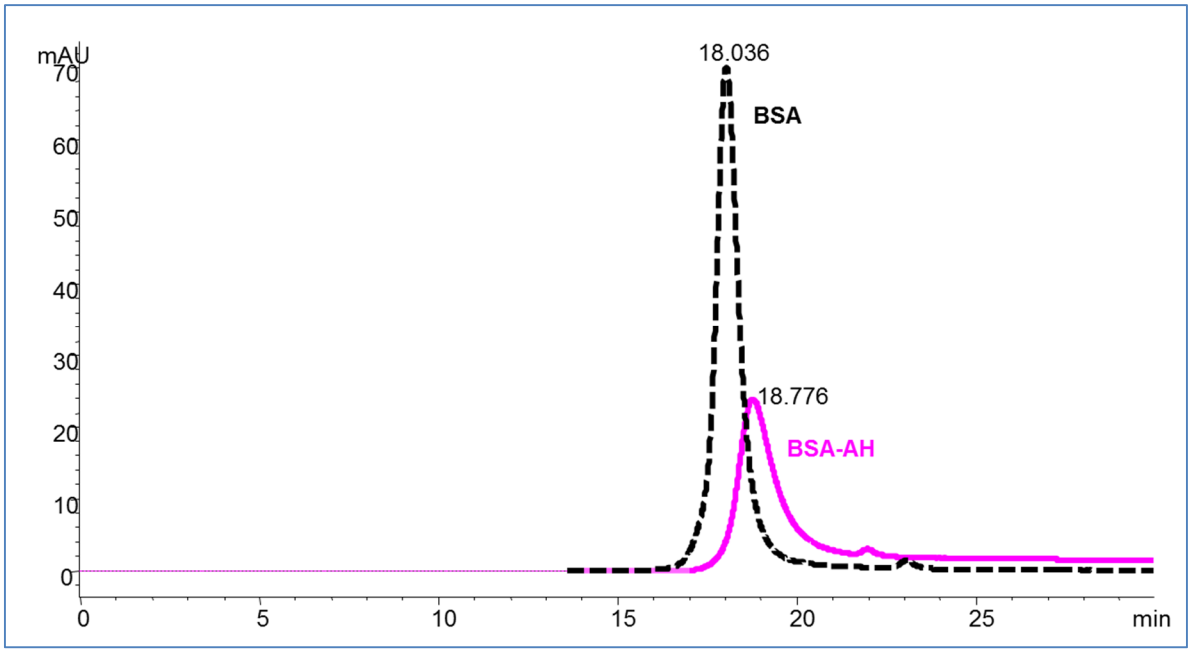

Figure 6.11: SEC–HPLC-UV 280 nm chromatogram of BSA (black) and derivatized BSA (pink).

The methodology described with the BSA reaction was then applied to TT. The TNBS assay for derivatized TT showed TT derivatization levels of 18% as well as a shift in MW observed by SEC-HPLC. Figure 6.12 represents a SEC-HPLC chromatogram of TT before and after activation. As for the BSA derivatization, a shift in retention time was observed to an apparent smaller molecular weight.

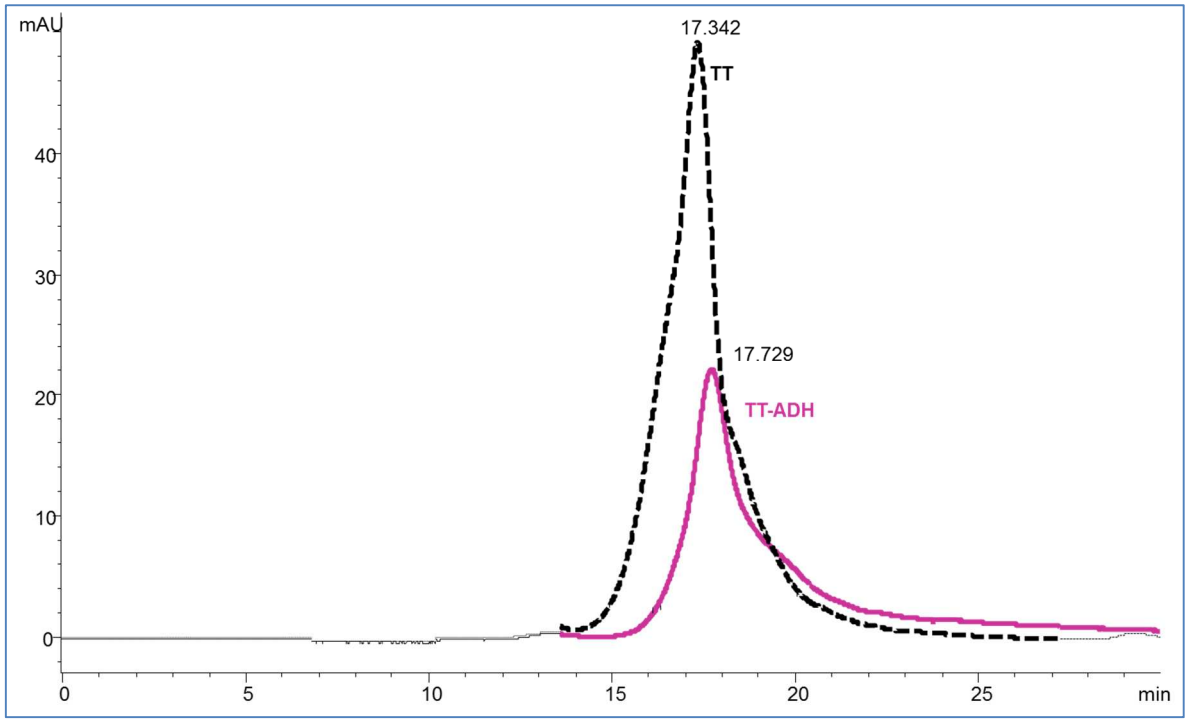

Figure 6.12: SEC–HPLC-UV 280 nm chromatograms of TT (black) and derivatized TT (pink).

6.3 Conjugation of carrier proteins to CPS

Various parameters for both the activation and conjugation processes were investigated. These included:

- Concentration of the polysaccharide solution.
- Concentration of carrier protein solution.
- Mass ratio of polysaccharide to protein in the reaction.
- Temperature of reaction.
- Full-length polysaccharide compared to size-reduced polysaccharide.
- Buffers used in the activation of polysaccharide and derivatization of protein.
- Volumes of reagents and buffers.
- Scale of reaction.

6.3.1 CPS:Bovine serum albumin (BSA) conjugates

The conjugation methodology was first established using BSA and then adapted for TT. All the experiments were performed on a small scale as a proof of concept and full-length 19F and size reduced 19F and 19A CPS were activated and coupled directly to BSA. The experimental parameters and reaction variables are summarized in Table 6.2. Ten conjugation reactions were performed of which nine were performed at 2 – 8 ºC and one at RT. The ratios of CPS: protein, CPS size and buffers were all tested to determine the optimal conjugation conditions.

Table 6.2: CPS and BSA variables for reactions employing CDAP chemistry at 2 – 8 ºC.

Reaction no.	CPS	CPS:Protein mg	Size (KDa)	Ratio of CPS:Protein	CPS Buffer	Protein Buffer	CDAP (mg)/mmol	0.2 M TEA (µL)/mmol	Quench with Glycine(mmol)
1	19F	25:25	1000	1:1	NaCl	Water	37.5/0.16	750/0.15	0.160
2	19F	25:12.5	1000	2:1	NaCl	Water	37.5/0.16	750/0.15	0.160
3	19A	25:12.5	96	2:1	Water	Water	18.75/0.08	375/0.075	0.053
4	19A	25:12.5	115	2:1	Water	Water	18.75/0.08	375/0.075	0.053
5	19A	25:12.5	96	2:1	NaCl	Water	18.75/0.08	375/0.075	0.090
6	19A	25:12.5	96	2:1	NaCl	Water	18.75/0.08	375/0.075	0.084
7	19F	25:12.5	115	2:1	NaCl	Water	18.75/0.08	375/0.075	0.084
8	19A	25:12.5	65	2:1	NaCl	MES	18.75/0.08	375/0.075	0.084
9	19A	25:8.3	65	3:1	NaCl	MES	18.75/0.08	375/0.075	0.084
*10	19A	25:8.3	65	3:1	NaCl	MES	18.75/0.08	375/0.075	0.084

*reaction 10 performed at RT

The SEC-HPLC chromatograms for reactions 2 using Pn19F and 8 using Pn19A (Table 6.2) are shown in Figures 6.13 (UV detector), 6.14 (RID detector) and 6.15 (expansion of the Pn19A conjugate chromatogram shown in Figure 6.13) are representative of a conjugation reaction between size-reduced CPS and ADH-activated BSA. The conjugates were first dialyzed and purified before SEC-HPLC. It can be seen using the UV chromatogram (Figure 6.13) that, while there is evidence of conjugate formation, not all of the protein was consumed during the reaction as a peak corresponding to unreacted protein was present. The presence of the peaks observed at UV 280 nm indicates the presence of free protein and therefore ratios of CPS to protein should be adjusted. At the same time, BSA buffers and activation were investigated.

This process was optimized and after the parameters tested for the BSA conjugates was concluded that the reaction at 2 - 8 ºC with a CPS to protein ratio of 2:1, with derivatized BSA in MES buffer and size reduced CPS in NaCl buffer would be optimum for this conjugate set up and should be used when constructing TT conjugates (reaction 8 in Table 6.2). No further purification besides dialysis or further analysis was conducted on this conjugate as the purpose of the model conjugate was to gather information and observe the HPLC outputs which assisted in identifying the size and presence of the CPS and conjugate as part of this proof of concept study.

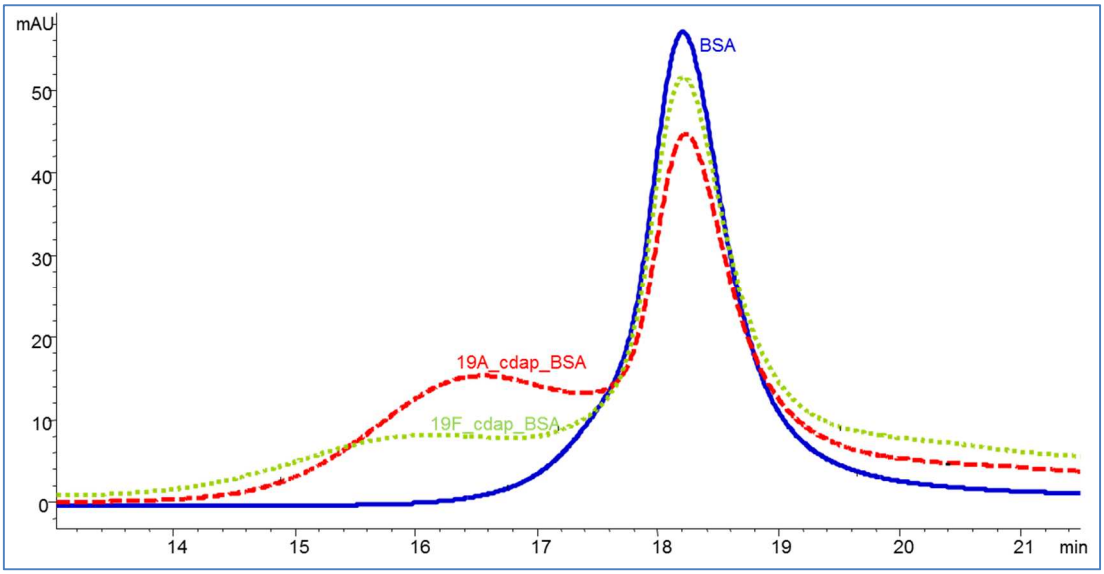

Figure 6.13: SEC-HPLC UV 280 nm chromatograms of 19F_CDAP_BSA-AH (green representing reaction 2), 19A_CDAP_BSA-AH (red representing reaction 8) and BSA (blue). Shodex 805/804 in series, 10 mM PBS buffer pH 6.8, the injection volume of 50 µL, flow rate 1 mL/min. Conjugation reaction between activated CPS and BSA analyzed by SEC-HPLC. Detection at 280 nm (mAU).

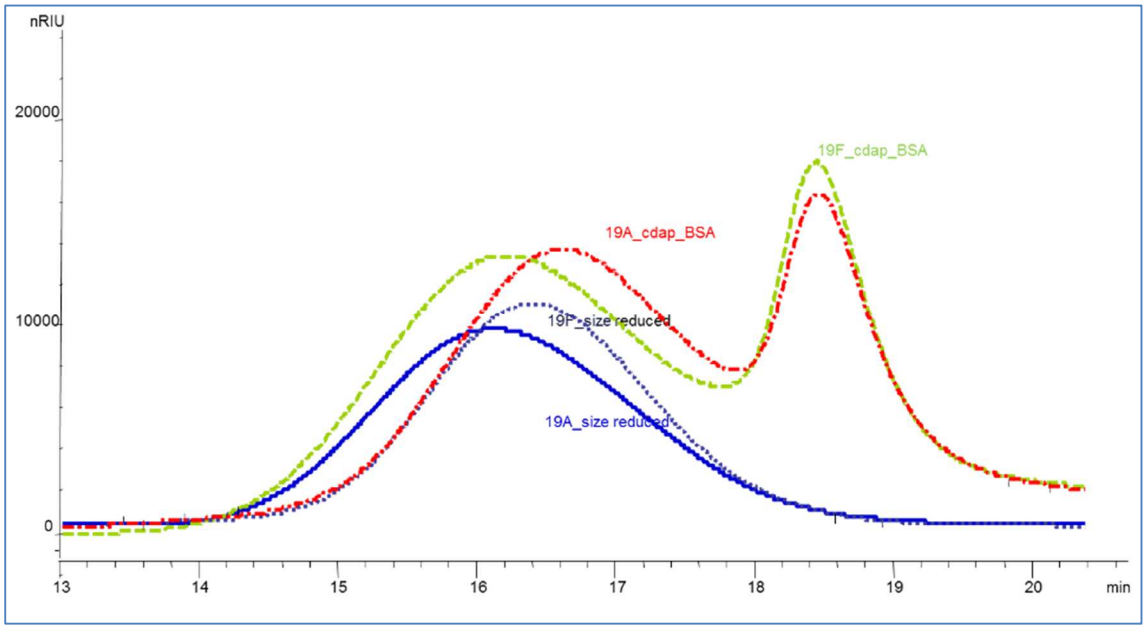

Figure 6.14: SEC-HPLC RID chromatograms of size reduced 19F (2.5 mg/mL – dark blue) and 19A (blue).CDAP activated Pn19F (green representing reaction 2) and Pn19A (red representing reaction 8) using Shodex 805/804 in series, 10 mM PBS buffer pH 6.8, the injection volume of 50 µL, flow rate 1 mL/min.

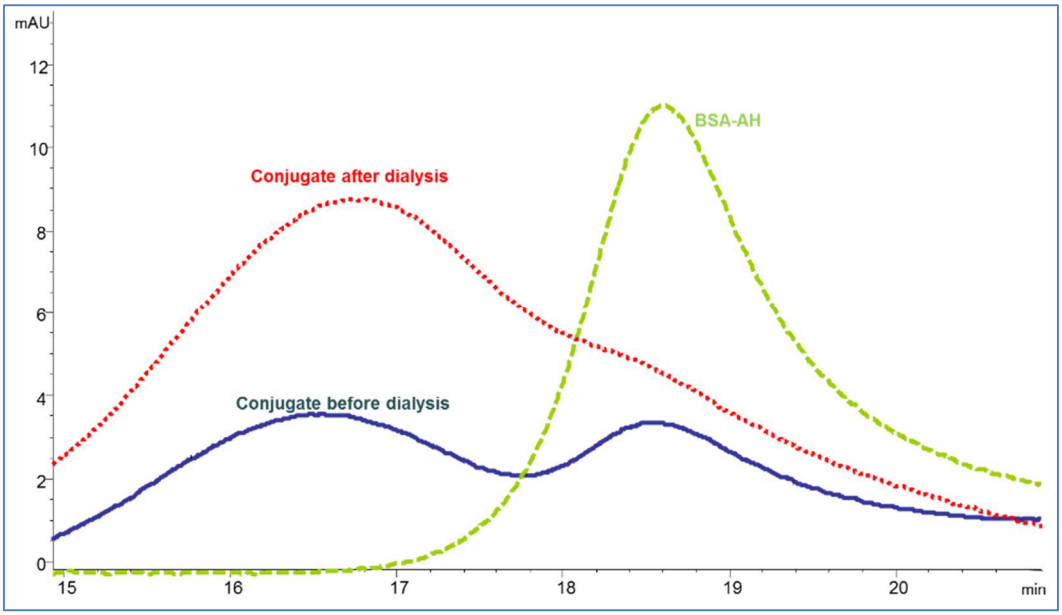

Figure 6.15: SEC-HPLC UV 280 nm chromatograms of Pn19A conjugated to BSA (reaction 8) before (red) and after (blue) dialysis. Shodex 805/804 in series, 10 mM PBS buffer pH 6.8, the injection volume of 50 µL, flow rate 1 mL/min. Derivatized BSA is shown in green.

6.3.2 CPS:Tetanus toxoid (TT) conjugates

As with BSA derivatization, TT was activated using ADH and EDC and conjugate to size reduced Pn19F and Pn19A to form Pn19F/ Pn19A: TT-ADH conjugates. The experimental design included both the polysaccharide and protein concentrations at varied ratio of CPS to protein as well as the amounts of buffers and reagents used in small scale to larger scale experiments (Table 6.3). The CPS buffer remained the same throughout the study whereas for the protein two buffers were investigated namely; water and 1M MES pH 5.5 and both gave similar results. MES according to the literature is the buffer of choice for TT and suited protein derivatization [85]. Two temperature ranges were investigated namely; 2 – 8 ºC and 18 – 22 ºC where both were found to be suitable for this conjugation method. The preferred temperature range for BSA was 2 – 8 ºC and for TT 18 – 22 ºC (RT).

Table 6.3: CPS and TT variables employing CDAP chemistry.

Reaction no.	CPS	CPS:Protein mg	Size (KDa)	Ratio of CPS:Protein	CDAP (mg)/mmol	0.2 M TEA (µL)/mmol	Temp ℃	Quench with Glycine(mmol)
1	19A	25:12.5	65	2:1	18.75/0.08	375/0.075	2-8	0.084
2	19A	25:12.5	65	2:1	18.75/0.08	375/0.075	2-8	0.084
3	19A	25:12.5	65	2:1	18.75/0.08	375/0.075	RT	0.084
4	19A	40:10	65	4:1	30.5/0.13	610/0.0122	RT	0.128
5	19A	25:12.5	65	2:1	18.75/0.08	375/0.075	RT	0.084
6	19F	25:12.5	115	2:1	18.75/0.08	375/0.075	RT	0.084
7	19A	150:37.5	65	4:1	225/0.96	4500/0.9	RT	0.96
8	19F	150:37.5	115	4:1	225/0.96	4500/0.9	RT	0.96
9	19F	100:50	115	2:1	75/0.32	1500/0.3	RT	0.32
10	19A	100:50	65	2:1	75/0.32	1500/0.3	RT	0.32
11	19A	200:100	65	2:1	150/0.64	3000/0.6	RT	0.64
12	19F	200:100	115	2:1	150/0.64	3000/0.6	RT	0.64

Reactions 11 and 12 from Table 6.3 were the conjugates used for the stability study and results presented in this section. Conjugate formation was tracked using the SEC-HPLC UV 280 nm signal as shown in Figure 6.16. The formation of a peak of higher molecular weight than that of the derivatized protein, indicative of the formation of a conjugate was observed by the shift in retention time. As for SEC-HPLC, bigger MW compounds are eluted first. The conjugates were first dialyzed and purified before SEC-HPLC. The RID signals for both size reduced polysaccharide and conjugates were shown in Figure 6.17.

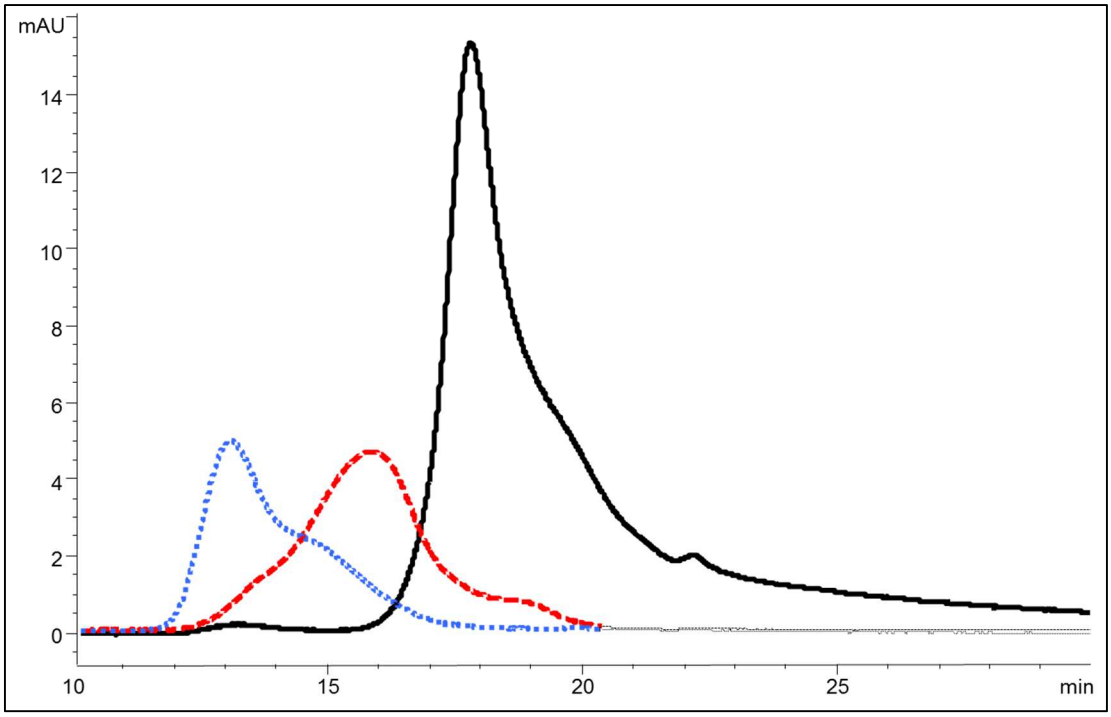

Figure 6.16: SEC-HPLC UV 280 nm chromatograms of TT-ADH (black), Pn19F (blue representing reaction 12 in Table 6.3) and Pn19A (red representing reaction 11 in Table 6.3) conjugates after dialysis Shodex 805/804 in series,10 mM PBS buffer pH 6.8, injection volume = 50 µL, flow rate 1 mL/min.

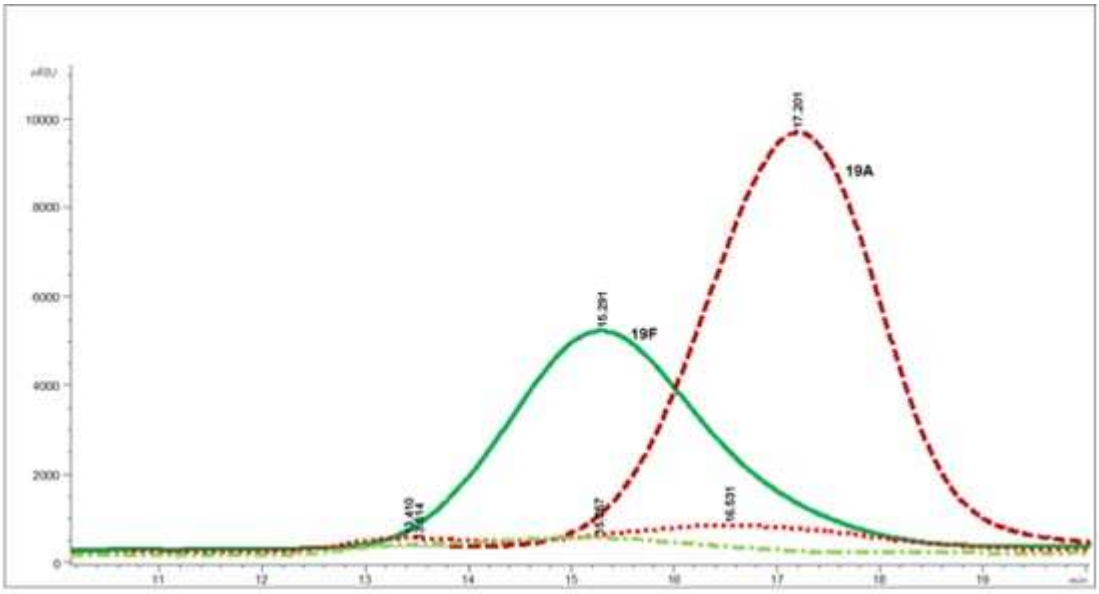

Figure 6.17: SEC-HPLC RID chromatograms of Pn19F CPS (dark green), Pn19A CPS (dark red), Pn19F (green) and Pn19A (red) conjugates after dialysis Shodex 805/804 in series,10mM PBS buffer pH 6.8, injection volume = 50 µL, flow rate 1 mL/min.

Proof of conjugation was established by the shift in retention (elution) time demonstrating an increase in the size of the carrier protein and the polysaccharide or both on SEC-HPLC. SEC-HPLC is an analytical tool that allows for monitoring of the conjugates before and after dialysis and assists in determining a shift in molecular size between polysaccharide, carrier protein and conjugate. It also shows concentration differences between samples. The main objective in these experiments using SEC-HPLC was to monitor the presence of polysaccharides and conjugates.

6.3.3 Purification of conjugates using ammonium sulfate

Upon completion of Pn19F and Pn19A conjugation, purification of the conjugates is performed to remove unreacted (unbound) polysaccharide, carrier protein and other impurities. The removal of these by-products is necessary in order to prevent an immune response to the by-product and not the conjugate in-vivo. There are many purification procedures used for the removal of free saccharide but for the purpose of this study, a simple, quick and efficient procedure was employed whereby the protein, and hence the conjugate, was precipitated from the solution under high salt concentrations, leaving the unconjugated CPS in solution [217].

To determine the efficiency of purification of the conjugates, in-house criteria of 5% or less of the unbound CPS must be present in the supernatant after purification. The unbound CPS is determined using the sodium deoxycholate (DOC) assay to separate the unbound CPS from bound CPS followed by the anthrone assay to determine the concentration of the unbound CPS. These assays are explained in detail in Chapter 2. The starting free saccharide concentration was slightly higher than the in-house criteria of 5% but because this was a proof of concept study to determine conjugation efficiency and stability, the data was normalized to determine the trend of steady increase in free saccharide over time depending on the storage conditions.

Table 6.4. Analytical assay results of saccharide and protein content.

Serotype	Total CPS (mg)	Free CPS (mg)	Total protein (mg)	CPS:Protein ratio	Conjugation efficiency (%)
19F	39	0.08	10	0.4:1	20
19A	30	0.01	10	0.2:1	15

The conjugation efficiency (Table 6.4) was calculated by taking the final result of the conjugated polysaccharide (39 mg 19F and 30 mg 19A) as a percentage of the total polysaccharide that underwent ammonium sulfate precipitation (200 mg). Due to the loss of polysaccharide and protein during the concentration step, this conjugation efficiency could potentially be a lot higher.

The purification method employed during this study was the use of ammonium sulfate, a highly saturated salt which is commonly used to purify proteins by altering the solubility of the proteins [218]. Salting out is a selective precipitation method that under higher salt concentrations tends to decrease protein solubility which leads to precipitation of the protein [219]. The amount of ammonium sulfate was based on previously studies performed on Pn6B and Hib at Biovac. After one fractionation a large amount of unbound CPS is observed and therefore a second ammonium sulfate precipitation is required (data not shown). The key indicator of the stability of the conjugate is the percentage unbound CPS (free saccharide). The conjugates after two ammonium sulfate fractionation steps are shown in Figures 6.18 and 6.19. The presence of a conjugate for both Pn19F (AT026) and Pn19A (AT025) was observed at UV280nm. Both conjugates presented as dimers indicating the presence of the conjugate. The protein shift is more to the right of the conjugate which is more to the left indicating that it is a bigger MW molecule. The method involved using a portion of the conjugate formed, concentrating it down to a gel like solution and adding approximately two volumes of ammonium sulfate. The mixture was stirred and left to precipitate overnight at 2 – 8 ℃. This mixture was centrifuged to pellet out the conjugate and the clear ammonium sulfate supernatant was discarded. This pelleted conjugate was subjected to a second round of precipitation before being reconstituted in PBS buffer (pH 7.2) and colorimetric analysis for protein as well as free and unconjugated saccharide was performed.
The conjugation efficiency as shown in Table 6.4 corresponds to the conjugates presented by SEC-HPLC in that the ratio of protein to conjugate after conjugation was lower for Pn19A than Pn19F which could demonstrates better binding of TT to Pn19F than to Pn19A CPS.

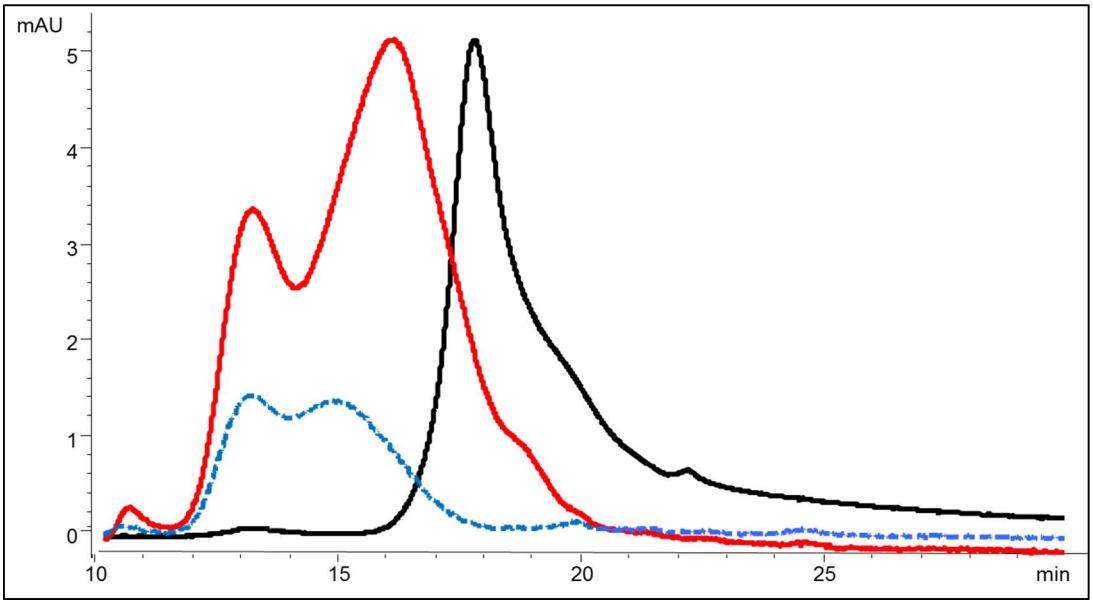

Figure 6.18: SEC-HPLC UV 280nm chromatograms of TT-ADH (black), Pn19F (blue) conjugates and Pn19A (red) conjugates after purification using ammonium sulfate, Shodex 805/804 in series, 10 mM PBS buffer pH 6.8, the injection volume of 50 µL, flow rate 1 mL/min. The void volume is at 10 min and the total volume is at 20 min.

The RID signals of the two conjugates shown in Figure 6.19 shows the presence of a dimer which indicated the presence of free saccharide and conjugates. The first peak is the free saccharide and the second larger peak is the conjugate indicating that the starting material has free saccharide present. The free saccharide peak as observed in Figure 6.19 elutes at a retention time of about 13 min and the dimer present in Figure 6.18 has a retention time spread across 11 – 20 min. The free polysaccharides results are discussed in the stability section as it is closely monitored and falls within the required literature values of less than 20%. These conjugates represent day zero of the stability study.

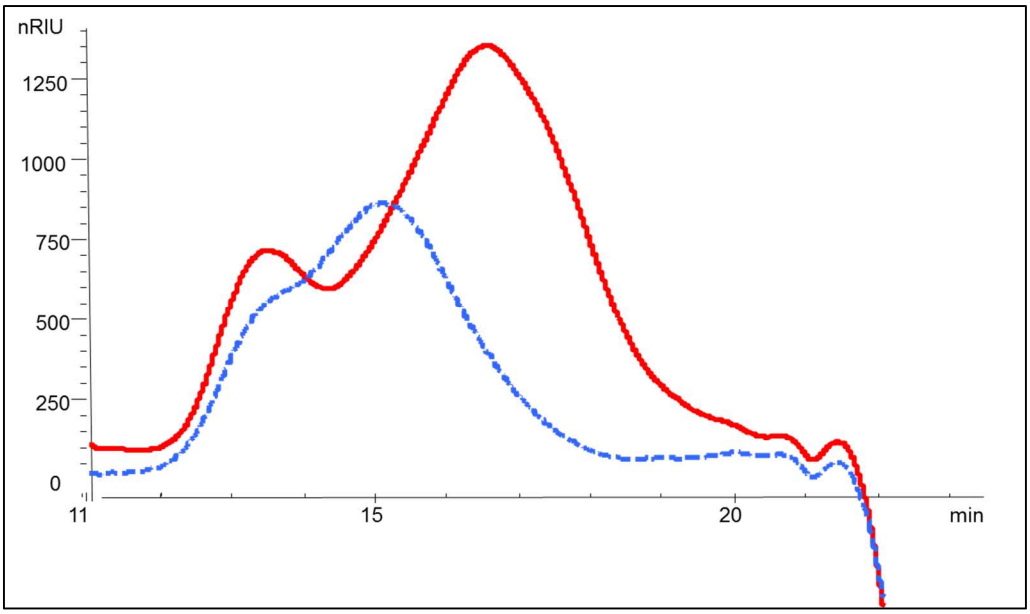

Figure 6.19: SEC-HPLC RID chromatograms of Pn19F (blue) and Pn19A (red) conjugates after purification using ammonium sulfate, Shodex 805/804 in series, 10 mM PBS buffer pH 6.8, the injection volume of 50 µL, flow rate 1 mL/min. The void volume is at 10 min and the total volume is at 20 min.

Another method to demonstrate conjugate formation is determining the presence of either protein or polysaccharide by SDS-PAGE. In general conjugated species either do not enter the gel or appear as high MW smears compared to the focused bands observed for unconjugated proteins or CPS [37]. This method allows for the analysis of unconjugated protein (using a Coomassie stain) or polysaccharide (using a PAS stain).

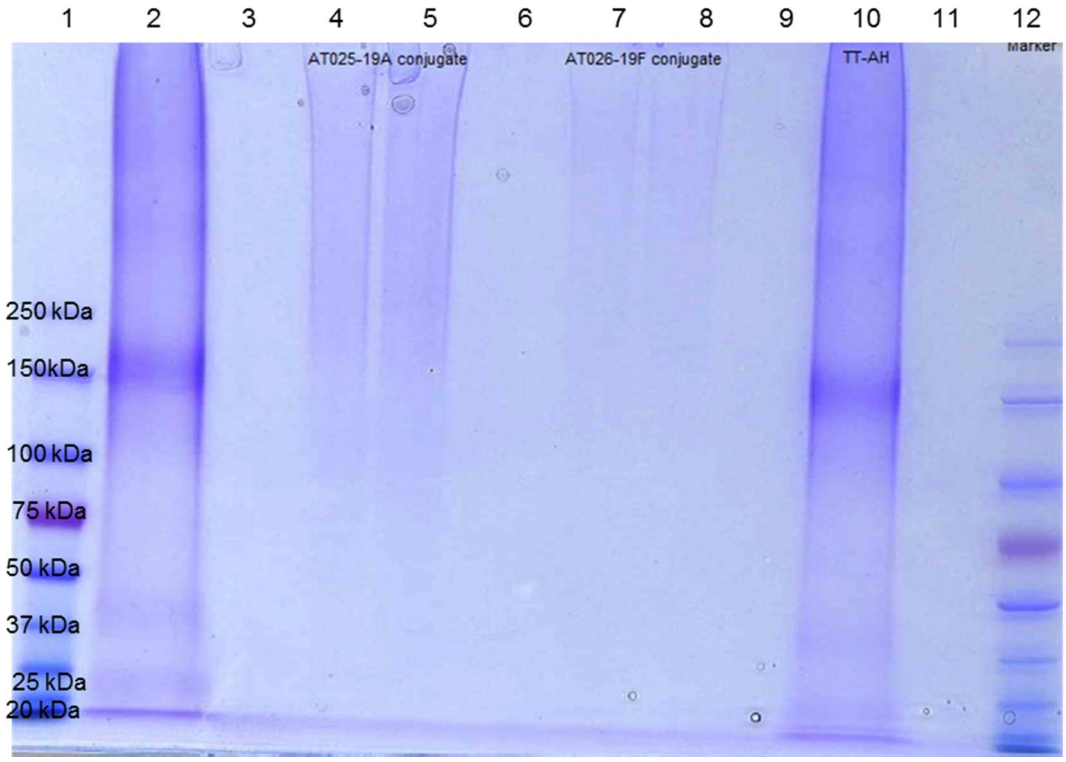

Figure 6.20: SDS-PAGE gel of Pn19F and Pn19A conjugates – reducing gel with Coomassie stain. Lane 1 and 12 contains precision all blue marker, lanes 2 and 10 shows the derivatized TT (positive control), lane 4 contains Pn19A conjugate in native form, lane 5 contains Pn19A conjugate reduced due to SDS, Lane 7 contains Pn19F conjugate in native form and lane 8 contains Pn19F conjugate reduce due to SDS.

The Coomassie stain shown in Figure 6.20 is used to identify the presence of protein in the samples; Lanes 1 and 12 are precision all blue markers, lanes 2 and 10 contain TT as a positive control; lanes 4 and 5, shows the Pn19A conjugates and lanes 7 and 8 contains the Pn19F conjugates. Lanes 3, 6, 9 and 11 were not utilized. The presence of the conjugates at the top of the well indicates that these conjugates are high in MW as shown by the MW marker bands of 250 kDa. The conjugates are polydispersed in MW indicated by the band smears from the top of the well. These high MW molecules are indicative of the polysaccharide-protein conjugate present. Based on the gel in Figure 6.20, it is demonstrated that all protein is conjugated the CPS. The yields of the conjugates were not calculated as the proof of concept of this study was to investigate the presence of the conjugates rather than the quantity of the conjugates. The purification of the conjugates posed a problem for Pn19F and Pn19A for both size exclusion chromatography and ammonium sulfate fractionation. Between the two methods, ammonium sulfate precipitation was more likely to yield greater results and was investigated in the laboratory.

6.4 Stability of Pn19F and Pn19A conjugates

The relative stability of the pneumococcal conjugate vaccines is expected to be based on the intrinsic stability of the polysaccharide, modulated by the conjugation chemistry and conjugate structure [101]. Pneumococcal serotypes 19F and 19A polysaccharides are chemically similar as they are linear copolymers that differ at one linkage point. Pn19A CPS was not included in the PCV7 vaccine as it was anticipated that the immunological similarities of vaccine serotype 19F would elicit cross-protection [220, 221]. This, however, was not the case and Pn19A was later included in PCV13 in 2010 [222].

It is proposed that Pn19A CPS is more labile towards hydrolysis than Pn19F CPS because the free hydroxyl on C-2 on the rhamnose on the repeating unit of serotype 19A (Na^+ salt) can participate in dephosphorylation of the anomeric phosphodiester [53]. The proposed mechanism of Pn19F and Pn19A CPS hydrolysis as illustrated in Figures 6.21 and 6.22.

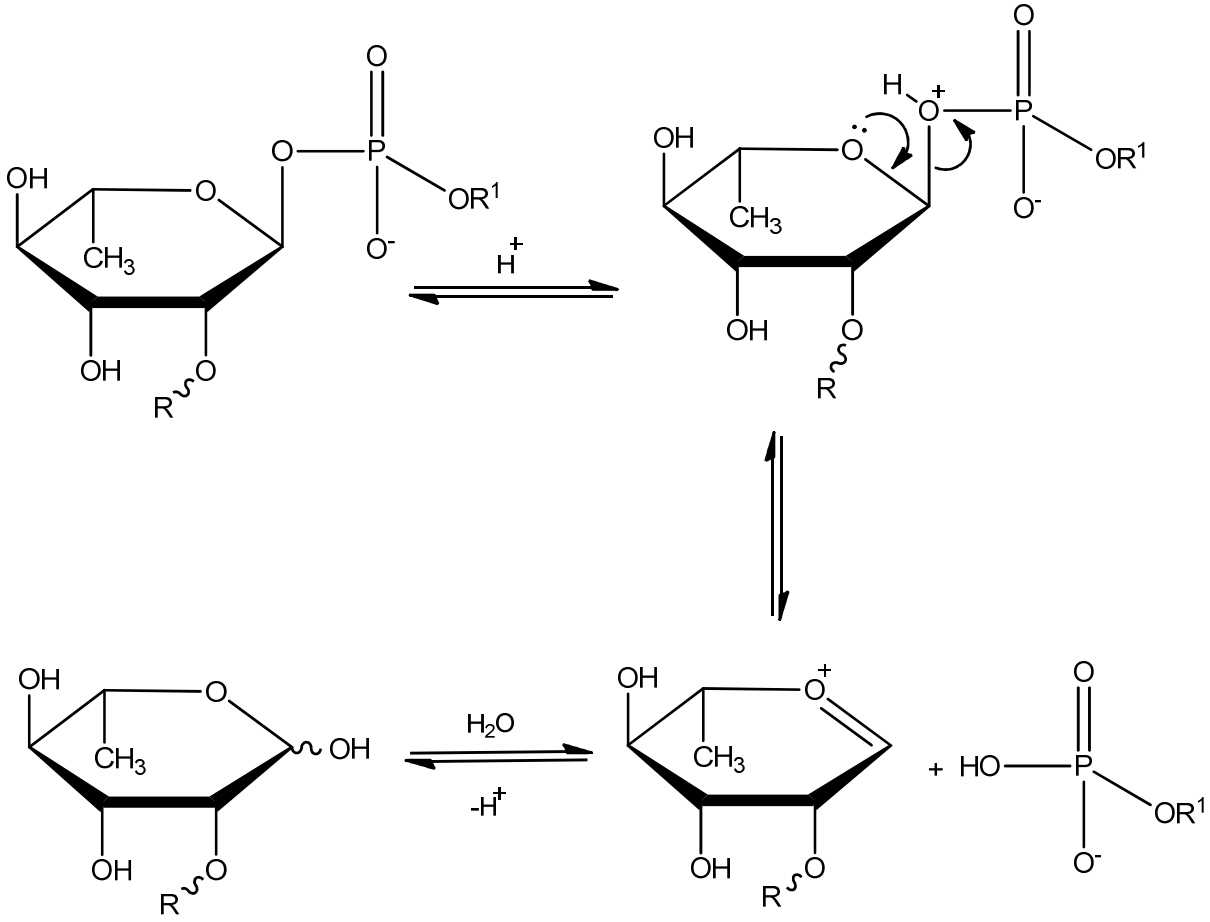

Figure 6.21: Pn19F repeating unit showing hydrolysis of the rhamnose-phosphate bond. R, R^1 represents the chain from Glc and ManAc respectively.

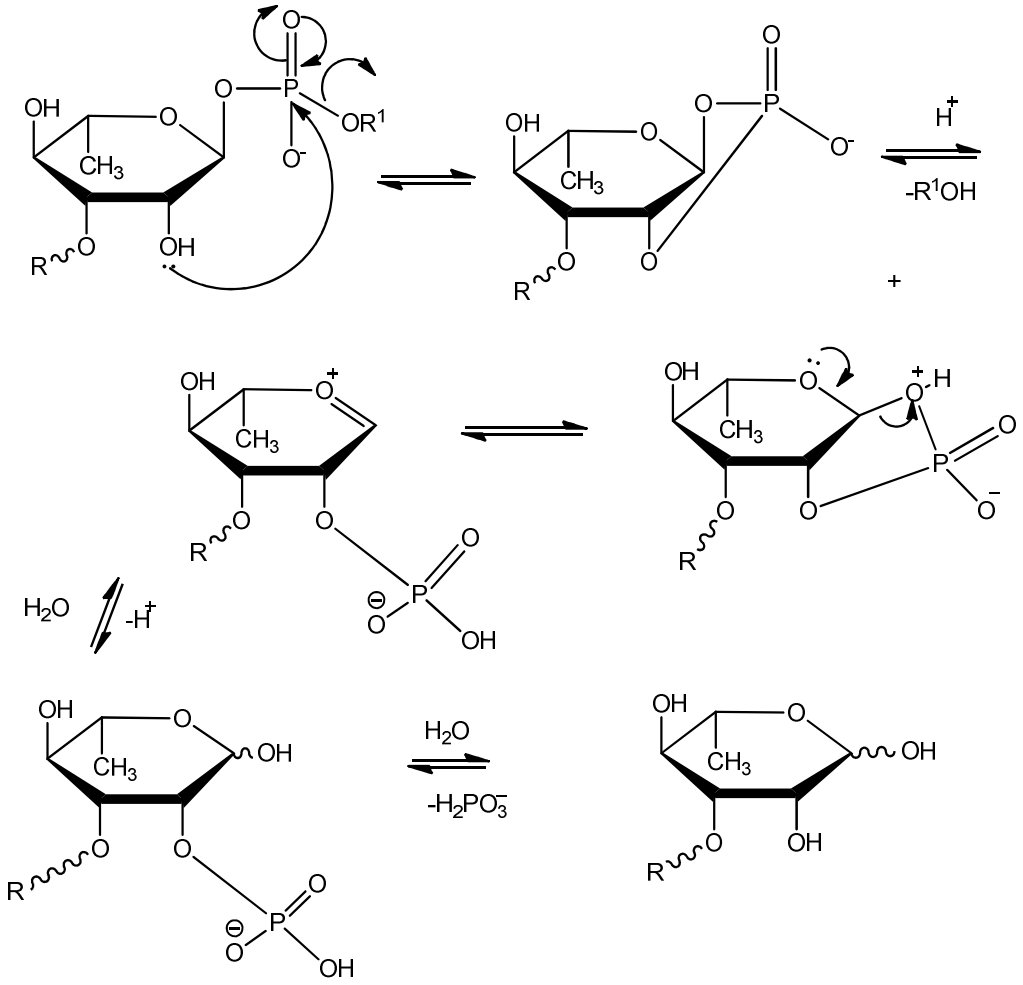

Figure 6.22: Pn19A repeating unit showing C2 hydroxyl-assisted hydrolysis of the phosphodiester linkage. R, R^1 represents the chain from Glc and ManAc respectively.

The aim of this stability study was to determine if the differences in the inherent stability of Pn19A and Pn19F could be detected in the conjugate bulks. In order to determine this, the effect of exposure to various storage temperatures over a period of 8 weeks was monitored weekly by colorimetric assays and chromatographic techniques. The colorimetric assays included anthrone and DOC assay for total and free polysaccharide content estimations, UV at 279 nm for protein estimations and SEC-HPLC for size distribution and molecular integrity of the conjugates and to a lesser extent NMR for structural information of protein and polysaccharide content. Immunoassays such as SDS-PAGE confirmed the presence of the conjugate and protein integrity at the start and end of the study. Monitoring of protein for denaturation and CPS for free polysaccharide aids in determining the integrity and stability of the conjugates.

This study was also performed as a proof of concept study to determine whether CDAP chemistry could be used in the preparation of liquid stable Pn19F and Pn19A: TT conjugates at temperatures of 2 - 8 ºC, 25 ºC and 37 ºC. This stability study was carried out on bulk conjugates only.

6.4.1 Methods

The liquid bulk conjugate was dispensed into 10 mL light blue polycarbonate containers with silicone lined polypropylene closures and incubated at 2 - 8 ºC, 25 ºC and 37 ºC. The stability protocol (Table 6.5) included the assays conducted during this study, the storage temperatures and time interval for testing of each conjugate.

Table 6.5: Temperature, time and tests performed weekly during this study.

Temperature	Time	Tests
37 ºC	6 weeks	Anthrone, DOC/Anthrone, UV, SDS-PAGE, HPLC, NMR
25 ºC	8 weeks	Anthrone, DOC/Anthrone, UV, SDS-PAGE, HPLC, NMR
2 - 8 ºC	8 weeks	Anthrone, DOC/Anthrone, UV, SDS-PAGE, HPLC, NMR

The assays performed during these experiments included anthrone (quantification), anthrone/DOC (free saccharide analysis), HPLC (size distribution), SDS-PAGE (size) and NMR (identity). The first (week 0) and final week (week 6 or 8) of the study included the full battery of tests whereas the weeks in between were limited to; anthrone, DOC/anthrone, UV, and HPLC.

6.4.2 Pn19F and Pn19A conjugate at 2 - 8 ºC

At the time of conjugate preparation, the conjugates presented with an initial free saccharide concentration. In order to compare the stability of the conjugates the data was normalized by subtracting the free sugar concentration obtained at time of preparation from the free sugar concentration at each time point. Normalized data for both conjugates presented in Figure 6.23 and Table 6.6. This study was performed at 2 - 8 ºC for 8 weeks. The real-time data was high confirming that the initial start concentrations for some conjugates would skew the interpretation of the results (data not shown).

Table 6.6: Pn19F and Pn19A conjugate at 2 - 8 ºC.

	Pn19F			Pn19A		
	0	**4**	**8**	**0**	**4**	**8**
Total CPS (mg/mL)	1.35	1.13	1.12	0.91	0.74	0.91
% Free CPS	0	5.95	3.33	0	5.46	2.33
Protein (mg/mL)	3.04	2.60	1.53	4.90	4.14	3.98

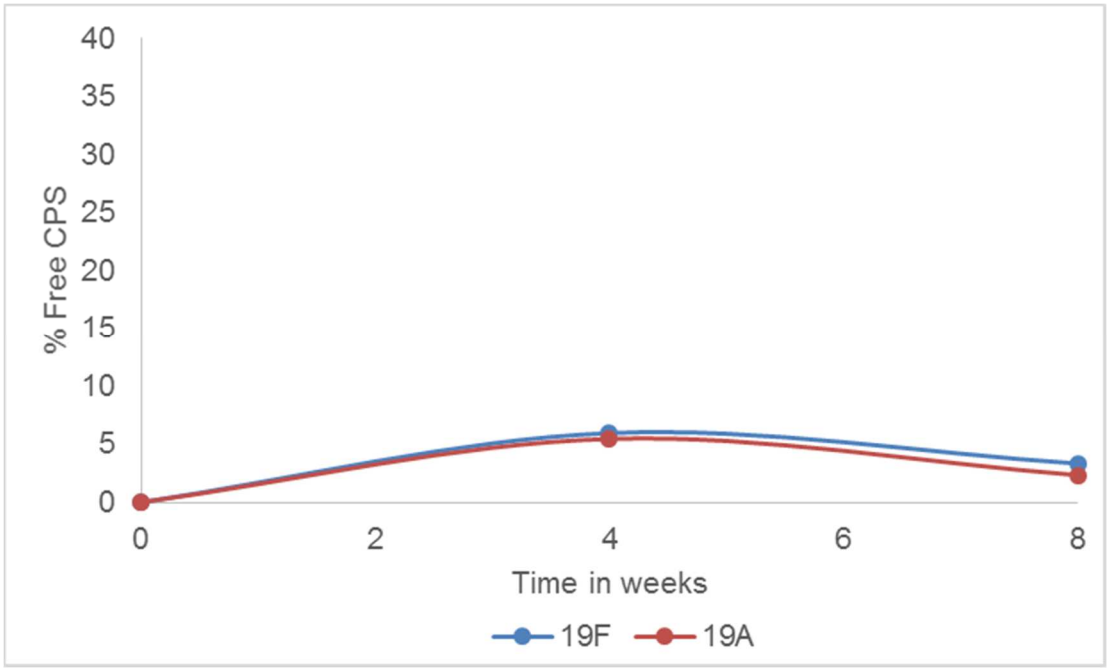

Figure 6.23: Pn19F and Pn19A conjugate over the course of 8 weeks period monitoring the percentage free saccharide at 2 - 8 ºC determined using the DOC/anthrone colorimetric assay.

After 8 weeks, the percentage free polysaccharide was below the WHO specifications of 20% [74]. The total polysaccharide concentration was 0.7 – 1.4 mg/mL and the protein concentration was 1.4 - 5 mg/mL for both Pn19F and Pn19A conjugates at 2 - 8 ℃ comparable to week 0. From the normalized data, the Pn19F and Pn19A conjugate start and end points in terms of free saccharide were very similar as shown in Figure 6.23. SEC-HPLC profiles for each of the time intervals are shown in Figures 6.24 to 6.27.

There is however a gradual increase in free saccharide for both Pn19F and Pn19A at week 0 compared to week 8 (Figure 6.32) which is indicated by the steady increase in high MW material on the shoulder of the broad peak (Figures 6.24 – 6.27). This slight/steady increase in low MW conjugate material is indicated by the longer elution time. Week 4 results are questionable as this could possibly be an artefact. The increase in MW material and peak size is confirmation that there is an increase in conjugate degradation which is expected as storage conditions over time would influence conjugate stability. The study revealed that there was no significant difference in the stability between Pn19F and Pn19A conjugates and the steady increase in percentage free saccharide remained below 20% throughout this study.

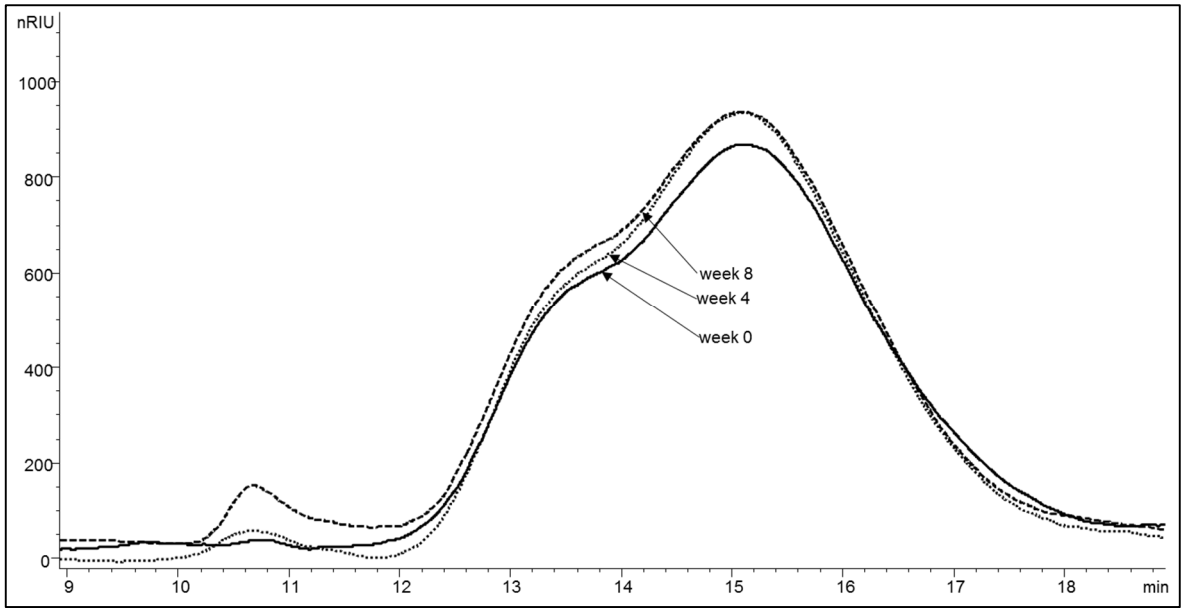

Figure 6.24: SEC-HPLC RID chromatograms of 19F_CDAP_TT in 10 mM PBS after 8 weeks at 2 - 8 ºC: Shodex 805/804 in series, PBS buffer, pH 7.0, the injection volume of 50 µL, flow rate 1 mL/min.

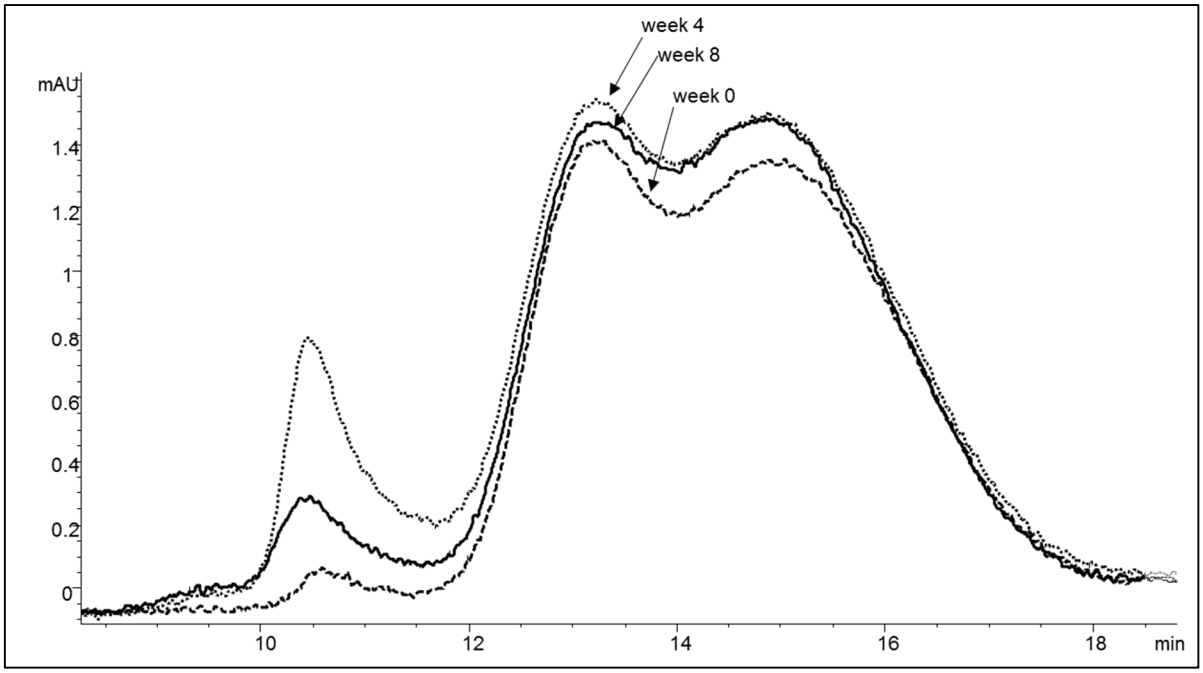

Figure 6.25: SEC-HPLC UV (280nm) chromatograms of 19F_CDAP_TT in 10 mM PBS after 8 weeks at 2 - 8 ºC: Shodex 805/804 in series, PBS buffer, pH 7.0, the injection volume of 50 µL, the flow rate 1 mL/min.

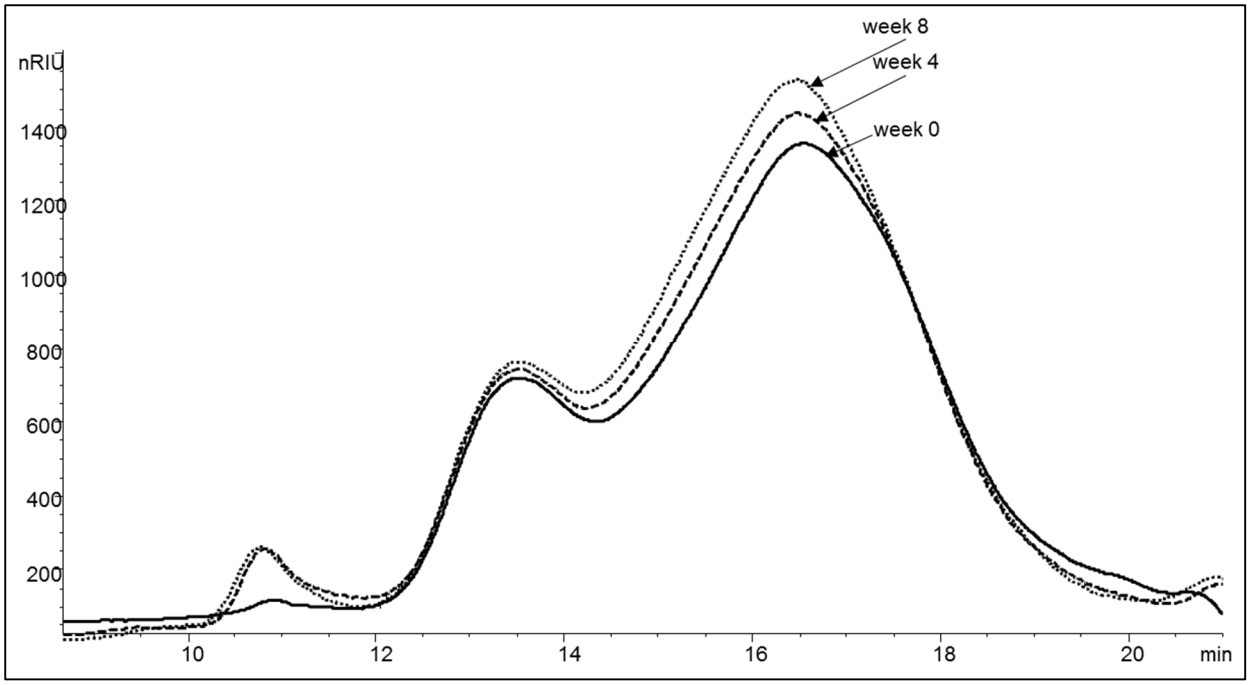

Figure 6.26: SEC-HPLC RID chromatograms of 19A_CDAP_TT in 10 mM PBS after 8 weeks at 2 - 8 ºC: Shodex 805/804 in series, PBS buffer, pH 7.0, the injection volume of 50 µL, flow rate 1 mL/min.

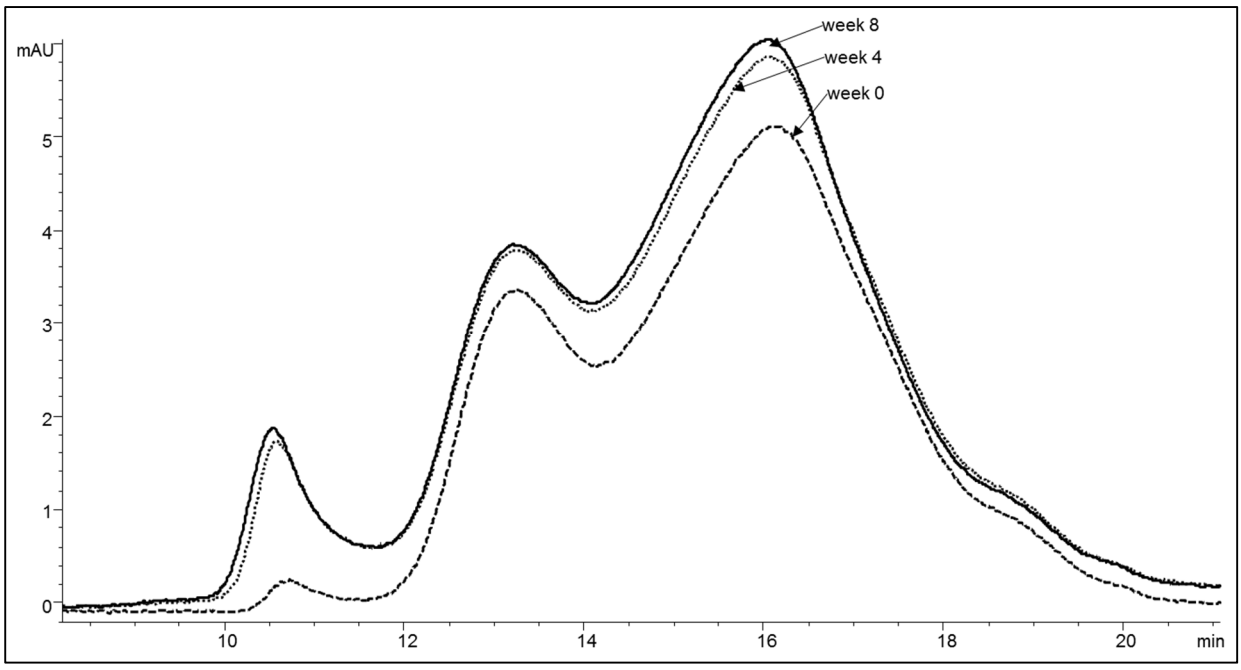

Figure 6.27: SEC-HPLC UV (280nm) chromatograms of 19A_CDAP_TT in 10 mM PBS after 8 weeks at 2 - 8 ºC: Shodex 805/804 in series, PBS buffer, pH 7.0, injection volume of 50 µL, flow rate 1 mL/min.

6.4.1 Pn19F and Pn19A at 25 ºC

In order to obtain information in a short time period, accelerated stability studies were conducted at elevated temperatures (25 ºC and 37 ºC). The results obtained during the accelerated stability studies could be used to predict the behaviour of the conjugates at the recommended storage temperature (2 – 8 ºC) assuming degradation is conserved over the entire temperature range (2 - 37 ºC) [223]. The intermediate temperature of 25 ºC between 2 - 8 ºC and 37 ºC was tested for 8 weeks. Table 6.7

summarizes the results obtained for Pn19F and Pn19A. The total polysaccharide concentration remained constant between 0.7 – 1.5 mg/mL and the protein concentration between 2 - 5 mg/mL at 25 ºC.

Table 6.7: Pn19F and Pn19A conjugates at 25 ºC.

	Pn19F					**Pn19A**				
	0	**2**	**4**	**6**	**8**	**0**	**2**	**4**	**6**	**8**
Total CPS (mg/mL)	1.35	1.32	1.16	1.20	1.45	0.91	0.88	0.73	1.17	1.03
% Free CPS	0	3.55	11.65	-0.18	8.37	1.01	0	8.19	18.93	9.34
Protein (mg/mL)	3.04	2.44	2.67	3.12	2.95	4.90	4.51	3.95	4.22	4.04

There was a gradual increase in free saccharide for both conjugates. Week 6 showed a significant increase in free saccharide for Pn19A and a significant decrease in Pn19F. This anomaly could be indicative of human error as the results returned to the normal trend at week 8 (Figure 6.28). SEC-HPLC profiles for each of the time interval were shown in Figures 6.29 - 6.32.

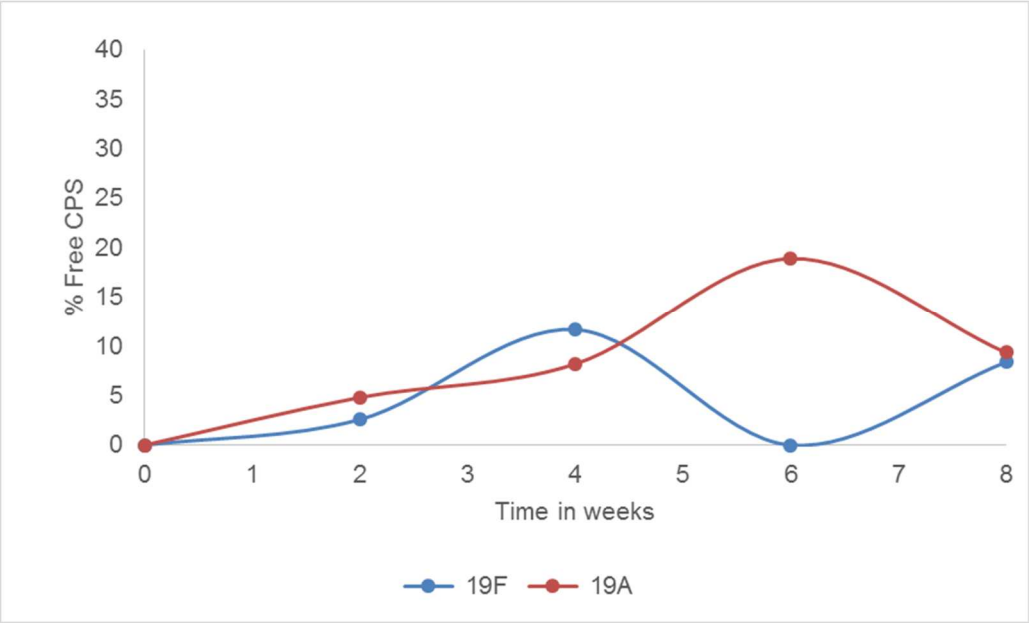

Figure 6.28: Pn19F and Pn19A conjugate over the course of 8 weeks period monitoring the percentage free polysaccharide at 25 ºC determined using the DOC/anthrone colorimetric assay.

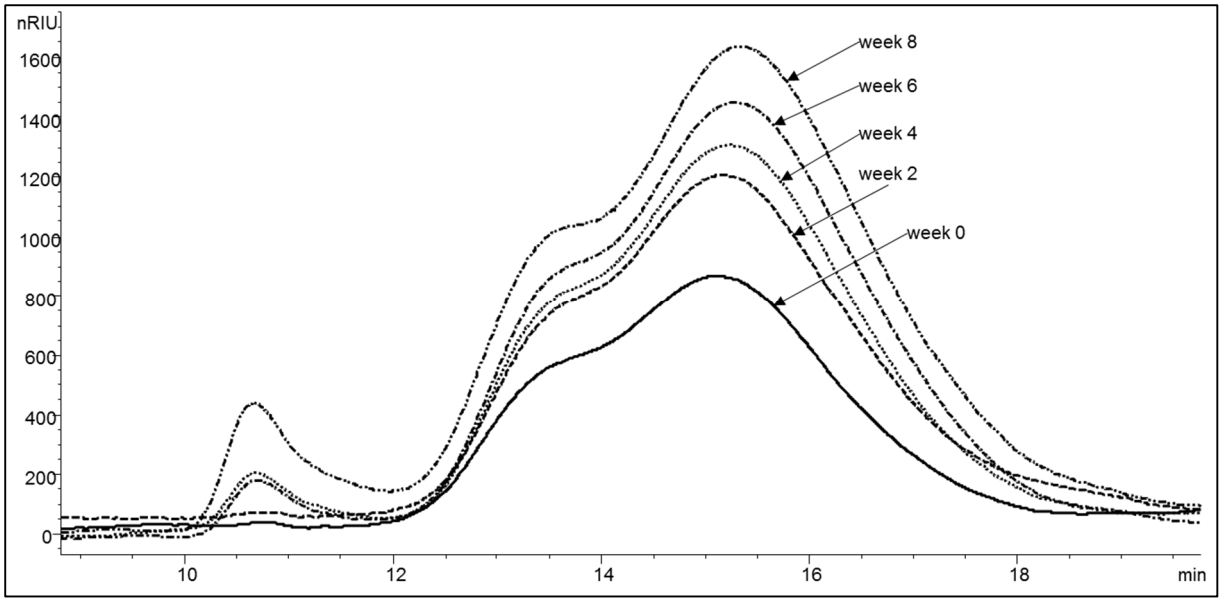

Figure 6.29: SEC-HPLC RID chromatograms of 19F_CDAP_TT in 10 mM PBS after 8 weeks at 25 ºC: Shodex 805/804 in series, PBS buffer, pH 7.0, the injection volume of 50 µL, flow rate 1 mL/min.

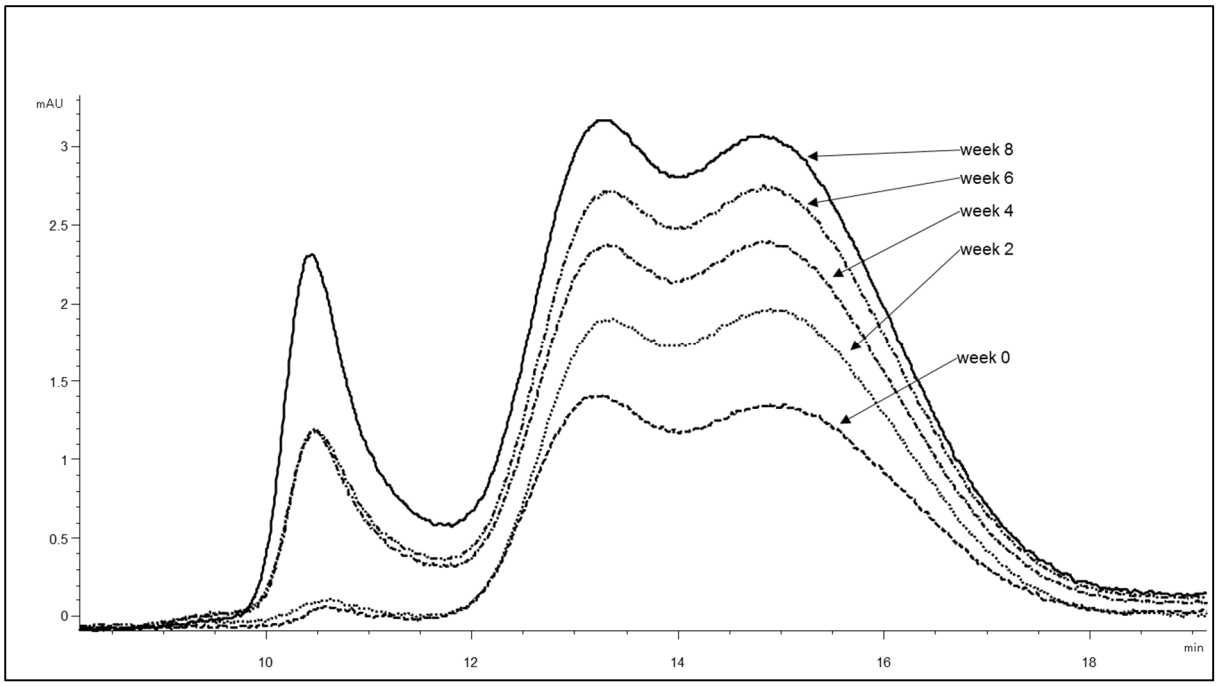

Figure 6.30: SEC-HPLC UV (280nm) chromatograms of 19F_CDAP_TT in 10 mM PBS after 8 weeks at 25 ºC: Shodex 805/804 in series, PBS buffer, pH 7.0, the injection volume of 50 µL, flow rate 1 mL/min.

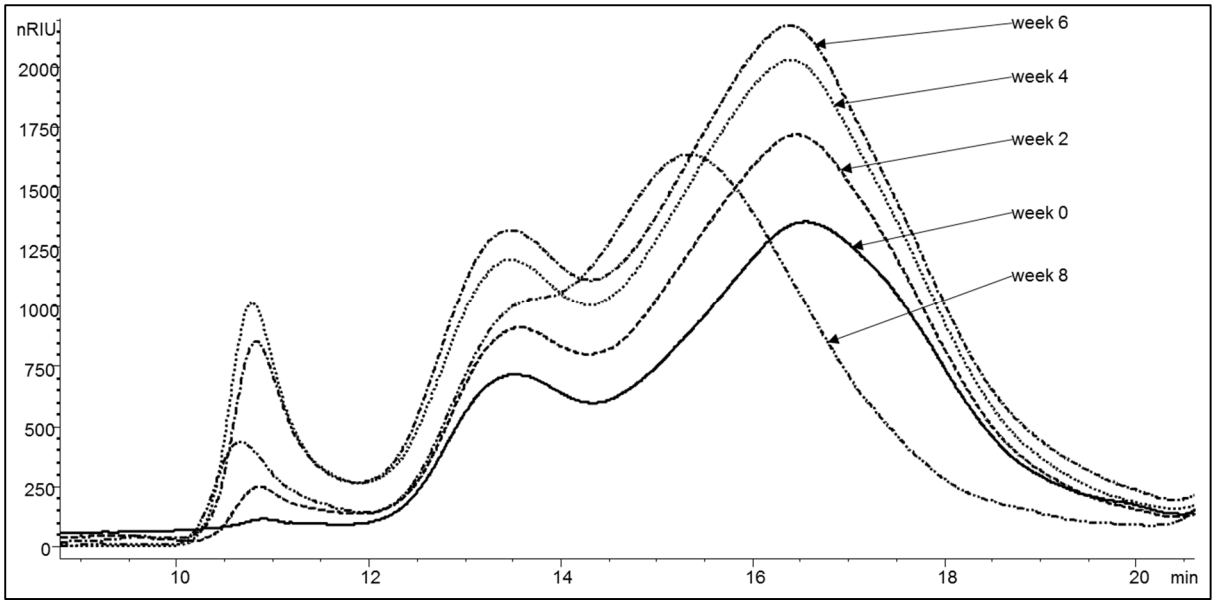

Figure 6.31: SEC-HPLC RID chromatograms of 19A_CDAP_TT in 10 mM PBS after 8 weeks at 25 ºC: Shodex 805/804 in series, PBS buffer, pH 7.0, injection volume = 50 µL, flow rate 1 mL/min.

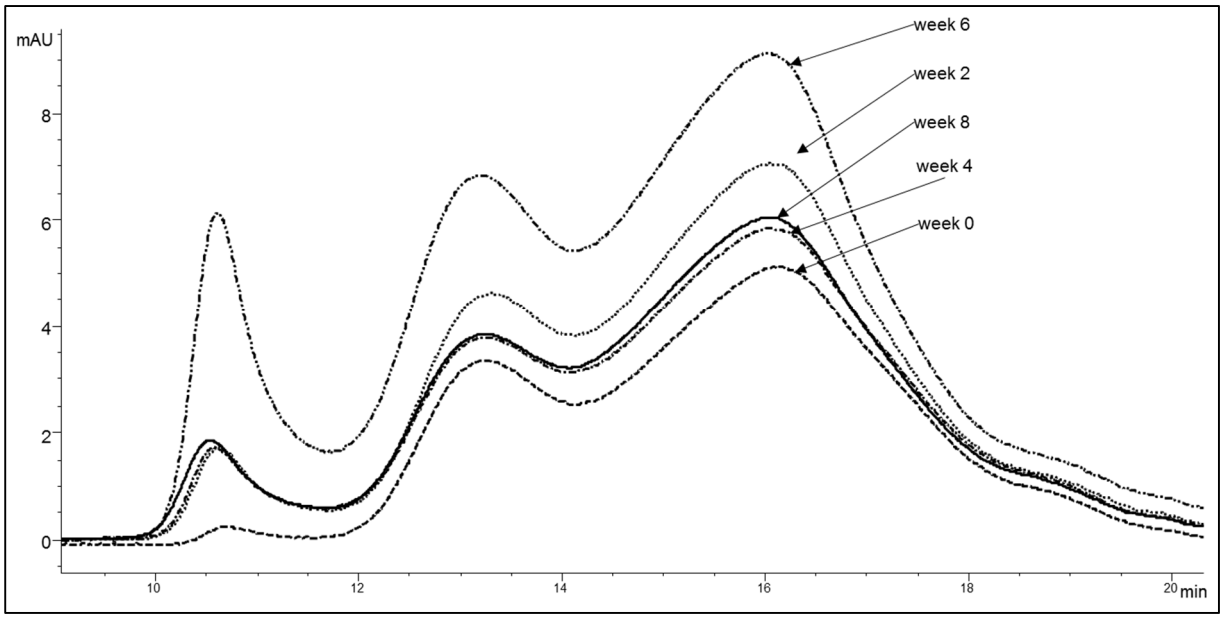

Figure 6.32: SEC-HPLC UV (280nm) chromatograms of 19A_CDAP_TT in 10 mM PBS after 8 weeks at 25 ºC: Shodex 805/804 in series, PBS buffer, pH 7.0, injection volume = 50 µL, flow rate 1 mL/min.

The SEC-HPLC clearly indicates degradation of both conjugates over the time period, with the generation of large MW material and a shift in retention time to smaller molecular weight material compared with week 0.

This degradation pattern was confirmed with the SDS-PAGE assay (Figure 6.33) of the conjugates after 8 weeks at 25 ºC with Coomassie stain emphasizing the presence of the protein. After 8 weeks at 25 ºC the smearing on the SDS-PAGE indicate a large range of MW material, and both conjugates in the native and reduced form show a large range of MW material indicating degradation had occurred when compared to the start of the study as shown in Figure 6.20.

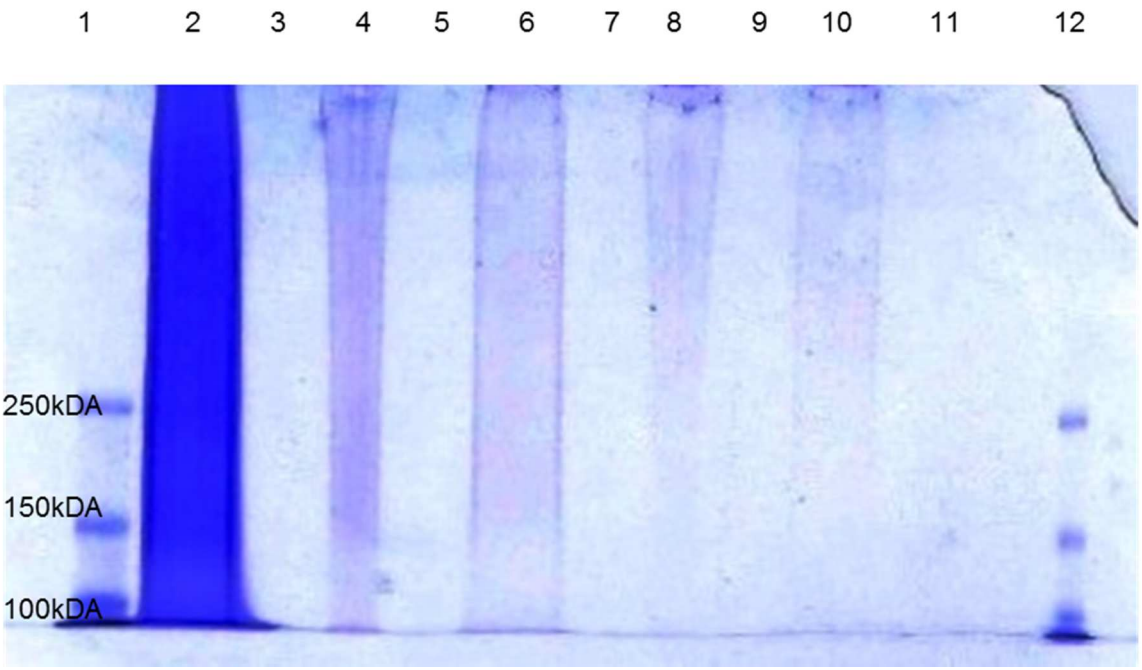

Figure 6.33: SDS-PAGE gel of Pn19F and Pn19A conjugates at 25 ℃ after 6 weeks – reducing gel with Coomassie stain. Lane 1 and 12 contains precision all blue marker, lane 2 shows the derivatized TT (positive control) lane 4 contains Pn19A conjugate in native form, lane 6 contains Pn19A conjugate reduced due to SDS, lane 8 contains Pn19F conjugate in native form and lane 10 contains Pn19F conjugate reduce due to SDS. Lanes 3, 5, 7, 9 and 11 were left clear.

6.4.2 Pn19F conjugates and Pn19A conjugates at 37 ºC

Table 6.8 summarises the results obtained during the 37 ºC stability study for both Pn19F and Pn19A conjugates. The protein and CPS concentrations remained constant for both conjugates. Marked increase in free saccharide was observed for both conjugates (Figure 6.34).

Table 6.8: Pn19F and Pn19A conjugate at 37 ºC.

	Pn19F							**Pn19A**						
	0	**1**	**2**	**3**	**4**	**5**	**6**	**0**	**1**	**2**	**3**	**4**	**5**	**6**
Total CPS (mg/mL)	1.35	1.46	1.42	1.44	1.26	1.49	1.52	0.91	0.951	0.92	0.91	0.86	0.87	0.97
% Free CPS	0	8.13	11.60	23.89	26.78	26.41	25.51	0	8.77	9.25	15.56	15.65	24.62	35.65
Protein (mg/mL)	3.04	3.25	2.39	3.02	2.62	3.10	3.03	4.90	4.36	4.12	3.82	3.65	3.89	3.89

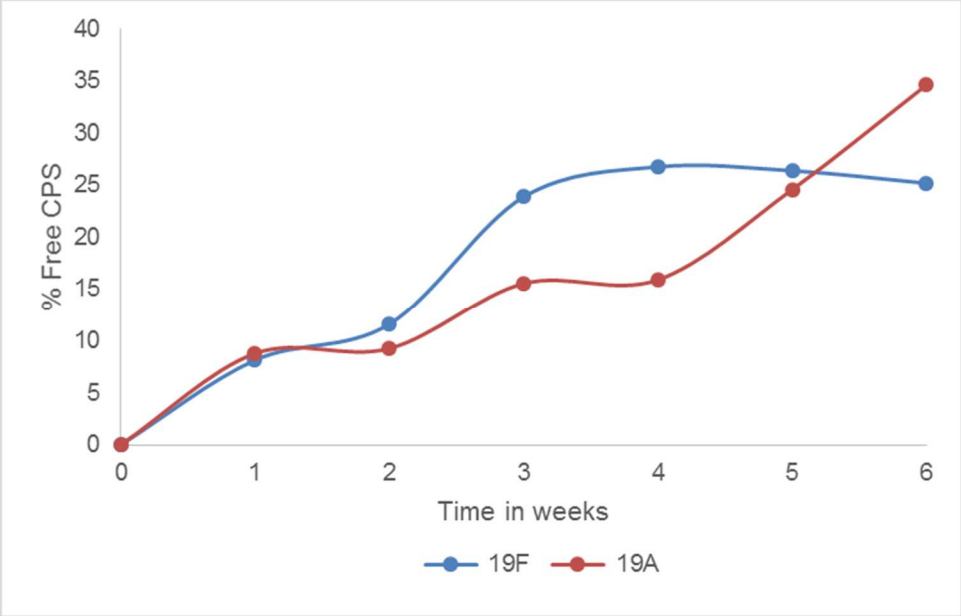

Figure 6.34: Pn19F and Pn19A conjugates over the course of 6 weeks period monitoring the percentage free polysaccharide at 37 ºC performing using the colorimetric assay, DOC/anthrone.

After 5 weeks of incubation the free polysaccharide was well above 20% which fell outside the WHO specifications. SEC-HPLC profiles for each of the time intervals are shown in Figures 6.35 - 6.38. The SEC-HPLC profiles for both serotypes at each experimental set point (time and temperature) showed an increase in the concentration of the conjugate. This increase saccharide concentration was observed to be due to sampling as the same vial was used each week to sample at each time and temperature point and therefore could have resulted in sampling error. A marked increase in both higher and smaller MW material after 2 weeks incubation was observed for both Pn19F and Pn19A.

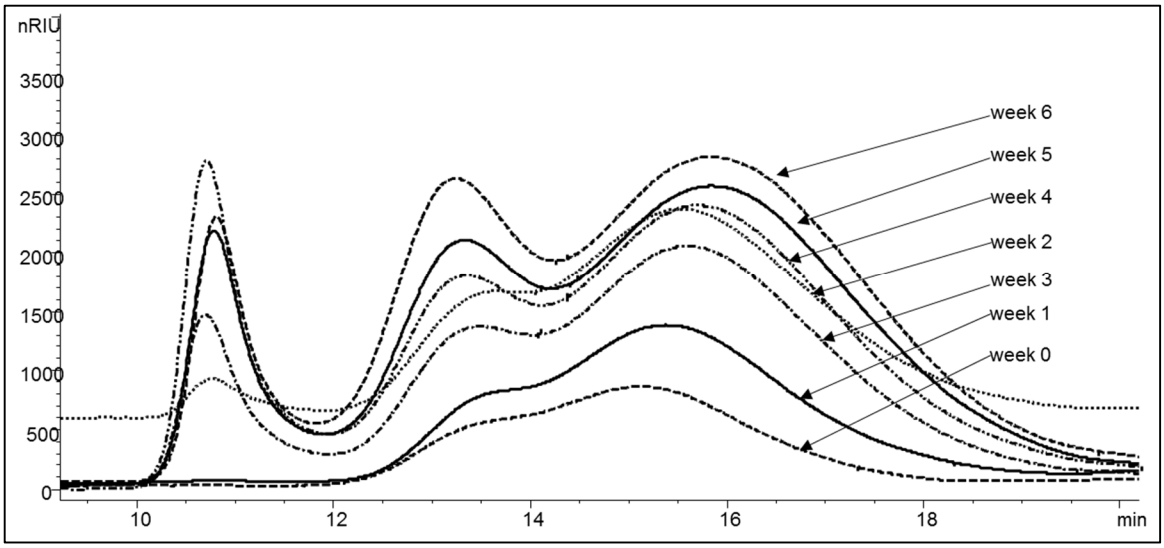

Figure 6.35: SEC-HPLC RID chromatograms of 19F_CDAP_TT in 10 mM PBS after 6 weeks at 37 ºC: Shodex 805/804 in series, PBS buffer, pH 7.0, the injection volume of 50 µL, flow rate 1 mL/min.

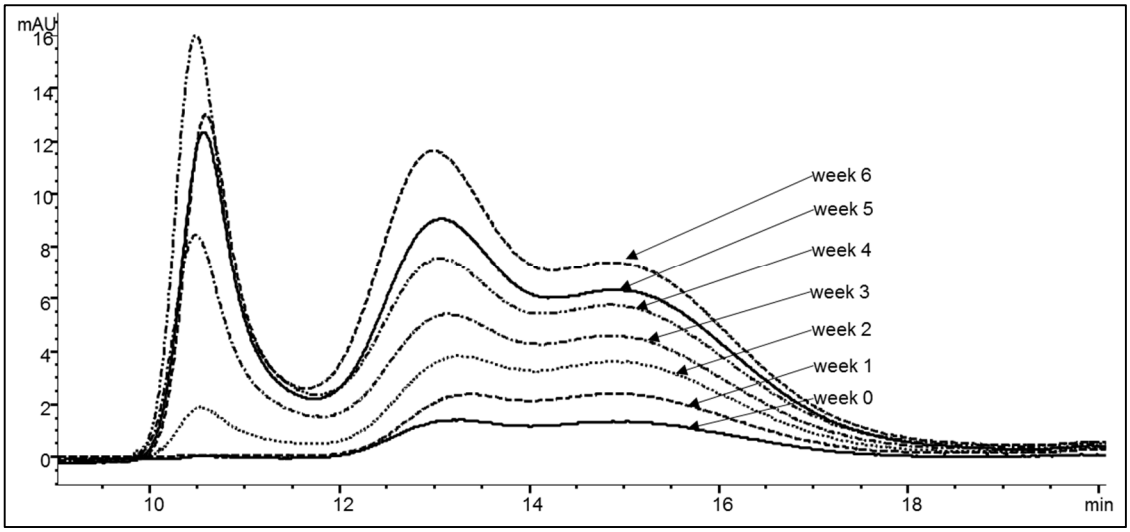

Figure 6.36: SEC-HPLC UV (280nm) chromatograms of 19F_CDAP_TT in 10 mM PBS after 6 weeks at 37 ºC: Shodex 805/804 in series, PBS buffer, pH 7.0, the injection volume of 50 µL, flow rate 1 mL/min.

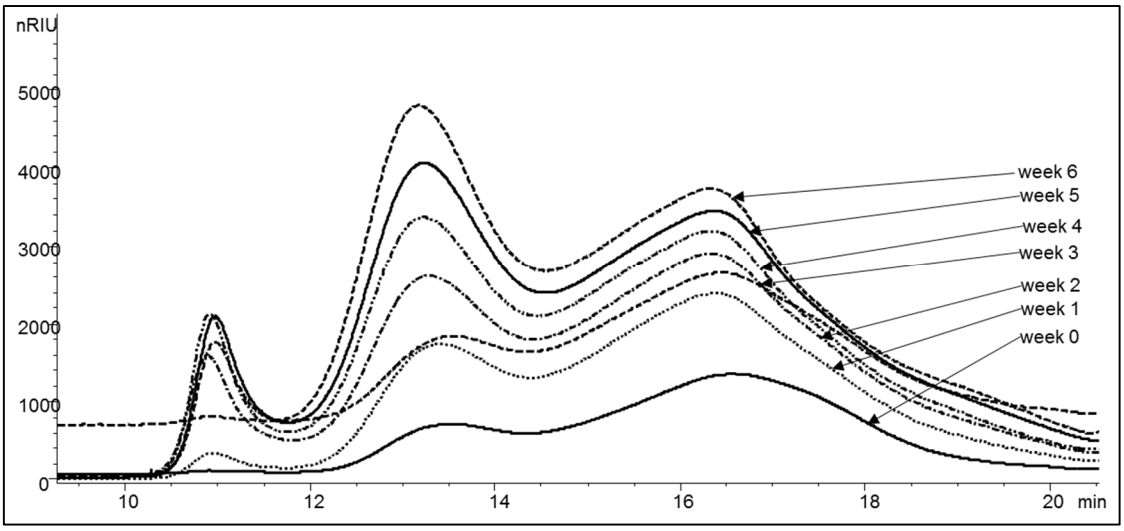

Figure 6.37: SEC-HPLC RID chromatograms of 19A_CDAP_TT in 10 mM PBS after 6 weeks at 37 ºC: Shodex 805/804 in series, PBS buffer, pH 7.0, the injection volume of 50 µL, flow rate 1 mL/min. The concentration of the samples seem to be increasing which is due to the increase in loss of sample and therefore leads to the remaining sample becoming more concentrated.

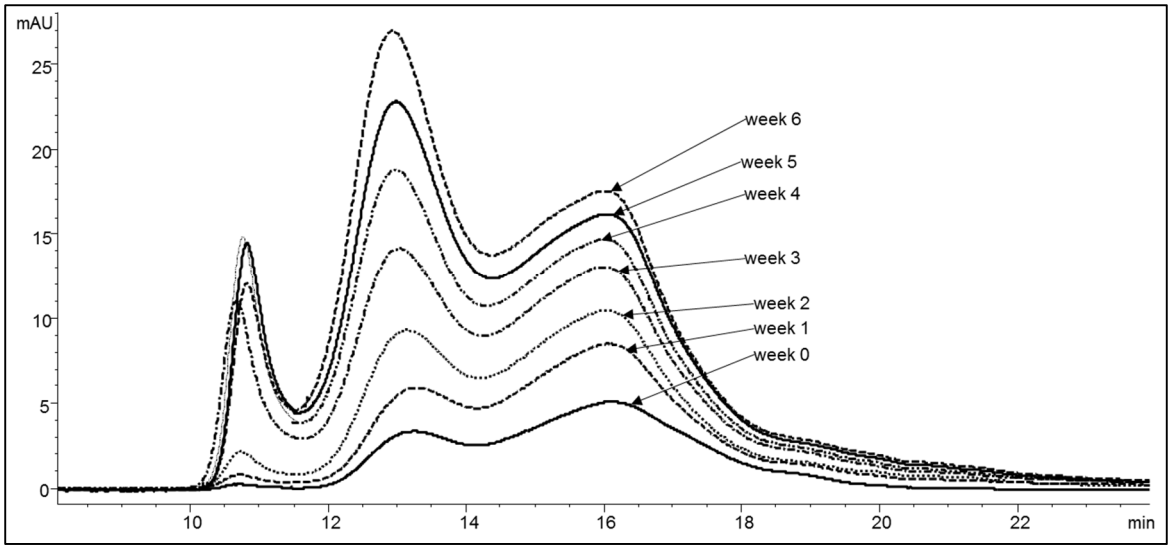

Figure 6.38: SEC-HPLC UV (280nm) chromatograms of 19A_CDAP_TT in 10 mM PBS after 6 weeks at 37 ºC: Shodex 805/804 in series, PBS buffer, pH 7.0, the injection volume of 50 µL, flow rate 1 mL/min.

The rate of increase of free saccharide was faster for serotype 19F than 19A but upon completion of the stability study the percentage increase plateaued and the same amount of free saccharide was seen for both serotypes.

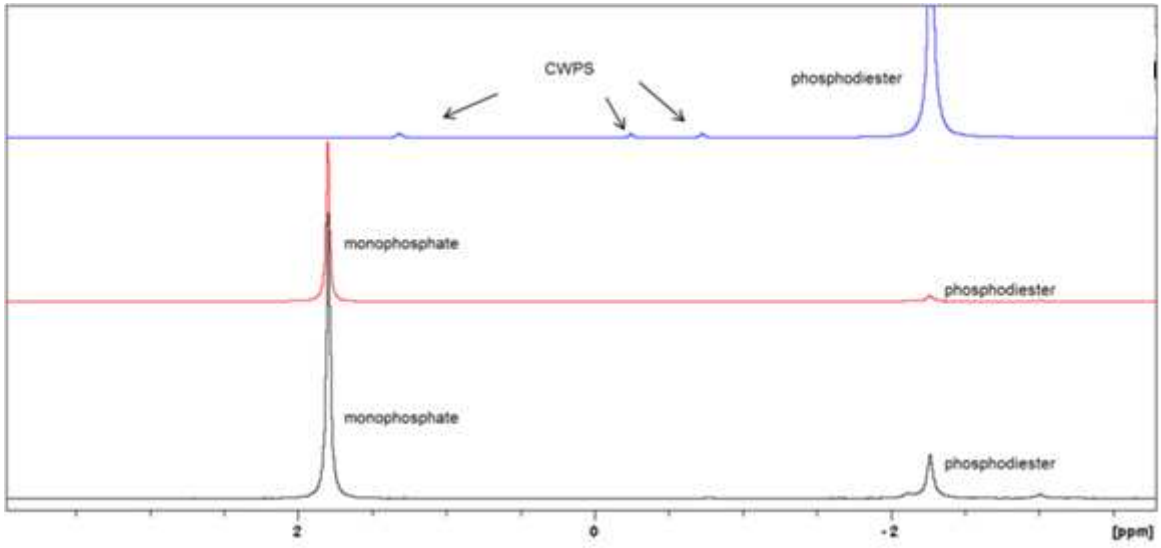

Figure 6.39: ^{31}P NMR spectroscopy of serotype 19F showing the polysaccharide (blue), the conjugate at the start of the stability study (red) at 37 ºC and the end of the accelerated stability study at 37 ºC (black).

Analysis of the conjugates by ^{31}P NMR was also employed to determine the extent of degradation of the conjugates over time. The ^{31}P chromatogram for Pn19F conjugate (Figure 6.39) indicates that the conjugate has undergone hydrolysis during the stability study with the phosphodiester bond between the rhamnose and the phosphate group been hydrolysed. The same spectroscopy profile was seen for serotype 19A (data not shown).

6.5 Conclusion

Accelerated studies at 37 ºC showed that the Pn19A conjugate remains stable for 2 weeks as indicated by the percentage free saccharide content remaining below the specification of 20% as well as consistent SEC-HPLC profiles, Pn19F and Pn19A both reached the same point of instability after 6 weeks at 37 ºC showing that there was little difference between the serotypes upon completion of the accelerated study.

The conjugates incubated at 25 ºC remained stable for 6 weeks thereafter there was an increase in percentage free saccharide above 20%. Real-time stability studies of the conjugates at 2 - 8 ºC showed that the conjugates were stable in the liquid form up to 2 months but it can be extrapolated that the stability of these conjugates would remain intact for a further 18 to 22 months. The NMR data when observing the ^{31}P NMR spectrum showed a clear indication of hydrolysis at the end of the stability study.

This study did not clearly differentiate the stabilities of Pn19A vs Pn19F and further analysis is required in order to ascertain whether the theory that Pn19F is more stable.

CHAPTER 7. GENERAL CONCLUSION

Pneumococcal infections caused by *Streptococcus pneumoniae* is one of the leading causes of death in children and the elderly worldwide. The burden of pneumococcal disease is known to be highest in children younger than 5 years of age and the elderly. The conjugate vaccine PCV7 contains antigens for serotypes 4, 6B, 9V, 14, 18C, 19F and 23F that were responsible for 60 - 80% of pneumococcal disease worldwide. After the introduction of PCV7 in developed countries (USA, Europe, and Australia) there was a steady decline in IPD caused by vaccine types but concurrently a gradual increase of IPD due to non-vaccine types (NVT). This rise in NVTs was mainly attributed to serotype 19A which, according to the CDC, had increased in IPD incidence in children younger than 5 years of age from 2.6 cases per 100000 population to 9.3 cases per 100000 population over a 6 year period [224]. This underlined the need for inclusion of NVTs such as 19A in pneumococcal conjugate vaccines.

The proof of concept approach and aim undertaken during this study was to investigate the process for the manufacture of a conjugate vaccine from cultivation to bulk formulation. The manufacturing process included clonal selection and isolation of a suitable working laboratory seed lot, fermentation for the production of CPS, purification for the extraction of CPS and conjugation of the main virulent factor of *S. pneumoniae,* the CPS for the bulk formulation of a conjugate vaccine for serotypes 19F and 19A. This study provided useful data on clonal selection and investigations into processes required to generate CPS for conjugation and ideally for vaccine development.

The cultivation process for the production of CPS extraction from *S. pneumoniae* was unique to this study as the cultivation using bag technology on bacteria is fairly new. This disposable bag technology makes the cultivation of bacteria more cost effective and because of the fast turnaround time ensures more cultivation can be performed compared to stirred tank reactors which require tedious cleaning and validation between fermentation runs. This makes it ideal for manufacturing facilities. Besides the bioreactor, some of the techniques used during cultivation of bacteria also proved promising. The process of cooling the cultivation broth upon completion of the fermentation run was unique to bacterial cultivation as it showed to increase CPS recovery levels when compared to not cooling the medium. This study also established the production of a high producer of CPS for serotype 19A with batch cultivation using disposable bag technology.

The purification method investigated during this study was based on Gotschlich and Biovac work and implemented using *S. pneumoniae* serotype 19A. The purified polysaccharide was subjected to a number of analytical tests in order to confirm that the purified polysaccharide batches conformed to the World Health Organisation specifications. These tests included identity (colorimetric assays), purity and size analysis. The structural studies using NMR proved the CPS cultivated and purified during this study was indeed Pn19A. CDAP conjugation performed on negatively charged polysaccharides such as Pn19F and Pn19A demonstrated similar behaviour to published data.

This proof of concept study confirmed that CDAP chemistry could be used on anionic polysaccharides and that ammonium sulfate purification could be used on these conjugates and that the ideal storage temperature for conjugates was between 2 - 8 ºC. Comparing the stability of Pn19A conjugates to Pn19F conjugates demonstrated that under extreme conditions the point of reference which in this case is the percentage free saccharide had the same end point at the same time. These conjugates thus show that they behave similarly under similar conditions proving that the stability study had limitations.

This study leaves room for future investigations. Multilocus sequence typing would be one such technique to identify serotype switching and characterize the pneumococcal population this particular strain belongs to. Genetic testing would aid in identifying the sequence type and thus correlate it to resistance and virulence.

Finally, additional studies to better understand the stability of these labile serogroup 19 conjugates will inform the development of future pneumococcal conjugate vaccines. This Ph.D. work contributes to the cultivation of serotype 19A using modern technology and fully characterizing the CPS of serotype 19F and 19A and contributed to the understanding of the stability of vaccines that could lead to improvement the design of pneumococcal conjugate vaccines.

REFERENCES

1. Austrian, R., *Pneumococcal otitis media and pneumococcal vaccines, a historical perspective*, in *Vaccine*. 2000. p. S71-7.
2. Restrepo, A.V., Salazar, B.E., Agudelo, M., et al., *Optimization of culture conditions to obtain maximal growth of penicillin-resistant Streptococcus pneumoniae.* BMC Microbiol, 2005. **5**(34): p. 1-8.
3. O'Brien, K.L., Wolfson, L.J., Watt, J.P., et al., *Burden of disease caused by Streptococcus pneumoniae in children younger than 5 years: global estimates.* Lancet, 2009. **374**(9693): p. 893-902.
4. Jordano, Q., Falco, V., Almirante, B., et al., *Invasive pneumococcal disease in patients infected with HIV: still a threat in the era of highly active antiretroviral therapy.* Clin Infect Dis, 2004. **38**(11): p. 1623-8.
5. Hausdorff, W.P., Bryant, J., Paradiso, P.R., et al., *Which pneumococcal serogroups cause the most invasive disease: implications for conjugate vaccine formulation and use, part I.* Clin Infect Dis, 2000. **30**(1): p. 100-21.
6. Von Gottberg, A., *Bacterial meningitis in the era of paediatric vaccination against the encapsulated pathogens.* CME, 2010. **26**: p. 252-259.
7. Trotter, C.L., McVernon, J., Ramsay, M.E., et al., *Optimising the use of conjugate vaccines to prevent disease caused by Haemophilus influenzae type b, Neisseria meningitidis and Streptococcus pneumoniae.* Vaccine, 2008. **26**(35): p. 4434-45.
8. Austrian, R., *The pneumococcus at the millennium: not down, not out.* J Infect Dis, 1999. **179 Suppl 2**: p. S338-41.
9. Austrian, R., *Pneumococcus: the first one hundred years.* Rev Infect Dis, 1981. **3**(2): p. 183-9.
10. Todar, K. *Streptoccus pneumoniae*. Online textbook of bacteriology 2008 [cited 2012; Available from: textbookofbacteriology.net/*S.pneumoniae*.html.
11. Chen, L., Ge, X., Dou, Y., et al., *Identification of hydrogen peroxide production-related genes in Streptococcus sanguinis and their functional relationship with pyruvate oxidase.* Microbiology, 2011. **157**(Pt 1): p. 13-20.
12. Mehr, S. and Wood, N., *Streptococcus pneumoniae--a review of carriage, infection, serotype replacement and vaccination.* Paediatr Respir Rev, 2012. **13**(4): p. 258-64.
13. Nahm, M.H., Apicella, M.A., and Briles, D., *Immunity to extracelluar bacteria*, in *Fundamental immunology*, W. Paul, Editor. 2003, Lippincott Williams & Wilkins Publishers.
14. Nuorti, J.P. and Whitney, C.G., *Prevention of pneumococcal disease among infants and children - use of 13-valent pneumococcal conjugate vaccine and 23-valent pneumococcal polysaccharide vaccine - recommendations of the Advisory Committee on Immunization Practices (ACIP).* MMWR Recomm Rep, 2010. **59**(RR-11): p. 1-18.
15. Schoub, B.D., Mphahlele, M.J., Ngcobo, N.J., et al., *Introducing new vaccines into the South African national immunisation programme - a case study.* Vaccine, 2012. **30 Suppl 3**: p. C1-2.
16. Ngcobo, N.J. and Cameron, N.A., *The decision making process on new vaccines introduction in South Africa.* Vaccine, 2012. **30 Suppl 3**: p. C9-13.

17. Bogaert, D., De Groot, R., and Hermans, P.W., *Streptococcus pneumoniae colonisation: the key to pneumococcal disease.* Lancet Infect Dis, 2004. **4**(3): p. 144-54.
18. Kim, J.O. and Weiser, J.N., *Association of intrastrain phase variation in quantity of capsular polysaccharide and teichoic acid with the virulence of Streptococcus pneumoniae.* J Infect Dis, 1998. **177**(2): p. 368-77.
19. Williams, S.R., Mernagh, P.J., Lee, M.H., et al., *Changing epidemiology of invasive pneumococcal disease in Australian children after introduction of a 7-valent pneumococcal conjugate vaccine.* Med J Aust, 2011. **194**(3): p. 116-20.
20. *Introduction of pneumococcal vaccine PCV10, two dose presentation*. A handbook for district and health facility staff 2013 [cited 2013; Available from: https://www.medbox.org/vaccine-preventable-diseases/introduction-of-pneumococcal-vaccine-pcv10-two-dose-presentation/preview?q=.
21. *Chapter 8: Identification and Characterization of Streptococcus pneumoniae*. Meningitis lab manual [cited 2012; Available from: http://www.cdc.gov/meningitis/lab-manual/chpt08-id-characterization-streppneumo.pdf.
22. Drijkoningen, J.J. and Rohde, G.G., *Pneumococcal infection in adults: burden of disease.* Clin Microbiol Infect, 2014. **20 Suppl 5**: p. 45-51.
23. Song, J.Y., Choi, J.Y., Lee, J.S., et al., *Clinical and economic burden of invasive pneumococcal disease in adults: a multicenter hospital-based study.* BMC Infect Dis, 2013. **13**: p. 202.
24. *Pneumonia*. WHO media centre fact sheet 2012; Available from: www.who.int/mediacentre/factsheets/fs331/en/index.html.
25. Alonso de Velasco, E., Verheul, A.F.M., Verhoef, J., et al., *Streptococcus pneumoniae: Virulence Factors, Pathogenesis, and Vaccines.* Microbiological Reviews, 1995. **59**(4): p. 591-603.
26. Goncalves, V.M., Zangirolami, T.C., Giordano, R.L., et al., *Optimization of medium and cultivation conditions for capsular polysaccharide production by Streptococcus pneumoniae serotype 23F.* Appl Microbiol Biotechnol, 2002. **59**(6): p. 713-7.
27. *Pneumococcal Disease*. Epidemiology and prevention of vaccine-preventable diseases: The Pink Book: Course text book 2012; Available from: http://www.cdc.gov/vaccines/pubs/pinkbook/downloads/pneumo.
28. *Pneumococcal Vaccine* Vaccines.gov [cited 2012; Available from: http://www.vaccines.gov/diseases/pneumonia/index.html.
29. Pace, D., *Glycoconjugate vaccines.* Expert Opin Biol Ther, 2013. **13**(1): p. 11-33.
30. Moreau, M. and Schultz, D., *Polysaccharide based vaccines for the prevention of pneumococcal infections.* Journal of Carbohydrate Chemistry, 2000. **19**(4-5): p. 419-434.
31. Grabenstein, J.D. and Klugman, K.P., *A century of pneumococcal vaccination research in humans.* Clin Microbiol Infect, 2012. **18 Suppl 5**: p. 15-24.
32. Zon, G., Szu, S., Egan, W., et al., *Hydrolytic stability of pneumococcal group 6 (type 6A and 6B) capsular polysaccharides.* Infection and Immunity, 1982. **37**(1): p. 89-103.

33. Jakobsen, H., Sigurdsson, V.D., Sigurdardottir, S., et al., *Pneumococcal serotype 19F conjugate vaccine induces cross-protective immunity to serotype 19A in a murine pneumococcal pneumonia model.* Infect Immun, 2003. **71**(5): p. 2956-9.
34. Biemans, R., Hermand, P.I., and Poolman, J., *Vaccine comprising Streptococcus pneumoniae capsular polysaccharide conjugates*. 2010: US 42419711.
35. Kadioglu, A., Weiser, J.N., Paton, J.C., et al., *The role of Streptococcus pneumoniae virulence factors in host respiratory colonization and disease.* Nat Rev Microbiol, 2008. **6**(4): p. 288-301.
36. Kayhty, H., Karanko, V., Peltola, H., et al., *Serum antibodies after vaccination with Haemophilus influenzae type b capsular polysaccharide and responses to reimmunization: no evidence of immunologic tolerance or memory.* Pediatrics, 1984. **74**(5): p. 857-65.
37. Lees, A., Puvanesarajah, V., and Frasch, C.E., *Conjugation Chemistry*, in *Pneumococcal Vaccines. The impact of Conjugate Vaccines*, G.R. SIber, K.P. Klugman, and P.H. Makela, Editors. 2008, ASM Press: USA. p. 163-175.
38. *Types of vaccines*. Understanding the Basics: general recommendations on immunization [cited 2012; Available from: http://www2.cdc.gov/nip/isd/ycts/mod1/courses/genrec/10351.asp?seg=H.
39. Geno, K.A., Gilbert, G.L., Song, J.Y., et al., *Pneumococcal Capsules and Their Types: Past, Present, and Future.* Clin Microbiol Rev, 2015. **28**(3): p. 871-99.
40. Robbins, J.B. and Schneerson, R., *Polysaccharide-protein conjugates: a new generation of vaccines.* J Infect Dis, 1990. **161**(5): p. 821-32.
41. Poland, G.A., *The burden of pneumococcal disease: the role of conjugate vaccines.* Vaccine, 1999. **17**(13-14): p. 1674-9.
42. Torres, A., Bonanni, P., Hryniewicz, W., et al., *Pneumococcal vaccination: what have we learnt so far and what can we expect in the future?* Eur J Clin Microbiol Infect Dis, 2015. **34**(1): p. 19-31.
43. Dinleyici, E.C. and Yargic, Z.A., *Pneumococcal conjugated vaccines: impact of PCV-7 and new achievements in the postvaccine era.* Expert Rev Vaccines, 2008. **7**(9): p. 1367-94.
44. von Gottberg, A., Cohen, C., de Gouveia, L., et al., *Epidemiology of invasive pneumococcal disease in the pre-conjugate vaccine era: South Africa, 2003-2008.* Vaccine, 2013. **31**(38): p. 4200-8.
45. Pilishvili, T., Lexau, C., Farley, M.M., et al., *Sustained reductions in invasive pneumococcal disease in the era of conjugate vaccine.* J Infect Dis, 2010. **201**(1): p. 32-41.
46. Wharf, C. *Synflorix, Pneumococcal polysaccharide conjugate vaccine (adsorbed)*. 2009 [cited 2012; Available from: http://www.ema.europa.eu/docs/en_GB/document_library/EPAR_-_Product_Information/human/000973/WC500054346.pdf.
47. Isaacman, D.J., McIntosh, E.D., and Reinert, R.R., *Burden of invasive pneumococcal disease and serotype distribution among Streptococcus pneumoniae isolates in young children in Europe: impact of the 7-valent pneumococcal conjugate vaccine and considerations for future conjugate vaccines.* Int J Infect Dis, 2010. **14**(3): p. e197-209.

48. Robbins, J.B., Austrian, R., Lee, C.J., et al., *Considerations for formulating the second-generation pneumococcal capsular polysaccharide vaccine with emphasis on the cross-reactive types within groups.* J Infect Dis, 1983. **148**(6): p. 1136-59.
49. Krishnamurthy, T., Lee, C.J., Henrichsen, J., et al., *Characterization of the cross-reaction between type 19F(19) and 19A(57) pneumococcal capsular polysaccharides: compositional analysis and immunological relation determined with rabbit typing antisera.* Infect Immun, 1978. **22**(3): p. 727-35.
50. Xu, Q., Pichichero, M.E., Casey, J.R., et al., *Novel type of Streptococcus pneumoniae causing multidrug-resistant acute otitis media in children.* Emerg Infect Dis, 2009. **15**(4): p. 547-51.
51. Beynon, L.M., Richards, J.C., Perry, M.B., et al., *Antigenic and structural relationships within group 19 Streptococcus pneumoniae: chemical characterization of the specific capsular polysaccharides of types 19B and 19C.* Can J Chem, 1992. **70**: p. 218-232.
52. Choi, E.H., Kim, S.H., Eun, B.W., et al., *Streptococcus pneumoniae serotype 19A in children, South Korea.* Emerg Infect Dis, 2008. **14**(2): p. 275-81.
53. Pujar, N.S., Huang, N.F., Daniels, C.L., et al., *Base hydrolysis of phosphodiester bonds in pneumococcal polysaccharides.* Biopolymers, 2004. **75**(1): p. 71-84.
54. Simberkoff, M.S., Lukaszewski, M., Cross, A., et al., *Antibiotic-resistant isolates of Streptococcus pneumoniae from clinical specimens: a cluster of serotype 19A organisms in Brooklyn, New York.* J Infect Dis, 1986. **153**(1): p. 78-82.
55. Levy, C., Varon, E., Bingen, E., et al., *[Pneumococcal meningitis in children in France: 832 cases from 2001 to 2007].* Arch Pediatr, 2008. **15 Suppl 3**: p. S111-8.
56. Laufer, A.S., Thomas, J.C., Figueira, M., et al., *Capacity of serotype 19A and 15B/C Streptococcus pneumoniae isolates for experimental otitis media: Implications for the conjugate vaccine.* Vaccine, 2010. **28**(12): p. 2450-7.
57. Lee, S., Lee, K., Kang, Y., et al., *Prevalence of serotype and multidrug-resistance of Streptococcus pneumoniae respiratory tract isolates in 265 adults and 36 children in Korea, 2002-2005.* Microb Drug Resist, 2010. **16**(2): p. 135-42.
58. Tyrrell, G.J., *The changing epidemiology of Streptococcus pneumoniae serotype 19A clonal complexes.* J Infect Dis, 2011. **203**(10): p. 1345-7.
59. *Pneumococcal polysaccharide conjugate vaccine (13-valent, adsorbed)*. Assessment report for Prevenar 13 2009; Available from: http://www.ema.europa.eu/docs/en_GB/document_library/EPAR_-_Public_assessment_report/human/001104/WC500057250.pdf.
60. Zon, G., Szu, S.C., Egan, W., et al., *Hydrolytic stability of pneumococcal group 6 (type 6A and 6B) capsular polysaccharides.* Infect Immun, 1982. **37**(1): p. 89-103.
61. Poolman, J., Frasch, C., Nurkka, A., et al., *Impact of the conjugation method on the immunogenicity of Streptococcus pneumoniae serotype 19F polysaccharide in conjugate vaccines.* Clin Vaccine Immunol, 2011. **18**(2): p. 327-36.

62. Hanage, W.P., Huang, S.S., Lipsitch, M., et al., *Diversity and antibiotic resistance among nonvaccine serotypes of Streptococcus pneumoniae carriage isolates in the post-heptavalent conjugate vaccine era.* J Infect Dis, 2007. **195**(3): p. 347-52.
63. Moore, M.R. and Whitney, C.G., *Emergence of nonvaccine serotypes following introduction of pneumococcal conjugate vaccine: cause and effect?* Clin Infect Dis, 2008. **46**(2): p. 183-5.
64. Frasch, C.E., *Preparation of bacterial polysaccharide-protein conjugates: analytical and manufacturing challenges.* Vaccine, 2009. **27**(46): p. 6468-70.
65. Jain, R. and Maithal, K., *Fermentation process for streptococcus pneumoniae*, B. Limited, Editor. 2011: WO 2011/151841 A1.
66. Constantino, P., Norelli, F., Olivier, R., et al., *Fermentation processes for cultivating streptococci and purification processes for obtaining CPS therefrom*. 2010, Norvatis Vaccines and Diagnostics SRL: US 0272755.
67. Singh, V., *Disposable bioreactor for cell culture using wave-induced agitation.* Cytotechnology, 1999. **30**(1-3): p. 149-58.
68. Ravenscroft, N. and Feavers, I.M., *Conjugate vaccines*, in *Handbook of Meningococcal Disease. Infection, Biology, Vaccination, Clinical Management*, F. M and M. MCJ, Editors. 2006, Weinheim: Wiley-VCH Verlag GmbH & Co KGaA. p. 343-369.
69. Weiser, J.N., Austrian, R., Sreenivasan, P.K., et al., *Phase variation in pneumococcal opacity: relationship between colonial morphology and nasopharyngeal colonization.* Infect Immun, 1994. **62**(6): p. 2582-9.
70. Prescott, L.M., Harley, J.P., and Klein, D.A., *Microbiology*. 5th ed. 2002: McGraw-Hill.
71. Fox, A., *Culture and Identification of infectious agents*, in *Bacteriology - Chapter two*. 2014, University of South Carolina School of Medicine: Chicago.
72. Gardam, M.A. and Miller, M.A., *Optochin revisited: defining the optimal type of blood agar for presumptive identification of Streptococcus pneumoniae.* J Clin Microbiol, 1998. **36**(3): p. 833-4.
73. Hoeprich, P.D., *Evaluation of an improved chemically defined medium for the culture of Diplococcus pneumoniae.* J Bacteriol, 1957. **74**(5): p. 587-90.
74. *Recommendations to assure the quality, safety and efficacy of pneumococcal conjugate vaccines*, in *Final Expert Committee on Biological Standardization* 2009, WHO: Geneva.
75. Dische, Z. and Shettles, L.B., *A new spectrophotometric test for the detection of methylpentose.* J Biol Chem, 1951. **192**(2): p. 579-82.
76. Morgan, W.T. and Elson, L.A., *A colorimetric method for the determination of N-acetylglucosamine and N-acetylchrondrosamine.* Biochem J, 1934. **28**(3): p. 988-95.
77. Ashwell, G., *Colorimetric analysis of sugars.* Methods of enzymology, 1957. **3**: p. 73-105.
78. *Protein assay instructions*. Protein assay kits 2012; Available from: www.thermo.com/pierce.
79. McCance, R.A., *The colorimetric determination of rhamnose.* Biochem J, 1929. **23**(6): p. 1172-4.
80. Elson, L.A. and Morgan, W.T., *A colorimetric method for the determination of glucosamine and chondrosamine.* Biochem J, 1933. **27**(6): p. 1824-8.

81. Chen, P.S., Toribara, T.Y., and Warner, H., *Microdetermination of Phosphorus.* Anal. Chem, 1956. **28**(11): p. 1756-1758.
82. Turula, V., Walters, S., Singh, S., et al., *Automated colorimetric polysacchairde assays*. 2008, Wyeth: US 0227207.
83. Ludwig, T.G. and Goldberg, J.V., *The anthrone method for the determination of carbohydrates in foods and in oral rinsing.* J Dent Res, 1956. **35**(1): p. 90-4.
84. Dubois, M., Gilles, K.A., Hamilton, J.K., et al., *Colorimetric method for determination of sugars and related substances.* Anal Chem, 1956. **28**(3): p. 350-356.
85. Noble, J.E. and Bailey, M.J., *Quantitation of protein.* Methods Enzymol, 2009. **463**: p. 73-95.
86. Pace, C.N., Vajdos, F., Fee, L., et al., *How to measure and predict the molar absorption coefficient of a protein.* Protein Sci, 1995. **4**(11): p. 2411-23.
87. Smith, P.K., Krohn, R.I., Hermanson, G.T., et al., *Measurement of protein using bicinchoninic acid.* Anal Biochem, 1985. **150**(1): p. 76-85.
88. Bradford, M.M., *A rapid and sensitive method for the quantitation of microgram quantities of protein utilizing the principle of protein-dye binding.* Anal Biochem, 1976. **72**: p. 248-54.
89. *Nucleic acids in polysaccharide vaccines*, in *European pharmacopoeia*. 2005, Council of Europe: Strasbourg.
90. Madhi, S.A., Izu, A., Violari, A., et al., *Immunogenicity following the first and second doses of 7-valent pneumococcal conjugate vaccine in HIV-infected and -uninfected infants.* Vaccine, 2013. **31**(5): p. 777-83.
91. Bhinge, S.D., Malipatil, S.M., and Sonawane, L.V., *Bioanalytical method development and validation for simultaneous estimation of cefixime and dicloxacillin by RP-HPLC in human plasma.* Acta Chim Slov, 2014. **61**(3): p. 580-6.
92. *Enzyme Linked Immunosorbent Assay (ELISA)*. Electrophoresis 2011 [cited 2017; Available from: https://www.nationaldiagnostics.com/electrophoresis/article/enzyme-linked-immunosorbent-assay-elisa.
93. Lee, C.J., *Quality control of polyvalent pneumococcal polysaccharide-protein conjugate vaccine by nephelometry.* Biologicals, 2002. **30**(2): p. 97-103.
94. Angersbach, S., Brand, S., Hipler, B., et al., *Monitoring of microbial growth curves by laser nephelometry*, in *BMG LABTECH Application Note 117;*. 2003, BMG LABTECH: Offenburg.
95. Tsai, C., *Purification and Characterization*, in *Biomacromolecules: Introduction to Structure, Function and Informatics*. 2006, Wiley-Liss: New Jersey. p. 31-54.
96. Jones, C., *NMR assays for carbohydrate-based vaccines.* J Pharm Biomed Anal, 2005. **38**(5): p. 840-50.
97. *Introduction to Fourier Transform Infrared Spectrometry*. Molecular Materials Research Center 2001 [cited 2012; Available from: http://mmrc.caltech.edu/FTIR/FTIRintro.pdf.
98. Chrambach, A. and Rodbard, D., *Polyacrylamide gel electrophoresis.* Science, 1971. **172**(3982): p. 440-451.
99. Trathnigg, B., Gorbunov, A., and Skvortsov, A., *Liquid adsorption chromatography of polyethers: experiments and simulation.* J Chromatogr A, 2000. **890**(2): p. 195-210.

100. *Size Exclusion Chromatography: Principles and Methods*. GE Healthcare Life Sciences 2000 [cited 2012; Available from: http://proteins.gelifesciences.com/~/media/protein-purification-ib/documents/handbooks/size-exclusion-chromatography-handbook.pdf?la=en.

101. Ravenscroft, N., Costantino, P., Talaga, P., et al., *Glycoconjugate Vaccines*, in *Vaccine Analysis: Strategies. Principles, and Control*, B. Nunnally, R.D. Sitrin, and V.E. Turula, Editors. 2015, Springer: USA. p. 301.

102. Talaga, P., Vialle, S., and Moreau, M., *Development of a high-performance anion-exchange chromatography with pulsed-amperometric detection based quantification assay for pneumococcal polysaccharides and conjugates.* Vaccine, 2002. **20**(19-20): p. 2474-84.

103. Kim, J.S., Laskowich, E.R., Arumugham, R.G., et al., *Determination of saccharide content in pneumococcal polysaccharides and conjugate vaccines by GC-MSD.* Anal Biochem, 2005. **347**(2): p. 262-74.

104. Jahnal, J.B., Ilieva, P., and Frimmel, F.H., *HPAE-PAD - a sensitive method for the determination of carbohydrates.* Fresenius J Anal Chem, 1998. **360**: p. 827-829.

105. Czechowska-Biskup, R., Rokita, B., Lotfy, S., et al., *Degradation of chitson and starch by 360-kHz ultrasound.* Carbohydrate polymers, 2005. **60**: p. 175-184.

106. Bystricky, S., Machova, E., Malovikova, A., et al., *Determination of the cross-linking effect of adipic acid dihydrazide on glycoconjugate preparation.* Glycoconj J, 1999. **16**(11): p. 691-5.

107. Hermanson, G., *Bioconjugate Techniques*. 2nd ed. 2008, Rockford, Illinois, USA: Academic Press.

108. Edmonds-Smith, C., *The development of a process and quality control methods for a conjugate vaccine against Streptococcus pneumoniae serotype 1*, in *Chemistry*. 2013, University of Cape Town: Cape Town. p. 280.

109. Qi, X.Y., Keyhani, N.O., and Lee, Y.C., *Spectrophotometric determination of hydrazine, hydrazides, and their mixtures with trinitrobenzenesulfonic acid.* Anal Biochem, 1988. **175**(1): p. 139-44.

110. Stramski, D. and Piskozub, J., *Estimation of scattering error in spectrophotometric measurements of light absorption by aquatic particles from three-dimensional radiative transfer simulations.* Appl Opt, 2003. **42**(18): p. 3634-46.

111. Shafer, D., Toll, B., Schuman, R., et al., *Activation of soluble polysaccharides with 1-cyano-4-dimethylaminopyridinium tetrafluoroborate (CDAP) for use in protein-polysaccharide conjugate vaccines and immunological reagents. II. Selective crosslinking of proteins to CDAP-activated polysaccharides* Vaccine, 2000. **18**: p. 1273.

112. McMaster, R., *Purification of polysaccharide-protein conjugate vaccines by ultrafiltration with ammonium sulfate solutions*. 2000, Aventis Pasteur, Inc.: US 6146902.

113. Guo, Y.Y., Anderson, R., McIver, J., et al., *A simple and rapid method for measuring unconjugated capsular polysaccharide (PRP) of Haemophilus influenzae type b in PRP-tetanus toxoid conjugate vaccine.* Biologicals, 1998. **26**(1): p. 33-8.

114. Popovic, T., Ajello, G., and Facklam, R., *Laboratory Methods for the Diagnosis of Meningitis caused by Neisseria meningitidis, Streptococcus pneumoniae, and Haemophilus influenzae*, CDC, Editor. 1999, WHO.
115. Kellogg, J.A., Bankert, D.A., Elder, C.J., et al., *Identification of Streptococcus pneumoniae revisited.* J Clin Microbiol, 2001. **39**(9): p. 3373-5.
116. Kaijalainen, T., *Identification of Streptococcus pneumoniae.* International journal of Circumpolar Health, 2006. **65**(5): p. 459-460.
117. Beveridge, T.J., *Use of the gram stain in microbiology.* Biotech Histochem, 2001. **76**(3): p. 111-8.
118. Bernheimer, A.W. and Pappenheimer, A.M., *Factors Necessary for Massive Growth of Group A Hemolytic Streptococcus.* J Bacteriol, 1942. **43**(4): p. 481-94.
119. Adams, M.H. and Roe, A.S., *A partially defined medium for cultivation of pneumococcus.* Bacteriology, 1945. **49**(4): p. 401-409.
120. Liberman, C., Takagi, M., Cabrera-Crespo, J., et al., *Pneumococcal whole-cell vaccine: optimization of cell growth of unencapsulated Streptococcus pneumoniae in bioreactor using animal-free medium.* J Ind Microbiol Biotechnol, 2008. **35**(11): p. 1441-5.
121. Bailey, F.J. and Herber, W.K., *Method of clonal growth of Streptococcus pneumoniae*. 1994, Merck & Co. Inc: US 5314822.
122. Hoeprich, P.D., *C14 Labelling of Diplococcus pneumoniae.* J Bacteriol, 1955. **69**(6): p. 682-8.
123. Leal, M., Pereira, D., Jessouroun, E., et al., *Investigation of cultivation condiitions for capsular polysaccharide production by Streptococcus pneumoniae serotype 14.* Electron J Biotechnol, 2011. **14**(5): p. 1-7.
124. Kim, S.N., Min, K.K., Kim, S.H., et al., *Optimization of Culture Conditions for Production of Pneumococcal Capsular Polysaccharide Type 1.* Microbiology, 1996. **34**(2): p. 179-183.
125. Massaldi, H., Bessio, M.I., Suarez, N., et al., *Features of bacterial growth and polysaccharide production of Streptococcus pneumoniae serotype 14.* Biotechnol Appl Biochem, 2010. **55**(1): p. 37-43.
126. Yesilkaya, H., Andisi, V.F., Andrew, P.W., et al., *Streptococcus pneumoniae and reactive oxygen species: an unusual approach to living with radicals.* Trends Microbiol, 2013. **21**(4): p. 187-95.
127. Pesakhov, S., Benisty, R., Sikron, N., et al., *Effect of hydrogen peroxide production and the Fenton reaction on membrane composition of Streptococcus pneumoniae.* Biochim Biophys Acta, 2007. **1768**(3): p. 590-7.
128. Pericone, C.D., Park, S., Imlay, J.A., et al., *Factors contributing to hydrogen peroxide resistance in Streptococcus pneumoniae include pyruvate oxidase (SpxB) and avoidance of the toxic effects of the fenton reaction.* J Bacteriol, 2003. **185**(23): p. 6815-25.
129. Goncalves, V.M., Takagi, M., Lima, R.B., et al., *Purification of capsular polysaccharide from Streptococcus pneumoniae serotype 23F by a procedure suitable for scale-up.* Biotechnol Appl Biochem, 2003. **37**(Pt 3): p. 283-7.

130. Marthos, B.V., Ferri, A.L., de Figueiredo, D.B., et al., *Capsular polysaccharide production by Streptococcus pneumoniae serotype 1: from strain selection to fed-batch cultivation.* Appl Microbiol Biotechnol, 2015. **99**(24): p. 10447-56.
131. Marshall, J., *Soytone as a nitrogen source in preparing meningcoccal conjugates*. 2008: US 0160044.
132. Corradini, C., Cavazza, A., and Bignardi, C., *High-Performance Anion-Exchange Chromatography Coupled with Pulsed Electrochemical Detection as a Powerful Tool to Evaluate Carbohydrates of Food Interest: Principles and Applications.* Carbohydrate Chemistry, 2012. **2012**: p. 1-13.
133. Avery, O.T. and Morgan, H.J., *The Occurrence of Peroxide in Cultures of Pneumococcus.* J Exp Med, 1924. **39**(2): p. 275-87.
134. Abadias, M., Teixido, N., Usall, J., et al., *Optimization of growth conditions of the postharvest biocontrol agent Candida sake CPA-1 in a lab-scale fermenter.* J Appl Microbiol, 2003. **95**(2): p. 301-9.
135. Chuck, A., Deshpande, R., Distler, A., et al., *Commercial production of recombinant erythropoietins.* Erythropoietins & Erythropoiesis Milestones in Drug Therapy MDT, 2006: p. 133-150.
136. Barkat, N., *BIological Products: Manufacturing, Handling, Packaging and Storage, Promising Pharmaceuticals*. Promising Pharmaceuticals, ed. D.P. Basnet. 2012: InTechOpen.
137. Okonkowski, J., Kizer-Bentley, L., Listner, K., et al., *Development of a robust, versatile, and scalable inoculum train for the production of a DNA vaccine.* Biotechnol Prog, 2005. **21**(4): p. 1038-47.
138. Gershater, C.J., *Inoculum preparation.* Encyclopedia of Bioprocess Technology, 2010: p. 1-16.
139. Leal, M.M., Pereira, D.S.G., Jessouroun, E., et al., *Investigation of cultivation conditions from capsular polysaccharide production by Streptococcus pneumoniae serotype 14.* Electron J Biotechnol, 2011. **14**(5): p. 1-7.
140. Hvalbye, B.K., Aaberge, I.S., Lovik, M., et al., *Intranasal immunization with heat-inactivated Streptococcus pneumoniae protects mice against systemic pneumococcal infection.* Infect Immun, 1999. **67**(9): p. 4320-5.
141. Aunins, J.G., Lee, A.L., and Volkin, D.B., *Vaccine production*. Second ed. The Biomedical Engineering Handbook, ed. E.J.D.B.B. Raton. Vol. 1. 2000: CRC Press LLC.
142. Parija, S., *Textbook of microbiology and immunology*. Second ed. 2009: Elsevier. 665.
143. Uittenbogaard, J.P., Zomer, B., Hoogerhout, P., et al., *Reactions of beta-propiolactone with nucleobase analogues, nucleosides, and peptides: implications for the inactivation of viruses.* J Biol Chem, 2011. **286**(42): p. 36198-214.
144. Rutala, W.A., Weber, D.J., Healthcare, et al. *Guideline for Disinfection and Sterilization in Healthcare Facilities*. 2008; Available from: http://www.cdc.gov/hicpac/pdf/guidelines/Disinfection_Nov_2008.pdf.
145. Liveyns, R.W., Gilles, D., and Arickx, M., *Purification of Pneumococcal Polysaccharides using CTAB/Celite*. 1989: Translation of Patent EP 0072513.

146. Camacho, A.I., Souza-Reboucas, J., Irache, J.M., et al., *Towards a non-living vaccine against Shigella flexneri: from the inactivation procedure to protection studies.* Methods, 2013. **60**(3): p. 264-8.
147. Bahler, B., Lee, T., Lotvin, J., et al., *Separation of contaminants from Streptococcus pneumoniae polysaccharide by pH manipulation*. 2006, Wyeth: US 2006/012134.
148. Marburg, S., Tolman, R.L., Kniskern, P.J., et al., *Pneumococcal polysaccharide conjugate vaccine*, M. Co, Editor. 1997: US 5623057.
149. Shukla, A., Etzel, M., and Gadam, S., *Process scale bioseparations for the biopharmaceutical industry*. 2006: CRC Press Taylor & Francis Group. USA. 565.
150. *CEPA High-speed centrifuges: For Laboratory and Industrial Processing*. 2013; Available from: http://www.tekniscience.com/documents/CEPA.pdf.
151. Guardia, M. and Hu, W.-S., *Mammalian cell bioreactors*. Encyclopedia of Bioprocess Technology: Fermentation, Biocatalysis, and Bioseparation, ed. S. Drew and M.C. Flickinger. 2002, New York: John WIley & Sons, Inc.
152. Jansson, P.E., Kenne, L., and Widmalm, G., *Computer-assisted structural analysis of polysaccharides with an extended version of CASPER using 1H- and 13C-n.m.r. data.* Carbohydr Res, 1989. **188**: p. 169-91.
153. Mikola, M., Seto, J., and Amanullah, A., *Evaluation of a novel Wave Bioreactor cellbag for aerobic yeast cultivation.* Bioprocess Biosyst Eng, 2007. **30**(4): p. 231-41.
154. Eibl, R., Kaiser, S., Lombriser, R., et al., *Disposable bioreactors: the current state-of-the-art and recommended applications in biotechnology.* Appl Microbiol Biotechnol, 2010. **86**(1): p. 41-9.
155. Gambillara, V., *The Conception and Production of Conjugate Vaccines Using Recombinant DNA Technology.* BioPharm International, 2012. **25**(1): p. 28-32.
156. Eibl, R., Werner, S., and Eibl, D., *Bag bioreactor based on wave-induced motion: characteristics and applications.* Adv Biochem Eng Biotechnol, 2010. **115**: p. 55-87.
157. *Wave Bioreactor systems: Cell culture procedures*. 2008, GE Healthcare.
158. *Wave Bioreactor systems: Cell culture procedures*. Upstream and Downstream 2007; Issue 1:[Available from: http://www.gelifesciences.com/gehcls_images/GELS/Related%20Content/Files/1314787424814/litdoc28932458_20161014161540.pdf.
159. Levine, H.L., *Vaccine Manufacturing in the Coming Decade*, in *World Vaccines Manufacturing Congress 2011*. 2011, BioProcess Technology Consultants: France.
160. Singh, V., *Method for culturing cells using wave-induced agitation*. 2001: US 6190913.
161. Schimdt, F.R., *Optimization and scale up of industrial fermentation processes.* Appl Microbiol Biotechnol, 2005. **68**.
162. Austrian, R., *Some observations on the pneumococcus and on the current status of pneumococcal disease and its prevention.* Rev Infect Dis, 1981. **3 Suppl**: p. S1-17.
163. Jin, S.D., Kim, Y.M., Kang, H.K., et al., *Optimization of capsular polysaccharide production by Streptococcus pneumoniae type 3.* J Microbiol Biotechnol, 2009. **19**(11): p. 1374-8.

164. Howden, R., *Use of anaerobic culture for the improved isolation of Streptococcus pneumoniae.* J Clin Pathol, 1976. **29**(1): p. 50-3.
165. Yavordios, D. and Cousin, M., *Procédé d'obtention de polyosides Capsulaires, polyosides capsulaires ainsi obtenus et leur application À la préparation de vaccins*. 1983: EP 0071515 a1.
166. Goncalves, V.M., Takagi, M., Carneiro, S.M., et al., *Introduction of air in the anaerobic culture of Streptococcus pneumoniae serotype 23F induces the release of capsular polysaccharide from bacterial surface into the cultivation medium.* J Appl Microbiol, 2006. **101**(5): p. 1009-14.
167. Klein, J.O., *The epidemiology of pneumococcal disease in infants and children.* Rev Infect Dis, 1981. **3**(2): p. 246-53.
168. Eibl, R. and Eibl, D., *Application of disposable bag bioreactors in tissue engineering and for the production of therapeutic agents.* Adv Biochem Eng Biotechnol, 2009. **112**: p. 183-207.
169. Harvey, L.M. and McNeil, B., *Liquid Fermentation Systems and Product Recovery of Aspergillus*, in *Aspergillus*, J.E. Smilth, Editor. 1994, Springer US: New York. p. 141-176.
170. Pericone, C.D., Overweg, K., Hermans, P.W., et al., *Inhibitory and bactericidal effects of hydrogen peroxide production by Streptococcus pneumoniae on other inhabitants of the upper respiratory tract.* Infect Immun, 2000. **68**(7): p. 3990-7.
171. Hu, W., Berdugo, C., and Chalmers, J.J., *The potential of hydrodynamic damage to animal cells of industrial relevance: current understanding.* Cytotechnology, 2011. **63**(5): p. 445-60.
172. Hammond, M., Nunn, H., Rogers, G., et al., *Identification of a leachable compound detrimental to cell growth in single-use bioprocess containers.* PDA J Pharm Sci Technol, 2013. **67**(2): p. 123-34.
173. Soubal, J., Peña, L., Santana, D., et al., *Procedure for the conjugation of the Streptococcus pneumoniae serotype 6B capsular polysaccharide to the tetanus toxoid.* Biotecnología Aplicada, 2013. **30**: p. 208-215.
174. Yuan, Y., Ruppen, M., and Sun, W., *Shortened purification process for the production of streptococcus pneumoniae polysaccharides*. 2008: US 0286838.
175. Gotschlich, E.C., Liu, T.Y., and Artenstein, M.S., *Human immunity to the meningococcus. 3. Preparation and immunochemical properties of the group A, group B, and group C meningococcal polysaccharides.* J Exp Med, 1969. **129**(6): p. 1349-65.
176. Katzenellenbogen, E. and Jennings, H.J., *Structural determination of the capsular polysaccharide of Streptococcus pneumoniae type 19A (57).* Carbohydr Res, 1983. **124**(2): p. 235-45.
177. Abeygunawardana, C., Williams, T.C., Sumner, J.S., et al., *Development and validation of an NMR-based identity assay for bacterial polysaccharides.* Anal Biochem, 2000. **279**(2): p. 226-40.
178. Jennings, H.J., Rosell, K.G., and Carlo, D.J., *Structural determination of the capsular polysaccharide of Streptococcus pneumoniae type -19 (19F).* Can. J. Chem, 1980. **58**: p. 1069-1074.

179. Hausdorff, W.P., Hoet, B., and Schuerman, L., *Do pneumococcal conjugate vaccines provide any cross-protection against serotype 19A?* BMC Pediatr, 2010. **10**(4): p. 1-7.
180. Chaplin, M.F. and Kennedy, J.F., *Carbohydrate Analysis: A Practical Approach*. 1994: ILR Press.
181. Dische, Z. and Shettles, L.B., *A specific color reaction of methylpentoses and a spectrophotometric micromethod for their determination.* J Biol Chem, 1948. **175**(2): p. 595-603.
182. Scott, J., *A reaction for the simple sensitive fluorimetric assay of heparin and 2-amino sugars.* Biochemistry 1979. **183**: p. 91-97.
183. Dische, Z. and Borenfreund, E., *A spectrophotometric method for the microdetermination of hexosamines.* J Biol Chem, 1950. **184**(2): p. 517-22.
184. Baginski, E.S., Epstein, E., and Zak, B., *Review of phosphate methodologies.* Ann Clin Lab Sci, 1975. **5**(5): p. 399-416.
185. Dreywood, R., *Qualititative test for carbohydrate material.* Ind. Eng, Chem. Analytical edition, 1946. **18**: p. 499.
186. Sattler, L. and Zerban, F.W., *The Dreywood Anthrone Reaction as Affected by Carbohydrate Structure.* Science, 1948. **108**(2800): p. 207.
187. Turula, V.E., Jr., Gore, T., Singh, S., et al., *Automation of the anthrone assay for carbohydrate concentration determinations.* Anal Chem, 2010. **82**(5): p. 1786-92.
188. Mokrasch, L.C., *Analysis of hexose phosphates and sugar mixtures with the anthrone reagent.* J Biol Chem, 1954. **208**(1): p. 55-9.
189. Koehler, L.H., *Differentitation of carbohydrates by anthrone reaction rate and color intensity.* Anal chem, 1952. **24**: p. 1576.
190. Cui, S., *Structural analysis of polysaccharides*, in *Food Carbohydrates: Chemistry, Physical Properties, and Applications*, L. Taylor & Francis Group, Editor. 2005, Taylor & Francis Group, LLC. p. 56.
191. Brummer, Y. and Cui, S.W., *Understanding carbohydrate analysis*, in *Food Carbohydrates: Chemistry, Physical Properties, and Application*, L. Taylor & Francis Group, Editor. 2005, CRC Press.
192. Clement, G., Dierick, J.F., Lenfant, C., et al., *Development and validation of a molecular size distribution method for polysaccharide vaccines.* Pharmeur Bio Sci Notes, 2014. **2014**: p. 40-59.
193. Wang, Q. and Cui, S., *Understanding the Physical Properties of Food Polysaccharides*, in *Food Carbohydrates: Chemistry, Physical Properties, and Applications*, L. Taylor & Francis Group, Editor. 2005, CRC Press.
194. Sanz, M.L. and Martinez-Castro, I., *Recent developments in sample preparation for chromatographic analysis of carbohydrates.* J Chromatogr A, 2007. **1153**(1-2): p. 74-89.
195. Cataldi, T.R., Campa, C., and De Benedetto, G.E., *Carbohydrate analysis by high-performance anion-exchange chromatography with pulsed amperometric detection: the potential is still growing.* Fresenius J Anal Chem, 2000. **368**(8): p. 739-58.

196. Chambers, R.E. and Clamp, J.R., *An assessment of methanolysis and other factors used in the analysis of carbohydrate-containing materials.* Biochem J, 1971. **125**(4): p. 1009-18.
197. Kim, J.S., Laskowich, E.R., Michon, F., et al., *Monitoring activation sites on polysaccharides by GC-MS.* Anal Biochem, 2006. **358**(1): p. 136-42.
198. DeJongh, D.C., Radford, T., Hribar, J.D., et al., *Analysis of trimethylsilyl derivatives of carbohydrates by gas chromatography and mass spectroscopy.* American Chemical Society, 1969. **91**(7): p. 1728.
199. Jones, C. and Mulloy, B., *The application of nuclear magnetic resonance to structural studies of polysaccharides.* Methods Mol Biol, 1993. **17**: p. 149-67.
200. Jonsson, H., *Exploring the structure of oligo- and polysaccharides: Synthesis and NMR spectroscopy studies*, in *Department of Organic Chemistry*. 2010, Stockholm: Stockholm. p. 61.
201. Xu, Q., Abeygunawardana, C., Ng, A.S., et al., *Characterization and quantification of C-polysaccharide in Streptococcus pneumoniae capsular polysaccharide preparations.* Anal Biochem, 2005. **336**(2): p. 262-72.
202. Lee, C.J. and Fraser, B.A., *The structures of the cross-reactive types 19 (19F) and 57 (19A) pneumococcal capsular polysaccharides.* J Biol Chem, 1980. **255**(14): p. 6847-53.
203. Cai, P., Moran, J., Pavliak, V., et al., *NMR structural analysis of the capsular polysaccharide from Streptococcus pneumoniae serotype 6C.* Carbohydr Res, 2012. **351**: p. 98-107.
204. Sorensen, U.B. and Henrichsen, J., *C-polysaccharide in a pneumococcal vaccine.* Acta Pathol Microbiol Immunol Scand C, 1984. **92**(6): p. 351-6.
205. Talaga, P., Bellamy, L., and Moreau, M., *Quantitative determination of C-polysaccharide in Streptococcus pneumoniae capsular polysaccharides by use of high-performance anion-exchange chromatography with pulsed amperometric detection.* Vaccine, 2001. **19**(20-22): p. 2987-94.
206. Kniskern, P.J., Miller, W.J., Hagopian, A., et al., *Process for making capsular polysaccharide from Streptococcus pneumoniae*. 1998, Merck & Co, Inc: US 5847112.
207. Zweig, S.E., *Advances in vaccine stability monitoring technology.* Vaccine, 2006. **24**(33-34): p. 5977-85.
208. Bobbitt, J.M., *Periodate oxidation of carbohydrates.* Adv Carbohydr Chem, 1956. **48**(11): p. 1-41.
209. Bystricky, S., Machova, E., Bartek, P., et al., *Conjugation of yeast mannans with protein employing cyanopyridinium agent (CDAP)--an effective route of antifungal vaccine preparation.* Glycoconj J, 2000. **17**(10): p. 677-80.
210. Kohn, J. and Wilchek, M., *1-Cyano-4-dimethylamino pyridinium tetrafluoroborate as a cyanylating agent for the covalent attachment of ligand to polysaccharide resins.* FEBS Lett, 1983. **154**(1): p. 209-10.
211. Kohn, J. and Wilchek, M., *A new approach (cyano-transfer) for cyanogen bromide activation of Sepharose at neutral pH, which yields activated resins, free of interfering nitrogen derivatives.* Biochem Biophys Res Commun, 1982. **107**(3): p. 878-84.

212. Wakselman, M. and Guibe-Jampel, E., *1-Cyano-4-dimethylamino-pyridinium Salts: New Water-soluble reagents for the cyanylation of the protein sulphydryl groups.* Chemical Society, Chemical Communications, 1976: p. 21-22.
213. Lees, A., Nelson, B.L., and Mond, J.J., *Activation of soluble polysaccharides with 1-cyano-4-dimethylaminopyridinium tetrafluoroborate for use in protein-polysaccharide conjugate vaccines and immunological reagents.* Vaccine, 1996. **14**(3): p. 190-8.
214. Suarez, N., Massaldi, H., Franco Fraguas, L., et al., *Improved conjugation and purification strategies for the preparation of protein-polysaccharide conjugates.* J Chromatogr A, 2008. **1213**(2): p. 169-75.
215. Broker, M., Costantino, P., DeTora, L., et al., *Biochemical and biological characteristics of cross-reacting material 197 CRM197, a non-toxic mutant of diphtheria toxin: use as a conjugation protein in vaccines and other potential clinical applications.* Biologicals, 2011. **39**(4): p. 195-204.
216. Knuf, M., Kowalzik, F., and Kieninger, D., *Comparative effects of carrier proteins on vaccine-induced immune response.* Vaccine, 2011. **29**(31): p. 4881-90.
217. Lees, A. and Shafer, D., *Simplified method for removing free protein during preparation of protein-polysaccharide conjugates and vaccines using restricted-access media*. 2001, The Henry M. Jackson Foundation for the Advancement of Military Medicine.: US 6284250.
218. Burgess, R.R., *Protein precipitation techniques.* Methods Enzymol, 2009. **463**: p. 331-42.
219. Lovrien, R. and Mayulis, D., *Extraction, Stabilization, and Concentration*, in *Current Protocols in Protein Science*, J.W.a. Sons, Editor. 1997.
220. *Invasive pneumococcal disease in children 5 years after conjugate vaccine introduction--eight states, 1998-2005*. MMWR Morb Mortal Wkly Rep 2008 Feb 15 [cited 57 6]; 2008/02/15:[144-8]. Available from: http://www.ncbi.nlm.nih.gov/pubmed/18272956.
221. Aguiar, S.I., Brito, M.J., Goncalo-Marques, J., et al., *Serotypes 1, 7F and 19A became the leading causes of pediatric invasive pneumococcal infections in Portugal after 7 years of heptavalent conjugate vaccine use.* Vaccine, 2010. **28**(32): p. 5167-73.
222. Bryant, K.A., Block, S.L., Baker, S.A., et al., *Safety and immunogenicity of a 13-valent pneumococcal conjugate vaccine.* Pediatrics, 2010. **125**(5): p. 866-75.
223. Berti, F., Romano, M.R., Micoli, F., et al., *Relative stability of meningococcal serogroup A and X polysaccharides.* Vaccine, 2012. **30**(45): p. 6409-15.
224. Johnson, H.L., Deloria-Knoll, M., Levine, O.S., et al., *Systematic evaluation of serotypes causing invasive pneumococcal disease among children under five: the pneumococcal global serotype project.* PLoS Med, 2010. **7**(10).